MIPAS Product Handbook

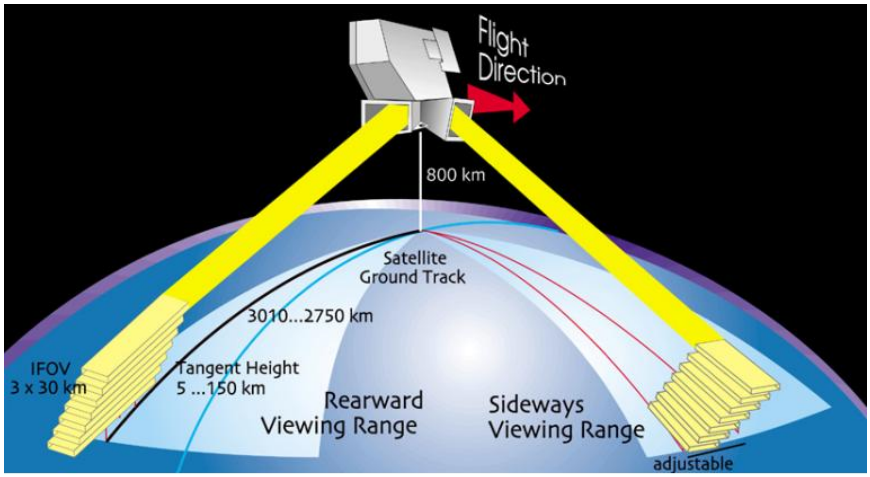

Issue 1.2, 1 September 2004

European Space Agency-EnviSat MIPAS Product Handbook, Issue 2.2, 27 February 2007

Table of contents

Abstract

Chapter 1

MIPAS Products User Guide

1.1 How to Choose MIPAS Data?

1.1.1 Geophysical measurements

MIPAS will be one of the atmospheric sensors on board ESA's polar orbiting ENVISAT to be launched towards the end of 2001. Operating in the mid-infrared (685 - 2410 cm^{-1}, or 14.6 - 4.15 μm) it will provide a number of geophysical parameters relevant for the study of atmospheric chemistry, climatology and tropospheric/stratospheric exchange processes.

During nominal in-orbit operation MIPAS will routinely sense the atmospheric limb emission while the instrument's line-of-sight (LOS) is periodically varied in discrete steps, within a tangent height range of about 8 km to 68 km. For each height step a single interferometer stroke ('sweep') is performed whilst interferograms are recorded in the five spectral bands, A: 685 - 970 cm^{-1}, AB: 1020 - 1170 cm^{-1}, B: 1215 - 1500 cm^{-1}, C: 1570 - 1750 cm^{-1}, D: 1820 - 2410 cm^{-1}. With a sweep measurement time of 4.45 s (high resolution, max. path difference = 20 cm), 16 tangent heights per scan and an orbit period of 100.6 minutes, typically 75 complete elevation scans will be acquired during each orbit. Scene measurements are interleaved by periodic radiometric offset ('deep space') measurements, in intervals of about 300 s. In addition, radiometric gain measurements, comprising sequences of blackbody target and deep space (D.S.) measurements, will be performed at approximately one week intervals.

The concept of the ENVISAT Payload Data Segment, PDS, foresees the routine generation and dissemination of calibrated, geolocated limb spectra (Level 1B products) and of so-called Level 2 data products. The latter covers vertical profiles of atmospheric pressure (p), temperature (T) as well as volume-mixing-ratio (VMR) profiles of the primary target species, O_3, H_2O, CH_4, N_2O, HNO_3 and NO_2. The table below provides a summary of MIPAS data products as well as auxiliary input data

Table 1.1 MIPAS Products Overview

Level 1B component		
Product ID	Description	Size
MIP_NL__0P	MIPAS raw (source packet) data, time ordered. Header and general quality information.	310 MBytes/ orbit
MIP_NL__1P	Included Data Sets: Calibrated limb radiance data in the five MIPAS spectral bands: A: 685-970 cm^{-1}. AB: 1020-1,170 cm^{-1}. B: 1215-1500 cm^{-1}. C: 1570-1750 cm^{-1}. D: 1820-2410 cm^{-1} Annotation data: Geolocation data, product quality information, processing parameters, noise assessment data, offset calibration data.	320 MBytes/ orbit
MIP_xx1__AX	Auxiliary products: * Calibration data (gain, offset validation, LOS, ILS) * others (e.g., characterisation data). * orbit state vector/attitude data.	variable size
Level 2 component		
MIP_NL__2P	Vertical profiles of pressure, temperature, volume mixing ratio of O3, H2O, CH4, N2O, NO2 and HNO3. Annotation data: Geolocation data, product quality information, residual spectra, fitted continuum data, processing parameters, others	8.5 MBytes/ orbit
MIP_NLE_2P	Included Data Sets: Vertical profiles of pressure, temperature, concentration of O3 and H2O. Annotation data: Geolocation data, product quality information, processing parameters, others.	8.5 MBytes/ orbit
MIP_xx2__AX	Auxiliary products * Pre-tabulated cross-section, microwindows data, atmospheric profiles, pointing information, processing parameters * ECMWF: Meteorology forecast data	variable size

1.1.2 Scientific background

Early in 1987 the European Space Agency asked a group of experts, the LISA (Limb Sounder of the Atmosphere) Consultancy Group, to assess the scientific utility of a limb sounder flown on a polar platform, to review and contrast the available technologies for limb sounding in the various parts of the electromagnetic spectrum, and to prepare outline specifications of a suitable instrument for use in a concept study.

The Group highlighted three major areas on which to focus remote sensing of the middle atmosphere in the late 1990s (ESA 1992 Ref. [1.34]), reaching the following conclusions:

Atmospheric Chemistry “there was a clear need to increase understanding of the processes which control the distribution of trace species in the middle atmosphere.

Climatology “ it was necessary to monitor the concentrations of trace species whose temporal changes affect the Earth's climate by modifying radiative transfer.

Operational Meteorology “ it was important to recognise the influence of the dynamic and radiative state of the lower stratosphere and upper troposphere on the atmosphere as a whole and hence its importance to operational meteorology.

To satisfy the scientific requirements defined above it is necessary to measure simultaneously a considerable number of species. To achieve this a set of instruments, operating in different parts of the spectrum, is essential. Light molecules with permanent dipole moments (such as OH, HO_2, ClO) have rotational features in the far infrared or microwave regions. Heavier molecules, such as NO_2 and HNO_3, can be identified and measured by analysing spectral features in the mid-infrared.

The Group concluded that the most appropriate type of instrument for such a mission would be a limb sounder capable of observing emitted radiances from the atmosphere. To cover the requisite wide spectral range this needed to be an interferometer. However, at the same time, it was clear that no one single instrument could be expected to adequately cover the complete spectral range required. The Group therefore recommended the provision of a complementary package of three instruments (mid-infrared, far-infrared and microwave) as the core of a middle atmosphere chemistry mission flown on a polar orbiting satellite. In so doing it highlighted the need for the measurements to be simultaneous (all related species), to be global in extent (pole to pole) and to cover day and night (diurnal variations).

1.1.2.1 Heritage of MIPAS

In deciding on the mission objectives for MIPAS and to focus on the mid-infrared, IMK not only took the views of the LISA Group into account but also the following:

¢ Within this part of the spectrum there is a wide variety of important molecules which have vibration-rotation spectra with absorption lines well suited for detection, so a large group of trace gases (e.g. the whole NO_y trace gas family, including the source gas N_2O) should be accessible to an instrument operating in this part of the spectrum.

¢ Atmospheric signals are generally higher here than in other parts of the spectrum because the location of the maximum of the Planck function (at 250 K) is at about 11 µm.

¢ Generally instruments working in the mid-infrared can be significantly smaller than those operating in the far-infrared. This is dictated by diffraction limits and the high spectral resolution needed to observe the chemical species of interest.

Another advantage of the mid-infrared is that instruments operating in this region can, in principle, be calibrated by observing cold space and black bodies. This gives them a significant advantage over those operating in the ultraviolet/visible region where reference calibration targets are not readily accessible.

The concept underlying the space version of MIPAS draws on the experience gained from several experiments exploiting Fourier transform spectrometers. In particular, the MIPAS-B (balloon) experiment can be regarded as a precursor of the MIPAS satellite experiment even if the type of interferometer is not exactly the same (see Fischer 1992 Ref. [1.38]). Since 1989 MIPAS-B has been successfully operated during several field experiments held in southern France as well as in Kiruna, northern Sweden (figure 1.1). The corresponding measurements have established the feasibility of detecting high quality emission spectra in the mid-infrared with the aid of a moderately cooled interferometer, i.e. sufficient sensitivity can be achieved by cooling the optical system to 200 K and the detectors to liquid Helium temperatures (Friedl-Vallon et. al. 1992 Ref. [1.40] , Fischer and Oelhaf 1996 Ref. [1.36]).

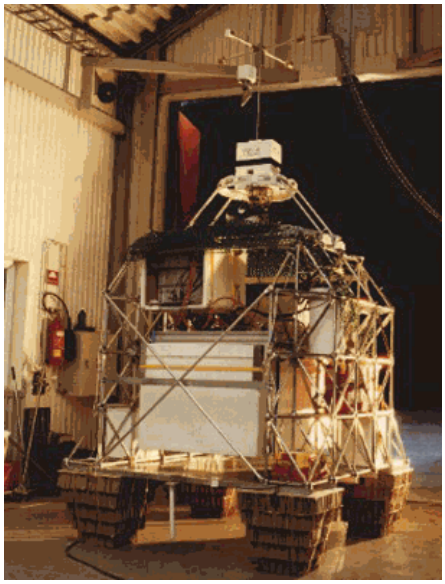

Figure 1.1 The MIPAS balloon gondola in Kiruna, North Sweden,1995

An instrument similar to MIPAS-B was flown on a Transall aircraft (MIPAS-FT) during the first half of the '90s (Gulde et al. 1994 Ref. [1.43]). These experiments showed quite clearly that even strong vibrations caused by an aircraft cannot seriously disrupt the operation of this type of interferometer. Strongly disturbed Phase-And magnitude spectra were corrected using the so-called double differencing method (Blom et al. 1996 Ref. [1.3]). Both types of experiment (i.e. balloon and aircraft) have helped establish the feasibility of MIPAS. Basic knowledge about interferometers gained from Fourier spectrometers measuring the attenuation of solar radiation in the atmosphere has also been taken into account during the development of the MIPAS space experiment. Here specific mention must be made of the ATMOS instrument which has yielded simultaneous measurements of a large number of trace constituents in the middle atmosphere (Farmer et al. 1987 Ref. [1.35]). A similar type of instrument has flown several times on a balloon platform and been used to investigate dynamical and chemical processes in the lower stratosphere (Camy-Peyret et al. 1993 Ref. [1.10]).

Analyses of MIPAS-B data have confirmed that cooled Michelson interferometers, operating in the mid-infrared, can observe many trace species simultaneously (Fischer and Oelhaf 1996 Ref. [1.36]). Vertical profiles of a large number of trace species have been derived, notably O_3, H_2O, HDO, CH_4, N_2O, $CFCl_3$, CF_2Cl_2, CHF_2Cl, CCl_4, CF_4, NO_2, HNO_3, HNO_4, N_2O_5 and $ClONO_2$; this despite the fact that the balloon instrument did not cover the whole of the mid-infrared (Fischer 1992 Ref. [1.38] , von Clarmann et al. 1994 Ref. [1.21] , Oelhaf et al. 1994 Ref. [1.55] , von Clarmann et al. 1995 Ref. [1.20] , Wetzel et al. 1995 Ref. [1.66]). In addition, ClO and HOCl concentrations have been estimated under disturbed chemistry conditions. Data from the MIPAS-FT has provided new information on

the horizontal distributions of various trace gases of relevance to stratospheric ozone research (Blom et al. 1994 Ref. [1.5] , Blom et al. 1995 Ref. [1.4] , Hopfner et al. 1996 Ref. [1.44]).

1.1.2.2 Atmospheric Chemistry

In many ways, the study of the stratosphere is the study of ozone and ozone-related chemistry. Infrared absorption and emission by ozone is a significant component in the radiation budget of the stratosphere, and is part of the Greenhouse Effect. Thus the absorption of shortwave radiation by ozone in the stratosphere is responsible for the temperature inversion which defines the height of the troposphere, the lowest part of the atmosphere where most biological activity takes place and where weather resides.

This inversion acts as a cap on vertical motion, limiting (but not stopping) the movement of water vapour and trace species into the stratosphere. The warming of the stratosphere, resulting from the absorption of solar radiation by ozone, controls air motion over a range of spatial scales. The restriction on vertical motion in the lower atmosphere, imposed by the stability of the stratosphere, has fundamental and wide-ranging effects on the global-scale circulation in the lower atmosphere. The limits on the vertical extent of convective activity, coupled with the influence of the Coriolis acceleration imposed by the Earth's rotation, determine the global pattern of zonal winds.

Ozone was first discovered to be present in the atmosphere in the mid-nineteenth century because the absorption of ultraviolet radiation by ozone in the stratosphere causes a sharp cut-off in levels of solar radiation reaching the ground. This occurs in the near-ultraviolet toward shorter wavelengths (i.e. ≤325 nm). This absorption was measured and used to estimate the total amount of ozone in the atmosphere. It led to the discovery that nearly all the ozone in the atmosphere is to be found well above the Earth's surface.

With the publication of the Chapman theory for the photochemical production of ozone in the upper atmosphere (Chapman 1930 Ref. [1.16]), the primary processes involved in the production of ozone and the establishment of its equilibrium vertical profile were enunciated. As first proposed by Chapman (Chapman 1930 Ref. [1.16]), ozone is created in the stratosphere as a result of the dissociation of molecular oxygen by ultraviolet radiation according to the reaction equation:

$$O_2 + h\nu \text{ “> } O + O \qquad \text{eq 1.1}$$

where the reaction of "O_2 + hυ"represents the absorption of a photon of light. This reaction is followed by:

$$O_2 + O + M \text{ “> } O_3 + M \qquad \text{eq 1.2}$$

where M is another molecule (probably O_2 or N_2) which allows the reaction to occur by absorbing excess energy and momentum.

Ozone is destroyed when it absorbs radiation shorter than 1.18 μm:

$$O_3 + hv + M \text{ “> } O_2 + O + M \qquad \text{eq 1.3}$$

The last two of these three reactions comprise a fast reaction cycle that neither destroys nor produces ozone, but which injects a large amount of energy into the stratosphere. Because of the speed of these two reactions, O and O_3 are, to a certain extent, 'equivalent' and their total concentration, [O] + [O_3], is often referred to as "odd oxygen". It is this absorption of ultraviolet energy by ozone, as represented by these equations, which is responsible for the temperature structure and consequent vertical stability of the stratosphere.

The primary production process (equation eq. 1.1) is balanced by reactions in which ozone is destroyed, such as:

$$O + O_3 \text{ “> } 2\,O_2 \qquad \text{eq 1.4}$$

As levels of oxygen decrease with height the absorption of photons in reaction 1 also decreases with height. Also, reaction 2 decreases with increasing height as the atmospheric density decreases, producing a level of maximum ozone in the stratosphere.

However, to achieve quantitative agreement with observed ozone profiles, many more ozone destroying reactions, plus some other minor source terms, must be included in the chemical scheme. These include reactions with water-related radicals (OH and HO_2), nitrogen compounds (NO and NO_2), chlorine compounds (Cl and ClO), bromine compounds (Br and BrO) and others. It is now known that more than 100 reactions and dozens of chemical species must be included for a chemical model of the stratosphere to calculate ozone amounts with reasonable accuracy over the whole globe. Furthermore, there are relatively few regions in the atmosphere, particularly those with the highest ozone levels, where the local concentration of ozone is determined by local photochemical equilibrium alone.

Despite of the fact that much of the basic knowledge of the stratosphere was developed several decades ago, the science of ozone is still far from being completely understood. Indeed, the recent (since 1985) development of the Antarctic ozone hole (figure 1.2) and contemporary observations of very low ozone amounts in the Arctic are stimulating active research in the field. There are a number of outstanding scientific questions which can be addressed with the aid of MIPAS data.

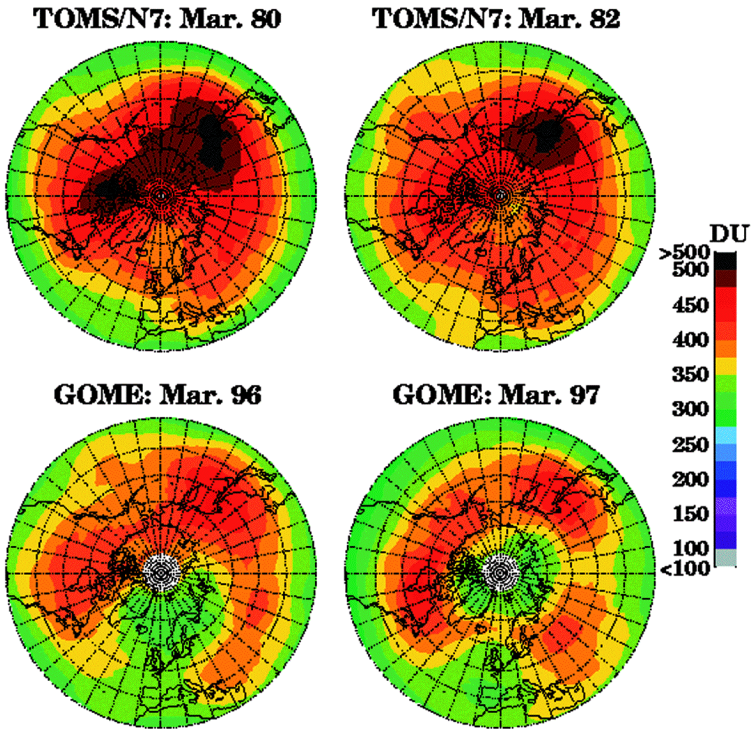

Figure 1.2 Arctic March total ozone (monthly means) observed in 1980 and 1982 by TOMS/Nimbus (top) and in 1996 and 1997 by GOME / ERS-2 (bottom) document the decline in polar total ozone in spring (source: WMO 1998)

Although, as indicated above, the general features of the stratospheric ozone layer and the global ozone budget now appear to be relatively well understood, there are a number of observations which are not properly explained by current scientific theory. Chemical and temperature data, particularly chemical tracer data, from MIPAS will contribute to further research in this area.

It is believed that the chemistry and dynamics of the stratosphere are qualitatively quite well understood. However, there are significant quantitative differences between the predictions of current models and observations of the distribution of stratospheric constituents which may have significant implications on the accuracy of long-term predictions of ozone change. In the lower stratosphere, the decline in ozone amounts at mid-latitudes has been roughly double the amount predicted by models, though otherwise there is in good agreement throughout most of the atmosphere. These differences are probably a result of insufficient (or inaccurate) knowledge of the chemical, microphysical and dynamical state of the region. In particular, stratosphere-troposphere exchange processes are not well understood on the

global scale. MIPAS is expected to provide additional insight in the mechanisms involved.

Changes are taking place in the ozone layer in the Arctic which seem to lie outside the predictions of current models. Since MIPAS will provide observations of many species, as well as of temperature, in the polar night, its data set will contribute significantly to work in this area. The relatively high vertical resolution of the MIPAS data set will permit smaller scale chemical effects to be studied over the whole globe. These observations may be crucial to advancing understanding of the effects of heterogeneous chemistry (i.e. chemistry on surfaces or in the liquid phase in droplets) which is responsible for much of the downward trend in total ozone levels.

Also, the MIPAS experiment should help to provide a baseline for the (future) monitoring of constituents involved in climate change. For example, a number of radiatively active gases, such as the CFCs, ozone and water vapour, will be measured with high accuracy over the whole globe by MIPAS.

Finally, the sensitivity of the MIPAS instrument will allow the observation of important atmospheric parameters in the mesosphere and lower thermosphere, namely the temperature, H_2O, CH_4, CO, CO_2, O_3 and NO. Based on these measurements several research aspects such as the ozone deficit in the lower mesosphere, the energy balance in this region, dynamic processes in the mesosphere can be investigated in some detail. Taking into account the good spectral resolution of MIPAS manifold studies of the non-Local Thermodynamic Equilibrium (LTE) in the middle and upper atmosphere can be performed with the measured spectra.

1.1.3 Principles of measurement

In this section we describe how MIPAS measures the interferograms that will later, during the level 1b and level 2 processing phases, be processed into spectra of atmospheric spectral radiance and in vertical profile of concentration of atmospheric molecules.

1.1.3.1 Overview

MIPAS 5.1. is a rapid scanning Fourier transform spectroradiometer. Compared to other types of spectrometers, Fourier transform spectrometers usually have a higher spectral resolution in the infrared, are easier to radiometrically calibrate and since they do not require a light-limiting slit, they tends to be more sensitive and can have a larger field of view.

Like most Fourier transform spectrometers (FTS), MIPAS is based on a variant of the traditional Michelson interferometer. The figure below shows the MIPAS interferometer.

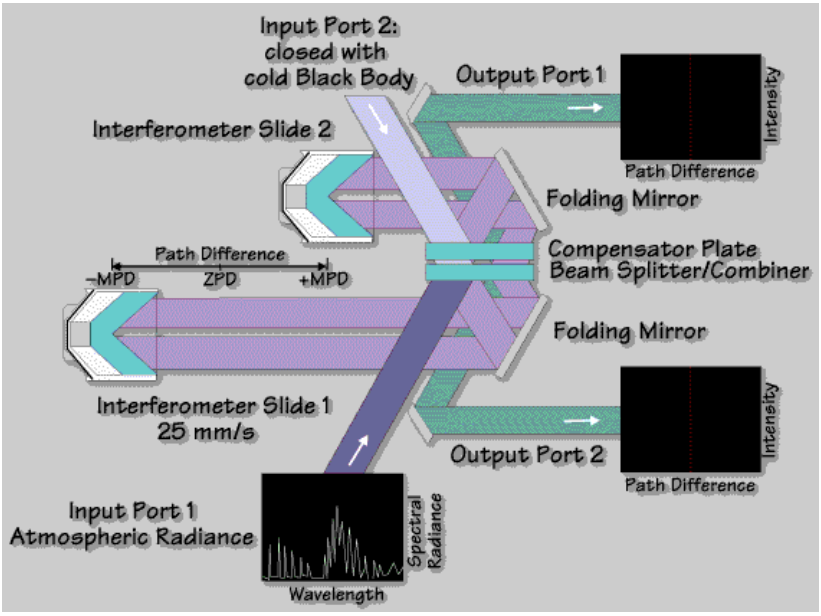

Figure 1.3

Infrared radiation (in blue on the figure) coming from the atmosphere is collected by the input telescope of the instrument. The radiation is then collimated by the input collimator and directed to one of the input port of the interferometer. In the interferometer, the radiation beam is divided in two equal fractions by the beamsplitter. About 50% of the radiation is reflected by the beamsplitter and the remaining 50% is transmitted by the beamsplitter. Both the transmitted beam and the reflected beam (in purple on the figure) are then directed to two cube corner retro-reflectors. The retro-reflectors reflect the radiation beams back to the beamsplitter where they are recombined. One more time, the beamsplitter separate the recombined beam in two separate beams (in green on the figure) and each beam is directed to an output port where they are collected by infrared detectors. The recombined beams generate an interference pattern. The intensity reaching the detector will depend on the interference pattern: the intensity is minimal if the radiation reaching the detector is in destructive interference; the signal is maximal if the interference is constructive.

If the corner-reflectors are moved with respect to one another, the difference in optical path between the reflected and transmitted beams will vary. If the optical path between the two beams varies, the interference pattern will also varies. The detector will record a succession of varying intensity as the interference changes from destructive to constructive and destructive again. This series of varying intensity is called an interferogram.

The interference pattern depends not only on the optical path difference between the two arms of the interferometer but also on the wavelength and on the spectral intensity of the incoming radiation. The interferogram thus contains information on the spectral distribution of energy of the incoming radiation. This information can be retrieved by "decoding" the interferogram. By performing a numerical Fourier transform of the recorded interferogram, the interferogram is transformed into the spectrum of the incoming radiation.

Because the corner-reflectors shear the beams, the radiation beam going to the corner-reflector do not overlap with the radiation beam reflected by the corner-reflectors. Because of that, the interferometer has two distinct output ports. Detectors are placed at each output ports. By symmetry, the system also has two input ports but the second input port is blocked by a cold target.

The spectral resolution of a FTS is mostly determined by the maximum optical path difference (MPD) between the two retro-reflectors. MIPAS has a MPD of +/-20 cm. This is achieved by independently moving the two cube corners by 5 cm backward and forward. The spectral resolution is about 0.6 / MPD. For MIPAS it is 0.035 cm^{-1}. This corresponds to about 0.06 nm at a wavelength of 4150 nm. It would be difficult, if not impossible, to achieve such a fine spectral resolution with a type of spectrometer other than a Fourier transform spectrometer.

This is very complicated, please explain more how a Fourier transform spectrometer works 1.1.4.1.1. .

The spectrum of the incoming radiation from the atmosphere contains information about the chemical constituents of the atmosphere and their concentration. A given molecule or atom of the atmosphere absorbs and emits radiation at specific wavelengths. It is thus possible to identify the presence of a specific molecule by checking if the studied spectrum contains the spectral line of that given molecule. The intensity of the line is proportional to the concentration of the molecules. Pressure and temperature also affect the pattern of spectral lines emitted by a given molecule. Since pressure and temperature are function of the altitude and because MIPAS takes measurement at several elevation angles, it is thus possible to determine vertical profiles of the concentration of given molecules from the spectra acquired with MIPAS.

1.1.3.2 Detector and spectral ranges

A set of four detectors by output port (for a total of eight detectors) records the interferogram. The data recorded by each output port are coadded to increase the signal to noise ratio (SNR). This set-up also provides a certain redundancy: if a detector in one output port fails, the corresponding detector in the second output port still provides useful data.

The four detectors are Hg:Cd:Te detectors but each has been optimized for a particular spectral range. Together, the four detectors cover the spectral range from 685 cm^{-1} to 2410

cm^{-1} in wavenumbers. In wavelengths, the corresponding spectral range is about 4150 nm to 14600 nm.

The four detectors are named A, B, C and D. Detectors A, C and D of port 1 and 2 are identical. Detectors B are different in port 1 and port 2. These 8 detectors can be combined in five spectral bands.

Table 1.2

Band	Detectors	Spectral range (cm^{-1})
A	A1 and A2	685 - 970
AB	B1	1020 - 1170
B	B2	1215 - 1500
C	C1 and C2	1570 - 1750
D	D1 and D2	1820 - 2410

1.1.3.3 Sampling the interferograms

As the corner-reflectors are moved, the interference pattern moves over the detectors. To record a useful interferogram, the modulated output has to be sampled at very regular optical path difference intervals (the required sampling accuracy for MIPAS is about 30 nm). This is done with help of a laser beam transmitted in the same optical set up, which is used to trigger the sampling electronics behind the detector at very precise values.

The interferogram of the monochromatic laser is pure sine wave. The interferogram is detected by a dedicated metrology detector and a fringe counter determines the OPD by the phase of the sine wave. The fringe counter forms a "clock signal that is sent to the ADC in the on-board signal processor electronics (SPE). The fringes trigger the sampling of the interferogram.

Variable phase delays in the detection electronics would also result in sampling jitters, thus the sampling frequency has to stay within a narrow range, which in turn leads to a requirement to have a very constant optical path difference speed (i.e. drive speed of the retro reflectors).

1.1.3.4 Calibration measurements

To radiometrically calibrate the spectra that will be generated during the Level 1b processing, it is necessary to have two calibration measurements: a "cold" and a "warm" measurement. These two measurements are necessary to determine the effective gain and offset of the instrument. These parameters are essential to perform the radiometric calibration of the measurements made by MIPAS.

1.1.3.4.1 Offset measurement

Looking at the deep space provides a "cold": scene, i.e. a scene with negligible infrared radiance. The interferogram acquired while looking at the deep space is mostly due to the instrument self-emission. Deep space measurements are made frequently, one every four elevation scans, in order to account for changing instrument self-emission due to temperature variations along the orbit. These measurements are performed at a reduced spectral resolution. The spectral resolution is coarser than the highest resolution of MIPAS by a factor 10. A single measurement will last 0.4 second.

The Offset Calibration is performed every four scans, and uses six sweeps at low resolution (three forward and three reverse), which must be combined to reduce the noise level to acceptable level. The baseline scenario uses 300 sweeps at low resolution in both forward and reverse directions. The total duration of the offset measurement is 16.15 seconds (including transition times), and measurements are then made every 300.5 seconds.

For an orbit of 100 minutes, assuming all measurements are performed with the same scan scenario, there are about 20 offset measurements per orbit, which is well above the necessary minimum determined from an estimation of the expected temperature variations.

1.1.3.4.2 Gain measurement

The "warm" measurement, i.e. a measurement with a relatively high radiance, is performed while the instrument is looking at an internal source. This source is a well characterized calibration blackbody with a controlled temperature.

The baseline is to look at the internal calibration blackbody once a week. These measurements are also performed at a reduced spectral resolution. The spectral resolution is coarser than the highest resolution of MIPAS by a factor 10. A single measurement will last 0.4 second.

In order to reduce the noise in the calibration measurements, many measurements are recorded and then coadded on the ground. The baseline scenario uses 300 sweeps at low resolution in both forward and reverse directions.

Calibration measurements are performed after the instrument slides have been stopped in order to re-establish a phase reference. The calibration sequence is therefore commanded as the first operation in any nominal measurement sequence. Radiometric Deep Space Calibration measurements precede those made looking towards the calibration blackbody to cover the worst case condition: i.e. the instrument entering measurement mode directly after the boost heater phase of the calibration blackbody 3.1.3.1.1.3. .

1.1.3.5 Onboard processing

The sampled interferograms are converted into digital number by the onboard analogue-to-digital converter (ADC). Before being sent to ENVISAT, the digital data is numerically filtered, it is decimated, the size of the digital word is reduced over a certain fraction of the interferogram and the data is compressed. See the level 0 processing 2.4.3.2. for details. The goal of all this processing is to reduce the data rate of the instrument to less than 550 kbits/s. The digital filtering and decimation can be disabled by telecommand from the ground but, in that case, the data rate increases to 8 Mbits/sec.

ENVISAT is in charge of telemetring the data to the ground station were it will be further processed.

1.1.3.6 Ground processing

The ground processing of MIPAS data is divided in two phases called level 1b and level 2.

The goal of the level 1 b processing is convert the raw interferogram measured by MIPAS and sent by ENVISAT into validated, corrected, radiometrically calibrated, spectrally calibrated and geolocated spectra of atmospheric radiance. The radiometric calibration uses the gain and offset measurements described above 1.1.3.4. . The spectral calibration is based on a comparison of the measured spectra with the spectral position of well known atmospheric lines used as reference. See the level 1b processing 2.4.3.2. for further details.

The goal of the level 2 processing is to retrieve vertical profile of atmospheric molecules from the calibrated spectra. It relies on state-of-the-art inversion models that derive vertical profile of temperature, pressure and volume mixing ratios of selected molecules from the fine spectral information provided by MIPAS. The five priority molecules that will be routinely retrieved on regular basis are water vapour (H_2O), ozone (O_3), methane (CH_4),

nitrogen dioxide (NO_2), nitreous oxyde (N_2O) and nitric acid (HNO_3). Other molecules can also be retrieved from the data. See the level 2 processing 2.4.3.2. for details.

1.1.3.7 Spatial coverage

MIPAS can collect data from various altitudes and various positions by using two scanning mirrors to point at different angles to the side and to the rear of ENVISAT. This scanning capability combined with the orbit of ENVISAT allows MIPAS to achieve a complete coverage of the Earth. See the section on geophysical coverage 1.1.4. for more details.

1.1.4 Geophysical coverage

1.1.4.1 Overview

MIPAS covers the infrared spectral region from 4100 nm to 14600 nm. It is designed to operate in both the day and the night parts of ENVISAT's orbit with an azimuth scan geometry in the anti-flight direction. This geometry ensures a complete global coverage. MIPAS is also capable of pointing perpendicularly to the flight track (i.e. in the range 80 to 110 degrees from flight direction), a scanning geometry that permits diurnal changes to be detected and special events to be observed. Latitudinal resolution is increased by looking backwards.

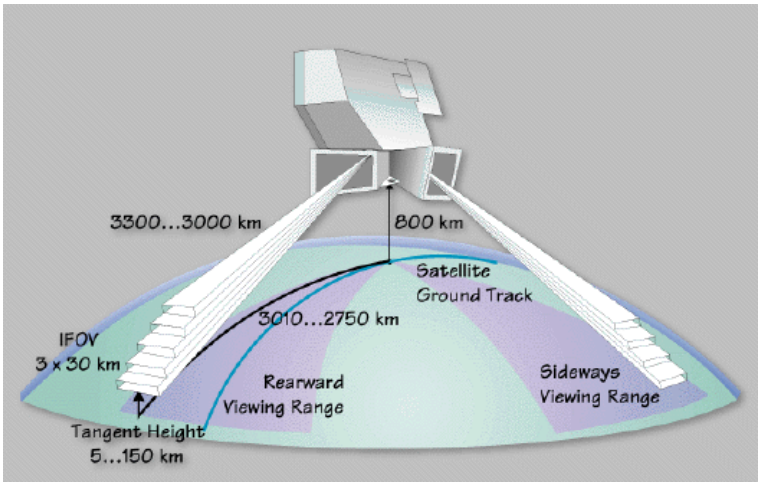

Figure 1.4 The scanning geometry (rear looking and sideways looking) of MIPAS

1.1.4.1.1 Basic principles of a Fourier transform spectrometer

The figure below represent a simplified version of a Michelson interferometer on which the design of MIPAS is based. In is essentially made of two flat mirror, perpendicular to one another and of a beamsplitter at 45 degrees. One of the two mirror (mirror #2) can be translated on an axis that is perpendicular to its surface. The system also includes a light detector that returns an electrical signal that is proportional to the intensity of the light that it collects.

On the figure the light from the source enters the interferometer from the left. The light beam strikes the beamsplitter. The beamsplitter separates the beam in two parts: one part is reflected to the mirror #1, the other part is transmitted to the mirror #2. Both part of the beam are reflected by one mirror and return to the beamsplitter. The beamsplitter once again separates the returning beams in two parts: one part is directed toward the detector and one part is directed back to the source. To simplify the explanation, we will suppose that the source is perfect laser, i.e. a source of monochromatic and coherent light.

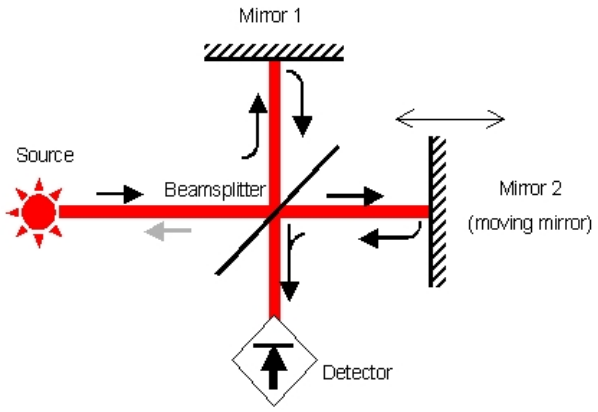

Figure 1.5

Two components of the initial beam reaches the detector: the beam that was reflected by the mirror #1 and the beam that was reflected by the mirror #2. These two beams are superposed when they reach the detector and their energy will add up.

Light is an electro-magnetic wave and it has a behaviour that is somewhat similar to classical waves. The result of an addition, also called interference, of two waves depends on the strength (energy) of each wave but also on the relative phase of the waves. If two waves add up so that their maximum are coinciding (figure below on the left), then the resulting wave has a maximum amplitude. This is called a constructive interference. On the other hand, if the two waves add up when a maximum of wave coincide with the minimum of the other wave (figure below, on the right), they cancel out and the result is nothing. This is called a destructive interference. Any other combination will result in a wave that has an amplitude between 0 and the maximum amplitude.

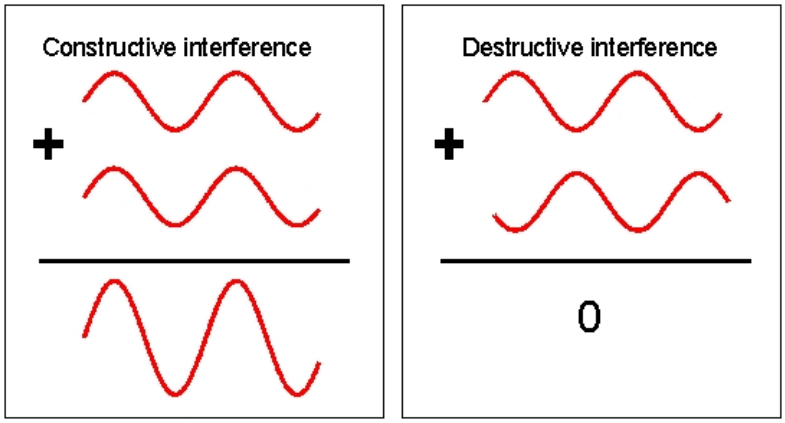

Figure 1.6

Light waves are waves that oscillates in space. Their phase (or the position of the maximum of amplitude) depends on the distance they have travelled. At the moment they are separated by the beamsplitter, the two beams that we were discussing above are in phase (they have the same phase) because they have travelled the same distance. After having been separated by the beamsplitter each beam travels its own path. One beam goes from the beamsplitter to the mirror #1, back to the beamsplitter and then to the detector. The other beam goes from the beamsplitter to the mirror #2, back to the beamsplitter and then to the detector. The difference of phase between the two beams depends on the difference of distance between the mirrors with respect to the position of the beamsplitter.

If this difference of travelled path is such that the two beams are in phase, the will interfere constructively on the detector and the detector will record a maximal signal. If the difference of travelled path is such that the two beams are in opposed phase, the will interfere destructively on the detector and the detector will record no signal. Anywhere in between these two extremes, the detector records a more less strong signal that depends on the difference of phase between the two beams.

The two beams will be in phase on the detector if the difference of distance between the two mirrors is an even multiple of a quarter of the wavelength (λ) of the light. At the opposite, the two beams will be completely out of phase if this distance is an odd multiple of quarter of the wavelength of the light. Because the light beams move back and forth between the mirror and the beamsplitter, the total difference of path (optical path) is twice the difference of physical distance.

If the moving mirror is translated back and forth along its axis, the difference of path between the two paths will vary and the interference pattern on the detector will alternate between constructive and destructive interference. The figure below shows the interference pattern and the corresponding signal recorded by the detector as a function of the position of the moving mirror.

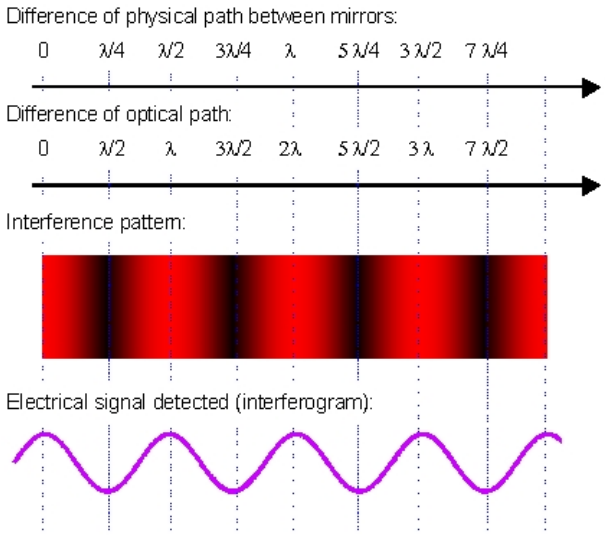

Figure 1.7

The interference pattern recorded by the detector is called an interferogram. The interference pattern depends on the position of the moving mirror and on the wavelength (λ) of the light beam. The amplitude of the interferogram also depends on the energy of the light entered the interferometer. The interferogram thus contains information about the wavelength and the energy of the light that entered the interferometer. This information is, however, somewhat hidden in the interferogram but it can be retrieved through the use of a mathematical operation. This mathematical operation is the Fourier transform. Applying a fast Fourier transform (FFT) to the interferogram transforms it into the distribution of energy as a function of the wavelength (a spectrum) of the incoming light. The adjective "fast" is added because it is a simplified Fourier transform function adapted to digital computers.

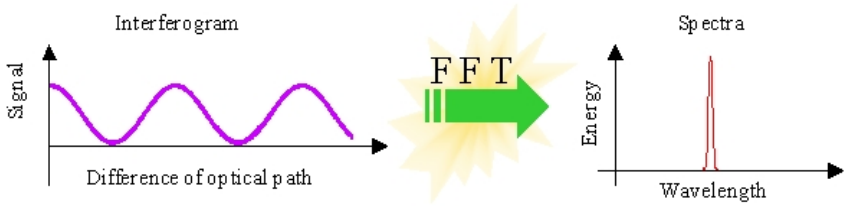

Figure 1.8

In our example, the interferogram is a cosine and the resulting spectrum is a spike because the incoming light comes from a monochromatic laser. However, the instrument works just as well with polychromatic light. The interferogram (and the resulting spectrum) is just more complicated. You can take a look at the image gallery 1.4. for an example of a typical MIPAS interferogram and its corresponding spectrum.

The Fourier transform spectrometer (FTS) has three main advantages over other types of spectrometers:

1. It does not require a slit like most other spectrometers so that it can accept a very large beam of light. This is useful to detect sources that are very faint.
2. It requires only one detector and not one detector per spectral interval like other types of spectrometers.
3. The spectral resolution is not limited by the size of the detector, it depends mainly on the maximum difference of path between the two mirrors. The longer the path is, the finer the spectral resolution is. It is relatively easy to achieve very fine spectral resolutions with a FTS.

1.1.4.2 Pointing

The overall MIPAS observational objectives can be described as being able to observe atmospheric parameters in the altitude range between 5 km and 160 km of altitude, globally, with step sizes between 1 and 10 km. To attain these objectives, MIPAS has two pointing mirrors: the elevation mirror and azimuth mirror.

The elevation mirror selects the limb altitude and corrects for variation in orbital altitude and the Earth's geoid geometry. The orientation of the azimuth mirror and the position of the satellite determine the latitude and the longitude of the observed part of the atmosphere. The azimuth mirror provides access to any limb target rearward within a 35 degree wide range around the anti-flight direction and sideways within a 30 degree wide range in the anti-Sun direction.

The baseline strategy is to keep the azimuth mirror at a fixed angle, while data from various altitudes are acquired by changing the orientation of the elevation mirror. The azimuth mirror is then moved to another orientation before acquiring new data. Varying the azimuth angle between scans allows MIPAS to measure from pole to pole. Since the azimuth mirror remains stationary during an elevation scan, the migration of the field of view due to the Earth's rotation (for backward looking) and to satellite movement (for sideways looking), has to be taken into account. For cross-track observation, simultaneous changes of both pointing mirror is possible in order to improve the horizontal resolution of a single atmospheric layer.

The time required to acquire one complete spectrum at a fixed elevation is 4.5 seconds at full spectral resolution. An elevation scan consists of 15 spectra (also called sweeps). Considering the time lost between sweeps and the time lost to reposition the pointing mirrors, the time required to complete an elevation scan is about 72 seconds. Typically there is a spacing of 3

km between successive measurements in the altitude range from the upper troposphere to the upper stratosphere and larger spacing above.

Typically, elevation scans performed in the rear and sideways looking modes while the satellite is moving, project a staircase pattern on which the single elevation scan will be positioned. The sampling intervals change their shape according to the sampling frequency during one elevation scan and the spacing between successive samples at the various altitudes. However since measurements in the mesosphere and thermosphere are not planned on a regular basis, an equal sampling distance has been assumed between the upper troposphere and the upper stratosphere. The altitude of the lower starting point of the elevation scan may be adjusted to the climatological height of the tropopause along the orbit. During sideways looking, the effective horizontal width of the FOV in the flight direction will be in the order of 60 km, due to the motion of the IFOV during interferogram recording.

1.1.4.3 Spatial coverage

In its nominal mode, MIPAS will have global coverage. Specialized observation modes will be used occasionally to study specific region of the globe.

At the tangent point, the IFOV of MIPAS is about 3 km in elevation by 30 km in azimuth.

Depending on the observation mode, the direction of looking and the angle of the elevation mirror, the horizontal spacing of a single measurement is between 100 and 800 km. Depending on the observation mode, the direction of looking and the angle of the elevation mirror, the vertical spacing between two consecutive measurements is between 1.5 and 10 km. See the section on observation modes 1.1.4.5. for details.

1.1.4.4 Temporal coverage

A typical elevation scan comprises fifteen high-resolution atmospheric scene measurements, each at one elevation. At full resolution, one measurement (i.e. one sweep) takes about 4.5 seconds. Considering the time lost between sweeps and the time lost to reposition the pointing mirrors, the time required to complete an elevation scan is about 72 seconds. Alternatively, an elevation scan can include up to 75 scenes measurements but with a spectral resolution reduced by a factor 10.

MIPAS will be in operation continuously over the full orbit of ENVISAT-1.

1.1.4.5 Observation modes

To cover the various scientific objectives of MIPAS, several observation modes are planned. Each mode is associated with a particular scientific objective and has different altitude coverage, altitude resolution and horizontal resolution.

Table 1.3

Observation Mode	Scientific Objective	Pointing direction	Coverage	Altitude range (km)	Vertical Spacing(km)	Horizontal spacing (km)
Nominal	Stratospheric chemistry and dynamics	rear	Global	6 - 68	3 - 8	530
Polar Winter Chemistry	Polar chemistry and dynamics	rear	Regional or occasional	8 - 55	2 - 10	450
Tropospheric-Stratospheric Exchange	Exchange between stratosphere and troposphere, troposphere chemistry	rear	Regional or occasional	5 - 40	1.5 - 10	400
Upper Atmosphere	Upper atmosphere	rear	Regional or occasional	20 -160	3 - 8	800
Dynamics	Small-scale structures in the middle atmosphere	rear	Regional or occasional	8 - 50	3 - 8	500
Diurnal Changes	Diurnal changes near the terminator	side	Regional or occasional	15 - 60	3	100
Impact of Aircraft	Study of major air traffic corridor	side	Regional or occasional	6 - 40	1.5 - 10	500

1.1.5 Peculiarities of MIPAS

The three atmospheric sensors on board ENVISAT, GOMOS, MIPAS and SCIAMACHY not only represent a continuation of the atmospheric ozone monitoring mission GOME/ERS-2 but significantly enrich the scope of observational capabilities - mainly the number of detectable species and their vertical distribution - making use of a variety of novel measurement techniques and enhanced spectral coverage.

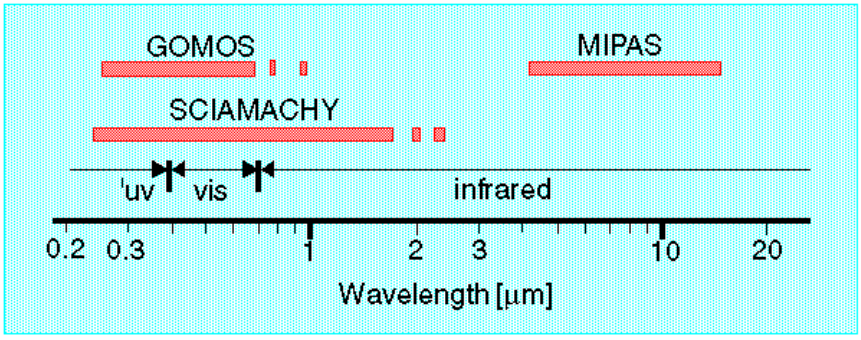

Figure 1.9 Spectral coverage provided by the three instruments.

Their three instruments' geophysical products will comprise a large number of atmospheric state parameters, primarily trace gas abundancies, and establish a high degree of complementarity in the provided information. Together, these data will supply the user community with unprecedent insights in the atmosphere's chemical and physical processes and facilitate major steps forward towards a better understanding of the future evolution of it's chemical and climatological balance.

The MIPAS instrument has been designed to acquire global measurements of the Earth's limb emission ranging from the upper troposphere up to the mesosphere. Analysis of numerous minor trace gases exhibiting spectral features in the 685 - 2410 cm^{-1} wavenumber interval (14.6 - 4.15 µm wavelengths) is envisaged posing challenging requirements on radiometric sensitivity, spectral resolution and pointing stability. MIPAS will provide accurate vertical profiles of atmospheric temperature and a number of key trace gases, including the entire NO_y family (except NO_3), and cover a height range from the upper troposphere up to the lower mesosphere. As MIPAS detects the atmosphere's thermal emission it is independent of sunlight conditions ('day & nightside' measurements) and

provides global coverage.

1.1.6 Summary of applications and products

The Michelson Interferometer for Passive Atmospheric Sounding (MIPAS) is a Fourier transform spectrometer that is part of the suite of instruments onboard ENVISAT. This instrument measures the infrared radiation emitted by the atmosphere as a function of the wavelength. It measures this radiation in the spectral range between 685 - 2410 cm^{-1} (14.6 - 4.15 µm) with a spectral interval of up to 0.025 cm^{-1}.

At the highest spectral resolution, it takes about 4.45 s to acquire a single spectrum. An elevation scanning mirror allows the instrument to measure at 16 different altitudes. In the course of a single orbit, MIPAS will typically acquire 75 scans made of spectra acquired at the 16 different elevations. Between measurements, the instrument also acquires calibration data used to perform the radiometric calibration.

The calibrated radiance spectra obtained with MIPAS are then feed to inversion models. These atmospheric models transform the spectra in vertical profiles of pressure, temperature and concentration of the following gases: O_3, H_2O, CH_4, N_2O, HNO_3 and NO_2. This information is valuable to monitor some of the gases that contribute to the greenhouse effect and to monitor the chemistry processes linked to the generation and destruction of ozone in the atmosphere.

The main data product obtained with MIPAS includes:

Level 1b:

- Radiometrically calibrated, spectrally corrected and geo-located spectra of radiance.

Level 2:

- Vertical profiles of pressure
- Vertical profiles of temperature
- Vertical profiles of volume mixing ratio of O_3, H_2O, CH_4, N_2O, HNO_3 and NO_2

1.2 How to use MIPAS data?

1.2.1 Software Tools

1.2.1.1 General tools

1.2.1.2 EnviView

1.2.1.3 MIPAS specific software tools

The BASIC Envisat Atmospheric Toolbox (BEAT)

Overview

The BEAT is a collection of executable tools and an application programming interface (API) which has been developed to facilitate the utilisation, viewing and processing of ESA GOMOS, MIPAS and SCIAMACHY data products. The purpose of the BEAT is not to duplicate existing commercial packages, but to complement them with new functions.

The main components of the BEAT are:

- support all Level-1b, Level-2, and auxiliary product formats for the Envisat atmospheric instruments (60 different product formats)
- fast and easy access to the data products using the EAT library from the C language, and from IDL and Matlab (e.g. from IDL and Matlab, only three calls are needed to get data out of a product file)
- selection of product files according to time and/or geolocation; finding of co-located data
- data import and export functionality to and from ASCII, binary, HDF-4, HDF-EOS, HDF5, HDF5-EOS
- data ingestion of GOME and TOMS products
- operations on spectral and spatial data: interpolation, resampling, gridding, binning, etc.
- microwindow operations (e.g. selecting a spectral range)
- integration of instrument-specific tools (e.g. GOMECAL, a new GOME calibration

tool)
- visualisation and analysis tool (VISAN)

Architectural Design Goals

The primary design features of BEAT are:
- An open source design enabling the user community to improve its quality.
- Portability through platform-independent design for use on major operating systems (e.g. SunOS, Solaris, Linux, and MS Windows).
- High-performance and flexibility.

A basic version of BEAT called will be released in mid December 2002.
More information is available from the envisat web site at http://envisat.esa.int/beat

1.3 Further reading

References

Papers and documents
Ref 1.1
DASA, “In-Flight Calibration Plan, PO-PL-DAS-MP-0031, Issue 2A, June 1997.

Ref 1.2
Bell R. J., “Introductory Fourier Transform Spectroscopy, Academic Press (1972)

Ref 1.3
Blom C.E. , M. Hopfner and C. Weddington, "Correction of Phase Anomalies of Atmopshjeric Emission Spectra by the Double Differencing Method", Appl. Opt., 35, (2649), 1996

Ref 1.4
Blom C.E. , H. Fischer, N. Glatthor, T. Guide, M. Hopfner and Ch. Piesch, "Spatial and Temporal variation of CIONO2, HNO3 and O3 in Arctic Winter 1992/93 as obtained by Airborne Infrared Emission Spectroscopy", J. Geophys. Res., 100, (9101), 1995.

Ref 1.5
Blom C. E., H. Fischer, N. Glatthor, T. Gulde and H. Hopfner, "Airborne Measurements during the European Arctic Stratospheric Ozone Experiment. Column Amounts of HNO3 and O3 derived from FTIR Emission Sounding", Geophys Res. Lett., 21, 1351, 1994.

Ref 1.6
Bomem, "Algorithm Technical Baseline Document for MIPAS Level 1b Processing",

PO-TN-BOM-GS-0012, September 1998.

Ref 1.7
Bomem, “MIPAS Detector Non-linearity Correction Critical Revision, PO-RP-BOM-GS-0017, Issue 1, May 1998

Ref 1.8
Bomem, "MIPAS In-flight Spectral Calibration and ILS retrieval", PO-TN-BOM-GS-0006, Issue 2A, June 1997.

Ref 1.9
Bomem, “Non-Linearity Characterization and Correction, PO-TN-BOM-MP-0019, Issue 1A, September 1996.

Ref 1.10
Camy-Peret C., J. M. Flaud, A. Perrin, C.P. Rinsland, A. Goldman and F. Murcray, "Stratospheric N2O5 CH4 and N2O profiles from IR solar occultation Spectra", J. Atmos Chem., 16, (31), 1993.

Carli B., B.M.Dinelli, P.Raspollini, M.Ridolfi, 'The problem of discrete representation and resampling in the case of limb-sounding measurements', accepted for publication in Applied Optics, (October 2000).

Ref 1.11
Carli B., M. Ridolfi, P. Raspollini, B. M. Dinelli, A. Dudhia, G. Echle, 'Study of the retrieval of atmospheric trace gas profiles from infrared spectra,' Final Report of ESA Study 12055-96-NL-CN (1998).

Ref 1.12
Carlotti M., B.M.Dinelli, P.Raspollini, M.Ridolfi, 'Geo-fit approach to the analysis of satellite limb-scanning measurements' submitted to Applied Optics, (Dec 2000).

Ref 1.13
Carlotti M., and M. Ridolfi, “Derivation of temperature and pressure from submillimetric limb observations, Applied Optics 38, 2398-2409 (1999).

Ref 1.14
Carlotti M. and B. Carli, “Approach to the design and data analysis of a limb-scanning experiment, Applied Optics, 33, 3237-3249 (1994).

Ref 1.15
Carlotti M., “Global-fit approach to the analysis of limb-scanning atmospheric measurements, Applied Optics 27, 3250-3254 (1988).

Ref 1.16
Chapman S., "A theory of the uper atmopsheric ozone", Mem. Roy. Meteor. Soc., 3, 103, 1930.

Ref 1.17
Clarmann T. v., A. Dudhia, G. Echle, J.-M. Flaud, C. Harrold, B. Kerridge, K. Koutoulaki, A. Linden, M. Lopez-Puertas, M. A. Lopez-Valverde, F.J. Martin-Torres, J. Reburn, J. Remedios, C. D. Rodgers, R. Siddans, R. J. Wells and G. Zaragoza, " Study on the Simulation of Atmospheric Infrared Spectra, Final Report of ESA Contract Number 12054/96/NL/CN (1998).

Ref 1.18
Clarmann T. v., and G. Echle, "Selection of Optimized Microwindows for Atmospheric Spectroscopy, Applied Optics 37, 7661-7669 (1998).

Ref 1.19
Clarmann T. v., A. Linden, G. Echle, A. Wegner, H. Fischer, M. Lopez-Puertas, in Proceedings of IRS '96: 'Current Problems in Atmospheric Radiation', Smith and Stamnes, ed. ISBN 0-937194-39-5 (Deepak Publishing, 1997). p. 557-560.

Ref 1.20
Clarmann T. v., A. Linden, H. Oelhaf, H. Fisher, F. Friedl-Vallon, C. Piesch, M. Seefeldner, W. Volker, R. Bauer, A. Engel, and U. Schmidt, "Determination of the Stratopsheric Organic Chlorine Budget in the Spring Arctic Vortex from MIPAS-B Limb Emission Spectra and Air Smapling Experiments", J. Geophys. Res., 100, 13979, 1995.

Ref 1.21
Clarmann T. v., H. Fisher, F. Friedl-Vallon, A. Linden, H. Oelhaf, C. Piesch, M. Seefeldner and W. Volker, "Retrieval of Stratospheric O3, HNO3, and ClONO2 Prfiles from 1992 MIPAS_B Limb Emission Spectra: Method, Results and Error Analysis", J. Geophys. Res., 98, 20495, 1994.

Ref 1.22
Clarmann T. v., H. Fischer, and H. Oelhaf, "Instabilities in retrieval of atmospheric trace gas profiles caused by the use of atmospheric level models, Applied Optics, 30, 2924-2925 (1991).

Ref 1.23
Clough, S. A., F. X. Kneizys and R. W. Davies, 'Line shape and the water vapor continuum', Atmospheric Research, 23 229-241 (1989).

Ref 1.24
Delbouille L. and G. Roland, "Assessement of finite Field-of-View effects on MIPAS ILS and review of resolution enhancement techniques, Answer to ESA NTO/ME/1573.

Ref 1.25
Department of Defense, Military Standard 2401, World Geodetic System (WGS), 1994.

Ref 1.26
Dornier, "MIPAS Assumptions on the Ground Segment", PO-RS-DOR-SY-0029, May 1996.

Ref 1.27

Echle G., T. von Clarmann, A. Dudhia, J.-M. Flaud, B. Funke, N. Glatthor, B.J. Kerridge, M. Lpez-Puertas, F.J. Martin-Torres , and G.P. Stiller, Optimized spectral microwindows for MIPAS-ENVISAT data analysis, App. Opt., Vol. 39, 5531-5540, 2000.

Ref 1.28
Echle G., T. v. Clarmann, A. Dudhia, M. Lopez-Puertas, F. J. Martin-Torres, B. Kerridge, and J.-M. Flaud, " Spectral microwindows for MIPAS-ENVISAT data analysis, in Proceedings of the European Symposium on Atmospheric Measurements from Space, ESA Earth Science Division, ed. (European Space Agency - Estec, The Netherlands, 1999). Vol. 2, p. 481-485.

Ref 1.29
Edwards D. P., "High Level algorithm definition document of the MIPAS Reference Forward Model, ESA Report PO-TN-OXF-GS-0004 (1997).

Ref 1.30
Edwards D. P. "GENLN2: A general line-by-line atmospheric transmittance and radiance model. Version 3.0 description and users guide, Report NCAR/TN-367+STR, Natl.Cent.for Atmos.Res., Boulder, Colo., (1992).

Ref 1.31
Edwards D. P. and L. L. Strow, "Spectral line shape considerations for limb temperature sounders, J. Geophys. Res. 96, 20859-20868 (1991)

Ref 1.32
Edlen B., Metrologia, 2, 12, (1966).

Ref 1.33
ESA, "ENVISAT MIPAS: An Instrument for Atmospheric Chemistry and Climate Research", SP-1229, March 2000.

Ref 1.34
ESA, "Limb Sounding techniques for Environmental Monitoring in the Nineties", ESA Report SP-1140, 1992.

Ref 1.35
Farmer C.B., O.F. Raper and F.G. O'Callaghan, Final Report on the First Flight of the ATMOS Instrument during the Spacelab 8 Mission, Spacelab 3 Mission and JPL Publication 97-82, 1987.

Ref 1.36
Fischer, H., Oelhaf, H., Remote Sensing of vertical profiles of atmospheric trace constituents with MIPAS limb emission spectrometers, Applied Optics, Vol. 35, Page 2787-2796, 1996.

Ref 1.37
Fisher H., "Remote Sensing of Atmospheric Trace Gases", Interdisc. Sci. Rev., 10, (185), 1993.

Ref 1.38
Fisher H., "Remote Sensing of Trace Constituents using Fourier Transform Spectrometry", Ber. Bunsenges Phy. Chem., 96, (306), 1992.

Ref 1.39
Friedl-Vallon, F., et al., Design and characterization of the balloon-borne Michelson Interferometer for Passive Atmospheric Sounding (MIPAS-B), to be submitted to Appl. Optics, 2001.

Ref 1.40
Friedl-Vallon, H. Fisher, T. von Clarmann, C. Frietzsche, H. Oelhaf, C. Piesch, M. Seefeldner, D. Rabus and W. Volker, Limb Emission Spectroscopy with the ballon-borne Michelson Interferometer for Passive Atmospheric Sounding (MIPAS)", Optiocal methods in Atmospheric Chemistry, SPIE 1715, 441, 1992.

Ref 1.41
Gill P. E., W. Murray, M. H. Wright, “Practical Optimization, Academic Press, Inc (1981).

Ref 1.42
Goldman A., R. S. Saunders, “Analysis of atmospheric infrared spectra for altitude distribution of atmospheric trace constituents -I: Method of analysis, J. Quant. Spectrosc. Radiat. Transfer 21, 155-162 (1979).

Ref 1.43
Guld T., Ch. Piesch, C.E. Blom, H. Fisher, F. Ferg, and G. Wildgruber, "The Airborne MIPAS Infrared Emission Experiment", Proc. of the Int. Airborne Remote Sensing Conference, ERIM, Vol. II, 301, 1994.

Ref 1.44
Hopfner M., C. Blom, T. Blumenstock, H. Fischer, T. Guide, "Evidence for the Removal of Gaseous HNO3 inside the Arctic Polar Vortex in January 1992", Geophys. Res. Lett., 23, 149, 1996.

Ref 1.45
Houghton J. T., “The Physics of Atmospheres , 2nd Ed, CUP, Cambridge, (1986).

Ref 1.46
Kalman R. E., “Algebraic aspects of the generalized inverse of a rectangular matrix, in Proceedings of Advanced Seminar on Generalized Inverse and Applications, M.Z.Nashed, ed. (Academic, San Diego, Calif., 1976). p. 111-124.

Ref 1.47
Levenberg K., “A method for the solution of certain problems in least squares, Quart. Appl. Math. 2, 164-168 (1944).

Ref 1.48
Lopez-Puertas M., M. A. Lopez-Valverde, F. J. Martin-Torres, G. Zaragoza, A. Dudhia, T. v.

Clarmann, B. J. Kerridge, K. Koutoulaki, and J.-M. Flaud, “Non-LTE studies for the MIPAS instrument, in in Proceedings of the European Symposium on Atmospheric Measurements from Space, ESA Earth Science Division, ed. (European Space Agency - Estec, The Netherlands, 1999). Vol. 1, p. 257-264.

Ref 1.49
Lpez-Puertas, M., G. Zaragoza, M. A. Lpez-Valverde, , F.J. Martin-Torres, G.M. Shved, R.O. Manuilova, A.A. Kutepov, O. Gusev, T.v. Clarmann, A. Linden, G. Stiller, A. Wegner, H. Oelhaf, D.P. Edwards, and J.- M. Flaud, Non-local thermodynamic equilibrium limb radiances for the MIPAS instrument on Envisat-1, J. Quant. Spectros. Radiat. Transfer, Vol. 59, 377-403, 1998.

Ref 1.50
Manuilova, R.O., O.A. Gusev, A.A. Kutepov, T. von Clarmann, H. Oelhaf, G.P. Stiller, A. Wegner, M. Lpez Puertas, F.J. Martin-Torres , G. Zaragoza, and J.M. Flaud, Modelling of non-LTE limb radiance spectra of IR ozone bands for the MIPAS space experiment, J. Quant. Spectros. Radiat. Transfer, Vol. 59, 405-422, 1998.

Ref 1.51
Marquardt D. W., “An Algorithm for the Least-Squares Estimation of NonLinear Parameters, J. Soc. Appl. Math. 11, 431 (1963).

Ref 1.52
McKee T. B., R. I. Whitman, J. J. Lambiotte jr., “A technique to infer atmospheric water-vapor mixing ratio from measured horizon radiance profiles, NASA TN D-5252 (1969).

Ref 1.53
Menke W., “Geophysical Data Analysis: Discrete Inverse Theory, Academic, San Diego, Calif. (1984).

Ref 1.54
Norton R. H., R.Beer, “New apodizing functions for Fourier spectrometry, J. Opt. Soc. Am., 66, 259, (1976), and errata corrige J. Opt. Soc. Am., 67, 419, (1977).

Ref 1.55
Oelhaf H., T. von Clarmann, H. Fisher, F. Friedl-Vallon, C. Fritzsche, A. Linden, C. Piesch, M. Seefledner, M. Wolfel, "Stratospheric ClONO2, HNO3 and O3 Profiles Inside the Arctic Vortex from MIPAS-B Limb Emission Spectyra during EASOE 1992", Geophys. Res. Lett., 21, 1263, 1994.

Ref 1.56
Press W. H., S. A. Teukolsky, W. T. Wetterling, B. P. Flannerly: “Numerical Recipes in Fortran, Second Edition Cambridge University Press (1992).

Ref 1.57
Raspollini P. and M.Ridolfi, 'Mapping of Temperature and Line-of-Sight Errors in Constituent Retrievals for MIPAS / ENVISAT Measurements', Atmospheric Environment,

Vol. 34, Nos. 29 “ 30, p. 5329 “ 5336 (2000).

Ref 1.58
Ridolfi M., B.Carli, M.Carlotti, T.v.Clarmann, B.M.Dinelli, A.Dudhia, J.-M.Flaud, M.Hoepfner, P.E.Morris, P.Raspollini, G.Stiller, R.J.Wells, 'Optimized forward model and retrieval scheme for MIPAS near-real-time data processing' Appl. Optics, Vol. 39, No. 8, p. 1323 “ 1340 (March 2000).

Ref 1.59
Rodgers C. D., “Retrieval of Atmospheric Temperature and Composition From Remote Measurements of Thermal Radiation, Reviews of Geophysics and Space Physics, 14, 609 (1976).

Ref 1.60
Rosenkranz P. W., “Shape of the 5 mm oxygen band in the atmosphere, IEEE Trans. Antennas Prop.AP-23, 498-506 (1975)

Ref 1.61
Sivia D. S., 'Data analysis. A Bayesian tutorial', Clarendon Press - Oxford (1998).

Ref 1.62
Strow L. L., H. E. Motteler, R.G. Benson, S.E. Hannon and S. De Souza-Machado, “Fast Computation of monochromatic infrared atmospheric transmittances using compressed look-up tables, J. Quant. Spectrosc. Radiat. Transfer, 59, 481-493, (1998).

Ref 1.63
Tikhonov A. N. and V. Y. Arsenin, “Solutions of ill-posed problems, V. H. Winston & Sons (1977).

Ref 1.64
Trieschmann, O., Weddigen, Ch., Thermal Emission from Dielectric Beamsplitters in Michelson Interferometers: A Schematic Analysis, Applied Optics, Vol. 39, pp. 5834-5842, 2000.

Ref 1.65
Twomey S., “Introduction to the mathematics of inversion in remote sensing and indirect measurements, Elsevier Scientific Publishing Company (1977).

Ref 1.66
Wetzel G., T. von Clarmann, H. Oelhaf and H. Fisher, "Vertical Profiles of N2O5 along with CH4, N2O and H2O in the Later Arctic Winter Retrieved from MIPAS-B Limb Emission Measurements", J. Geophys. res., 100,. 23173, 1995.
Conference proceedings
Ref 1.67
Battistini E., B.M. Dinelli, M. Carlotti B.Carli, P.Raspollini, M.Ridolfi, F. Friedl-Vallon, M. Hoepfner, H.Oel-haf, O. Trieschmann, G. Wetzel, 'Performances of MIPAS/ENVISAT Level 2 inversion algorithm with data measured by the balloon instrument MIPAS-B', International Radiation Symposium (IRS 2000), Saint - Petersburg State University, St.

Petersburg, Russia, 24 - 29 July 2000.

Ref 1.68
Battistini, E., B.M. Dinelli, M. Carlotti, B.Carli, P.Raspollini, M.Ridolfi, F. Friedl-Vallon, M. Hoepfner, H. Oelhaf, O. Trieschmann, G. Wetzel,

Performances of MIPAS/ENVISAT Level 2 inversion algorithm with data measured by the balloon instrument MIPAS-B, Proc. Int. radiation Symposium 2000, Deepak Publ., in press, 2001.

Ref 1.69
Bennett, V. L., A. Dudhia and C. D. Rodgers, 'Microwindow Selection for MIPAS using Information Content', ESAMS'99 Proceedings, 18-22 January 1999, Noordwijk, NL.

Ref 1.70
Carli B., E.Battistini, M.Carlotti, T.v.Clarmann, B.M.Dinelli, A.Dudhia, G.Echle, J.-M.Flaud, A.Gignoli, M.Hoepfner, E.Lunedei, F.Mencaraglia, P.E.Morris, P.Raspollini, M.Ridolfi, G.Stiller, A.Vigiani, R.J.Wells, 'MIPAS Level 2 Algorithm', European Symposium on Atmospheric Measurements from Space, ESTEC Noordwijk, The Netherlands, 18-22 January 1999.

Ref 1.71
Carlotti M., B.M.Dinelli, P.Raspollini, M.Ridolfi, 'Geo-fit approach to the analysis of satellite limb-scanning measurements', OSA topical meeting on Fourier Transform Spectroscopy and optical remote sensing of the atmosphere, Coeur d'Alene, Idaho (USA), (5 " 8 February 2001).

Ref 1.72
Clarmann T. v., M.Ridolfi et al., 'Advanced MIPAS-Level-2 Data Analysis (AMIL2DA)', ERS " ENVISAT symposium, 16 " 20 October 2000 Gothenburg, Sweden (poster presentation).

Ref 1.73
Friedl-Vallon, F, H. Oelhaf, M. Hopfner, A. Kleinert, A. Lengel, G. Maucher, H. Nordmeyer, O. Trieschmann, and G. Wetzel, Pre-launch assessment of MIPAS/ENVISAT near real-time Level 2 algorithm with data obtained from the balloon-borne MIPAS-B instrument, Part 1 - Instrument characterisation, Level 1b data processing and consistency checks., 9th int. Workshop on Atmospheric Science from Space using Fourier Transform Spectroscopy, Kyoto, Japan, 2000.

Ref 1.74
Friedl-Vallon, F., Maucher, G., Oelhaf, H., Trieschmann, O., Wetzel, G., Fischer, H., The balloon-borne Michelson interferometer for passive atmospheric sounding (MIPAS-B2). Instrument and results, Larer, A.M., (Hrsg.), Optical Spectroscopic Techniques and Instrumentation for Atmospheric and Space Research III: Proc. Of SPIE's 44th Annual Meeting, Denver, Colorado, July 19-21, 1999, SPIE Proceedings Series 3756, S. 9-16, Bellingham, Washington, 1999.

Ref 1.75
Friedl-Vallon, F., Kleinert, A., Trieschmann, O., Oelhaf, H., and Wetzel, G., Radiometric calibration of MIPAS-B2 spectra, 8th int. Workshop on Atmospheric Science from Space using Fourier Transform Spectroscopy, Meteo-France, Toulouse,1998.

Ref 1.76
Hoepfner M., H.Kemnitzer, G.Stiller, B.Carli, A.Gignoli, P.Raspollini, M.Ridolfi, M.Carlotti, A.Vigiani, J.- M.Flaud, 'An optimised forward and retrieval model for MIPAS near real-time data evaluation', 7th Interna-tional Workshop on Atmospheric Science from Space using Fourier Transform Spectrometry, Oberpfaffen-hofen, Munich, Germany (poster presentation), 12 " 14 May 1997.

Ref 1.77
Jay, V.L., A.Dudhia, C.D.Rodgers, H. Oelhaf, O. Trieschmann, Channel selection for high-resolution remote sounding instruments, Proc. Int. Radiation Symposium 2000, Deepak Publ., in press, 2001.

Ref 1.78
Kleinert, A., Trieschmann, O., Quality assessment of the statistical phase determination approach and implication on the calibration accuracy for an emission spectrometer, 9th int. Workshop on Atmospheric Science from Space using Fourier Transform Spectroscopy, Kyoto, Japan, 2000.

Ref 1.79
Kleinert, A., Friedl-Vallon, F., Characterisation of the non-liearity of the MIPAS-B2 detector system, 8th int. Workshop on Atmospheric Science from Space using Fourier Transform Spectroscopy, Météoo-France, Toulouse,1998.

Ref 1.80
Lengel, A., Multiple-line deconvolution of MIPAS-B2 high altitude spectra as a method to retrieve the ILS from flight data, 5th Workshop on Infrared Emission Measurements by FTIR, Quebec, Feb. 9-11, 2000.

Ref 1.81
Lpez-Puertas, M., M.A. Lpez-Valverde, F.J. Martin-Torres, G. Zaragoza, A. Dudhia, T. von Clarmann, B.J. Kerridge, K. Koutoulaki, and J.-M. Flaud, Non-LTE Studies for the MIPAS Instrument, Atmospheric Mea-surements from Space, ESA-ESTEC WPP-161, Vol. 1, 257-264, Noordwijk, The Netherlands, 18-22 January 1999.

Ref 1.82
Nett H., J.Langen, G.Perron, M.Ridolfi, S.Casadio, 'MIPAS Calibration and Processor Validation', ERS " ENVISAT symposium, Gothenburg, Sweden, 16 " 20 October 2000.

Ref 1.83
Nett H., B.Carli, M.Carlotti, A.Dudhia, H.Fisher, J.-M.Flaud, J.Langen, G.Perron, P.Raspollini, M.Ridolfi, 'MIPAS Ground Processor and Data Products', IGARSS'99 Remote Sensing of the System Earth, - A Chal-lenge for the 21st Century, Hamburg (Germany), 28

June - 2 July 1999.

Ref 1.84
Oelhaf H., G. Wetzel, M. Hopfner, F. Friedl-Vallon, N. Glatthor, G. Maucher, G. Stiller, O. Trieschmann, Th. von Clarmann, M. Birk, G. Wagner, Interconsistency checks of ClONO2 retrievals from MIPAS-B spectra by using different bands and spectroscopic parameter, Proc. Int. Radiation Symposium 2000, Deepak Publ., in press, 2001.

Ref 1.85
Oelhaf H., A. Engel, H. Fischer, D. McKenna, C. Schiller, U. Schmidt, F. Stroh, Validation of trace gas measurements of the ENVISAT instruments MIPAS, GOMOS and SCIAMACHY using in-situ and remote sensing balloon borne techniques, ERS-ENVISAT Symposium, Gothenburg, 16-20 October 2000

Ref 1.86
Oelhaf, H., H. Fischer, G. Wetzel, M. Stowasser, F. Friedl-Vallon, G. Maucher, O. Trieschmann, R. Ruhnke, and Y. Sasano, Intercomparison of ILAS/ADEOS with MIPAS-B measurements in late March 1997, SPIE Vol. 3501, 92-100, 1998.

Ref 1.87
Oelhaf, H., G. Wetzel, M. Stowasser, F. Friedl-Vallon, G. Maucher, O. Trieschmann, R. Ruhnke, H. Fischer and Y. Sasano, Validation of ILAS on ADEOS with MIPAS-B2 and lessons learnt for the validation of ENVISAT instruments, Proc. 8th Intern. Workshop on Atmospheric Science from Space using Fourier Transform Spectroscopy, pp. 241-249, Toulouse, 16-18 Nov. 1998.

Ref 1.88
Oelhaf, H., et al., Remote Sensing of the Arctic stratosphere with the new balloon-borne MIPAS-B2 instrument, in Polar stratospheric ozone, Proc. 3rd European Workshop 18 to 22 September 1995, Schliersee, Bavaria, Germany, J. A. Pyle, N. R. P. Harris, and G. T. Amanatidis eds., European Commission, pp. 270-275, 1996a.

Ref 1.89
Raspollini P., M.Hoepfner, M.Ridolfi, 'Performances of the near real-time code for MIPAS data analysis', Pro-ceedings of EUROPTO, Satellite Remote Sensing of Clouds and Atmosphere IV, Vol. 3867, pag. 177-186, September 1999.

Ref 1.90
Raspollini P., M.Ridolfi, M.Hoepfner, 'Performances of the near real-time code for MIPAS data analysis', pub-lished in the proceedings of Nato Advanced Study Institute (ASI) 'Chemistry and radiation changes in the ozone layer', Kolimpari, Crete, Greece, 15 “ 24 May 1999.

Ref 1.91
Raspollini P., M.Ridolfi, B.Carli, M.Carlotti, E.Battistini, M.Hoepfner, G.Stiller, A.Dudhia, P.E.Morris, R.J.Wells, J.-M.Flaud, 'An optimised forward and retrieval model for MIPAS near real time data processing', Proceedings of the advanced study course on “Interactions between Chemical Compounds, the Ozone Layer and UV-B fluxes", Halkidiki, Greece,

October 1998.

Ref 1.92
Raspollini P., B.Carli, M.Carlotti, A.Dudhia, B.M.Dinelli, J.-M.Flaud, M.Hoepfner, P.E.Morris, M.Ridolfi, G.P.Stiller, R.J.Wells: ' Optimization and performance of the retrieval algorithm for MIPAS near-real-time data processing', 8th International Workshop on Atmospheric Science from Space using Fourier Transform Spec-trometry, Météoo France, Toulouse, France 16 - 18 Nov. 1998.

Ref 1.93
Ridolfi M. E.Battistini, B.Carli, M.Carlotti, B.M.Dinelli, P.Raspollini, H. Oelhaf, F. Friedl-Vallon, M. Hoe-pfner, A. Kleinert, A. Lengel, G. Maucher, H. Nordmeyer, O. Trieschmann, G. Wetzel, 'Pre-launch assessment of MIPAS/ENVISAT near real-time Level 2 algorithm with data obtained from the balloon borne MIPAS-B instrument: Part I: Instrument characterization, Level 1b data processing and consistency checks. Part II: Level 2 data analysis, results and performances', 9th International Workshop on Atmospheric Science from Space using Fourier Transform Spectroscopy, Kyoto (Japan), 22 " 24 May 2000.

Ref 1.94
Ridolfi M., B.Carli, M.Carlotti, T.v.Clarmann, B.M.Dinelli, A.Dudhia, J.-M.Flaud, M.Hoepfner, P.E.Morris, P.Raspollini, G.Stiller, R.J.Wells, 'An optimized forward model and retrieval scheme for MIPAS near-real-time data processing', ERS " ENVISAT symposium, Gothenburg, Sweden, 16 " 20 October 2000.

Ref 1.95
Ridolfi M. M.Hoepfner, P.Raspollini, 'Expected Performances of Near Real Time MIPAS Data Analysis' Fifth European Workshop on Stratospheric Ozone, Saint Jean de Luz (France). The paper has been published by the European Commission in the Air Pollution Research Report n. 73, 27 Sept. " 01 Oct. 1999.

Ref 1.96
Ridolfi M., M.Hoepfner, P.Raspollini: "Implementation of the Voigt line-shape calculation in the forward model for operational MIPAS retrievals", 13th International Conference on Spectral Line Shapes, Firenze (poster pre-sentation), June 1996.

Ref 1.97
Ridolfi M., B.Carli, M.Carlotti, A.Dudhia, J.-M.Flaud, M.Hoepfner, P.E.Morris, P.Raspollini, G.P.Stiller, R.J.Wells: 'An optimized forward and retrieval model for MIPAS near-real-time data processing', SPIE Vol. 3501, pag.170 Optical Remote Sensing of the Atmosphere and Clouds (1998). Oral presentation of the paper by M.Ridolfi at the first International Asia-Pacific Symposium on Remote Sensing of the Atmosphere, Environ-ment, and Space, Beijing, China, 14 - 17 September 1998.

1.4 Image gallery

This section presents examples of simulated MIPAS data.
Level 0 interferogram

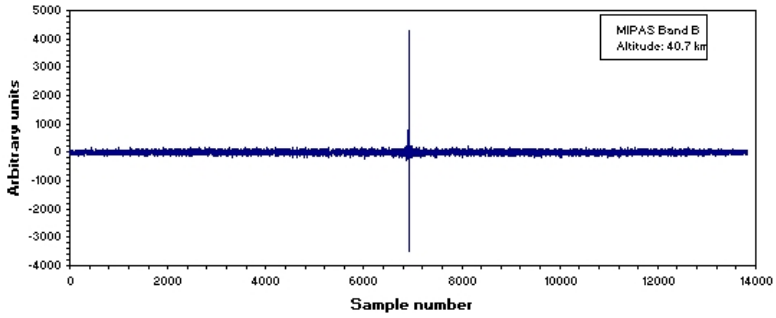

Figure 1.10 Interferogram (MIPAS Band B, target at 40.7 km of altitude)

Level 1b Calibrated radiance spectrum

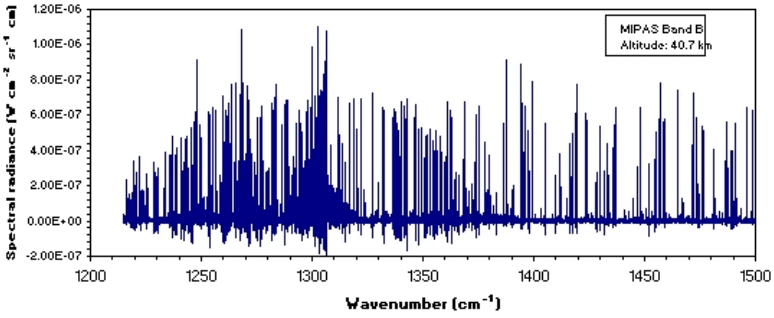

Figure 1.11 Spectrum (MIPAS Band B, target at 40.7 km of altitude)

Level 2 Retrieved vertical profile

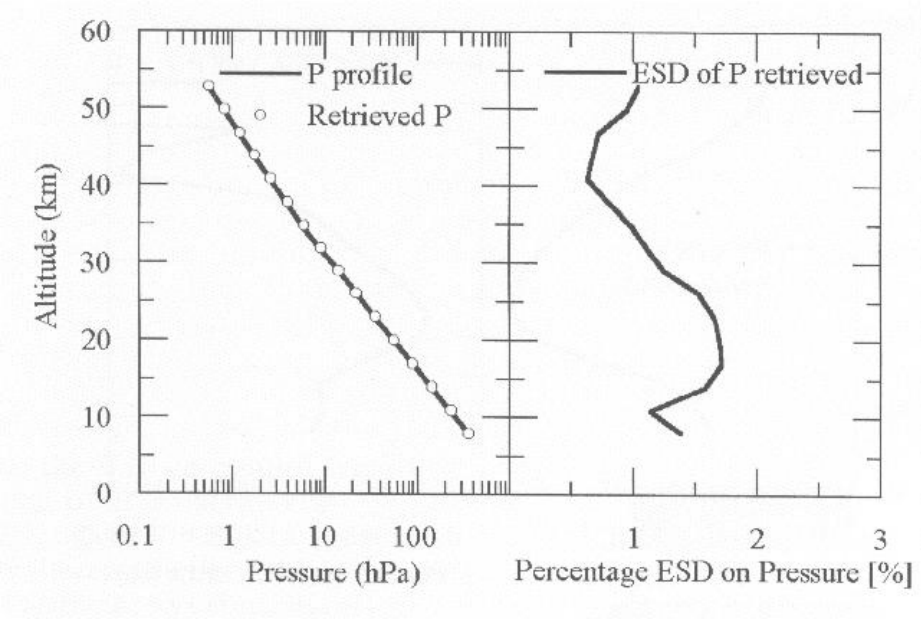

Figure 1.12 Simulation of vertical profile of pressure (left) and estimated standard deviation (right)

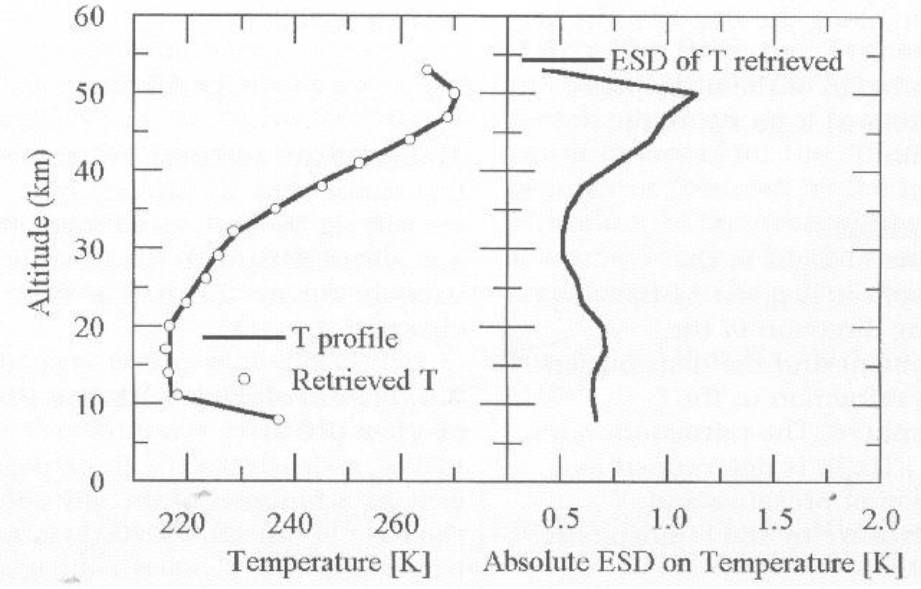

Figure 1.13 Simulation of vertical profile of temperature (left) and estimated standard deviation (right)

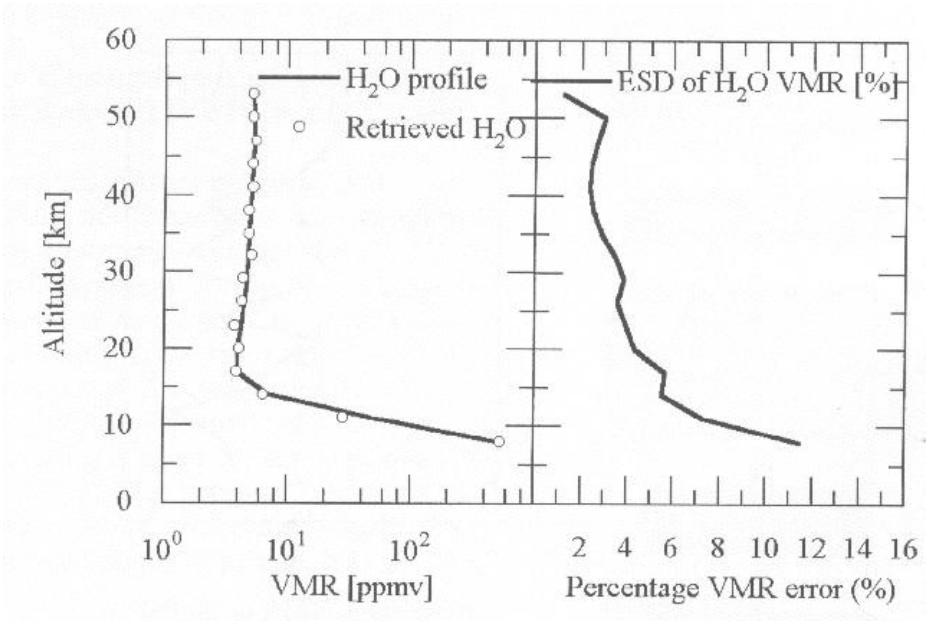

Figure 1.14 Simulation of vertical profile of volume mixing ratio of water vapor (left) and estimated error (right)

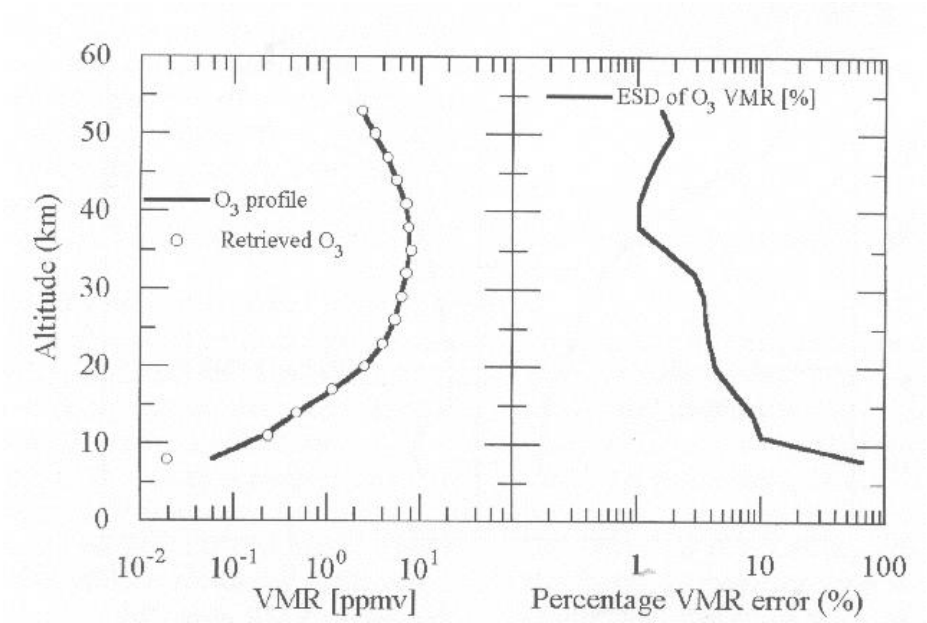

Figure 1.15 Simulation of vertical profile of volume mixing ratio of ozone (left) and estimated error (right)

Chapter 2

MIPAS Products and Algorithms

2.1 Introduction

MIPAS is a Fourier transform spectrometer. It is an interferometric instrument that measures interferograms. The interferograms have to be transformed in calibrated spectra of atmospheric spectral radiance. The spectra can then be fed to various inversion models to compute vertical profiles of atmospheric molecules. From the most raw interferograms to the final atmospheric profiles, there is series of necessary processing steps. These steps are described in the following sections.

The processing is separated in two major parts: space segment and ground segment processing. Space segment is performed in space, it includes generation of the data by the instrument and its subsystems, onboard processing, transmission to the spacecraft and transmission to the ground. Ground segment includes reception and decoding of the data

and processing into higher level data products. The ground segment is divided into two major processing phases: level 1b and level 2 processing. The goal of level 1b processing is to decode the instrument source packets and transform them into calibrated and geolocated spectra of atmospheric radiance. The goal of the level 2 processing is to transform the spectra generated by the level 1 b processing into vertical profiles of concentration of various atmospheric molecules.

The following flowchart illustrates the flow of data processing:

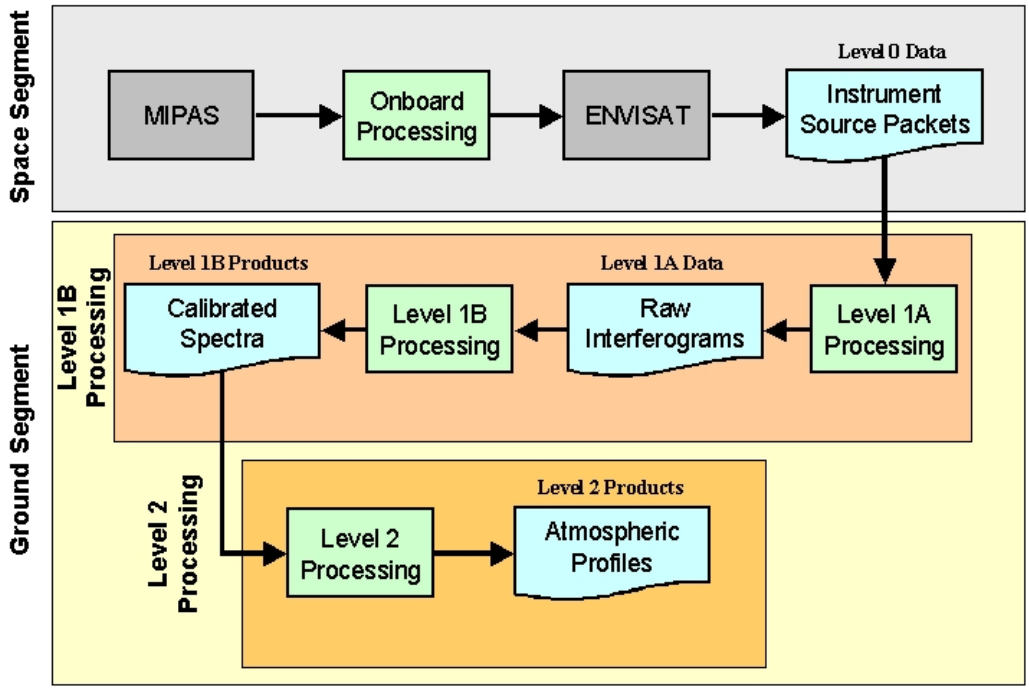

Figure 2.1 Data processing flowchart for MIPAS.

2.2 Definition and convention

2.3 Product evolution history

2.4 Algorithms and products

2.4.1 Level 0 products and algorithms

Level 0 data is the data stream received directly from the instrument without any further processing. Since MIPAS performs some onboard processing, this does not mean that Level 0 data is free of processing. The interferogram recorded by the detectors undergo a series of modification before being downlinked to the ground station. The main processing steps are:

- filtering and decimation 2.4.1.1.
- word length reduction 2.4.1.2.
- data compression
- formatting into instrument source packets

2.4.1.1 Decimation and filtering

In order to lower the size of the signals to be transmitted, measured interferograms are filtered and decimated. This operation is part of the onboard processing.

Neglecting the dispersion phenomenon inducing a non-null phase, an observed interferogram is basically a real and symmetrical function. The symmetry is about ZPD and, by extension about every multiple of MPD.

The Fourier transform of such an interferogram is a real and symmetrical spectrum with symmetry about every multiple of the sampling frequency. In other words, the full spectrum will show on one half the true physical spectrum and on the other half the image of this spectrum. Depending on the convention, this second half may be displayed as negative frequencies or as frequencies above the sampling frequency divide by 2, as displayed in the figure below.

For a given sampling rate of s_s (equal to 7692 cm^{-1} for MIPAS, corresponding to a laser operating at 1300 nm), the Nyquist sampling theorem states that this sampling frequency

defines a fixed spectral band of maximum width $s_s / 2$. This spectral band is quite large and can be reduced. The principle of data compression is to sample at a lower rate by decimating the interferogram (taking one point out of n) already sampled by the metrology laser system. The result is a reduced number of interferogram data points that permits a smaller data throughput.

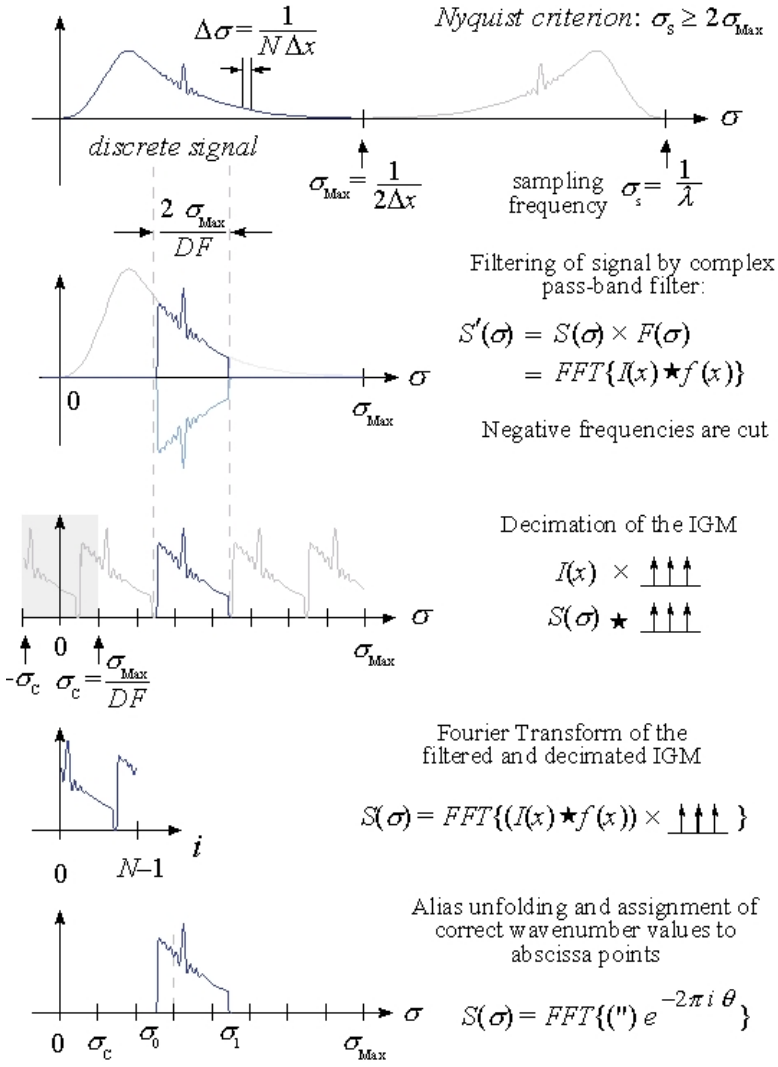

Figure 2.2 Filtering and decimation scheme

When a spectrum is band limited between s_0 and s_1 , the sampling frequency can be reduced up to $2s_1$ without any information loss as stated by the Nyquist sampling theorem. Reducing the sampling frequency further can produce spectral overlap that disturbs the interesting

information (aliasing effect). However, since there is a useless spectral region from 0 to s_o , it is possible to sample at a lower rate than $2s_1$ and still keep all the information. For a real filtered signal, where both the desired physical band and its image are present, the lowest possible sampling frequency preserving the information is twice the spectral bandwidth .

For MIPAS, complex filters have been devised in such a way that it has no image passband, by defining its imaginary part anti-symmetrical such that it produces a compensating negative image. After such a filtering, the only undersampling condition is:

$$s_s = s_1 - s_o \qquad \text{eq 2.1}$$

Thus, the decimation factor can be two times larger after complex filtering. The integer ratio of the initial sampling frequency to the new one is called the decimation factor, noted DF. Since the folding frequencies are not restricted to be out of the band of interest, there is no additional restriction on the decimation factor. It is then possible to better optimize the decimation factor. This is where a gain can be made with respect to data reduction.

The shape of the apodisation function applied to the filtering impulse response (FIR) is critical. It must produce sufficient smoothing of the filter, but must avoid widening it to the point of reducing too much the effective bandwidth of the pass bands and the possible data compression. MIPAS FIR filters respect these criteria and are defined over 256 taps using 16-bit coefficients. The isolation of the various MIPAS filters range from 65 to 87 dB.

The processing needed for the proper recovery of the wavenumber axis for each spectrum consists of computing a Fourier transform of the decimated signal, unfolding of the spectral axis (for cases where spectral limits do not exactly correspond to an integer factor of the band width), followed by axis limit identification. Further details about this procedure can be found in the ATBD Ref. [1.6].

2.4.1.2 Word length reduction

During the formatting of the data stream by the SPE, the word length (or bit size) of the interferogram is reduced on a fraction of the interferogram. Due to the typical shape of an interferogram (see the figure below), the full dynamic range (16 bits) is used only near the ZPD. Far from the ZPD, only a small fraction of the ADC range is used. The regions far from the ZPD, on both side of the interferogram, can thus be coded using a smaller number of bits without loosing any information. The size of the data transmitted is thus significantly reduced.

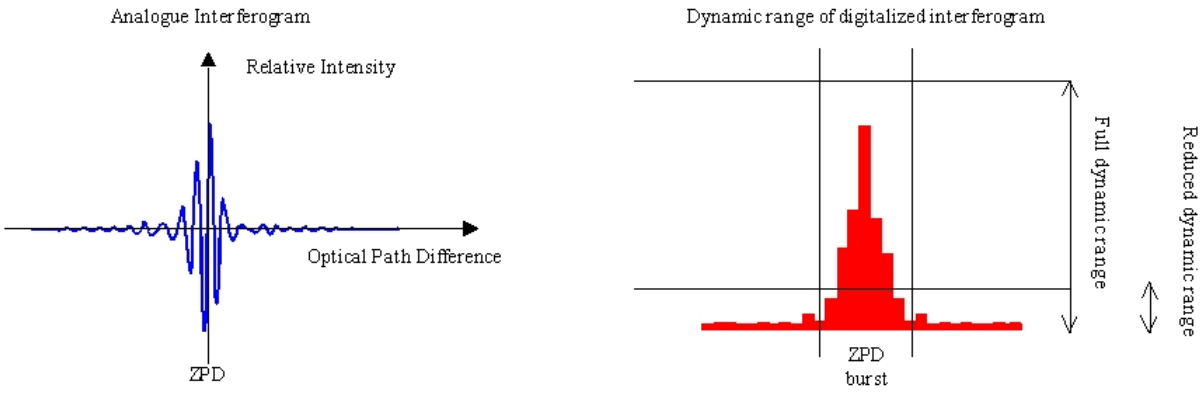

Figure 2.3 Typical analogue (left) and digitalised (right) interferograms.

2.4.1.3 Data compression

2.4.1.4 Formatting into instrument source packets

2.4.2 Level 1a intermediary products and algorithms

On the ground, the raw interferogram are reconstructed by combining and decoding instrument source packets. Using additional information contained in the transmitted information, the reconstructed interferograms are also sorted into calibration and scene data. The result of this reconstruction and sorting operation is the level 1a data. Level 1a data are intermediary data, they are the starting point of the subsequent processing phase that will lead to level 1b data. Level 1a data are not archived and not normally distributed.

The processing of the level 1a data is essentially accomplished by a single high level function called Load data 2.4.2.1. .

2.4.2.1 Load Data function

Level: 1a

Main objectives:

The Load Data function performs the initial processing of all incoming on-board instrument data. It converts separate data packets into single measurements properly identified and grouped. Auxiliary data is properly calibrated and complete reconstructed interferograms are sent to the proper function depending on the type of data.

It is assumed that incoming data have been demultiplexed and time ordered. These operations are normally common to all instruments of the platform and they will not be covered in the present document.

Specific objectives:

Specific objectives of the function are:

- Receive MIPAS 5.1. data source packets from the on-board instrument (Level 0)
- Extract data packets and form single measurements
- - Perform Error Correction (transmission errors)
- Calibrate relevant auxiliary data
- - UTC time computation
  - Calibration blackbody PRT reading conversion into Kelvin
- Sort measurement data according to the type of measurement (i.e. scene, blackbody, or deep space)
- Stack the calibration measurements 1.1.3.4. into the relevant groups
- Generate and deliver preprocessed data (Level 1a)

Organigram:

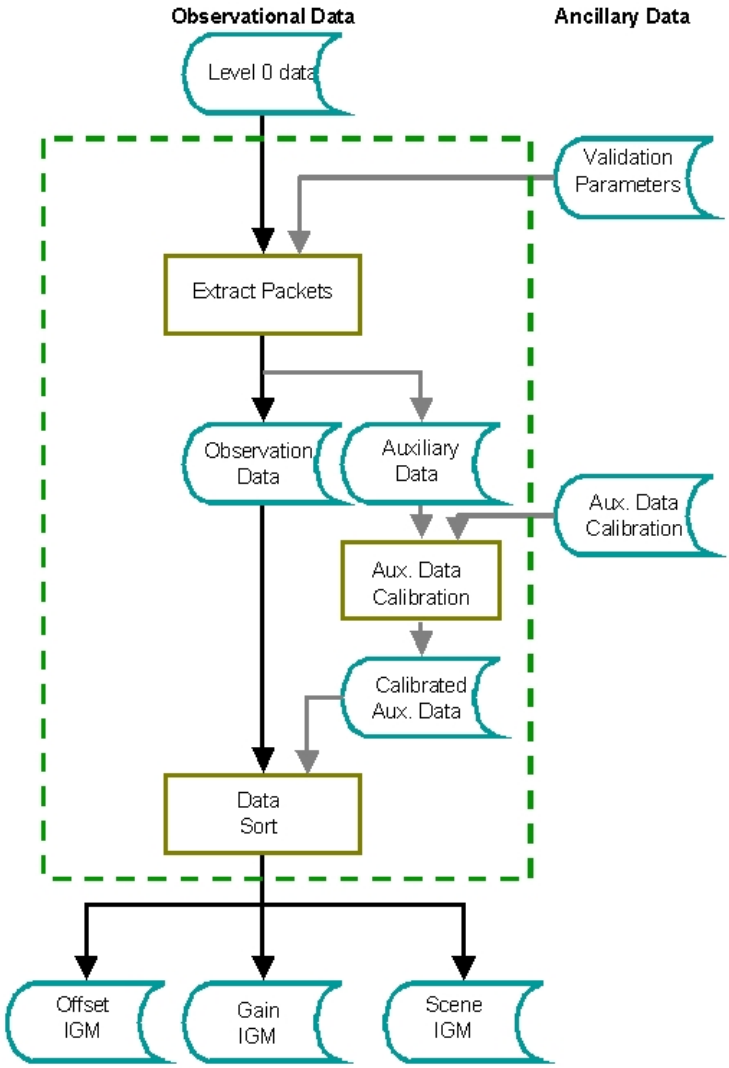

Figure 2.4

Input:

- Level 0 data and auxiliary data

Output:

- Reconstructed and annotated interferograms (Level 1a data):
  - Offset interferogram
  - Gain interferogram
  - Scene interferogram

2.4.3 Level 1b products and algorithms

2.4.3.1 Algorithms

The goal of the level 1b processing is to transform the interferograms generated at the end of the level 1a processing into calibrated and corrected spectral radiance spectra. The overall processing , divided in high level functions, will be processed in the following order:

- Calculate offset calibration 2.4.3.1.1.
- Calculate gain calibration 2.4.3.1.2.
- Calculate spectral calibration 2.4.3.1.3.
- Calculate radiance 2.4.3.1.4.
- Calculate instrumental line shape retrieval 2.4.3.1.5.
- Calculate pointing 2.4.3.1.6.
- Calculate geolocation 2.4.3.1.7.

The following flowchart shows how the Level 1b ground processing is organised:

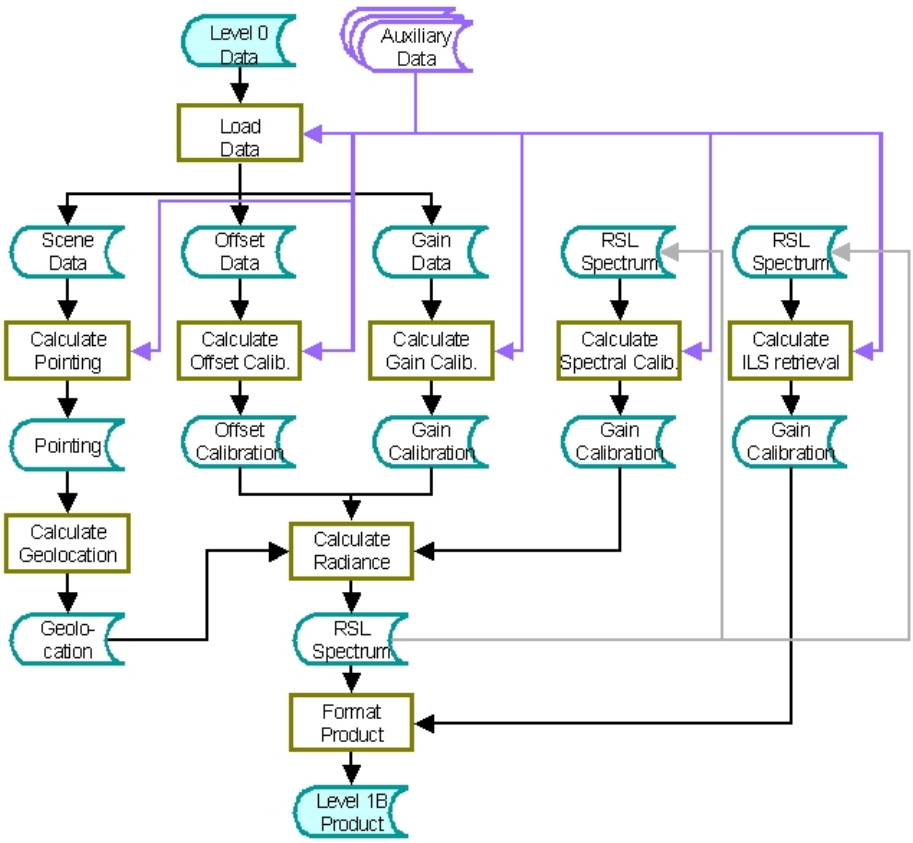

Figure 2.5 Level 1B processing flowchart

During the Level 1b processing there are also some auxiliary functions, applied to both the scene and the calibration data, that are part of several of the above high level functions. These auxiliary functions are:

- Detection and correction of spikes 2.4.3.1.8.
- Detection and correction of fringe count errors 2.4.3.1.9.
- Correction of detector non linearity 2.4.3.1.10.
- Responsivity scaling 2.4.3.1.11.

All these algorithms are described in more details in the "Algorithm Technical Baseline

Document for MIPAS Level 1b Processing Ref. [1.6]".

2.4.3.1.1 Calculate Offset Calibration function

Level: 1b

Main objectives:
The main objective of the Calculate Offset Calibration function is to deliver offset calibration measurement data in a form suitable for radiometric calibration of the spectra by the Calculate Radiance function. Specific objectives: Specific objectives of the function are:

- Perform spikes detection
- Sort offset data according to the direction of interferometer sweep.
- Coadd six interferograms in each band.
- Detect and correct fringe count errors in spectral bands C and D.
- - Gain spectral interpolation
  - Calculate coarse spectra
  - Calculate calibrated spectra
- Responsivity scaling
- Correct for detector non-linearity.
- Equalize and combine interferograms in band A.
- Assess NESR performance.
- - Accumulate statistics from deep space readings to obtain the NESR of the instrument
  - Check the validity of incoming readings

Organigram:

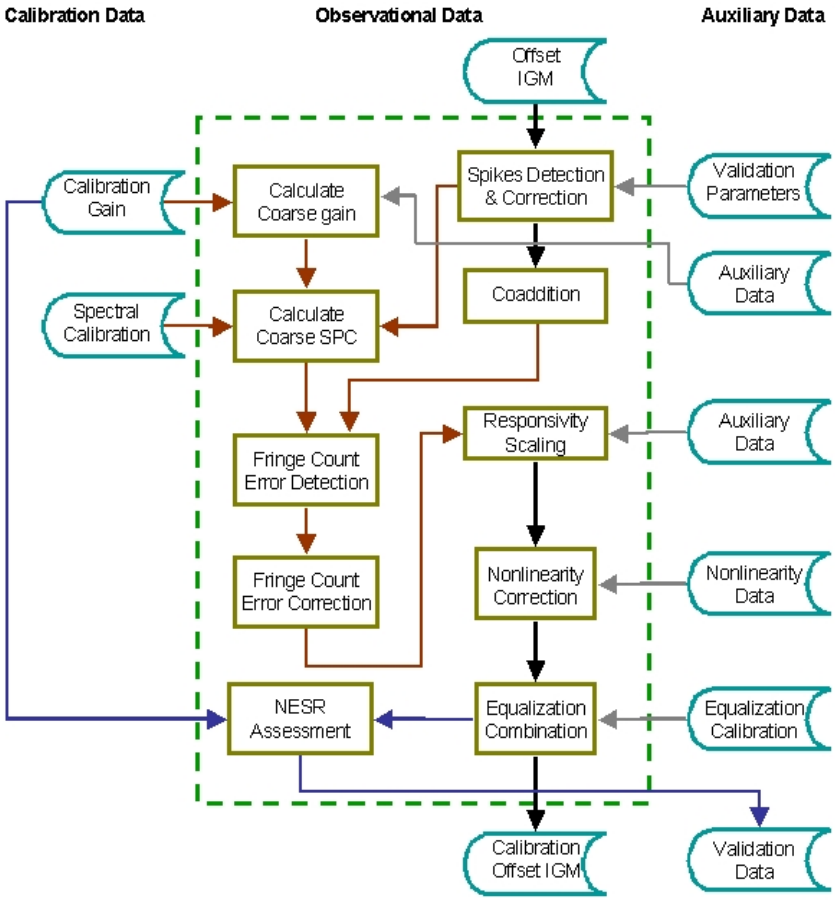

Figure 2.6

Input:

- Level 1a Offset (deep space) interferograms
- Calibration gain from previous calibration sequence [MIP_CG1_AX] 6.4.2.
- Spectral calibration data [MIP_CS1_AX 6.4.5.] 6.4.2.
- Non-linearity characterization
- Validation parameters

Output:

- Calibration offset interferograms (coadded and corrected for spikes and fringe count errors) [MIP_NL__1P:OFFSET CALIBRATION ADS 6.5.34.]
- Validation data (NESR of deep space measurements)

Detailed description: The radiometric offset is an estimate of the instrument contribution, due to its elf-emission, to the total measurement. This estimate of the instrument contribution is made by simply pointing the instrument to deep space and performing a measurement cycle as in the nominal case. For practical reasons, the deep space measurement is taken at a tangential height of around 150 km. Also, due to the potential difference in phase between different sweep directions of the instrument, a measurement is taken in each of the forward and reverse directions of the interferometer. In the ground segment, the closest in time offset measurement (in the correct sweep direction) is simply

subtracted from each interferogram during processing. Click here for details on the offset measurement 1.1.3.4.1. .

The signals detected during offset measurements arise mainly from noise sources in detectors/ amplifiers and from thermal emission of the optical components within the interferometer. Even if the spectrum will be weak, it is believed that fringe count errors can be effectively determined. The scheme applied to scene and calibration measurements will most probably detect the occurrence of fringe errors, and the use of all interferograms (including offsets) maximizes the chance of detecting and correcting the errors as soon as possible after their occurrence.

The zero offset measurements will be subtracted from the relevant individual interferograms. Logically, these measurements should be made at the same spectral resolution as the scene measurements themselves, in order that the vectors are directly comparable. However, it is not expected that any high resolution features will be present in the offset spectra, which means that the measurements may be made at low resolution, with an interpolation on the ground segment. This has the advantage of reducing the duration of the offset measurement.

Offset calibration is performed such that the closest in time available valid offset measurement is used until a new valid offset measurement becomes available. If no offset data are found at the beginning of the Level 0 product input data set, then the first available offset found leading to valid measurement shall be used for all initial scenes. If one or more invalid offset measurements are detected in the middle of the input stream, then a “closest in time strategy shall be applied, which means that complete scans shall be calibrated with the closest valid offset. If no valid offset at all is found in the input data, then the offset calibration data contained in the offset validation file shall be used.

2.4.3.1.2 Calculate Gain Calibration function

Level: 1b

Main objectives:
The main objective of the Calculate Gain Calibration function is to deliver a file representing the radiometric gain of the instrument, computed using gain calibration measurements, in a form suitable for radiometric calibration of the spectra by the Calculate Radiance function.
Specific objectives: Specific objectives of the function are:

- Perform spikes detection
- Sort the gain calibration measurements according to types of measurement and sweep direction.
- Coadd interferograms to increase SNR.
- Detect and correct fringe count errors in spectral bands C and D.
- - Gain spectral interpolation
  - Calculate coarse spectra

- Gain shift correction
- Calculate calibrated spectra

- Responsivity scaling
- Correct DS and CBB measurements for non-linearity of each affected detector.
- Subtract offset due to contribution of the instrument.
- Equalize and combine interferograms in band A.
- Compute coarse spectra using a FFT algorithm applied on the zero-padded interferograms.
- Interpolate gain spectral vectors to provide the gain on a predefined spectral axis.
- Calculate expected blackbody radiance from temperature readings corresponding to blackbody measurements.
- Calculate the complex ratio of theoretical to calculated spectrum (gain computation).
- Gain coaddition
- Check for radiometric accuracy of the incoming data.

Organigram:

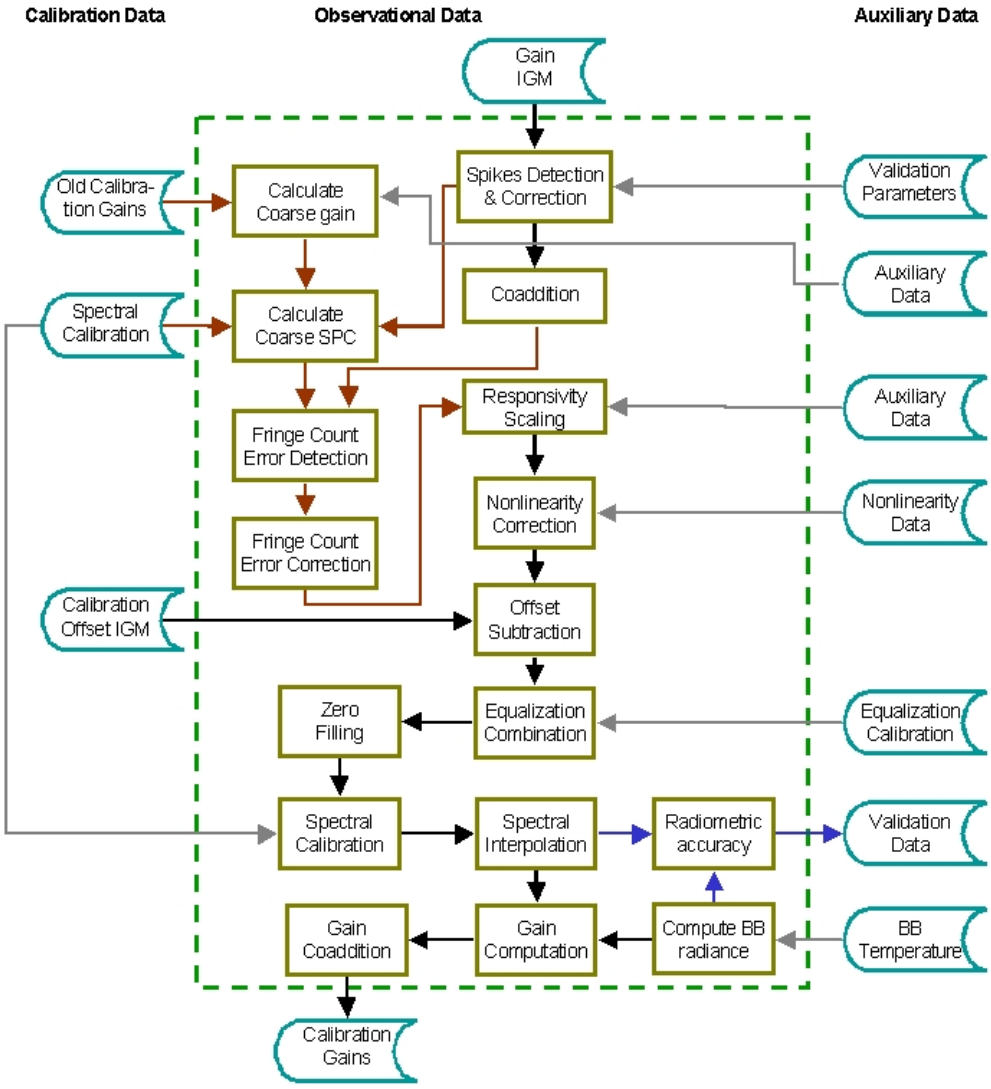

Figure 2.7

Input:
- Level 1a Gain (calibration blackbody) interferograms
- Old calibration gains [MIP_CG1_AX] 6.4.2.
- Calibration offset interferograms
- Spectral calibration data [MIP_CS1_AX 6.4.5.] 6.4.2.
- Non-linearity characterization
- Calibration blackbody 3.1.3.1.1.3. temperatures
- Validation parameters

Output:
- Calibration gains [MIP_NL__1P: GAIN CALIBRATION ADS #1] 6.4.2.
- Spectral accuracy data for validation [MIP_NL__1P: GAIN CALIBRATION ADS #2] 6.4.2.

Detailed description: The radiometric gain calibration requires all deep space and blackbody measurements of the gain calibration sequence. Since in this case the instrument is again contributing to the observed signal, it is also necessary to perform deep space measurements before the blackbody measurements in order to subtract the appropriate instrument offset. (In this instance, the term "Deep Space Radiometric Calibration" is used to distinguish the measurements from the regular Offset Calibration made with the scan sequences. The Deep Space (DS) Radiometric Calibrations are used only to correct the Calibration Blackbody (CBB) measurements and must be explicitly commanded. In fact, several measurements of each kind will be needed. This is because the signal to noise ratio of a single, offset-corrected, blackbody measurement is not high enough, particularly in band D, to achieve the required radiometric accuracy. Therefore a single gain calibration implies several successive measurements.

It is expected that there will be no high frequency features in either the CBB spectrum or in the instrument contribution (as assumed also for the offset calibration). These assumptions will be verified on the ground during instrument Assembly and Integration Test (AIT), but the assumption is reasonable. Therefore, each CBB or Deep Space sweep of the instrument will be made at low-spectral resolution, i.e. with a duration of 0.4 seconds. The baseline scenario uses 300 sweeps at low resolution in both forward and reverse directions for both CBB and DS measurements.

The gain data is processed by the Level 1b processor at the beginning before scene data. During processing, the gain file is not be modified by the processor.

2.4.3.1.3 Calculate Spectral Calibration function

Level: 1b

Main objectives:
The Calculate Spectral Calibration function performs the processing of some selected (radiometrically) calibrated scene measurements and generates the spectral calibration data.
Specific objectives: Specific objectives of the function are:

- Compute a corrected spectral axis

Organigram:

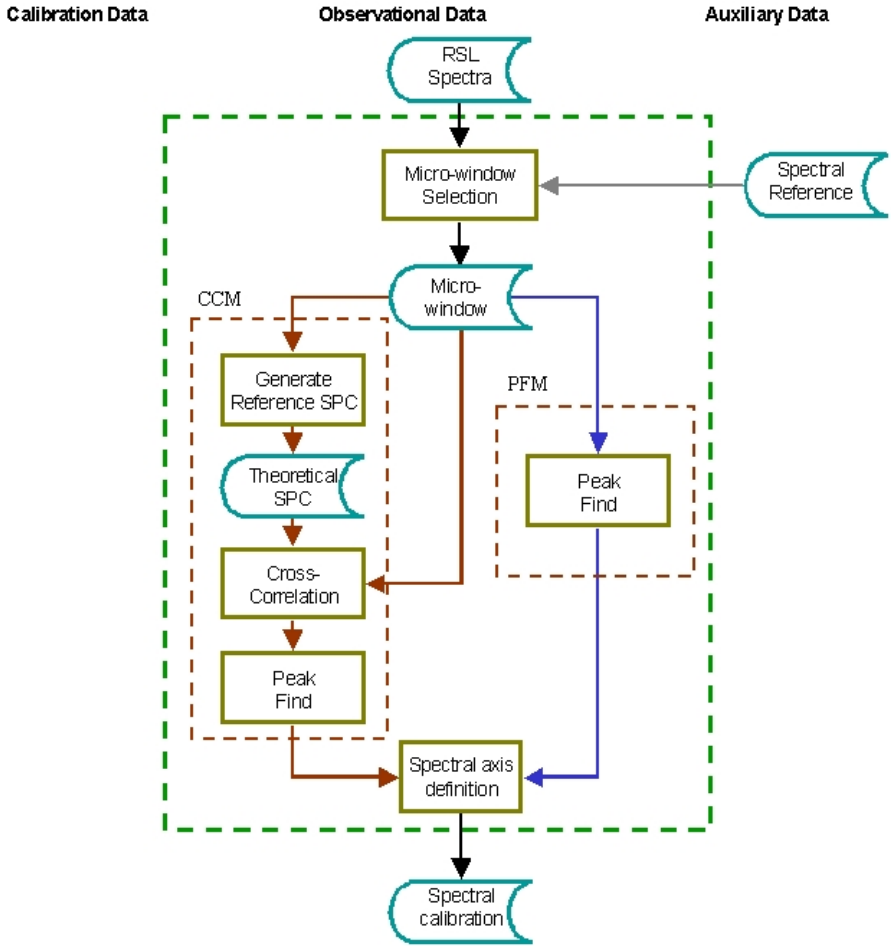

Figure 2.8

Input:

- Radiometrically and spectrally and locally calibrated (RSL) atmospheric spectra
- List of reference spectral lines

Output:

- Corrected spectral axis (spectral calibration data)

Detailed description:

Spectral calibration is performed in MIPAS using standard limb measurements from the atmosphere already corrected for the Doppler effect by the Calculate Radiance function. Specific reference spectral lines will be retrieved in the observed spectra according to the extremities of specific microwindows listed in a reference lines database. From these microwindows will be performed the line position identification, with respect to a database containing the exact known theoretical position of the reference lines. In order to reduce noise, equivalent scenes are coadded, i.e., scenes with altitude included in the range of the processing parameter file. The computed known values of the reference lines positions will be used to establish the assignment of the calibrated wavenumber to the index of spectral data points. Following this operation, spectral calibration will be used for the wavenumber assignment of all subsequent measurements until a new spectral calibration is performed.

The Calculate Spectral Calibration will be performed when it is appropriate to update the spectral calibration, with a current baseline of twice per day.

Because it is related to the same parameters, the spectral shift can be considered as a part of the instrument line shape. The disadvantage is that it is then necessary to perform a deconvolution of the ILS from an observed spectrum to get the proper wavenumber assignment. Here we will assume that the spectral shift is included in the spectral calibration, i.e. it is calibrated out by the spectral calibration procedure without any ILS deconvolution.

It is also assumed that the spectral calibration will be the same throughout the spectral range. It is assumed that the definition of the optical axis is common to all four detectors on the output ports, for both output ports. It is also assumed that the residual misalignment between the two output ports is low enough so that the difference in wavenumber is negligible.

Two algorithms have been proposed to perform spectral calibration: the Peak Finding Method (PFM) and the Cross-Correlation Method (CCM). The feasibility of both these methods have been demonstrated, and both algorithms have demonstrated strengths and weaknesses. The PFM has shown to be a little simpler to implement and faster to execute, but the CCM presents the advantage of giving information related to the precision of a given fit. A switch between in the level 1b processor setup allows the selection of one of these two methods.

The
PFM method uses an analytical model to describe the target line minimising the squared difference between the modelled and observed spectral lines within preselected spectral windows. The optimisation involves the simultaneous fit of four independent parameters using a simplex algorithm. The fitted parameters correspond to an additive offset, the line width, a line amplitude scaling factor and the line centre wavenumber.

For the
CCM method, the cross-correlation function of the measured spectral line and a modelled spectrum (within predefined spectral windows) is computed. The frequency shift in the observational data is obtained by computing the position of the peak in the cross-correlation function.

The precision of the peak identification algorithm is proportional to the number of

equivalent scenes that are coadded, as the noise affecting the signal decreases when multiple readings are superposed. This number will probably vary between 1 and 5 (to attain stability and a precision equal or less than 0.001 cm^{-1}), and will be defined in auxiliary data.

Spectral calibration is performed such that the latest available valid spectral measurement is used until a new valid spectral measurement becomes available. If in the middle of the input stream invalid spectral calibration are calculated, then a "previous closest in time strategy is applied, which means that complete scans shall be calibrated with the previous valid spectral calibration. If no valid spectral calibration at all is available, then the spectral calibration data contained in the current ILS and spectral calibration file is used. Spectral calibration data is written to auxiliary file simultaneously with ILS retrieved data. Otherwise the file is not be modified by the processor.

2.4.3.1.4 Calculate Spectral Radiance function

Level: 1b

Main objectives:
The Calculate Radiance function performs the processing of the scene measurements and generates a radiometrically calibrated spectrum. This function assumes that gain, offset and spectral calibrations are available as soon as they are produced, so that they can be used for the processing of all scene measurements following these calibrations. If this is not the case, then processing will proceed with the latest available calibration data. Specific objectives: Specific objectives of the function are:

- Perform spikes detection
- Detect fringe count errors in spectral bands C and D, and in the case of misalignment adjust the phase of the gain and offset according to the current fringe count.
-
  - Gain spectral interpolation
  - Calculate coarse spectra
  - Calculate calibrated spectra
- Responsivity scaling
- Correct scene measurements for non-linearity of each affected detector.
- Equalize and combine interferograms in band A.
- Subtract offset due to contribution of the instrument.
- Compute spectra using a FFT algorithm applied on the zero-padded interferograms.
- Correct spectral axis for Doppler shift and perform spectral interpolation onto a predefined uniform spectral axis.
- Interpolates spectrum over a pre-determined user's grid
- Radiometric calibration by a complex multiplication of the actual scene spectrum with the actual gain.
- Perform scene measurement quality verification.
- Report of NESR
-

Organigram:

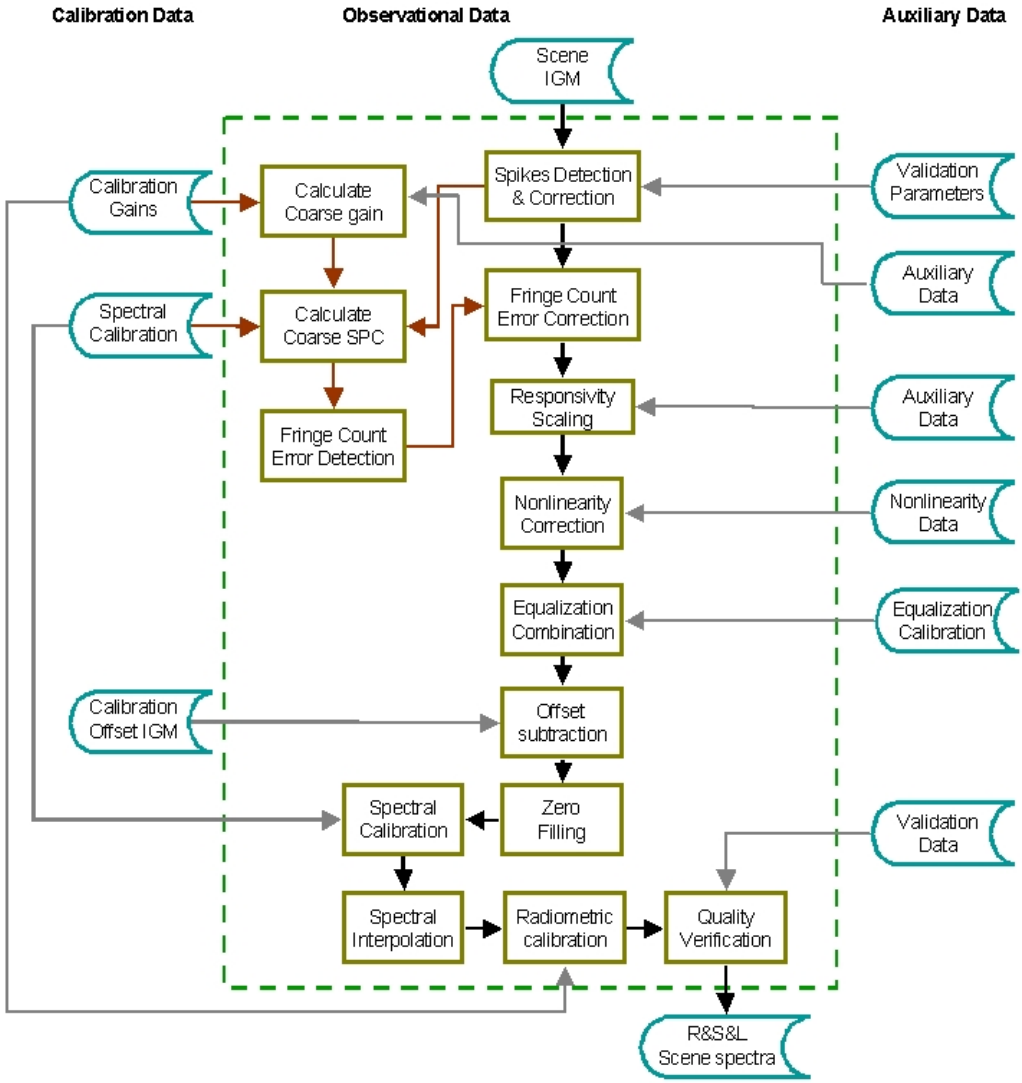

Figure 2.9

Input:

- Level 1a Scene IGM
- Calibration gains
- Calibration offset
- Spectral calibration
- Non-linearity characterization data

Output:

- Radiometrically and spectrally and locally calibrated spectral radiance of the scene

Detailed description:

2.4.3.1.5 Calculate ILS Retrieval function

Level: 1b

Main objectives:
The Calculate ILS Retrieval function performs the instrument line shape (ILS) retrieval from radiometrically and spectrally calibrated spectra. The result of this operation is made available to the output data products. Specific objectives: Specific objectives of the function are:

- Select specific microwindows containing precisely one reference peak of well-known wavenumbers.
- Obtain or generate the reference theoretical spectral line corresponding to this microwindow.
- Fit an ILS to the incoming spectrum by minimizing residuals between the reference line and the parametric ILS.
- Store the iterated ILS parameter set and the specific wavenumbers as a Level 1b product.
-

Organigram:

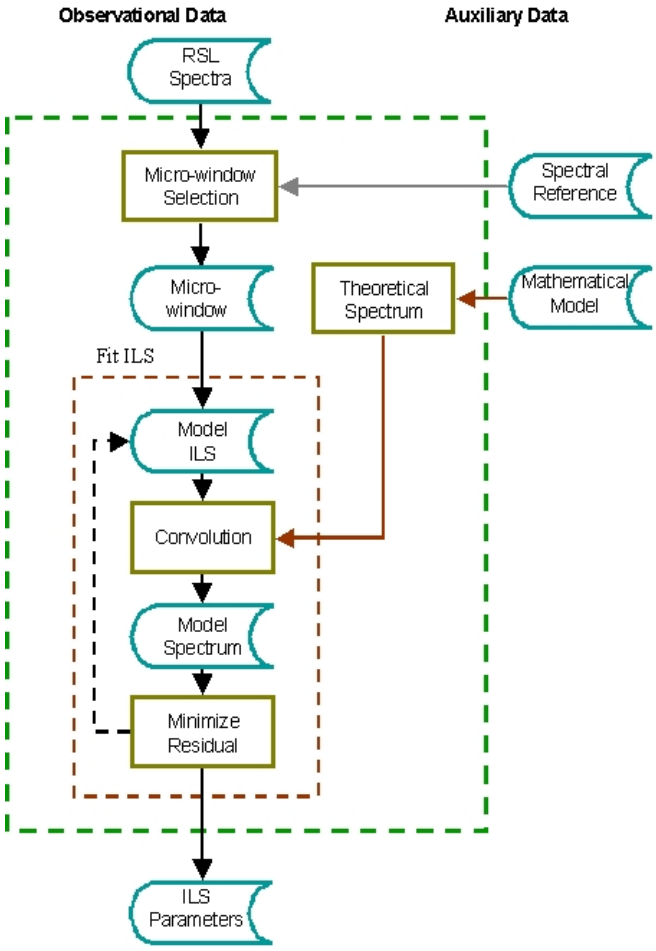

Figure 2.10

Input:

- Radiometrically and spectrally and locally calibrated spectrum [MIP_NL__1P:MIPAS LEVEL-1B MDS 6.5.37.]
- Spectral reference data [MIP_MW1_AX 6.4.9.]
- ILS model

Output:

- ILS parameters for the ILS model [MIP_NL__1P:ILS/SPECTRAL CAL GADS 6.5.10.]

Detailed description:

ILS retrieval has been studied extensively in the technical note (see Ref. [1.8]). A

deconvolution approach has shown to be inadequate, but a second approach has shown to give good enough results. The chosen ILS retrieval method is called the " Parametric ILS Fitting Method (PIFM). This method proceeds with a theoretical ILS, obtained by a modelization with a limited number of parameters, convolved with the theoretical line and iteratively fits the results onto the experimental data.

Appropriate peaks for spectral calibration that represent known features of standard scene measurements have been identified and studied in the document (see Ref. [1.8]). The precision of the peak identification algorithm is proportional to the number of equivalent scenes that are coadded, as the noise affecting the signal decreases when multiple readings are superposed. This number will probably vary between 2 and 10, and will be defined in auxiliary data.

The operation of ILS retrieval is more computer intensive than others tasks presented up until now, but this operation will be requested only from time to time, not on a regular basis as the computation of spectral calibration for example. Topics of the exact frequency at which the ILS retrieval shall be done is addressed here.

It has been chosen to extract the ILSin each detector band of the instrument on an appropriate spectral line located anywhere inside the band. The list of reference spectral lines will be stored in a table kept as auxiliary data.

The auxiliary data file containing retrieved ILS parameter data and spectral calibration data shall be produced by the Level 1B processor according to the processing parameter file. An initial ILS and spectral calibration auxiliary file will be given as an input to the processor at all processing stations and shall be used until the next file will be made available. ILS and spectral calibration data will be written to the auxiliary file simultaneously (i.e., only ca. once per week). Otherwise the file shall not be modified by the processor.

2.4.3.1.6 Calculate Pointing function

Level: 1b

Main objectives:
The Calculate Pointing function performs the line of sight (LOS) pointing calibration in order to generate corrected LOS pointing angles. This includes:

- Compute correction of elevation pointing angle,
- Compute corrected pointing angles of actual scene (sweep).

Specific objectives:
Specific objectives of the function are:

- Compute the actual pointing error at time of ZPD crossing
- Compute actual azimuth pointing angle
- Compute correction of elevation angle

- Compute actual elevation pointing angle

Organigram:

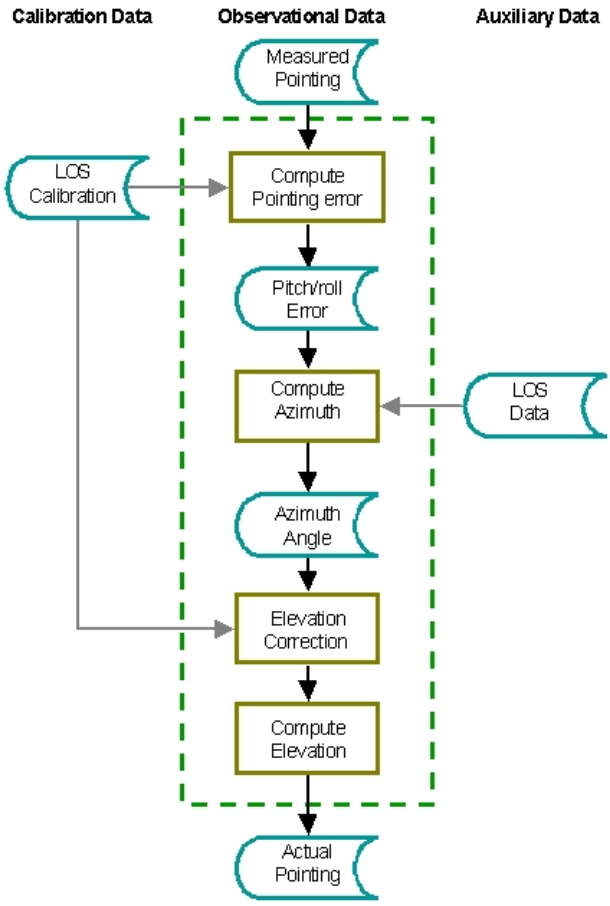

Figure 2.11

Input:
- Measured LOS angles
- LOS calibration data

Output:
- Corrected LOS angles

Detailed description:
The Calculate Pointing function is based on the following assumptions. It is assumed that commanded elevation angles are only partially corrected with respect to known pointing errors according to the best knowledge based on-ground characterisation and LOS calibration measurements. The remaining elevation error, obtained from LOS calibration

measurements, shall be computed in the ground segment (PDS) and be used to correct in measurement mode the measured elevation angles. The corrected elevation angles and the measured azimuth angles are used to compute the geolocation (height/longitude/latitude) of the actual scene (target).

2.4.3.1.7 Calculate Geolocation function

Level: 1b

Main objectives:
The main objectives of the Calculate Geolocation function are:
- Compute tangent height of actual scene
- Compute RMS error of tangent height of actual scene
- Compute longitude / latitude of actual scene.

Specific objectives: Specific objectives of the function are:
- Compute orbital position of spacecraft at ZPD time
- Compute tangent height, longitude and latitude
- Estimate error on computed tangent height

Organigram:

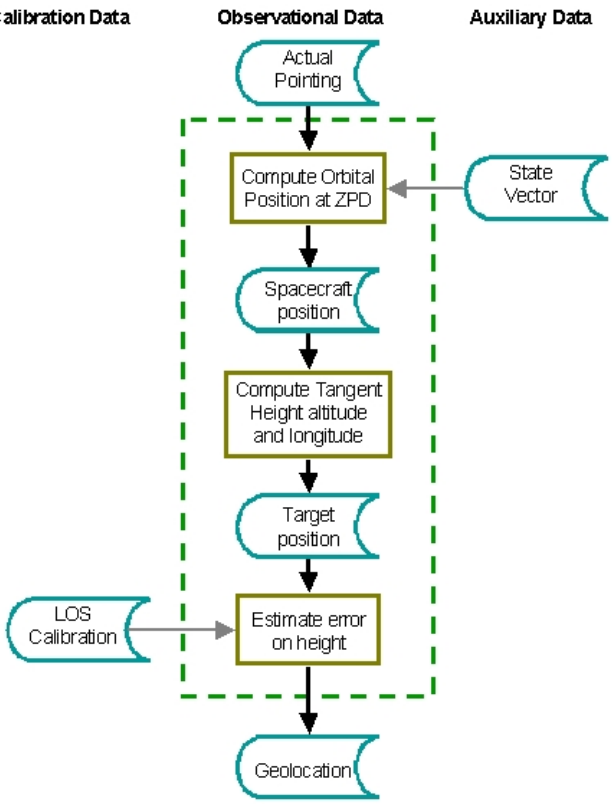

Figure 2.12

Input:
- Corrected LOS angles
- LOS calibration data
- State vectors

Output:
- Geolocation (latitude, longitude and tangent height of target)

Detailed description: The Calculate Geolocation function calculates the tangent point geolocation and related information. The function has as input the orbit state vector and corrected pointing angles.

2.4.3.1.8 Detection and correction of spikes

Level: 1b

Main objectives:
Detect and correct spurious spikes in an interferogram Specific objectives: Specific objectives of the function are:
- Inspect the interferogram around the ZPD to detect the presence of spikes
- Reject the interferogram if it is in a calibration measurement, otherwise replace detected spikes by the mean of the neighbor points.
-

Organigram:

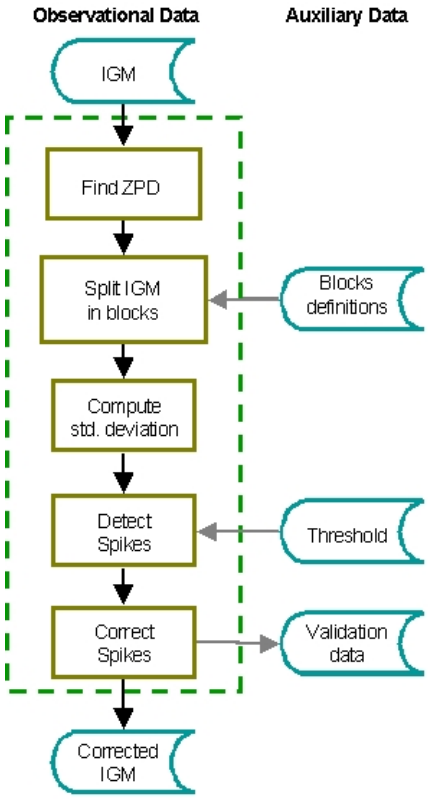

Figure 2.13

Input:

- Interferogram to inspect and correct

Output:

- Corrected interferogram
- Spikes position

Detailed description:

This function has the purpose of detecting spurious spikes in an interferogram. The presence of spikes in an interferogram can be caused by cosmic radiation or transmission errors. The affected points in a scene interferogram are corrected by taking the mean between immediate non-affected points. This scene will be flagged of having corrected for one or more spikes. If a spike is detected in a gain or in an offset measurement, this measurement will be discarded in order to avoid corrupting all of the subsequent calibrated spectra.

The algorithm performing spike detection scans groups of points in the interferogram (odd

number with central block corresponding to ZPD block) in search of spikes. In each block, except for the central ZPD region of the middle block, the standard deviation of the interferogram values is computed, and a spike is identified if a given point amplitude exceeds a predefined threshold for values in the real or the imaginary parts. To improve the accuracy of the algorithm, A second pass is done excluding the data points identified as spikes to calculate the final standard deviation of the group.

For each detected spike, the value at the specific wavenumber is replaced by a mean of the two immediate points in the interferogram vector. The real part and the imaginary part are corrected independently.

The spike correction will always cause some distortions with respect to the original spectrum, but it has been shown that this distortion is within the radiometric accuracy requirement. Interferograms that have been corrected for spikes are flagged as such.

2.4.3.1.9 Detection and correction of fringe count errors

Level: 1b

Main objectives:
Detect and correct fringe count errors (FCE) in the interferograms Specific objectives: Specific objectives of the function are:

- For FCE detection:
  - FFT the ZPD region of the interferogram
  - Multiply the resulting spectrum by the latest available gain (interpolated)
  - Calculate the spectral phase of the roughly calibrated spectrum
  - Perform a linear regression of the phase vs. wavenumber
  - Calculate the OPD shift
- For FCE correction:
  - Perform the FFT of the shifted interferogram
  - Calculate the phase function necessary to correct the calculated shift
  - Multiply the spectrum with the calculated phase function
  - perform an inverse FFT on the spectrum

Organigram:

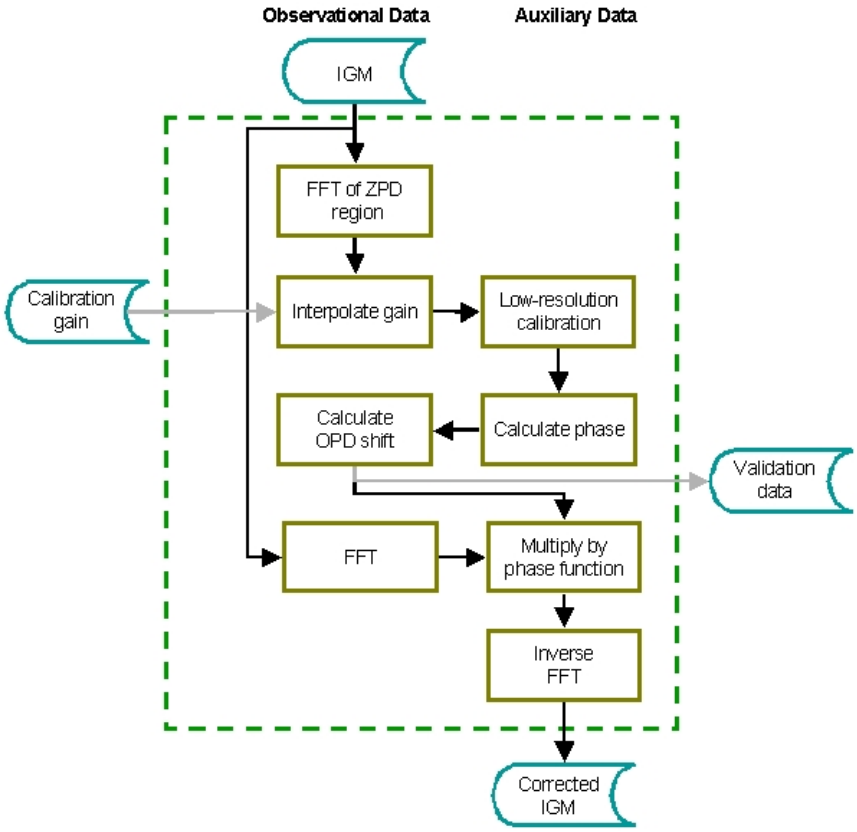

Figure 2.14

Input:

- interferogram to inspect

Output:

- Phase corrected interferogram

Detailed description: The basic ground processing for MIPAS contains no explicit phase correction or compensation. For a given interferometer sweep direction, it is assumed that the gain and offset calibrations and also the scene measurements have the same phase relationship, i.e. they are sampled at precisely the same intervals. This sampling is determined by a metrology fringe counting system using a reference laser source within the interferometer subsystem, with the fringe counts forming a " clock signal to the ADC in the on-board signal processor electronics (SPE). The fringes trigger the sampling of the interferogram. If, for any reason, a fringe is lost, then the phase of subsequent measurements will be affected and if these are calibrated using a gain or offset measurement taken before the occurrence of the fringe loss, then errors will be introduced into the final spectrum. The ground processing scheme includes a method for detecting and correcting fringe losses by analyzing the residual phase of calibrated spectra, computed from the central ZPD region of each interferograms. Hence there is no specific measurement required as part of calibration for this aspect.

The proposed approach assumes that fringe count errors occur at turn-around, i.e. between

two measurements. Under this assumption, the effect of a fringe count error is to shift all measurements following the error by N points. The problem manifests itself at calibration because all the measurements involved may not have the same sampling positions, i.e. they do not have the same phase relationship.

Fringe count errors occurrence within a measurement is believed much less probable, and its effect is the same as if the error would have been at the turn-around. Thus it will be covered by the above assumption.

Fringe count errors can occur in all types of measurements done by the MIPAS instrument, except of course the LOS calibration measurements during which the sweeping mechanism is stopped. Depending on the type of measurement, the effect is not the same and therefore, the detection and correction approach will be different. Because the phase is not strictly the same for forward and reverse sweeps, the fringe count error detection and correction will be done independently for the two sweep directions. For all measurements, the fringe count reference interferogram of a given sweep direction will be the last gain interferogram of that sweep direction. The last gain interferogram can be either a deep space or a blackbody interferogram, depending on the acquisition scenario requested.

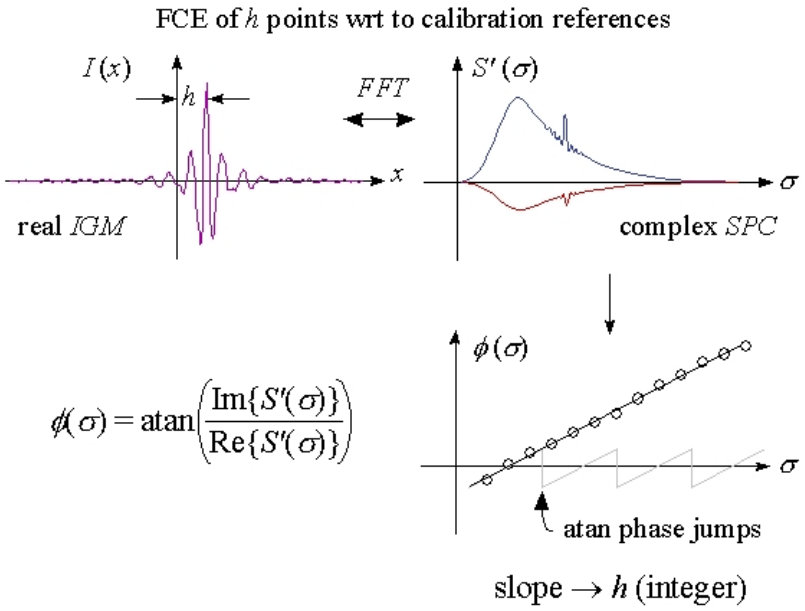

Figure 2.15 Fringe Count Error handling

Fringe count errors detection

The approach selected for fringe count error detection consists in a coarse radiometric calibration of the actual measurement at very low resolution, followed by an analysis of the residual phase. The radiometric calibration is done using the last available gain measurement. When the optical path difference (OPD) axis definition of the actual

measurement is the same as the gain used for radiometric calibration, then the residual phase should be zero. A shift will produce a phase error increasing linearly with wavenumber.

The algorithm simply performs a linear regression on the residual phase of the calibrated spectrum to reveal an integer shift due to a fringe count error on the observed interferogram. The spectral phase is expressed as tan arctangente of the ratio of the imaginary part over the real part of the spectrum.

Fringe count errors correction

Once the OPD shift is known, the decimated interferogram must be shifted by a fractional number of points corresponding to this shift divided by the current DF. This requires some sort of interpolation. The current approach is to perform a multiplication of the Fourier transformed of the shifted IGM by the phase function obtained in the detection procedure.

With this method, no manipulation is done on the OPD axis of the interferogram, but each data point is corrected to represent the value of its desired current OPD position.

It should be mentioned that fringe count errors will affect interferograms of all bands. For the MIPAS instrument, detection is done only for bands C and D.

The approach for fringe count error detection and correction will be the same for all types of measurements. However, the implementation will be somewhat different for the different types. This is discussed below. The fringe count error detection will be performed systematically on all incoming interferograms. However, the correction procedure will be applied only if a non-zero shift is detected.

FCE handling in offset measurements

Detection and correction are done with respect to the last available gain calibration. All the offsets corresponding to one orbit are aligned to the fringe count phase of this last gain. If one or more fringe count errors occur during the computation of one orbit, the ground processing will detect the same shift for all subsequent offset interferograms and will apply the same (always recalculated) correction on these offsets until the end of the processing of the orbit.

FCE handling in gain measurements

At the beginning of a gain measurement sequence, there is no reference against which one can check for fringe count errors. Thus, there is no relation between the actual measurement and the previous fringe counting reference. This is the main reason why we start with a new gain measurement.

Fringe count errors during gain calibration are checked by comparison with the first measurement of the sequence, typically a blackbody measurement (either forward or reverse). The first step is to determine the OPD shift between that measurement and the

previous gain. The same procedure as for normal error detection and correction is then followed.

This corrected gain will then be used for detection of fringe count errors on all subsequent interferograms. In principle, the calibrated spectra obtained with this corrected gain should show no additional phase until a fringe count error occurs. Then, all error-free measurements will be coadded normally. Each time a fringe count error will be detected, a new coaddition group will be formed. When the complete calibration sequence is over, then all the coadded measurements are corrected with respect to the last measurement and the remaining processing of the radiometric calibration is performed normally. Correcting the gain with respect to the last measurement presents the advantage that all subsequent error-free measurements need no correction.

After processing the data corresponding to one orbit, if one or more FCE are detected, the current gain is shifted according to the last fringe count error measured. This is done in order to avoid correcting all the offsets and scenes in subsequent orbits.

FCE handling in scene measurements

When a scene is measured, its fringe count is checked against the last available gain calibration. All the scenes corresponding to one orbit are aligned to the fringe count phase of this last gain. If one or more fringe count errors occur during the computation of one orbit, the ground processing will apply the same correction on these scenes until the end of the processing of the orbit.

After that, the gain is shifted according to the last FCE to match the offsets and scenes of subsequent orbits. This way, the worst that could happen is that all the scenes of only one orbit would need to be shifted. All the subsequent processing of the orbits to follow would not suffer needlessly of a single previous FCE event.

This approach also minimizes the accumulating of numerical error on gains, that can be modified only after successive orbits. In practice, FCE are expected to occur very infrequently during processing of one orbit; but even if this would be the case, the fact of aligning offsets and scenes to the last available gain calibration would limit the error accumulation on the gain calibration vector.

This procedure will slightly increase the throughput for the reference gains used for the ground segment computation. There will be one each time at least one fringe count is detected during one orbit. But, as fringe count errors are expected to occur infrequently, there would usually still only be one gain vector per week and, should an error occur, only the gain would be modified after the processing of the corresponding orbit. The fact of realigning gain calibration vectors between orbits should save a lot of operations, as one would otherwise be correcting every interferogram until the next gain calibration (the saving occurs independently of whether there are frequent fringe errors or not).

2.4.3.1.10 Correct non-linearity function

Level: 1b

Main objectives:
Correct the non-linearity of the response of the detectors of MIPAS. Specific objectives: Specific objectives of the function are:

- apply the non-linearity polynomial on a detector per detector basis for each interferogram
-

Organigram:

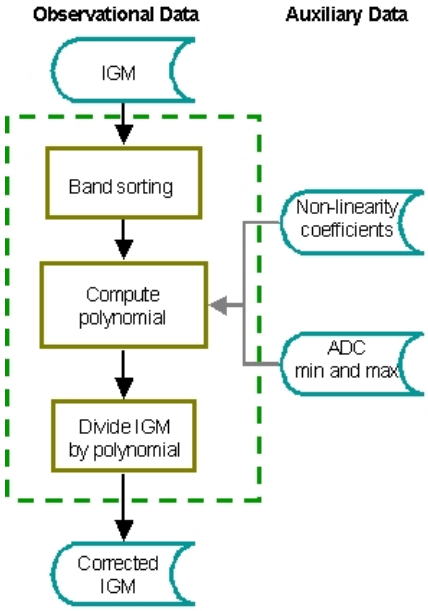

Figure 2.16

Input:

- Interferogram to correct
- Set of non-linearity coefficient for each band/detector

Output:

- corrected interferogram

Detailed description:
The detectors from the first three MIPAS bands (detectors A and B) are photoconductive detectors, subject to non-linearity depending on the total photon flux falling on them. Here, the non-linearity means that the response of the detector differs from a linear behavior as a function of the incoming flux. This phenomenon occurs at high fluxes.

The non-linearity can be a source of significant radiometric errors if it is not properly handled (as much as 40% in band A). As explained in (Ref. [1.9]), the non-linearity produces a change in the effective responsivity as well as the apparition of spectral artifacts. The present method corrects for the decrease of responsivity with DC photon flux in the radiometric calibration, within the required radiometric accuracy. The approach is the following:

A characterization must first be performed on ground, and then in space at specific intervals, at instrument level, of the total height of the unfiltered and undecimated interferogram with the on-board calibration blackbody at different pre-selected temperatures. These values will be used during the characterization phase for a computation of the non-linear responsivity coefficients. These values will be used to correct for the non-linearity of the detectors by means of a specific algorithm called the Adaptive Scaling Correction Method (ASCM).

Although they are intended to be combined in a single band, the optical ranges of the detectors A1 and A2 are not the same. They will then exhibit a different behavior with respect to photon flux. As a result, they will require different non-linearity corrections. Because of this, the signals from these detectors are not equalized and combined on board the instrument in the SPE. This operation is instead performed by the ground processor following non-linearity correction. The other two PC detectors, B1 and B2, are not combined in any case as they produce the bands AB and B. Other than the need to keep A1 and A2 separate in the baseline output set up at the SPE, the non-linearity measurements and correction has no impact upon the calibration scenario.

The important effect of detector non-linearity is on the radiometric accuracy performance. The present radiometric error budget allocated to the non-linearity in the 685 “ 1500 cm^{-1} (where the detectors are the most non-linear) shall be better than the sum of 2 x NESR and 5% of the source spectral radiance, using a blackbody with a maximum temperature of 230K as source.

A polynomial correction is then applied on each incoming interferogram, at the very beginning in the processing chain, with the purpose of compensating for the global effects of responsivity.

For the measured responsivity curves of the MIPAS engineering and demonstration model (EDM), the correction of the non-linearity error due to the change of effective responsivity and from the cubic artifacts have shown to lead to an accuracy within the allocated budget.

The polynomial used to correct the non-linearity is of the form:

$$k = 1 + d_0 F + d_1 F^2 + d_2 F^3 + d_3 F^4 \qquad \text{eq 2.2}$$

where F is the total flux on the detector (estimated as the difference between the maximum and minimum values of the digitized interferogram by the ADC before filtering and decimation and multiplied by the amplification gains) and the d_i are coefficients determined by the non-linearity characterisation for each detector. In absence of non-linearity effect, these coefficients are 0. The interferograms are corrected by dividing them by this polynomial.

2.4.3.1.11 Responsivity scaling

Level: 1b

Main objectives:
Scale interferograms acquired with different gains to a common baseline. Specific objectives:
Specific objectives of the function are:

- Scale interferograms acquired with different gains to a common baseline.
-

Organigram:

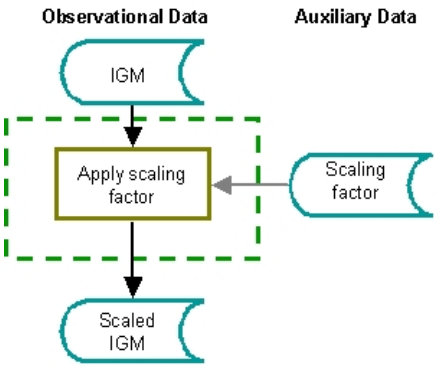

Figure 2.17

Input:

- Interferograms (gain, offset and scene measurements)
- gains scaling factors

Output:

- Scaled interferograms

Detailed description:
The gains of MIPAS are adjusted depending on the relative intensity of the target so as to maximize the dynamic range of the instrument. For instance the gains are not the same for deep space measurement and for CBB measurements. Since interferograms acquired with different gains will be combined during the radiometric calibration processing, it is necessary to scale these interferograms to a common baseline.

In practice, three scaling items need to be considered, as a result of the pre-amplifier warm (PAW) system:

1) A scaling to account for a commanded gain change

The gains are predefined and are commanded by an 8-bit word sent via the instrument control unit. Since different gains may be commanded, a data scaling in the ground segment to equalize performance must be foreseen. The commanded gain is available in the auxiliary data stream and so this is a simple scaling effect based on the extracted word.

2) A temperature dependent scaling to account for changes in responsivity of the detectors.

The detector units are specified to provide a stable response based upon assumed knowledge of their temperature (i.e. the responsivity may vary but it must be well characterized). For this reason, a correction of performance with time/temperature must be foreseen. This is made based on the measured detector temperature (available via thermistor values in the auxiliary data) and using characterization curves generated during characterization tests on ground.

3) A temperature dependent scaling (gain & possibly phase) to account for the variations in the performance of the electronics of the PAW and the SPE around the orbit.

At present, it is not thought necessary to correct for these effects around the orbit as predictions show the variations will not cause the units to drift out of specification. The In-Flight Calibration Plan Ref. [1.1] foresees to make around orbit measurements during Commissioning Phase to check whether there are any such variations.

2.4.3.2 Products

2.4.3.2.1 High level organisation

Level 1b products consist of formatted geolocated, radiometrically and spectrally calibrated spectra of atmospheric radiance. It also includes ILS data, identifiers for the various correction and calibration processes and data quality control indicators. The structure of the Level 1b products is described on the following diagram:

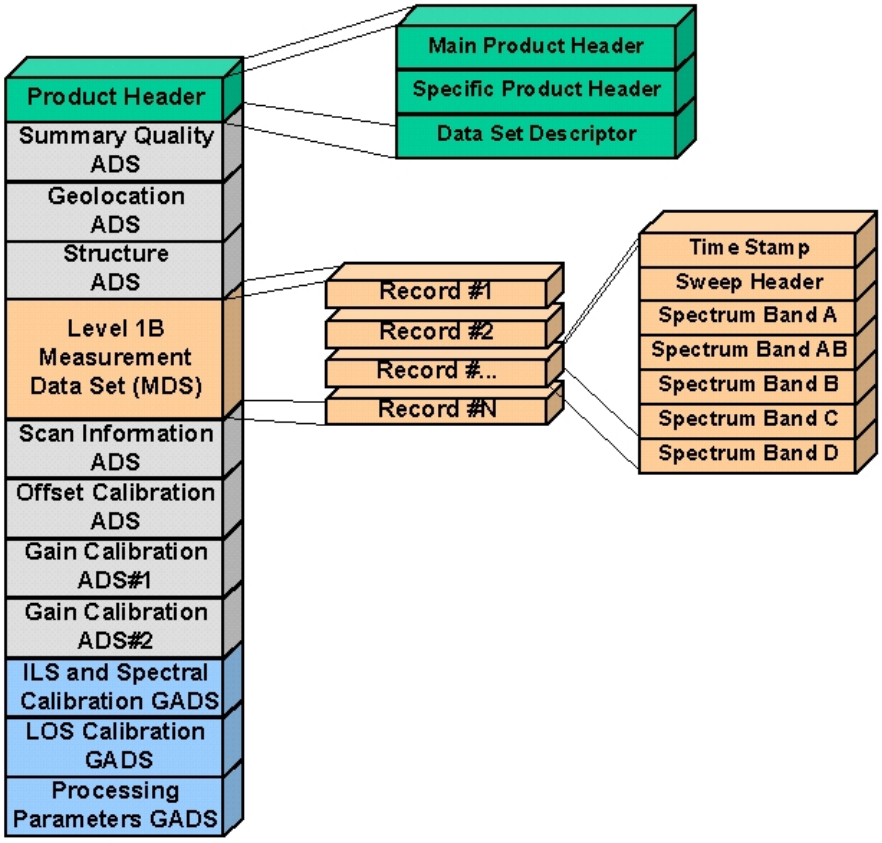

Figure 2.18 Level 1b data product structure

The main elements of the level 1b product are:

- The Product header
- The Summary quality ADS
- The Geolocation ADS
- The Structure ADS
- The Level 1B measurement data set
- The Scan info ADS
- The Offset calibration ADS
- The Gain calibration ADS#1 and ADS#2
- The ILS and Spectral Calibration GADS
- The LOS Calibration GADS
- The Processing parameters GADS

The current detailed structure of the level 1b data product can be found here 6.2.1. .

2.4.3.2.2 Product header

The product header is divided into three parts:
- Main product header 2.4.3.2.2.1.
- Specific product header 2.4.3.2.2.2.
- Data set descriptor 2.4.3.2.2.3.

2.4.3.2.2.1 Main product header

The main product header is the same for all ENVISAT products. It specifies basic product information such as origin of data, processing site, processing software version, UTC time of data sensing and processing, orbit and velocity parameters of ENVISAT, quality indicators for input data, etc.

The current detailed structure of the MPH can be found here 6.5.1. .

2.4.3.2.2.2 Specific product header

The SPH contains the information applicable to the whole Level 1b product file such:
- UTC measurement time intervals (ZPD time)
- geographic coverage of scene data (latitude and longitude of first and last scan)
- number of total, nominal and special event scans in product file
- number of sweeps per scan
- number of sweeps per deep space (offset) measurements 1.1.3.4.1.
- first and last wavenumbers of the spectral axis (for each band)
- first and last wavenumbers of the NESR curve reported
- MPD during the sweeps of the nominal scans

The current detailed structure of the SPH can be found here 6.5.38. .

2.4.3.2.2.3 Data set descriptor

The DSD provide information on structure and size of included or referenced measurement and annotation data.

2.4.3.2.3 Summary quality ADS

This ADS contains notes on the quality of the data in the data product file. It is summary file that list the number of bad sweeps. It includes:

- The number of corrupted sweeps
- The number of corrupted sweeps with instrument errors.
- The number of corrupted sweeps with observational errors
- The number of sweeps with a too large phase error
- The number of sweeps for which the fringe count error in band B differs from band AB.
- The number of sweeps for which the flux is out of range for one or more detectors.

The current detailed structure of this ADS can be found here 6.5.35. .

2.4.3.2.4 Geolocation ADS

This ADS contains information on the geolocation of the product. It includes:

- ZPD time of the first, last and sweep closest in time to the center of the scan.
- WGS84 latitude and longitude of the first, last and sweep closest in time to the center of the scan.

The current detailed structure of this ADS can be found here 6.5.32. .

2.4.3.2.5 Structure ADS

This ADS gives information about the size and organization of the MDSR of the data product. It is separated into various ADSR, each referring to a given MDSR. Each includes:

- Number of sweep in current elevation scan
- Number of point in NESR vector
- Number of spectral peaks fitted during spectral calibration
- Size of blocks used in spectral calibration

The current detailed structure of this ADS can be found here 6.5.36. .

2.4.3.2.6 Level 1b measurement data set

This part of the data product, is the part that contains the actual level 1b product. The level 1b MDS is a series of structured measurement data set records (MDSR). Each MDSR corresponds to an individual scene measurement (single sweep). The MDSR contain a time

stamp, the specific header for the sweep and the radiometrically and spectrally and locally calibrated spectra in the five spectral bands of MIPAS.

Each MDSR contains:

- ZPD time of the sweep
- Sweep ID number and relative number is elevation scan
- The position of the spacecraft at ZPD time of that sweep
- The azimuth and elevation angles of that sweep
- The rate of variation of the altitude of the target
- The geodetic latitude and longitude of the tangent point of that sweep
- Validity and quality flags
- Instrument mode
- Number, position and relative intensity of detected spikes
- Number of detected and corrected fringe count errors
- Doppler stretching applied
- Sweep direction (forward or reverse)
- Interferogram minimum and maximum values at ADC for each detector (used by non-linearity correction 2.4.3.1.10. algorithm)
- The spectral data points of bands A, AB, B, C and D in W cm^{-2} sr^{-1} cm (real part of the radiometrically and spectrally and locally calibrated spectral radiance).

The current detailed structure of the Level 1b MDS can be found here 6.5.37. .

2.4.3.2.7 Scan information ADS

This ADS gives information related to the instrument configuration during the elevation scans and level 1b processing issues. It includes:

- Identification number of set of numerical filters used
- Decimation factors per detector
- Number of samples taken at the ADC (fringes counted)
- Commanded (as opposed to actual) elevation and azimuth angles
- Elevation scan number since last valid offset measurement
- Solar time at target
- Satellite and to target azimuth angle
- Target to sun azimuth and elevation angles
- Date and time of scene used for spectral calibration
- Linear spectral correction factor (not including Doppler effect) and its standard deviation
- Number of peaks fitted during spectral calibration
- For each peak:
  - identification number of microwindow
  - Exact wavenumber of reference line
  - Detected frequency shift
  - correlation coefficient
  - number of coadded scenes for spectral calibration
- PAW gain scaling factor

- NESR data

The current detailed structure of this ADS can be found here 6.5.33. .

2.4.3.2.8 Offset calibration ADS

This ADS contains the offset calibration measurement applied to the current data product as well as related information about this measurement. It contains:

- Validity flag for each spectral band
- Number of fringe count errors in gain calibration data
- Sweep direction (forward or reverse)
- For each band:
  - ZPD time of the first sweep
  - Decimation factors
  - Number of corrected spikes in interferogram
  - Position of corrected spikes in interferogram
  - Amplitude of corrected spikes in interferogram
  - Number of data point before decimation
  - Complex interferogram data

The current detailed structure of this ADS can be found here 6.5.34. .

2.4.3.2.9 Gain calibration ADS#1

This ADS contains the calibration gain applied to the current data product as well as related information about this measurement. It contains:

- Quality indicators
- Interferogram minimum and maximum values at ADC for each detector (used by non-linearity correction 2.4.3.1.10. algorithm)
- Average temperature of the PRT of the calibration blackbody
- Number of coadded blackbody interferograms 1.1.3.
- Number of coadded deep space interferograms 1.1.3.
- temperature of FEO
- Sweep direction (forward or reverse)
- For each spectral band:
  - decimation factor
  - number of detected spikes
  - Position of corrected spikes in interferogram
  - Amplitude of corrected spikes in interferogram
  - Number of points in band
  - first and last wavenumbers of gain data
  - The gain data in W cm^{-2} sr^{-1} cm

The current detailed structure of this ADS can be found here 6.5.30. .

2.4.3.2.10 Gain calibration ADS#2

This ADS contains information about the radiometric accuracy. It contains:

- Time of creation
- Quality indicators
- Sweep direction (forward or reverse)
- For each spectral band:
  - number of points in band
  - first and last wavenumbers of data
  - mean of gain variation (cumulated with last valide gains) in W cm^{-2} sr^{-1} cm
  - standard deviation of gain variation (cumulated with last valide gains) in W cm^{-2} sr^{-1} cm

The current detailed structure of this ADS can be found here 6.5.31. .

2.4.3.2.11 ILS and spectral calibration GADS

This GADS contains information on the spectral calibration and ILS retrieval. It contains:

- Time of creation
- ZPD time of the first sweep of scene used for ILS retrieval
- Quality indicators for ILS retrieval
- Level 1 b product file name that contains the data used for the ILS retrieval
- Number of ILS retrieved
- ILS parameters including:
  - microwindow identification number
  - wavenumber of the line used
  - number of coadded scenes
  - ILS parameters
- ZPD time of the first sweep used for spectral calibration
- Quality indicator for spectral calibration
- Level 1 b product file name that contains the data used for the spectral calibration
- Linear spectral correction factor (nor including Doppler effect) and its standard deviation
- Number of fitted peaks
- For each peak:
  - identification number of microwindow
  - Exact wavenumber of reference line
  - Detected frequency shift
  - correlation coefficient
  - number of coadded scenes for spectral calibration

The current detailed structure of this GADS can be found here 6.5.10. .

2.4.3.2.12 LOS calibration GADS

This GADS contains information on the LOS calibration. It contains:

- Time of creation
- Quality indicator
- Angular frequency of first order harmonic pointing error (for x and y axis)
- Estimated bias error (for x and y)
- Estimated amplitude of first order harmonic error (for x and y)

- Estimated phase of first order harmonic error (for x and y)
- Variance of both estimated amplitude and phase of first order harmonic error (for x and y)'
- Number of averaged orbits

The current detailed structure of this GADS can be found here 6.5.7. .

2.4.3.2.13 Processing parameters GADS

This GADS contains information on various elements of the level 1b processing. It includes:

- Nominal metrology laser wavenumber
- Number of points in each five bands
- First and last wavenumber of each band
- Number of points around the ZPD of band A and AB
- Values of various rejection thresholds
- Number of spectral blocks used for spike detection
- Spectral calibration method used (CCM or PFM)
- Simplex tolerance, maximum allowed number of iterations and initial guess values (for ILS retrieval).
- ILS model parameters
- Maximum and minimum azimuth angles in side observation geometry and in rearward observation geometry
- Default yaw, pitch and roll angles, default mispointing angles and default mispointing rates (for LOS calibration)
- The last modification time of various section in this file

The current detailed structure of this GADS can be found here 6.5.63. .

2.4.4 Level 2 products and algorithms

2.4.4.1 Algorithms

2.4.4.1.1 Introduction

The middle infrared emission spectra measured by MIPAS (output of Level 1b processor 2.4.3.2.) contain features of most atmospheric constituents. Therefore, a series of spectra

measured in the limb-scan configuration can be processed to determine the volume mixing ratio (VMR) profiles of numerous atmospheric trace species. Since middle infrared emission spectra are strongly sensitive to temperature, and in general limb observations are strongly affected by the observation geometry (that, in Level 2 processing is usually identified by the value of pressure at tangent altitudes, 'tangent pressure'), a correct interpretation and analysis of the observed spectra for the retrieval of the atmospheric constituents requires a good knowledge of these quantities, which have to be determined for each limb scan sequence.

The retrieval of pressure and temperature (p, T), as well as the VMR of five high priority species, namely O_3, H_2O, HNO_3, CH_4, N_2O and NO_2 will be routinely performed in near real time (NRT). The retrieval of these parameters from calibrated spectra (provided by Level 1b processor 2.4.3.2.) is indicated as NRT Level 2 processing.

The requirement for NRT analysis is very demanding because of both the time constraints (short delay between measurement and processing, and computing time shorter than measurement time) and the need for a validated algorithm capable of producing accurate and reliable results in an automated operative mode.

The main functional components of the Level 2 processor are:

The pre-processor:

is the software that manages the environment in which the retrieval modules are run. Typical tasks of this code are: selection of the observations to be processed in the subsequent retrievals, preparation of inputs (including all auxiliary data) needed by the retrieval modules, calculation of the quantities that must be calculated only once for processed scan, preparation and formatting of the output files (Level 2 products).

Go here 2.4.4.1.2. for further details on the Level 2 pre-processor.

The retrieval modules:

Satrting from the inputs prepared by the pre-processor (i.e. from selected intervals of the calibrated and apodized spectra calculated in Level 1b, a set of auxiliary data and processing setup parameters) these modules perform p,T and VMR retievals.

The retrieval modules have been implemented (in the ENVISAT Payload Data Segment) by industry on the basis of the algorithms defined in the frame of a scientific study. In this study, a "scientific" version of the retrieval code has been developed, optimized for the requirements of speed and accuracy. This code is called Optimized Retrieval Model (ORM) and includes p, T and VMR retrieval components. The objective of the study was to develop physical and mathematical optimisations of a baseline retrieval scheme and to validate them against a set of test scenarios. A summary description of the algorithms implemented in the retrieval modules is reported here 2.4.4.1.3.1. . Full details of these algorithms are reported both in the Level 2 Algorithm Theoretical Baseline Document (ATBD) 2.4.4.1.1.1. and in Ridolfi M.and CO Ref. [1.58].

2.4.4.1.1.1 Level 2 Algorithms Theoretical Baseline Document (ATBD)

Click here to download a .pdf file (1.9 Mb) containing the MIPAS Level 2 ATBD.

2.4.4.1.2 The Level 2 pre-processor

Tasks performed by the the Level 2 Framework Processor

The overall loop structure for the processing of one product is

- Read Level 1b Product and Auxiliary Files
- Perform Preprocessing
- For each selected Scan of the Product
- Compute Initial Guess 2.4.4.1.2.1. for p,T Retrieval 2.4.4.1.3.3.
- Perform p,T Retrieval 2.4.4.1.3.3.
- Receive/Store p,T Retrieval Results
- For all selected VMR Retrievals :
- Compute Initial Guess 2.4.4.1.2. for VMR Retrieval
- Perform VMR Retrieval 2.4.4.1.3.3.
- Receive/Store VMR Retrieval Results
- End of Loop over all Retrievals
- End of Loop over all selected Scans
- Write Level 2 Product

All tasks except the p,T retrieval and the VMR retrievals are performed by the framework processor modules, while the retrieval modules are collected in the retrieval component library (RCL).

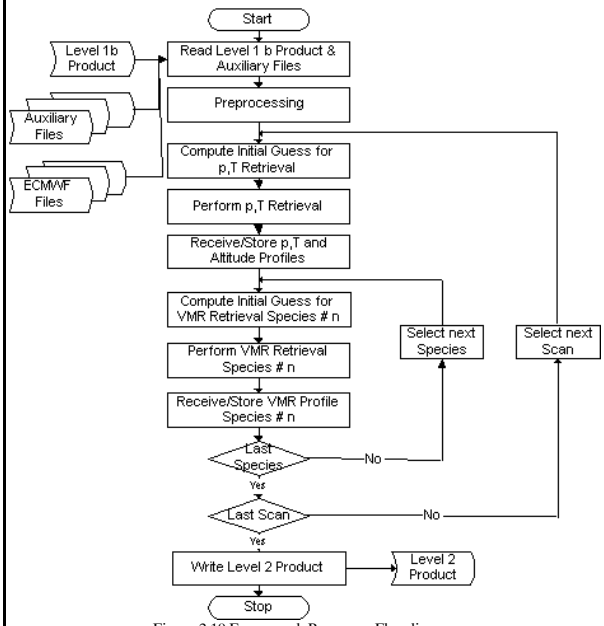

Figure 2.19 Framework Processor Flowdiagram

Preprocessing Preprocessing consists of the following steps:

- For each selected scan of the product
- Check Health of Level 1b Data
- Selection of Microwindows
- Extraction of Spectral Data from the Level 1b Product
- Apodisation of Selected Spectral Data
- Compute Apodised Instrument Lineshape for each Microwindow
- Compute Variance Co-variance Matrix of the Observations
- end of loop over all scans

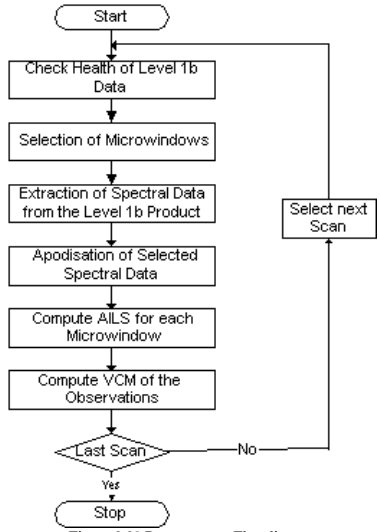

Figure 2.20 Preprocessor Flowdiagram

Check Health of Level 1b Data The purpose of this function is to determine the spectral data of each scan, that may be used for the retrievals.

All information on quality of MIPAS measurement data is contained in the Level 1b product. In a first step the quality indicator (PCD) contained in the Measurement Data Structure (MDS) of the Level 1b product is evaluated for each measured tangent altitude (sweep) of the scan. If health checking proofs that spectral data related to a particular tangent altitude (sweep) is corrupted, a logical flag will be set equal to "false" indicating that those spectral data are not used during p,T retrieval and VMR retrievals for this scan. Corruption of spectral data may concern a single spectral band or all spectral bands (in total five bands).

Beside quality indicators (PCD), the MDS-DSR contains information on uncorrected / remained spikes in interferograms. This information is also evaluated in order to identify spectral bands corrupted by spectral artifacts caused by possible spiking (e.g. by cosmic radiation) occurred during recording of interferograms onboard the instrument. Spectral bands corrupted by spikes are also flagged by setting a logical variable equal to "false" so that no spectral data related to those spectral bands will be extracted for p,T and VMR retrieval.

Output of this function are two logical vectors which are evaluated by the function "Selection of Microwindows".

Selection of Microwindows The purpose of this function is to select a optimized set of microwindows 2.4.4.1.3.1. for each retrieval and each scan.

The information on a variety of spectral intervals valid for p,T and VMR retrieval, called microwindows (MW´s), is stored in the microwindow database 2.4.4.4. . A dedicated set of MW´s to be used for each retrieval and scan is called a MW a occupation matrix. Those latitude dependent occupation matrices are stored in the occupation matrix database 2.4.4.4. (MIP_OM2_AX) which may be replaced occasionally to take into account seasonal effects or different measurement scenarios. The matrix elements of each occupation matrix identify which MW (identified by the columns) at which sweep (identified by rows) shall be selected and thus the matrix elements of an occupation matrix uniquely identify the spectral data points to be extracted from the Level 1b product.

The algorithm will select the first occupation matrix in the file which :

- is valid for the scans latitude
- has the correct number of sweeps
- is valid for the altitudes of sweeps

and does not make use of corrupted data (see Check Health of Level 1b Data).

If no valid occupation matrix is found the corresponding retrieval of the scan will be skipped. If no valid occupation matrix for the p,T retrieval is found , all retrievals of the scan will be skipped.

Table 2.1 Example of an Occupation Matrix

Sweep\Microwindow	PT__0169	PT__0175	PT_0218
Sweep 0	FALSE	TRUE	TRUE
Sweep 1	FALSE	TRUE	TRUE
Sweep 2	FALSE	TRUE	TRUE
Sweep 3	TRUE	TRUE	TRUE
Sweep 4	TRUE	FALSE	TRUE
Sweep 5	FALSE	FALSE	TRUE
Sweep 6	FALSE	FALSE	TRUE
Sweep 7	TRUE	TRUE	TRUE
Sweep 8	TRUE	TRUE	TRUE
Sweep 9	TRUE	TRUE	TRUE
Sweep 10	TRUE	TRUE	FALSE
Sweep 12	TRUE	TRUE	FALSE
Sweep 13	TRUE	TRUE	FALSE
Sweep 14	FALSE	TRUE	FALSE
Sweep 15	FALSE	TRUE	FALSE

To each occupation matrix a logical retrieval vector is associated. This vector defines the altitudes of the retrieved profile. Usually this is foreseen to be identical to the altitudes of the sweeps, but in general case it may be only a subset.

Note: The occupation matrix database references the used microwindows by name (label). The information defining the microwindows themselves is contained in the microwindow database. Therefore the occupation matrix database and microwindow database are closely linked, and it is essential to select a consistent pair of them for each processing run.

Extraction of Spectral Data from the Level 1b Product This function extracts for each sweep the spectral data points related to the cut-off wavenumbers (first and last wavenumber) of the microwindows plus some additional data points which are needed to perform resampling (if necessary) and apodisation of spectral data.

The maximum resolution of the MIPAS instrument is the inverse of the maximum path difference of the interferometer (1/40 cm = 0.025 cm-1). The instrument can also be operated with a smaller optical path difference, which will allow to increase the possible number of sweeps within a scan. Spectral resolution will be lower in this case. On the other hand the retrieval modules need to receive the spectral data always on a fixed (PS2 setting) grid called the "general coarse wavenumber grid". Therefore resampling of level 1b spectral data is necessary if the spectral grid of input spectra deviates from the general coarse

wavenumber grid. Nominally, the spectral grid of level 1b spectra and the general coarse wavenumber grid are identical, resampling is expected being a non routinely performed operation.

If the spectral grid of Level 1b spectra deviates from the general coarse wavenumber grid the following two cases have to be considered:

- Input spectra are given on a spectral grid which is a multiple integer of the general coarse wavenumber grid. In this case input spectra simply need to be undersampled, i.e. one sample is taken out of N samples.
- Input spectra are given on a spectral grid which is not a multiple integer of the general coarse wavenumber grid. In this case spectral interpolation of Level 1b input spectra to the general coarse wavenumber grid is performed using an apodised sinc interpolation function.

Apodisation of Selected Spectral Data All observed spectral data is the result of the convolution of the instrument line shape with the atmospheric spectra entering the instrument. The instrument line shape (ILS) is a function looking similar to a sinc eq. 5.3 -function, hence has sidelobes with significant impact on the convolution result. As a consequence the forward model of the retrievals would have to consider spectral lines, which are many wavenumbers away from the selected microwindows. To avoid this, the influence of the sidelobes is suppressed by a convolution of the observations with an apodisation function. The resulting apodised observation is identical to the convolution of the atmospheric spectra entering the instrument with the apodised instrument line shape AILS.

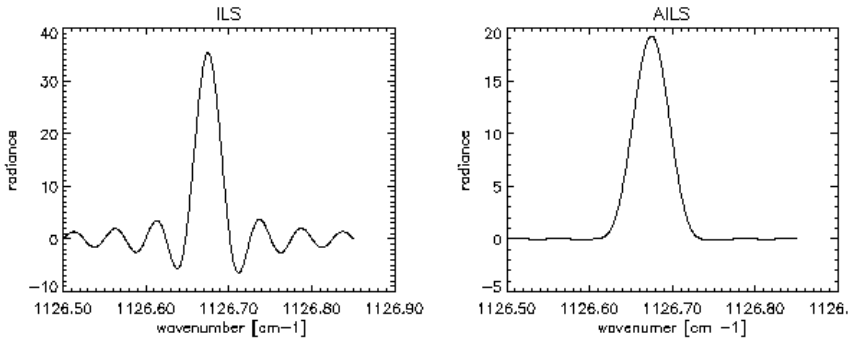

Figure 2.21 Example of ILS and AILS

To summarize :

The spectra as found in the level 1b product are :

Observed spectra = Atmospheric Spectra x ILS eq 2.3

Apodisation leads to:

Apodised Spectra = (Atmospheric Spectra x ILS) x Apodisation Function eq 2.4

During the retrievals least square fit the simulated apodised spectra are computed according to:

Simulated Apodised Spectra = Simulated Atmospheric Spectra x eq 2.5
(ILS x Apodisation Function)

where (ILS x Apodisation Function) is called the AILS.

Compute Apodised Instrument Lineshape for each Microwindow As explained in the section "Apodisation of Selected Spectral Data" the retrieval modules will have to convolute the simulated atmospheric spectra with the apodised instrument lineshape AILS. The AILS is computed by the preprocessor using auxiliary data from the PS2 file. The exact shape of AILS is a function of the wavenumber. The change of the AILS shape within the small range of wavenumbers within one microwindow can be neglected, while the change from one microwindow the next has to be considered. Therefore one AILS is computed for each microwindow using the microwindows central wavenumber.

The AILS is computed in two steps:

- Compute the ILS
- Convolute the ILS with the Apodisation Function

where the apodisation function must be identical to the one use for apodisation of the spectral data. The MIPAS level 2 processor uses the Norton Beer function that purpose (see Norton R. H., R.Beer Ref. [1.54]).

Compute Variance Covariance Matrix of the Observations The least square fit performed during the retrievals will take into account the accuracy of the measurements, allowing bigger deviations between simulation and observation where variance is big and small deviations where the variance is small. The standard deviation of each measurement is defined by the NESR , which is reported in the level 1b product as function of wavenumber. The measurements at different wavenumbers are assumed to be independent, but the processing step of Apodisation of Selected Spectral Data introduces a correlation between the apodised spectral data points used by the retrieval. Another correlation is added in the case that the measurement have to interpolated to the nominal processing grid (see Extraction of Spectral Data from the Level 1b Product). Therefore the Variance Covariance Matrix of the Observations VCM^{obs} has non zero off-diagonal elements. Since the preprocessing does not introduce correlations between spectral data of different microwindows or altitudes the VCM of the observations holds non zero values only in small quadric sub matrices along the main diagonal. Each sub-matrix is the VCM of one microwindow at a certain altitude. Each of this sub matrices is computed by preprocessor and passed to the retrieval modules.

Note: The VCM of the observations is not the VCM reported in the level 2 product. The level 2 product contains the variance and covariance data of the retrieved quantities.

2.4.4.1.2.1 The Initial Guess Processor

The first iteration of each retrieval starts with profiles called "initial guess". During the retrieval these profiles will be iteratively updated such that the deviation from simulated spectra to observed spectra is minimized.

The purpose of the initial guess processor is to provide an optimized set of initial guess profiles in order to reduce the number of iterations needed during the retrieval. Since the runtime of the retrieval is directly proportional to the number of iterations, it is of major importance to find a good initial guess.

Please note that for each retrieval only a subset of the initial guess profiles in varied, while the others are fixed. In the p,T retrieval the VMR profiles will not be modified, but used. In each VMR retrieval only one VMR species is retrieved, while p,T, altitude and the other VMR profiles a are kept fixed. The p,T retrieval will be the first retrieval for each scan, the order of the other VMR retrievals can be defined by PS2 settings (see also here 2.4.4.1.3.1.).

For the details of the initial guess processor see Framework-DPM section.
Input to the Initial Guess Profiles The initial guess processor uses several sources of profiles to compute the best initial guess set of profiles for each retrieval. They are listed and explained in this section.
IG2 file Contains climatological profiles (p,T,VMR and continua). Profiles are different for different latitude bands (altitude range: 0-120 km). They are generated from long term climatological observations. Profiles from this source will be called IG2 profiles in the following.
ECMWF files Contain profiles for geopotential, temperature, relative humidity and ozone on a fixed pressure grid. Geopotential can be converted to altitude (altitude range:~ 0-25.5 km), relative humidity to H20-VMR. ECMWF profiles depend on latitude and longitude. Each ECMWF profile may be flagged invalid independently of the other profiles. ECMWF profiles are delivered by the European Center of Midrange Weather Forecast every 6 hours, each profile type in a separate file. Profiles from this source will be called ECMWF profiles in the following.
FM2 (Forward Model File) The idea of the Forward Model File is, that for a given initial guess from IG2 file and given settings from PS2 auxiliary file the simulated spectra computed in the first iteration of p,T retrieval are determined. Therefore they can be pre-computed off-line.

The FM2 file contains precomputed spectra, the jacobian 2.4.4.1.3.3.2. and microwindow grouping for a standard p,T retrieval scenario (nominal occupation matrix). Furthermore it contains the full IG2 data used to generate the FM2 file. Spectra and jacobian 2.4.4.1.3.3.2. are computed for different altitudes in this file. When the FM2 is used, interpolation to the current altitudes is performed. FM2 information is latitude dependent. Most probably, FM2 usage saves the first iteration. FM2 files contain a reference to the PS2 settings -file used,

when the FM2 file was generated. If this file does not agree with the PS2 file used in the current retrieval, FM2 usage will be rejected. Whenever a FM2 file is selected to be used by the workorder file of MIPAS level 2 processor, IG2 information must be taken from this file. Therefore FM2 file may be thought of as an enhanced IG2 file . The processing of one product may use either IG2 file or FM2 file. For details of FM2 usage see also Framework-DPM.

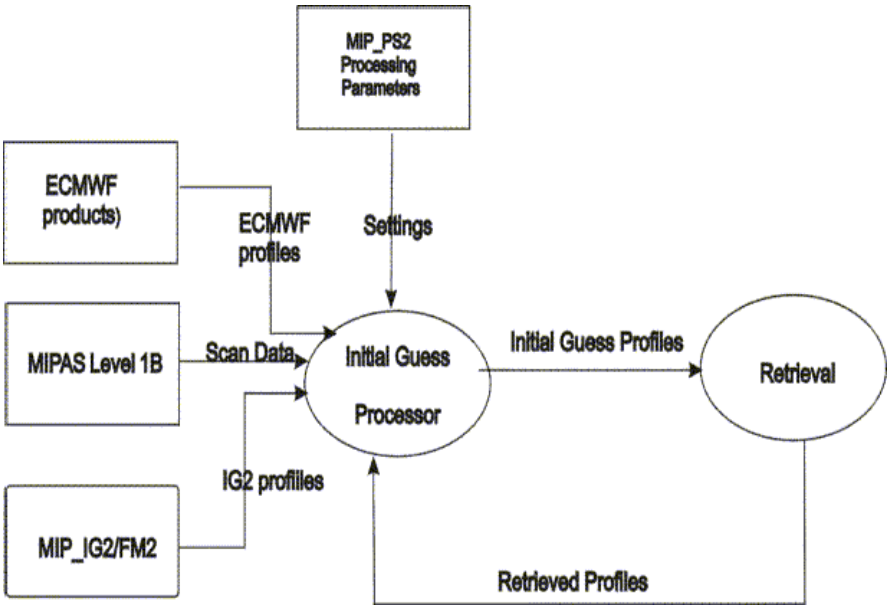

Figure 2.22 Dataflow of Initial Guess Processor

Retrieved Profiles The most recent information available on the pressure, temperature and VMR profiles are the profiles retrieved by the MIPAS level 2 processor itself. Therefore the initial guess processor is able to make use of its own retrieval results.

Retrieved profiles may originate from the same scan (but a preceding retrieval) as the current retrieval or from any preceding processed scan of the current product. Because of the usage of the retrieved profiles, the Initial Guess Processor must not be part of the preprocessing, but part of the processing main loop. Initial Guess Processor Algorithm The initial guess processor strategy is that the source of initial guess should be as near in time and space (latitude/longitude) as possible to the currently processed scan. Therefore retrieved profiles are preferred to ECMWF profiles, and ECMWF profiles are preferred to IG2 profiles. Only in cases of p,T retrieval with no retrieved profiles and no ECMWF data available precomputed spectra (FM2) shall be used. Merging of Profiles ECMWF profiles do not cover the full altitude range needed and have to be extended with scaled IG2 data. This operation will be called "merging". A Priori Profiles: If ECMWF data is used "a priori profiles" are the result of merging IG2 profiles with ECMWF data. If only IG2 profiles are used, "a priori profiles" are identical to IG2 profiles. Usage of Retrieved Profiles When retrieved profiles are available three cases have to be considered:

- An initial guess for pressure, temperature and altitude is needed for VMR retrieval.

- In nominal processing this shall always be the result of the p,T retrieval of the current scan. The retrieved p,T and altitude profile will be used without change. If p,T retrieval fails the VMR retrievals of the current scan shall be skipped.
- An initial guess for a VMR profile is needed for VMR or p,T retrieval.
- The initial guess will be computed as optimum estimate from retrieved profile and a priori profile. Optimum estimate is a weighted averaging using the VCM of the retrieved profile , and a VCM computed from PS2 settings for the a priori profile.
- An initial guess is needed for pressure, temperature and altitude for a p,T retrieval.
- In this case temperature profile will be computed by optimum estimate. For pressure no computations are performed, because pressure will be used as the free parameter to define the grid. Altitudes will be computed using hydrostatic equilibrium and one altitude value from a priori profile.

Initial Guess for Continuum Profiles Initial guess continuum profiles will always be taken from IG2 (FM2), because :

- ECMWF data does not contain information for continua

- Usage of retrieved continua is difficult, because of their strong altitude dependency and the fact of necessary exponential (= linear with pressure) extrapolation/interpolation for "holes" in occupation matrix and "holes" caused by micro-window grouping.

Go back to Mipas level 2 processing introduction 2.4.4.

2.4.4.1.3 The retrieval modules

2.4.4.1.3.1 General features of the adopted approach

In contrast with the data processing of already flown operational limb sounding instruments (e.g. on the Nimbus-7 and UARS Satellites), which have been mainly of radiometric type, MIPAS data analysis will be confronted with the exploitation of broad band and high resolution spectral measurements which contain information about several atmospheric constituents that are each observed in several spectral elements. The multiplicity of unknowns and the redundancy of the data to be handled lead to the adoption of a retrieval strategy based upon the following three choices.

2.4.4.1.3.1.1 Use of Microwindows

The redundancy of information coming from MIPAS measurements makes it possible to

select a set of narrow (less than 3 cm^{-1} width) spectral intervals containing the best information on the target parameters, while the intervals containing little or no information can be ignored. The use of selected spectral intervals, called 'microwindows', allows the size of analyzed spectral elements to be limited and avoids the analysis of spectral regions which are characterized by uncertain spectroscopic data, interference by non-target species, Non-Local Thermal Equilibrium (NLTE) and line mixing effects. More generally, priority can be given to the analysis of spectral elements with most information on the target species and less affected by systematic errors, e.g. for VMR retrievals transitions with weak temperature dependence can be preferred in order to minimize mapping of temperature uncertainties on to the resulting VMR vertical profiles. 2.4.4.3.

By analyzing the sensitivity of the radiance to changes of target parameters, lists of appropriate microwindows have been selected for the retrieval of H_2O, O_3, HNO_3, CH_4, N_2O and NO_2 as well as for the joint retrieval of pressure and temperature Clarmann T. v., A. Dudhia, and CO Ref. [1.17] . A microwindow database 2.4.4.4. has been created and is currently being refined with respect to minimization of retrieval errors, following the approach illustrated in Clarmann T. v., and G. Echle Ref. [1.28] .

2.4.4.1.3.1.2 Sequential retrieval of the species

The unknowns of the retrieval problem are:

- the observation geometries, that are identified by the 'tangent pressures', i.e. the values of pressure corresponding to the tangent points of the limb measurements (pressure is the independent variable and it is used as the altitude coordinate of all the profiles) ;
- the profile of temperature;
- the profile of VMR of the five target species;
- the atmospheric continuum, that includes all the emission sources that are frequency independent within a microwindow.
- zero-level calibration correction, that accounts for additive microwindow dependent offsets that could remain uncorrected after Level 1b 2.4.3.2. processing.

These unknowns are retrieved using the following sequence of operations. First temperature and 'tangent pressures' are retrieved simultaneously (p,T retrieval), then the target species VMR profiles are retrieved individually in sequence. The reason of this approach is that a simultaneous retrieval of all the species would require a huge amount of computer memory, because the size of the matrices to be handled by the retrieval is proportional to the product between the unknown parameters and the number of observations.

The feasibility of the simultaneous retrieval of pressure and temperature has been investigated in Carlotti M., and M. Ridolfi Ref. [1.13] and Clarmann T. v., A. Linden,and CO Ref. [1.19] . Simultaneous p,T retrieval exploits the hydrostatic equilibrium assumption, that provides a relationship between temperature, pressure and geometrical altitude. The use of the hydrostatic equilibrium assumption is discussed in this section eq. 2.37 .

The sequence of the target species retrieval has been determined according to the degree of their reciprocal spectral interference and is: H_2O, O_3, HNO_3, CH_4, N_2O and NO_2 .

In p, T retrieval the quantities to be fitted are the 'tangent pressures', the temperature profile sampled in correspondence of the 'tangent pressures' and the parameters of atmospheric continuum and zero-level calibration correction. In each VMR retrieval, the fitted quantities are the VMR altitude distribution of the considered gas sampled at the tangent pressures and the parameters of atmospheric continuumand instrumental zero-level calibration correction.

2.4.4.1.3.1.3 Global Fit analysis of the Limb-Scanning sequence

A global fit approach Carlotti M Ref. [1.15] is adopted for the retrieval of each vertical profile. This means that spectral data relating to a complete limb scan sequence are fitted simultaneously. Compared to the onion-peeling method McKee T. B., R. I. Whitman, J. J. Lambiotte jr Ref. [1.52] , Goldman A., R. S. Saunders Ref. [1.42] , the global fit provides a more comprehensive exploitation of the information and a rigorous determination of the correlations between atmospheric parameters at the different altitudes. Besides, it permits the full exploitation of hydrostatic equilibrium condition and is better compatible with the modeling of the finite field of view (FOV) of the instrument.

2.4.4.1.3.2 Mathematics of the retrieval

In the inversion algorithm the syntetic spectra simulated using a radiative transfer model (forward model) through an inhomogeneous atmosphere are fitted to the observed spectra. The simulations are fitted to the observations by varying the input parameters of the model (such as pressure, temperature, VMR, etc...) according to a non-linear Gauss-Newton procedure. Further details of the mathematics of the retrieval model can be found here 2.4.4.1.3.2.1. .

2.4.4.1.3.2.1 Details

The problem of retrieving the altitude distribution of a physical or chemical quantity from limb-scanning observations of the atmosphere falls within the general class of problems that requires the fitting of a theoretical model, describing the behavior of the observed system, to a set of available observations Ref. [1.65], Ref. [1.41], Ref. [1.53], Ref. [1.61].

The instrument observes the radiance $L(\tilde{\nu},\theta)$ emitted by the atmosphere at different values of the spectral frequency $\tilde{\nu}$ and of the limb-viewing angle θ. The theoretical model (or forward model $F(\mathbf{p},\mathbf{q})$) simulates the observations through a set of parameters p and q: p represents

the quantities that affect the radiance but are not retrieved, and q the quantities that are retrieved, i. e. the distribution profile of the atmospheric quantity under investigation.

The retrieval procedure consists of the search for the set of values of the parameters q that produces the "best" simulation of the observations.

It has to be noted that the real atmospheric profile is a continuous function, but, since there will always be a finite number of measurements (n), in order to constrain the problem, the unknown function is approximated with a discrete representation that we indicate with a vector x of dimension m, where m < n. Between the m discrete points, an interpolated value is then used in the forward model.

Assuming a normal (Gaussian) distribution for the measurement errors, the approach generally used for determining the parameters which produce the best simulation of the observation is the least-square fit. This procedure, deriving from the theory of the maximum likelihood estimation Ref. [1.61], looks for the solution x that minimizes the χ^2 function, defined as the square summation of the differences between observations and simulations, weighted by the measurement noise.

Given n measurements S_i and the corresponding simulations $F_i(p, \tilde{\mathbf{x}})$ calculated by the forward model using the assumed profile $\tilde{\mathbf{x}}$, and calling n the vector of the differences between observations and simulations and V_n the variance-covariance matrix (VCM) associated to the vector n, the quantity to be minimized with respect to the unknown parameters x is:

$$\chi^2 = \mathbf{n}^T \mathbf{V}_n^{-1} \mathbf{n} \qquad \text{eq 2.6}$$

If the observations are suitably chosen, matrix V_n is not singular and its inverse exists. However, in case the spectrum is sampled on a grid finer than 1/(2 * MPD) where MPD is the Maximum Path Difference, the inverse of matrix V_n does not exist. In this case the generalized inverse Ref. [1.46] of V_n is used in equation eq. 2.6 .

In general, the observations do not depend linearly on the unknown parameters x. As a consequence equation eq. 2.6 is not a quadratic function of the unknowns, and an analytic expression for the values of the unknowns which minimizes equation eq. 2.6 cannot be determined.

However, sufficiently close to the minimum, we may assume that the χ^2 function is well approximated by a quadratic form, obtained expanding equation eq. 2.6 in the Taylor series about the initial guess profile:

$$\chi^2(\mathbf{x}) = \chi^2(\tilde{\mathbf{x}}) + \nabla\chi^2\,\mathbf{y} + \frac{1}{2}\,\mathbf{y}^T \nabla^2 \chi^2\,\mathbf{y} \qquad \text{eq 2.7}$$

where ∇ and ∇^2 indicate respectively the gradient and the Hessian matrix of the χ^2 function and $\mathbf{y} = \mathbf{x} - \tilde{\mathbf{x}}$ is a vector of dimension m, providing the correction to be applied to the assumed value of parameter $\tilde{\mathbf{x}}$ in order to obtain its correct value x.

Writing the gradient and the Hessian matrix of the χ^2 function explicitly, and indicating with K the Jacobian matrix, i.e. a matrix of n rows and m columns, whose entry k_{ij} is the derivative of simulation i made with respect to parameter j, we obtain:

$$\chi^2(\mathbf{x}) = \chi^2(\tilde{\mathbf{x}}) - 2\left(\mathbf{K}^T\mathbf{V}_n^{-1}\mathbf{n}\right)^T\mathbf{y} + 2\,\mathbf{y}^T\left(\mathbf{K}^T\mathbf{V}_n^{-1}\mathbf{K} - \frac{\partial\mathbf{K}}{\partial\mathbf{x}}\mathbf{V}_n^{-1}\mathbf{n}\right)\mathbf{y} \qquad \text{eq 2.8}$$

If the problem is linear or if near the minimum the residuals have a null average, the term with $\partial\mathbf{K}/\partial\mathbf{x}$ can be neglected in equation eq. 2.8 and the value of y which minimizes the χ^2 function is the Gauss-Newton solution Ref. [1.41]:

$$\mathbf{y} = (\mathbf{K}^T\mathbf{V}_n^{-1}\mathbf{K})^{-1}\mathbf{K}^T\mathbf{V}_n^{-1}\mathbf{n} \qquad \text{eq 2.9}$$

Therefore, the solution matrix of the inverse problem, defined as the matrix that calculates the unknowns from the measured quantities, is equal to:

$$\mathbf{D} = (\mathbf{K}^T\mathbf{V}_n^{-1}\mathbf{K})^{-1}\mathbf{K}^T\mathbf{V}_n^{-1} \qquad \text{eq 2.10}$$

If the hypothesis of linearity is not satisfied, with this procedure the minimum of the χ^2 function is not reached but only a step is done toward the minimum. The vector $\mathbf{x} = \mathbf{y} + \tilde{\mathbf{x}}$, with y computed using equation eq. 2.9 , represents only a better estimate of the parameters than $\tilde{\mathbf{x}}$. In this case the whole procedure must be reiterated starting from the new estimate of the parameters (Newtonian iteration) and equation eq. 2.9 has to be written as:

$$\mathbf{x}_{iter} - \mathbf{x}_{iter-1} = (\mathbf{K}_{iter-1}^T\mathbf{V}_n^{-1}\mathbf{K}_{iter-1})^{-1}\mathbf{K}_{iter-1}^T\mathbf{V}_n^{-1}\mathbf{n}_{iter-1} \qquad \text{eq 2.11}$$

where iter indicates the iteration index, $\mathbf{x}_{iter-1}$ the result of the previous iteration, $\mathbf{K}_{iter-1} = \partial\mathbf{F}(\mathbf{p}, \mathbf{x}_{iter-1})/\partial\mathbf{x}_{iter-1}$ the Jacobian relative to the profile $\mathbf{x}_{iter-1}$, $\mathbf{n}_{iter-1} = \mathbf{S} - \mathbf{F}(\mathbf{p}, \mathbf{x}_{iter-1})$ the residuals.

Convergence criteria are therefore needed in order to establish when a value close enough to the minimum of the χ^2 function has been reached. However, this procedure is successful only in the case of sufficiently weak non-linearities. If we start from a position of the χ^2 function that is far from the minimum, its second order expansion may be a poor approximation of the shape of the function, so that the calculated correction can be misleading, and increase rather than decrease the residuals. For this reason, a modification of the Gauss-Newton method, the Levenberg Ref. [1.47] - Marquardt Ref. [1.51], Ref. [1.56] method, is used. The modification involves the introduction in equation eq. 2.11 of a factor λ which reduces the amplitude of the parameter correction vector.

$$\mathbf{x}_{iter} - \mathbf{x}_{iter-1} = (\mathbf{K}_{iter-1}^T\mathbf{V}_n^{-1}\mathbf{K}_{iter-1} + \lambda\mathbf{I})^{-1}\mathbf{K}_{iter-1}^T\mathbf{V}_n^{-1}\mathbf{n}_{iter-1} \qquad \text{eq 2.12}$$

The factor λ is initialized to a user-defined (less than 1) number, and during the retrieval iterations it is increased or decreased depending on whether the χ^2 function increases or decreases. At convergence the Levenberg - Marquardt method provides the same solution that is obtained with equation eq. 2.11 because they aim at the same minimum of the χ^2

function.

If V_n is a correct estimate of the errors of the observations and the real minimum of the χ^2 function is found, the quantity defined by equation eq. 2.6 has an expectation value of (n - m) and a standard deviation equal to $\sqrt{n-m}$. The value of the quantity $\chi^2/(n-m)$ provides therefore a good estimate of the quality of the retrieval. Values of $\chi^2/(n-m)$ that deviate too much from unity indicate the presence of incorrect assumptions in the retrieval.

The errors associated with the solution of the inversion procedure can be characterized by the variance-covariance matrix V_x of x given by:

$$\mathbf{V_x} = \mathbf{D}_c \mathbf{V}_n \mathbf{D}_c^T = (\mathbf{K}_c^T \mathbf{V}_n^{-1} \mathbf{K}_c)^{-1} \qquad \text{eq 2.13}$$

where D_c and K_c are respectively the solution matrix and the Jacobian matrix evaluated at convergence.

Matrix V_x maps the experimental random errors onto the uncertainty of the values of the retrieved parameters. Actually, the square root of the diagonal elements of V_x measures the root mean square (r.m.s.) error of the corresponding parameter. The off-diagonal element $(V_x)_{ij}$ of matrix V_x, normalized to the square root of the product of the two diagonal elements $(V_x)_{ii}$ and $(V_x)_{jj}$, provides the correlation coefficient between parameters i and j.

According to the theory of maximum likelihood, if an a-priori information on the unknown parameters is available, (x_a and V_a^{-1} being respectively the vector containing the a-priori values of the unknown and its VCM) the χ^2 expression to be minimized is Ref. [1.59]:

$$\chi^2 = (\mathbf{x} - \mathbf{x}_a)^T \mathbf{V}_a^{-1} (\mathbf{x} - \mathbf{x}_a) + \mathbf{n}^T \mathbf{V}_n^{-1} \mathbf{n} \qquad \text{eq 2.14}$$

and equation eq. 2.11 becomes:

$$\mathbf{x}_{iter} - \mathbf{x}_{iter-1} = (\mathbf{K}_{iter-1}^T \mathbf{V}_n^{-1} \mathbf{K}_{iter-1} + \mathbf{V}_a^{-1})^{-1} \left(\mathbf{K}_{iter-1}^T \mathbf{V}_n^{-1} \mathbf{n}_{iter-1} + \mathbf{V}_a^{-1} (\mathbf{x}_{iter-1} - \mathbf{x}_a)\right) \qquad \text{eq 2.15}$$

while equation eq. 2.13 becomes:

$$\mathbf{V_x} = (\mathbf{K}_c^T \mathbf{V}_n^{-1} \mathbf{K}_c + \mathbf{V}_a^{-1})^{-1} \qquad \text{eq 2.16}$$

If we assume that the complementary information consists of a vector n_1 with a VCM V_{n_1} connected by the Jacobian K_1 to the unknowns y, equation eq. 2.15 can be written as:

$$\mathbf{x}_{iter} - \mathbf{x}_{iter-1} = \left[\mathbf{K}_{iter-1}^T \mathbf{V}_n^{-1} \mathbf{K}_{iter-1} + \mathbf{K}_1^T \mathbf{V}_{n_1}^{-1} \mathbf{K}_1\right]^{-1} \left[\mathbf{K}_{iter-1}^T \mathbf{V}_n^{-1} \mathbf{n}_{iter-1} + \mathbf{K}_1^T \mathbf{V}_{n_1}^{-1} \mathbf{n}_1\right] \qquad \text{eq 2.17}$$

This expression, which is implicitly used in equation eq. 2.9 for the combination of the information provided by independent microwindows, is used for the exploitation of non-radiometric information (external information). In section 5.1. the problems associated

with the use of external information on the unknown parameters will be reviewed on the light of the choices implemented in the MIPAS Level 2 retrieval modules.

2.4.4.1.3.3 Main components of the retrieval

As already stated in the previous section, the objective of the retrieval program is the determination of the atmospheric parameters that better fit the simulations to the observations.

Starting from some first-guess values of the unknown parameters 2.4.4.5. and using information on observation geometry and instrumental characteristics, the forward model computes the simulated spectra, which are compared with the measured spectra provided by MIPAS Level 1b processor 2.4.3.2. . The difference between simulated and measured spectra provides the vector of the residuals used to evaluate the cost function (χ^2) to be minimized (see mathematical details here) 2.4.4.1.3.2.1. . A new profile is generated by modifying the first guess with the corrections provided by the Gauss-Newton formula. The inversion requires the knowledge of the Jacobian matrix. The improved profile can be used as new guess for generating simulated spectra which are again compared with the measured ones. The iterative procedure stops when the convergence criteria are fulfilled.

The main components of the retrieval algorithm are therefore:

- forward model 2.4.4.1.3.3.1.
- jacobian calculation 2.4.4.1.3.3.2.
- convergence criteria 2.4.4.1.3.3.3.

2.4.4.1.3.3.1 Forward model

The purpose of the forward model is to simulate the spectra measured by the instrument in the case of known atmospheric composition. The signal measured by the spectrometer is equal to the atmospheric radiance which reaches the spectrometer modified by the instrumental effects, mainly due to the finite spectral resolution and the finite Field of View (FOV) of the instrument. The atmospheric radiance that reaches the instrument when pointing to the limb at tangent altitude z_t is calculated by means of the radiative transfer equation:

$$L(\tilde{\nu}, z_t) = \int_{x_t}^{x_0} \left[B(\tilde{\nu}, x) c(\tilde{\nu}, x) \eta(x) \right] \exp\left(- \int_{x}^{x_0} c(\tilde{\nu}, x') \eta(x') dx' \right) dx \qquad \text{eq 2.18}$$

where x is the position along the line of sight between the observation point x_0 and the point x_i at the farthest extent of the line of sight, B($\tilde{\nu}$, x) is the source function, c($\tilde{\nu}$,x) is the absorption cross-section, η(x) is the number density of absorbing molecules. The exponential term represents the atmospheric transmittance between x and x_0 . In the case of local thermodynamic equilibrium B($\tilde{\nu}$, x) is equal to the Planck function.

The measured signal S($\tilde{\nu}$,z_t) is simulated convolving the atmospheric limb radiance $L(\tilde{\nu},z_t)$ with the Apodized Instrument Line Shape (AILS, defined in section 2.4.4.1.3.3.1.5.) and with the MIPAS FOV function (FOV(z_t), discussed in section 2.4.4.1.3.3.1.6.):

$$S(\tilde{\nu},z_t) = \iint L(\tilde{\nu}-\tilde{\nu}',z_t-z_t')\,AILS(\tilde{\nu}')d\tilde{\nu}'\;FOV(z_t')dz_t' \qquad \text{eq 2.19}$$

The computation of equation eq. 2.18 and equation eq. 2.19 requires many operations that must be repeated for several variables, each with numerous values. The search for a sequence of operations that avoids repetition of the same calculations and minimizes the number of memorized quantities is the first objective of the optimization process.

The following sequence of operations has been chosen:
1. definition of the frequency grid in which the atmospheric radiance is calculated (section 2.4.4.1.3.3.1.1.);

2. definition of the tangent altitude grid of the simulations and of an atmospheric layering (common to all the simulations) used for discretising their radiative transfer integral; determination of the 'paths' (i.e. combination of layer and limb view) that require a customized calculation of the values of pressure and temperature and definition of the values of pressure and temperature characteristics of each of these 'paths' (section 2.4.4.1.3.3.1.2.);

3. computation of absorption cross-sections, relating to all the selected paths and all the gases (section 2.4.4.1.3.3.1.3.);

4. computation of radiative transfer integral (section 2.4.4.1.3.3.1.4.);

5. AILS convolution (section 2.4.4.1.3.3.1.5.);

6. FOV convolution (section 2.4.4.1.3.3.1.6.)
The implementation of each of these operations is described below.

2.4.4.1.3.3.1.1 Dependence on spectral frequency

Limb radiance spectra contain spectral features varying from the sharp, isolated, Doppler-broadened lines at high altitudes to wide, overlapping, Lorentz-broadened lines at low altitudes. In order to resolve the sharp features at high altitude, a 'fine grid' of spectral resolution of the order of 0.0005 cm^{-1} is required. Furthermore the overlapping wings at low altitudes require the grid to be ubiquitous. The choice of a small spacing implies a large number of spectral points and an equally large number of calculations.

However, even if a fine grid of 0.0005 cm^{-1} is needed, not all the points of this grid are equally important for the reconstruction of the spectral distribution and the full radiative transfer calculation needs only be performed for a subset of fine grid points, the remaining spectrum being recovered by interpolation. This subset is denoted the 'irregular grid' and depends on the microwindow boundaries and on the Instrument Line Shape.

In principle it is possible to determine an optimal irregular grid for each tangent altitude, taking advantage of the particular line broadening associated with each observation geometry. However, while this might lead to a reduction in total number of fine grid points for which radiative transfer calculations are required, this prevents the savings obtained with calculations common to all tangent altitudes. As a consequence, an irregular grid is determined which is valid for all tangent altitudes, and therefore common to all observation geometries.

The number of points that are selected for the irregular grid depends upon the interpolation law that is used for the reconstruction of the spectral distribution. Several interpolation functions were investigated, but since the same interpolation is also required for the calculation of Jacobian, which, unlike the radiances, can have negative values, logarithmic and inverse interpolations had to be discarded and finally a simple linear interpolation was chosen.

The procedure for the generation of the 'irregular grid' is to start with a set of complete fine grid limb radiance spectra for different tangent altitudes. Then, for each point, a `cost' function is determined, representing the maximum radiance error (at any altitude, after AILS convolution) that would arise if the point were to be replaced by an interpolated value. The point with the smallest interpolation cost is then eliminated and the process repeated for the remaining grid. The iteration continues until no further points can be removed without exceeding a maximum error criterion, chosen to be 10 % of the noise-equivalent signal radiance. In figure 2.23 an example of the high resolution radiance of a representative microwindow computed for the irregular grid points, as well as its convolved radiance and the difference between the original and interpolated radiance, is shown.

Typically it is found that only 5-10 % of the complete fine grid is sufficient for a satisfactory reconstruction of the spectral distribution.

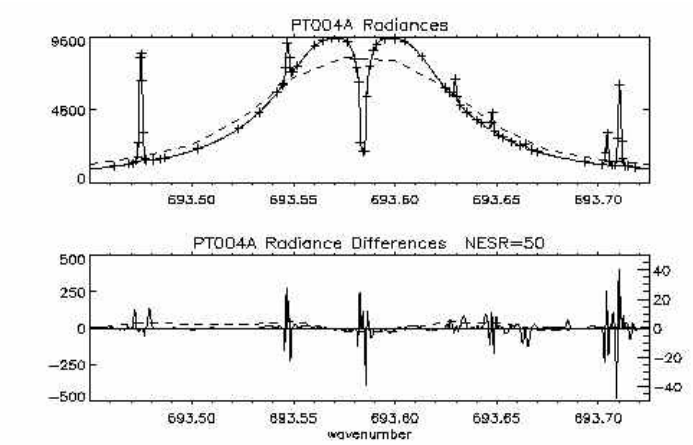

Figure 2.23 44 km tangent height spectral radiance from a microwindow (frequency range 693.45 - 693.725 cm⁻¹) selected for p, T retrieval. The upper plot shows the high-resolution radiance (solid line), the irregular grid points (+), and the convolved radiance (dashed line). The lower plot shows the difference between the original and interpolated radiances, on both the high-resolution grid (solid line, left axis) and the convolved radiances (dashed line, right axis).

2.4.4.1.3.3.1.2 Ray-tracing and definition of the atmospheric layering

The radiative transfer integral, given by equation, is a path integral along the line of sight in the atmosphere. The line of sight is determined by the viewing direction of the instrument and, due to refraction, is not a straight line, but bends towards the earth. The refractive index of air is a function of both pressure and temperature (the dependence on frequency is negligible in the spectral region of MIPAS measurements, as well as the dependence on water vapor, since MIPAS does not penetrate in the lower troposphere) and can be determined with the Edlen Edlen B. Ref. [1.32] model. Since the Earth is assumed locally spherical, the local radius of curvature being determined by the simplified WGS84 model Department of Defense Ref. [1.25] which has been adopted for the Earth shape, the atmospheric layering is spherical too. In these conditions, the optical path x is linked to the altitude r by the following expression:

$$dx = \frac{1}{\sqrt{1 - \frac{n^2(r_t)\, r_t^2}{n^2(r)\, r^2}}} dr \qquad \text{eq 2.20}$$

with r altitude referred to the earth center, n(r) refractive index and r_t tangent altitude.

Equation eq. 2.20 has a singularity at the tangent point ($r = r_t$), however the singularity can be removed by changing the integration variable from r to $y = \sqrt{r^2 - (r_t)^2}$.

It results that:

$$dy = \frac{dr}{\sqrt{1 + \frac{r_t^2\left(n^2(r) - n^2(r_t)\right)}{n^2(r)\,y^2}}} \qquad \text{eq 2.21}$$

and the limit of this expression for r --> r_t can be computed analytically considering the dependence of the refractive index, the pressure and the temperature on the altitude.

The path integral equation is computed as a summation over a set of discrete layers. A common set of layers is defined for all the spectra of the sequence. The boundaries of these layers are defined in correspondence of the grid of the simulated tangent altitudes. We recall that spectra are simulated at the tangent altitudes of the limb scan sequence and at some additional tangent altitudes that are used for the FOV convolution (as discussed in section 2.4.4.1.3.3.1.6.). Extra levels are added to the simulation grid as long as either the variation of temperature or the Voigt half-width of a reference line across each layer are greater than a maximum threshold supplied by the user.

For each layer that results from this process, appropriate 'equivalent' pressure and temperature, namely the Curtis-Godson Houghton J. T. Ref. [1.45] quantities, have to be determined. These are calculated weighting the pressure and temperature along the ray-path with the number density of each absorbing gas. This technique allows a coarse discretisation of the atmosphere to be implemented. The equivalent value of parameter G (pressure or temperature respectively) relative to the gas g, the layer l and the limb view t, is calculated as:

$$\left(G_e\right)_{g,l,t} = \frac{\int_{z_{l-1}}^{z_l} G(z)\, X_g(z)\, \eta(p(z),T(z))\, \frac{dx_t}{dz}\, dz}{col_{g,l,t}} \qquad \text{eq 2.22}$$

where z is the altitude, z_l and z_{l-1} are the heights of the boundaries of the layer, $X_g(z)$ is the VMR of the g-th gas, x_t is the line of sight characterized by the tangent altitude z_t , $\eta(p(z),T(z))$ is the air number density, and $col_{g,l,t}$ is the slant column relative to the considered gas, layer and limb view:

$$col_{g,l,t} = \int_{z_{l-1}}^{z_l} X_g(z)\, \eta(p(z),T(z))\, \frac{dx_t}{dz}\, dz \qquad \text{eq 2.23}$$

It has to be noted that in principle, Curtis-Godson pressures and temperatures have to be computed for each gas, each layer and each limb view. However, when the approximations of flat layers and straight line of sight are valid, both the numerator and the denominator of equation eq. 2.22 are proportional to the secant of the angle θ between the line of sight and the vertical direction and the same values of p_e and T_e are obtained independently of the limb angle. We have verified that the use of secant law approximation causes very small errors at all altitudes, except at the tangent layer, as it is shown in figure 2.24 .

In this approximation, since a layering common to all spectra of the scan is defined, it is

sufficient to calculate the values of p_e and T_e for all the layers of the lowest limb view, and only for the lowest layer of the other limb-views, all the other layers being characterized by the same values of p_e and T_e as the lowest limb view.

This optimization is crucial, not only because less equivalent pressures and temperatures have to be calculated, but mainly because absorption cross-sections have to be calculated and stored for a smaller number of p, T combinations.

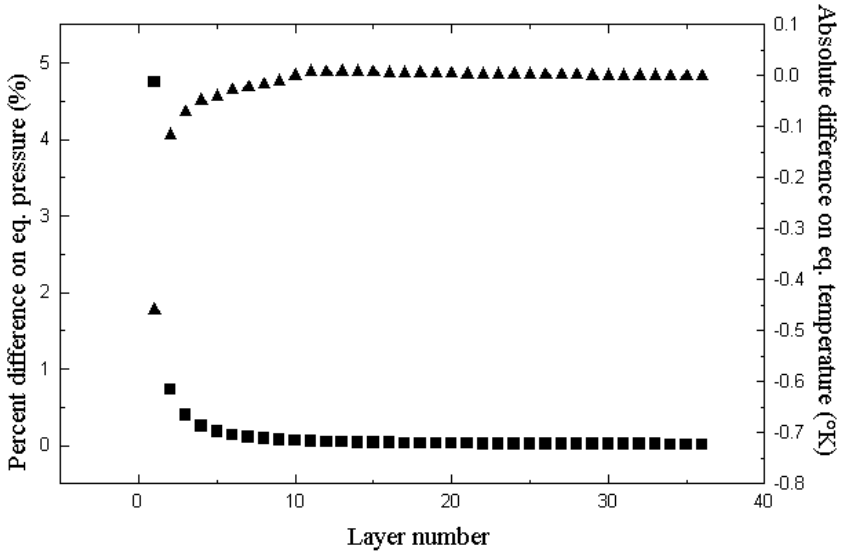

Figure 2.24 Differences between Curtis-Godson pressures and temperatures of the layers of the limb view with tangent altitude 30 km and the corresponding quantities of the same layers in the case of the lowest limb view (tangent altitude 6 km). On the left axis the percent differences on equivalent pressures (squares) are reported, on the right axis the absolute differences on equivalent temperature (triangle) are shown. The layers are counted from the tangent layer at 30 km and are 2 km thick.

2.4.4.1.3.3.1.3 Computation of cross-sections

The computation of cross-sections in equation is a very time consuming part of the forward model, due to the large number of spectral lines to be considered, the high spectral resolution required and the number of p, T combinations for which they have to be computed.

In the code the cross-sections can either be calculated line by line (LBL), using a pre-selected spectroscopic database and fast Voigt profile computation, or be read from look-up tables (LUTs).

The use of LUTs is advantageous only if they can be stored in random access memory (RAM), and the feasibility of this depends on the amount of memory required. Cross-section LUTs have to be tabulated for all the considered microwindows, for each absorber g, and for an appropriate range of p,T values. For a single microwindow (typical width 0.5 cm^{-1}), the number of data points required is of the order of:

1000 spectral pts. x 100 pressures x 10 temperature pts. = 10^6 grid points eq 2.24

A pictorial representation of a typical table is shown in figure 2.25 . For a retrieval, up to 100 such tables have to be stored (tens of microwindows with a few absorbers per microwindow), requiring too much memory for most practical applications.

In order to overcome this difficulty, the solution suggested by Strow in Strow L. L., H. E. Motteler Ref. [1.62] was adopted. It consists of compressing this information using `Singular Value Decomposition'. Any matrix K (m x n) can be decomposed as the product of three other matrices:

$$K = U\Sigma V \qquad \text{eq 2.25}$$

where U (m x n) and V (n x n) are orthonormal matrices, and Σ is a diagonal matrix containing n singular values. Assuming that most of the information is contained in the j ($<<$ n) largest singular values, the n dimension of the decomposition matrices can be truncated to give:

$$K \approx U' \Sigma' V' = U' W' \qquad \text{eq 2.26}$$

where the reduced matrices U' (m x j) and W' (j x n) are much smaller matrices than the original matrix K.

In this application, the matrix K contains the logarithm of the cross-section and is decomposed and stored as matrices U'($\tilde{\nu}$,j) and W'(j,x), where x represents any pair of (p,T) conditions. Typically the number j of singular values is less than 10, giving compression factors of the order of 10 - 100.

The number of singular values, as well as the number of pressure and temperature increments, are optimized so that the maximum difference between the resulting LUT and LBL convolved limb radiance is below the microwindow radiance noise criteria (equal to NESR/10). In figure 2.26 the differences between LUT and LBL limb radiances before and after AILS convolution are reported for a representative microwindow.

The combined use of irregular grids and LUTs means that the absorption cross-sections need only be reconstructed at a subset of fine grid points. Therefore the m dimension is effectively reduced by an order of magnitude, which usually makes U' the smaller of the two components of the LUT.

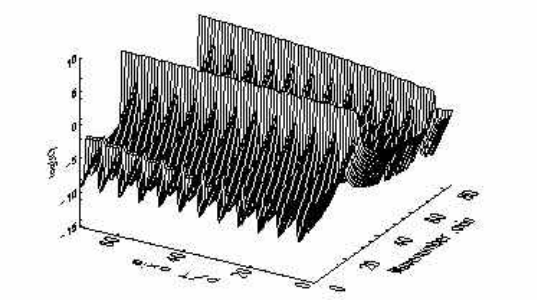

Figure 2.25 Plot of the logarithm of the CO₂ cross-section (k) tabulated for the spectral interval 693.45-693.725 cm<sup>-1. Each of the 12 major cycles in p, T axis corresponds to a different temperature, and within each are 6 different -ln) values varying from Lorentz to Doppler broadening.

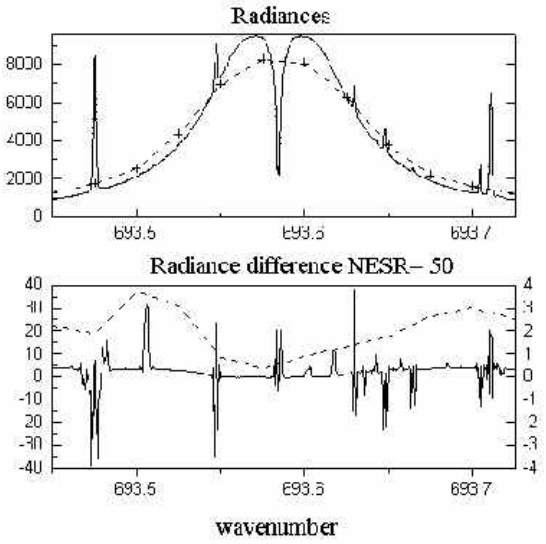

Figure 2.26 44 km tangent height radiance from a microwindow (frequency range 693.45 - 693.725 cm-1) selected for p,T retrieval. The upper plot shows the high-resolution radiance obtained with LBL calculation of cross-section (solid line) and with the use of LUTs (dotted line), as well as the convolved radiance (dashed line for LBL calculation and (+) for use of LUTs). The lower plot shows the difference between the two methods, before AILS convolution (solid line, left axis) and after AILS convolution (dashed line, right axis).

2.4.4.1.3.3.1.4 Computation of the radiative transfer integral

The radiative transfer integral (equation) is computed as a summation over discrete layers as follows:

$$L = \sum_{l=1}^{N} B_{l,t}\left(1-\exp\left(-\tau_{l,t}\right)\right)\left(\prod_{k=l+1}^{N}\exp\left(-\tau_{k,t}\right)\right) \qquad \text{eq 2.27}$$

where $\tau_{l,t}$ is the single layer optical depth:

$$\tau_{l,t} = \sum_{g=1}^{Ngas} c_{g,l,t} col_{g,l,t} + c_{cont\,l,t} col_{air\,l,t} \qquad \text{eq 2.28}$$

l = 1 and l = N (N is equal to twice the number of layers) are respectively the index of the farthest and the nearest integration step along the line of sight with respect to the observer, t is the index of the limb view, $B_{l,t}$ is the Planck function computed for the equivalent temperature of the main gas of the retrieval in layer l and limb view t. $c_{g,l,t}$ and $col_{g,l,t}$ are respectively the absorption cross section and the column of the gas g.

The second term of equation eq. 2.28 is the contribution to the single layer optical depth of all emission sources characterized by a constant amplitude in a microwindow, the so-called 'atmospheric continuum': $c_{cont\,l,t}$ is an altitude and microwindow dependent absorption cross-section, that is fitted by the retrieval program, $col_{air\,l,t}$ is the air column.

Since the atmosphere is assumed horizontally homogeneous and with a spherical symmetry, the computation of equation eq. 2.27 is further accelerated taking into account that the two contributions of the same layer from opposite sides of the tangent point are characterized by different transmissions, but by the same emission.

Therefore equation eq. 2.27 becomes:

$$L = \sum_{l=1}^{N/2} B_{l,t}\left(1-\exp\left(-\tau_{l,t}\right)\right)\left(1+\exp\left(-\tau_{l,t}\right)\prod_{k=l+1}^{N/2}\exp\left(-2\tau_{k,t}\right)\right)\prod_{j=1}^{l-1}\exp\left(-\tau_{j,t}\right) \qquad \text{eq 2.29}$$

This expression is computed at the irregular frequency grid and at the grid of the simulated tangent altitudes, i.e. the grid containing the measured limb views 5.3.5. and the additional ones needed for the FOV convolution (see section 2.4.4.1.3.3.1.6.).

The zero-level calibration correction (caused by self-emission of the instrument, scattering of light into the instrument or third order non-linearity of the detectors) has to be finally applied to the spectrum. This is performed adding to the atmospheric spectrum equation eq. 2.29 a microwindow dependent (but tangent altitude independent) offset which is then fitted by the retrieval program.

2.4.4.1.3.3.1.5 AILS convolution

The Instrument Line Shape (ILS) function is, by definition, the response of the spectrometer to a monochromatic radiance. In the case of a perfect Fourier transform spectrometer, observing a stable source of evenly distributed radiance, the ILS is equal to the convolution of the sinc eq. 5.3 function, associated with the finite spectral resolution of the instrument, with a term due to the finite angular aperture. If the angular aperture is circular, this term is equal to a rectangular function shifted in wavenumber and with a width that varies linearly with the wavelength Bell R. J. Ref. [1.2] . In a real instrument alignment errors and irregular angular aperture lead to a more elaborate ILS. Furthermore, the uneven distribution of the source radiance could introduce the major complication of a frequency and tangent altitude dependent ILS distortion. The atmospheric radiance at the limb is indeed characterized by an exponential energy distribution through the input diaphragm. Fortunately, it has been demonstrated Delbouille L. and G. Roland Ref. [1.24] that even the strongest exponential energy distribution across the field of view does not significantly affect the ILS. The main effect of the non-uniform energy distribution across the input aperture is instead that a significant difference can exist between the effective tangent altitude and the geometrical one, and this effect is taken into account by FOV convolution (section 2.4.4.1.3.3.1.6.).

The ILS function, which is an input of the forward model, is therefore a function independent of the tangent altitude and will take into account alignment and aperture effects, but not the instrument responsivity and phase error corrections, which are corrected for in the Level 1B 2.4.3.2. processing.

Measured MIPAS spectra are apodized before entering the retrieval process. This choice is dictated by the use of selected spectral intervals ('microwindows') for the retrieval of the VMR profiles. The advantages of using 'microwindows' have been already discussed in section 2.4.4.1.3.1.1. . The measured spectrum is equal to the convolution of the atmospheric spectrum with the ILS, and since the ILS is characterized by ' sidelobes' decreasing linearly in amplitude, the atmospheric signal at a given frequency affects the measured signal in a broad spectral interval. Therefore, the simulation of a narrow microwindow of the measured spectrum requires the calculation of a broad spectral interval. Apodization reduces the amplitude of the side lobes of the ILS and accordingly the size of the spectral interval in which the atmospheric spectrum must be calculated. It causes a loss of spectral resolution, but if a reversible apodization function is used, no information is lost. When the spectrum is convolved with the apodization function, correlation between different spectral points is introduced which appear as off-diagonal terms in the VCM of the observations.

The 'Norton-Beer strong' Norton R. H., R.Beer Ref. [1.54] function is used as apodizing function. The effects of the ILS and the apodization are simultaneously considered by convolving the atmospheric radiance with the apodized instrument line shape (AILS), obtained convolving the ILS with the apodization function.

The atmospheric radiance computed at the irregular grid points should first be interpolated on the regular fine grid (spacing 0.0005 cm^{-1}) and then convolved with the AILS function in

order to obtain the spectrum on the coarse grid (spacing 0.025 cm^{-1}). Actually, these two operations are simultaneously performed skipping the step of interpolating the spectrum on the regular fine grid, with a saving in both computation time and memory requirements.

2.4.4.1.3.3.1.6 Instrument field of view convolution

The main effect of the exponential variation of the atmospheric radiance as a function of the limb angle through the input aperture is that a non-negligible difference exists between the signal observed along the central line of the FOV and the integrated signal.

The spread of the FOV in the altitude domain is measured experimentally and tabulated in a FOV pattern distribution FOV(z) whose shape is constructed with a linear interpolation from a tabulated function. The FOV pattern is assumed to be constant as a function of the scan angle.

The effect of field of view is taken into account performing, for each spectral frequency, the convolution between the tangent altitude dependent spectrum and the FOV pattern. This convolution requires the forward model calculation for a number of lines of sight that span the vertical range of the FOV around the tangent altitude. In order to reduce the number of computations, in the Level 2 algorithm, the variation of the spectrum as a function of tangent altitude is determined by interpolating a polynomial through the spectra calculated at contiguous tangent altitudes in the range of the FOV pattern.

Where the radiance profile varies rapidly with tangent altitude, additional spectra may be simulated at intermediate tangent levels to maintain the numerical accuracy of the convolution. In figure 2.27 the values of the spectrum at a significant frequency calculated with an analytical convolution at altitudes between 9.5 and 12.5 km are plotted as a function of the corresponding values of the spectrum calculated with a reference numerical convolution. The results of the analytical convolution for both quartic and parabolic interpolation are shown for a critical case (in the atmospheric model used for these simulations, the tropopause is located at 11 km). The deviation of the curve from a straight line indicates the presence of a potential error in the computation of the analytical derivative of the spectrum with respect to the tangent pressure (section 2.4.4.1.3.3.2.).

The simultaneous computation of the whole sequence of limb scanning spectra, which is required by the global fit approach, allows a simple and efficient computation of the FOV convolution and avoids the reiterated computation of spectra with adjacent tangent altitudes.

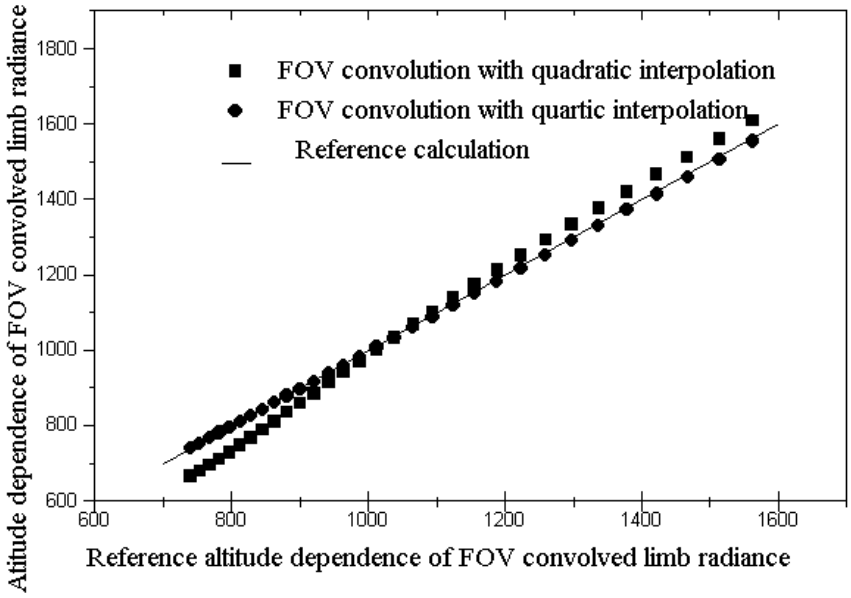

Figure 2.27 FOV convolved limb radiance values, at a significant frequency, calculated analytically at altitudes between 9.5 and 12.5 km versus corresponding reference values obtained by means of numerical convolution. The analytical convolution performed using a quadratic interpolation (made drawing a parabola through 3 spectra with tangent altitudes in the range of FOV pattern) is compared with the one obtained drawing a polynomial of the fourth degree (quartic interpolation) through 5 spectra with tangent altitudes in the FOV pattern range. The reference FOV convolved spectral values are computed simulating spectra at 100 m distant tangent altitudes. The deviation of the curves from a straight line indicates the presence of an error in the interpolated spectrum and hence of a potential error in the computation of the analytical derivatives.

2.4.4.1.3.3.2 Jacobian calculation

Another important part of the retrieval code is the fast determination of the derivatives of the radiance with respect to the retrieval parameters. In the following we will first present the five different types of derivatives which have to be computed and then explain the procedure implemented for their calculation. As already stated in section 2.4.4.1.3.1. , the retrieval parameters are: (1) volume mixing ratios of atmospheric trace gases at tangent pressures, (2) atmospheric continuum values at tangent pressures, (3) the tangent pressures themselves, (4) temperature at tangent pressures, and (5) the zero-level calibration correction. As described in section 2.4.4.1.3.4.4. , a retrieval grid is chosen which coincides with the tangent points. As

a consequence, the number of parameters in (1), (3) and (4) is equal to the number of tangent points. By contrast, the atmospheric continuum (2) and the zero-level calibration correction (5) are assumed to be microwindow dependent, and the atmospheric continuum also tangent altitude dependent. Thus, the number of atmospheric continuum parameters is equal to the number of microwindows times the number of tangent altitudes at which the individual microwindows are used, while the number of zero-level calibration correction parameters is equal to the number of microwindows.

The numerical computation of the derivatives requires, for each retrieved parameter, an extra forward model calculation with an increment applied to that parameter. Whenever possible, derivatives are computed analytically in the sense that analytical formulas of the derivatives are implemented in the program (this is the case of the retrieval parameters (1), (2), (3) and (5)). Where the calculation of sufficiently precise analytical derivatives requires computations as time consuming as the calculation of spectra (parameters (4)), an optimized numerical procedure is implemented.

Derivatives with respect to parameters (1) and (2) are handled in a similar way. The aim is the calculation of the derivatives of the spectrum L provided by equation eq. 2.27 with respect to the atmospheric retrieval parameters x_n on each tangent level n. The expression for these derivatives reads:

$$\frac{dL}{dx_n} = \sum_{j=1}^{N} \left(\frac{dL}{dB_j} \frac{dB_j}{dx_n} + \frac{dL}{d\tau_j} \frac{d\tau_j}{dx_n} \right) \qquad \text{eq 2.30}$$

. If we neglect the 2nd order dependence of equivalent temperatures on the parameters x_n , the first term of (4.12) eq. 2.30 is equal to 0. The second term requires the calculation of the derivative of the radiance with respect to the optical depth and the derivative of the optical depth with respect to the retrieval parameter. The derivative of the radiance with respect to the optical depth is equal to:

$$\frac{dL}{d\tau_j} = B_j \left(\prod_{k=j}^{N} \exp(-\tau_k) \right) - \sum_{i=1}^{j-1} B_i \left(1 - \exp(-\tau_i)\right) \prod_{k=i+1}^{N} \exp(-\tau_k) \qquad \text{eq 2.31}$$

In this expression, the first term is the derivative of the emission of layer j attenuated by all layers between j and the observer, while the second term is the derivative of the attenuation for the radiation of each layer up to layer j-1 and represents the emission spectrum measured by the observer due to the first (j-1) layers.

The derivative of the optical depth with respect to each parameter of the atmospheric continuum reads simply:

$$\frac{d\tau_j}{dx_{cont_n}} = \frac{d\tau_j}{dc_{cont_j}} \frac{dc_{cont_j}}{dx_{cont_n}} = col_{air_j} \frac{dc_{cont_j}}{dx_{cont_n}} \qquad \text{eq 2.32}$$

where c_{cont_j} is the continuum cross section of the j-th layer and x_{cont_n} the continuum parameter,

i.e the continuum cross section value at the n-th tangent level relative to a given microwindow. Due to the limited influence of the single change of a continuum parameter on the whole continuum profile, the only terms $dc_{cont\,j}/dx_{cont\,n}$ which are different from 0 are the ones corresponding to layers between tangent levels (n+1) and (n-1).

The derivative of the optical depth with respect to the VMR parameters is equal to:

$$\frac{d\tau_j}{dx_{g,n}} = \frac{d\tau_j}{dc_{g,j}}\frac{dc_{g,j}}{dx_{g,n}} + \frac{d\tau_j}{dcol_{g,j}}\frac{dcol_{g,j}}{dx_{g,n}} = col_{g,j}\frac{dc_{g,j}}{dx_{g,n}} + c_{g,j}\frac{dcol_{g,j}}{dx_{g,n}} \qquad \text{eq 2.33}$$

Neglecting the dependence of equivalent temperature and pressure on the VMR parameters it follows that $dc_{g,l}/dx_{g,n} = 0$. During the calculation of the Curtis-Godson equivalent quantities, only the derivatives of the partial columns of each layer with respect to the VMR at the tangent level have to be determined.

The analytical derivative of the spectrum with respect to the tangent pressure (3) can be very complicated, since changes in the column, in the line-shapes and in the temperature have to be considered when tangent pressure is perturbed. The problem was overcome by exploiting the fact that the effect of FOV convolution is to shift the 'effective' tangent pressure of the spectrum. Therefore, the derivative of the spectrum with respect to tangent pressure is calculated performing an analytical derivative of the expression that provides the convolution between the spectrum interpolated as a function of tangent pressure and the FOV pattern. The accuracy of the derivative calculated in this way is strictly connected with the accuracy of the interpolated spectrum in the range where the FOV pattern is defined (figure 2.27).

The temperature derivatives are determined in a 'fast numerical' way. In contrast with slow numerical derivatives, in the 'fast numerical' calculation the derivatives are computed in parallel with the spectra, avoiding unnecessary repeated calculations. The implemented fast numerical derivatives with respect to tangent temperature make use of the limited influence of the change of one temperature parameter on the overall temperature profile: only the Curtis-Godson equivalent temperatures of the neighboring layers above and below the tangent altitude (relating to the considered parameter) are affected. Hence, in addition to the calculation of cross-sections and radiative transfer corresponding to the unperturbed original temperature profile, needed for the forward calculation, only cross-sections relating to the layers affected by the current temperature parameter change and radiative transfer as modified by the changed cross-sections are computed.

The derivatives with respect to the zero-level calibration correction (5) are equal to 1, since the zero-level calibration correction is simply an additive term of the simulated spectrum.

With the adopted optimizations the additional computing effort required for the Jacobian calculation is only twice the effort needed for one forward model run. This is a very interesting result, considering that the full numerical calculation of the derivatives would require as many forward model re-runs as many are the fitting parameters (≈ 100).

2.4.4.1.3.3.3 Convergence criteria

The convergence criteria adopted in our code are a compromise between the required accuracy of the parameters and the computing speed of the algorithm. The following three convergence conditions are used to achieve this:

- Condition on linearity: at the current iteration 'iter' the relative difference between the actual χ^2 and the expected value of chi-square computed in the linear approximation (χ^2_{LIN}) must be less than a fixed threshold t $_1$:

$$\left| \frac{\chi^2(\mathbf{x}_{iter}) - \chi^2_{LIN}(\mathbf{x}_{iter})}{\chi^2(\mathbf{x}_{iter})} \right| < t_1 \qquad \text{eq 2.34}$$

where χ^2_{LIN} is computed using the expression:

$$((\mathbf{I} - \mathbf{KD})\mathbf{n})^T (\mathbf{V}_n)^{-1} ((\mathbf{I} - \mathbf{KD})\mathbf{n}) \qquad \text{eq 2.35}$$

- Condition on attained accuracy: the relative correction that has to be applied to the parameters for the subsequent iteration is below a fixed threshold t$_2$ i.e.:

$$\mathrm{Max}_j \left| \frac{(\mathbf{x}_{iter-1})_j - (\mathbf{x}_{iter})_j}{(\mathbf{x}_{iter})_j} \right| < t_2 \qquad \text{eq 2.36}$$

.

Different thresholds are used for the different types of parameters depending on their required accuracy. Furthermore, whenever an absolute accuracy requirement is present for a parameter, the absolute variation of the parameter is checked instead of the relative variation considered in equation eq. 2.36 . The non-target parameters of the retrieval, such as continuum and instrumental offset parameters are not included in this check. Parameters equal to zero are excluded from this check as well.

- Condition on computing time: the maximum number of iterations must be less than a given threshold.

The convergence is reached if either condition equation eq. 2.34 or condition equation eq. 2.36 is satisfied. If only the condition on computing time is satisfied, the retrieval is considered unsuccessful.

2.4.4.1.3.4 Choices and assumptions in the forward and retrieval

algorithms

In this section we report de description of specific issues regarding both the strategy adopted in the version algorithm and the simplifications / shourtcomings implemented in the forward model

2.4.4.1.3.4.1 Use of complementary information in the inversion model

MIPAS limb scanning retrievals have redundancy of measurements, such that stable vertical profiles of atmospheric state parameters can be retrieved without constraining the retrieval with a-priori knowledge. On the other hand, when some complementary information on the unknown parameters is available, the quality of retrieved parameters can be improved by including this information in the retrieval process.

The external information can be either of 'general' type (as in the case of climatological data or model forecasts) which, as such, may apply to several MIPAS observations made at different locations and at different time, or of 'specific' type, which relates to individual MIPAS scans.

The exploitation of 'general' information is not desirable because the same external information can be used for the retrievals of several sequences so that the results of these retrievals are affected by a common bias and can no longer be considered independent measurements. The correlation between subsequent profiles would add extra complexity in the use of the data in geographical maps and averages.

On the other hand, complementary information relating to the individual MIPAS sequences (e.g. line of sight data, or data relating to the same air mass actually sounded by the considered MIPAS scan) can be profitably included in the retrieval, as stated in section 2.4.4.1.3.2.1. , using equation instead of equation. In fact, engineering data defining the instrument Line Of Sight (LOS) are updated at each scan and therefore constitute an effective and 'specific' source of information which can be routinely used in p,T retrievals without introducing a bias in the retrieved profiles.

The LOS engineering information consists of both a vector z containing the tangent altitudes of the current scan and of a VCM V_z related to the vector z.
A relationship between the engineering tangent heights and the unknowns of the p,T retrieval is provided by hydrostatic equilibrium constraint. This law, generally fulfilled in normal atmospheric conditions, especially in the stratosphere, provides a relationship between pressure, temperature and altitude. Assuming known pressure and temperature distributions and a reference altitude $z_1 = z(p_1, T_1)$, the altitude z_i relating to pressure p_i is calculated as:

$$z_i = z_1 + \frac{R}{M} \sum_{j=1}^{i-1} \frac{\overline{T_j}}{g_j} \log\left(\frac{p_j}{p_{j+1}}\right) \qquad \text{eq 2.37}$$

where M is the average molecular weight of the atmosphere, R the universal gas constant, g_j the acceleration of gravity relating to the j-th atmospheric layer (its dependence on altitude and latitude is derived from the WGS84 model Department of Defense Ref. [1.25]) and $\bar{T}_j$ is the average temperature of the j-th atmospheric layer.

The engineering measurements of tangent altitudes are linked with the unknowns of the inversion problem (p, T) by equation eq. 2.37 . In particular, equation eq. 2.37 can be locally linearized providing:

$$\mathbf{z} = \mathbf{K}_z \mathbf{y} \qquad \text{eq 2.38}$$

Matrix K_z is the Jacobian connecting the engineering tangent altitudes with the unknowns p,T and is obtained deriving equation with respect to p and T. In this case the solution of the retrieval problem is found by simultaneously inverting equation and equation eq. 2.38 . The solution formula is in this case provided by equation and is equal to:

$$\mathbf{x}_{iter} - \mathbf{x}_{iter-1} = \left[\mathbf{K}_{iter-1}^{T}\mathbf{V}_n^{-1}\mathbf{K}_{iter-1} + \mathbf{K}_z^{T}\mathbf{V}_z^{-1}\mathbf{K}_z\right]^{-1}\left[\mathbf{K}_{iter-1}^{T}\mathbf{V}_n^{-1}\mathbf{n}_{iter-1} + \mathbf{K}_z^{T}\mathbf{V}_z^{-1}\mathbf{z}\right] \qquad \text{eq 2.39}$$

In our approach climatological data only contribute to the definition of the first guess profile, and profiles which are used within the forward calculation but not retrieved (i.e. contaminants). The first guess is obtained by combining climatological data and the previously retrieved profile with optimal estimation equation. In this case, the optimal estimation helps in reducing the number of retrieval iterations, but does not directly contribute to the retrieval error.

2.4.4.1.3.4.2 Profile regularization

In some cases the retrieved profiles vary as a function of altitude with an oscillation that is greater than it is physically reasonable to expect. This oscillation is intrinsic to the retrieval problem, because the solution is represented in a base of functions different from the base of the observations identified by the Jacobian: if the base of the solution contains some components that are nearly orthogonal to the base of the measurements, these components are sensitive to small variations of noise with a consequent instability of the solution.

The techniques intended to reduce these instabilities are called 'regularisation' techniques. For instance, Tikhonov-Phillips [26] Ref. [1.63] regularisation consists in the minimization of the function:

$$\chi^2 = \mathbf{n}^{T}\mathbf{V}_n^{-1}\mathbf{n} + \mu\left(\mathbf{x}-\mathbf{x}_0\right)^{T}\mathbf{L}^{T}\mathbf{L}\left(\mathbf{x}-\mathbf{x}_0\right), \qquad \text{eq 2.40}$$

where x is the unknown, L is an appropriate operator which determines the type of constraint, m is the regularisation parameter which determines the relative weight of the two conditions and x_0 is the a-priori estimate of the solution, which is usually set equal to zero.

The solution minimizing the function equation eq. 2.40 , in a Newtonian iteration, is given by:

$$\mathbf{x}_{iter} - \mathbf{x}_{iter-1} = (\mathbf{K}_{iter-1}{}^{T}\mathbf{V}_n{}^{-1}\mathbf{K}_{iter-1} + \mu\ \mathbf{L}^{T}\mathbf{L})^{-1}\left(\mathbf{K}_{iter-1}{}^{T}\mathbf{V}_n{}^{-1}\mathbf{n}_{iter-1} + \mu\ \mathbf{L}^{T}\mathbf{L}(\mathbf{x}_{iter-1} - \mathbf{x}_0)\right) \quad \text{eq 2.41}$$

.

As indicated by equation eq. 2.40 , the Tikhonov-Phillips regularization minimizes a modified χ^2 and, depending on the choice of the a-priori estimate x_0, a bias may be introduced in the retrieved profile. The bias can be avoided by choosing the a-priori estimate equal to the profile estimate of the current iteration: $\mathbf{x}_0 = \mathbf{x}_{iter-1}$. In this case the solution equation eq. 2.41 is equal to:

$$\mathbf{x}_{iter} - \mathbf{x}_{iter-1} = (\mathbf{K}^{T}_{iter-1}\mathbf{V}_n{}^{-1}\mathbf{K}_{iter-1} + \mu\ \mathbf{L}^{T}\mathbf{L})^{-1}\left(\mathbf{K}^{T}_{iter-1}\mathbf{V}_n{}^{-1}\mathbf{n}_{iter-1}\right) \quad \text{eq 2.42}$$

Levenberg-Marquardt solution is a particular case of equation eq. 2.42 , obtained with L=I.

Like in the case of the Levenberg-Marquardt method, also in the case of equation eq. 2.42 the regularization operates only on the correction $\mathbf{y} = \mathbf{x}_{iter} - \mathbf{x}_{iter-1}$ that is determined in the current iteration and stepwise the same exact solution is eventually reached. For this reason the choice of $\mathbf{x}_0 = \mathbf{x}_{iter-1}$ is considered in the literature Rodgers C. D. Ref. [1.59] not to be a real regularization.

We find however that the choice of $\mathbf{x}_0 = \mathbf{x}_{iter-1}$ serves our objective of not changing the function to be minimized (in order to avoid the associated bias) while successfully damping in the retrieval the undesirable components. The operator L provides a filter to the oscillatory components of the correction y. These components are added to the retrieved profile to the extent that they are well measured. In this way the convergence path, followed by the Newtonian iterations, is modified even if still aiming at the same convergence point. When the convergence criteria are satisfied a different solution is found in which the oscillatory components, if poorly determined by the measurements, have not yet been amplified as much as otherwise possible. This is obtained with a possible increase of the number of iterations but with an equally good value of the χ^2 function. The apparent contradiction of an unbiased solution different from the 'exact' one and satisfying to the same convergence criteria can be explained considering that the ' damping' introduced by the operator L acts only on the poorly determined components, which by definition cause a small difference in the observations and therefore do not change significantly the χ^2 function.

An optional regularisation of the type equation eq. 2.42 is implemented in MIPAS Level 2 processor with $L^T L$ equal to a strip-diagonal matrix in which elements different from 0 are only the diagonal elements and the first off-diagonal ones. Due to the constant (user-defined) value of μ, this regularisation proves to be more effective than the Levenberg-Marquardt method in damping oscillations in both iteration and altitude domain. The value of μ is determined on the basis of operational needs.

2.4.4.1.3.4.3 Levels versus layers

The retrieval allows only the determination of a discrete representation of the vertical profile. Several options can be considered for the discretisation of the unknown profile, the most common being a representation at discrete levels with linearly interpolated values at intermediate altitudes Carlotti M. and B. Carli Ref. [1.14] and a representation at discrete layers with constant value within the thickness of the layer.

Since the spectrum contains information mainly on the average VMR in each layer and not on the specific values of VMR at adjacent levels and since a non-unique relation exists between VMR at adjacent levels and the average mixing ratio in the layer between the levels, more stable results can be obtained with the layer representation rather than with the level representation Clarmann T. v., H. Fischer, and H. Oelhaf Ref. [1.22] .

However, the level representation is more easily used in plots and is considered to result into a more user friendly product. Considering the small mathematical difference that in any case exists between the two representations, the representation at levels has been chosen.

2.4.4.1.3.4.4 Retrieval vertical grid

The vertical resolution and the accuracy with which the retrieved profile is determined are generally anti-correlated (see Ref. [1.14]) and are strongly dependent on the grid where the retrieved points are represented ('retrieval grid'). In the case of onion peeling method, the unknown values can only be retrieved at the measurement grid, i.e. the grid of the measured tangent altitudes. With global fit, the 'retrieval grid' can be different from the 'measurement grid'. Since in Level 3 data processing global maps on pressure surfaces are produced, the possibility offered by the global fit of using fixed pressure levels which will in general be different from the tangent altitude levels could directly meet user needs.

The performances of the retrieval code when the two different retrieval grids are used have been compared for different measurement and retrieval scenarios with the method described in Carlotti M. and B. Carli Ref. [1.14] . This analytical procedure allows the estimation of the random error that is associated with each value of the retrieved profile when a given vertical resolution is adopted, or, conversely, of the vertical resolution that can be reached when the random errors must be contained within a given limit.

When the retrieval is performed on the measurement grid and then the profile is interpolated to a fixed grid, the vertical resolution of the resulting profile is degraded and its accuracy improved Carlotti M. and B. Carli Ref. [1.14] , Carli B., M. Ridolfi and CO Ref. [1.11] . It has been found that there is little difference in vertical resolution and accuracy between retrieving on the measured grid and retrieving on a fixed grid shifted with respect to the measured one.

On the other hand, if the retrieval is performed on the nominal 3 km grid and the measurements have been performed on a 'stretched' grid (e.g. 3.5 km spacing), undesirable oscillations are present in the retrieved profile. These can be avoided only if the retrieval grid is made coarser than any possible measurement grid or if some profile regularisation is imposed.

The final choice was to retrieve vertical profiles at an altitude grid defined by the tangent altitude levels, since this provides the best information that can be derived from the measurements and the most stable results.

2.4.4.1.3.4.5 Vertical resolution

The vertical resolution of the retrievals depends on both experimental choices (instantaneous FOV and scanning altitude step), and on the profile representation within the retrieval (spacing of the retrieved points). Improvements in the vertical resolution are always obtained at the expenses of either retrieval accuracy or, through the measurement time, horizontal resolution. A preliminary model of MIPAS FOV has been used, which assumes the FOV shape to be a trapezium with the greater base equal to 4 km and the smaller base equal to 3 km. Assuming this FOV shape, a 3 km spacing has been found to be a good resolution/accuracy compromise for both the measurements and the retrieval grid.

2.4.4.1.3.4.6 Assumptions

In order to limit the complexity of the code and meet the computing time requirements, some simplifications have been adopted in the forward model. In particular, some effects have up to now been neglected in both the spectroscopic and the atmospheric model.

Neglected effects in the spectroscopic model are:

- line mixing Edwards D. P. and L. L. Strow Ref. [1.31] , Rosenkranz P. W Ref. [1.60] occurring when collisions between a radiating molecule and the broadening gas molecules cause the transfer of population between rotational-vibrational states. Line mixing affects especially the Q-branches where transitions between ro-vibrational energy levels closer than K_BT (K_B is the Boltzmann constant, T is the temperature) are packed together. The most apparent effect of line-mixing is a reduction of the cross-section in the wings of the branch. The impact of line-mixing effects, mainly significant for CO_2 lines, is reduced by using an appropriate selection of microwindows.
- pressure shift Rosenkranz P. W Ref. [1.60] , that is significant only at high pressures, is not foreseen to affect MIPAS spectra, because MIPAS penetrates to the tangent altitude of 8 km as a minimum.

Both these effects could be taken into account without an increase of the computing time if they are modeled by the program that generates the LUTs.

Concerning the atmospheric model, the following assumptions have been made:

- Assumption on local thermodynamic equilibrium (LTE).

Level 2 algorithm assumes the atmosphere in local thermodynamic equilibrium: this means that the temperature of the Boltzmann distribution is equal to the kinetic temperature and that the source function in equation eq. 2.18 is equal to the Planck function at the local kinetic temperature. This LTE model is expected to be valid at the lower altitudes where kinetic collisions are frequent. In the stratosphere and mesosphere excitation mechanisms such as photochemical processes and solar pumping, combined with the lower collision relaxation rates make possible that many of the vibrational levels of atmospheric constituents responsible for infrared emissions have excitation temperatures which differ from the local kinetic temperature. It has been found Lopez-Puertas M. and CO Ref. [1.48] that many CO_2 bands are strongly affected by non-LTE. However, since the handling of Non-LTE would severely increase the retrieval computing time, it was decided to select only microwindows whose emission is in thermodynamic equilibrium to avoid Non-LTE calculations in the forward model.

- Assumption of horizontally homogeneous atmosphere

Limb sounding attains good sensitivity due to the long path lengths obtainable, but this necessarily requires measurements which `average' the atmosphere over long horizontal distances. With limb-scanning, there is the associated problem that the profile of acquired tangent points is sheared horizontally, partly by the variation in elevation angle and partly by the satellite motion. A third problem is the assumption that the retrieved value at one altitude can be used to model the contribution of the atmosphere at that level along the ray paths for lower tangent heights, whereas in reality these paths all intersect the altitude surface at different locations. Each of these effects has a horizontal length scale of the order of several hundred kilometers, and ignoring these effects is the equivalent of assuming that the atmosphere is horizontally homogeneous over this distance.

Studies Carli B., M. Ridolfi and CO Ref. [1.11] have shown that the retrieval accuracy is particularly sensitive to horizontal temperature gradients. For example, ignoring a temperature gradient of 3 K / 100 km (a typical maximum, e.g. associated with crossing the polar vortex) can lead to composition retrieval errors of tens of %, although these errors are localized and usually associated with regions in which the atmospheric composition is also changing rapidly.

Several approaches Carlotti M., B.M.Dinelli and CO Ref. [1.12] , Carlotti M., B.M.Dinelli, P.Raspollini, M.Ridolfi Ref. [1.71] have been considered in order to allow for horizontal inhomogeneity, but none of them appear to be suitable for NRT operational processing. We must, therefore, be aware of the assumption of horizontally homogeneous atmosphere when observing air masses with steep gradients.

2.4.4.1.3.5 Algorithm validation

To validate the approximations implemented in the forward model internal to the Level 2 processor (that is called 'Optimized Forward Model' = OFM), comparisons were made with

a specially developed line-by-line code based on GENLN2 Edwards D. P Ref. [1.30] . This code was compared with several existing codes and was elected as our reference forward model (RFM) Edwards D. P Ref. [1.29] . The main results of the RFM / OFM intercomparisons are:

- Ray-tracing: for N_2O, 10 km tangent-height path (representing the most 'difficult' case involving both large VMR gradients and refraction effects) RFM-OFM calculations differ by less than 0.7% in the slant column calculations, less than 0.004% in the Curtis-Godson pressure calculation and less than 0.002 K in Curtis-Godson temperature calculation.
- Cross-section calculations: RFM and OFM full spectral calculations agree to better than 1 % near major absorption features.
- Limb spectral calculations: RFM-OFM limb radiance calculations agree to within NESR/4 (the values of the NESR in the different spectral ranges are reported on the figure below:

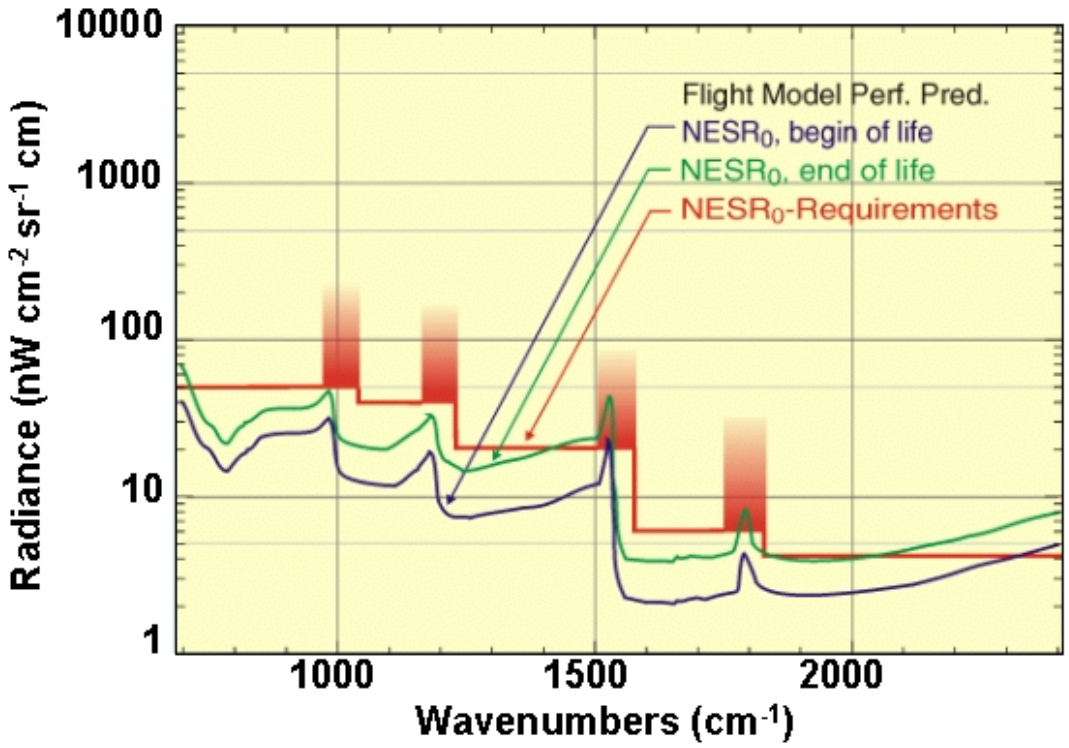

Figure 2.28

The factor 4 is intended to account for the possible building up of systematic effects and for the achievement of a NESR better than the requirements.

The retrieval code has been validated by performing retrievals from spectra generated by its

own forward model and by the RFM. Tests are in progress (January 2001) using with spectra obtained with the balloon instrument MIPAS-B2.

The results obtained so far indicate that both forward model error, i.e. error due to imperfect modeling of the atmosphere, and convergence error, i.e. error due to the fact that the inversion procedure does not find the real minimum of the χ^2 function, are much smaller than the measurement error due to radiometric noise.

2.4.4.1.3.6 Performances

2.4.4.1.3.6.1 Accuracy performance of Level 2 retrieval algorithm

The main error sources that affect the accuracy of the retrieved profiles are:

- noise error, due to the mapping of radiometric noise in the retrieved profiles;
- temperature error, which maps into VMR retrieved profiles;
- systematic error, due to incorrect input parameters.

The amplitude of noise error has been evaluated (through equation eq. 2.13) with test retrievals that use observations simulated starting from assumed atmospheric profiles (reference profiles) and perturbed with random noise of amplitude consistent with MIPAS noise specification.

The effect of temperature error on VMR retrievals is determined using tabulated propagation matrices which estimate the effect for different measuring conditions. Current results indicate that temperature error can be a significant component of the error budget and consideration is being given to methods to improve the accuracy of temperature retrieval. (details on p,T error propagation 2.4.4.3.)

Errors of the third type include systematic errors, such as spectroscopic errors or errors due to imperfect knowledge of the VMR profiles of non-target species. These errors are taken into account in the definition of the optimum size of each microwindow and for the selection of the optimal set of microwindows 2.4.4.4. that should be used for the retrieval. The quantifiers that are calculated for these operations can also be used for the determination of the total error budget.

The relevance of systematic errors in the total error budget depends on whether optimistic or conservative error estimates are used. The current estimate of the ultimate retrieval accuracy is summarized in the following plot that reports the total error as a function of the altitude for each of the retrieved constituents and for temperature.

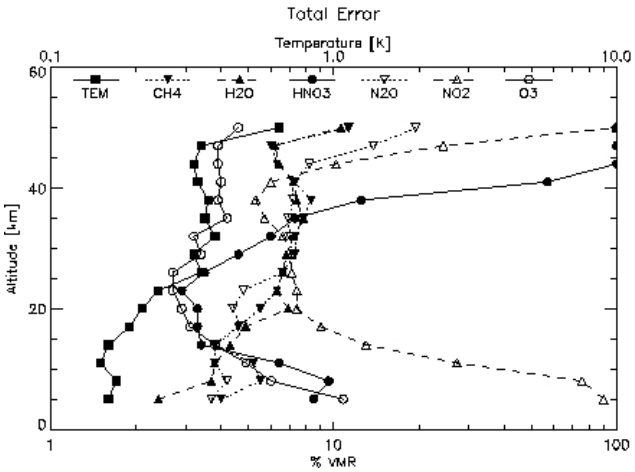

Figure 2.29

2.4.4.1.3.6.2 Runtime performance

Note: here is a section illustrating only the runtime performance of the ORM. What about the L2 processor ????

The runtime performances of the ORM have been tested using different computers. Tests have been performed on simulated observations using two different sets of microwindows, a preliminary standard set and a set which optimizes the trade-off between accuracy and run-time performance. In these tests we used initial guess profiles of the retrieval that are sufficiently close to the reference profiles (the ones used to simulate the observations), so that convergence is reached in only one iteration. The results of these tests are shown in the table below.

Considering that the measurement time per scan is 75 seconds and that more than one computer can be used for the operational analysis data, we can conclude that the run-time requirements are fully satisfied also for retrievals that need more than one iteration.

Table 2.2 Table: Runtime (sec.) for p,T and 5 target species retrieval (1 iteration)

Computer description	Standard set of MWs	Optimized set of MWs
SUN SPARC station 20 120 MHz CPU, 128 Mb RAM	550 (*)	348 (*)
PENTIUM PC 200 MHz CPU, 256 Mb RAM	352	210
Ultra Sparc station 5	181	Not Available
IBM RS6000 Model 397	149	Not Available
Digital DEC-SERVER Mod. 4100 600 MHz CPU, 1 Gb RAM	74	51

(*) This run-time is strongly affected by the use of swap space

2.4.4.2 Products

2.4.4.2.1 Level 2 Products Description

There exists 2 forms of level 2 products. The level 2 product 2.4.4.2.1.1. itself and the level 2 NRT / meteo product 2.4.4.2.1.2. containing a subset of the data contained in the relating level 2 product.

2.4.4.2.1.1 Level 2 Product

Table 2.3

Product Header 2.4.4.2.1.3.	Main Product Header 2.4.4.2.1.3.1.
	Specific Product Header 2.4.4.2.1.3.2.
	Data Set Descriptors 2.4.4.2.1.3.3.
Summary Quality ADS 2.4.4.2.1.4.	
Scan Geolocation ADS 2.4.4.2.1.5.	
Structure ADS 2.4.4.2.1.6.	
Scan Information MDS 2.4.4.2.1.7.	
p,T Retrieval MDS 2.4.4.2.1.8.	
Species #1 VMR Retrieval MDS 2.4.4.2.1.9. [a]	
Species #2 VMR Retrieval MDS 2.4.4.2.1.9. [a]	
Species #3 VMR Retrieval MDS 2.4.4.2.1.9. [a]	
Species #4 VMR Retrieval MDS 2.4.4.2.1.9. [a]	
Species #5 VMR Retrieval MDS 2.4.4.2.1.9. [a]	
Species #6 VMR Retrieval MDS 2.4.4.2.1.9. [a]	
Continuum and Offset MDS 2.4.4.2.1.10.	
PCD Information ADS 2.4.4.2.1.11.	
MW Occupation Matrix ADS 2.4.4.2.1.12.	
Residual Spectra ADS 2.4.4.2.1.13.	
Parameters ADS 2.4.4.2.1.14.	

a:	Sequence of species is given in Specific Product Header

The level 2 product consists of following elements (see index)
The detailed structure of the level 2 product can be found here .

2.4.4.2.1.2 Level 2 NRT /Meteo Product

Table 2.4

Product Header 2.4.4.2.1.3.	Main Product Header 2.4.4.2.1.3.1.
	Specific Product Header 2.4.4.2.1.3.2.
	Data Set Descriptors 2.4.4.2.1.3.3.
Summary Quality ADS 2.4.4.2.1.4.	
Scan Geolocation ADS 2.4.4.2.1.5.	
Structure ADS 2.4.4.2.1.6.	
Scan Information MDS 2.4.4.2.1.7.	
p,T Retrieval MDS 2.4.4.2.1.8.	
O_3 Retrieval MDS 2.4.4.2.1.9.	
H_2O Retrieval MDS	
MW Occupation Matrix ADS 2.4.4.2.1.12.	
Parameters ADS 2.4.4.2.1.14.	

The level 2 NRT / Meteo product consists of following elements (see index)
The detailed structure of the level 2 NRT / Meteo product can be found here .

2.4.4.2.1.3 Product Header

The product header is divided into three parts:
- the Main Product Header 2.4.4.2.1.3.1.
- the Specific Product Header 2.4.4.2.1.3.2.
- the Data Set Descriptors 2.4.4.2.1.3.3.

2.4.4.2.1.3.1 Main Product Header

The main product header is the same for all ENVISAT products. It specifies basic product information such as origin of data, processing site, processing software version, UTC time of data sensing and processing, orbit and velocity parameters of ENVISAT, quality indicators for input data, etc.

The detailed structure of the MPH can be found here 6.5.1. .

2.4.4.2.1.3.2 Specific Product Header

The SPH is the same for both forms of level 2 products. It contains information applicable to the whole level 2 product file such:
- UTC measurement time intervals (ZPD time)
- geographic coverage of scene data (latitude and longitude of first and last scan)
- number of total, nominal and special event scans in product file
- MPD during the sweeps of the nominal scans
- sequence of VMR retrievals within the product
- number of sweeps per scan

The detailed structure of the level 2 SPH can be found here 6.5.50. .

2.4.4.2.1.3.3 Data Set Descriptors

The DSD provide information on structure and size of included or referenced measurement and annotation data.

2.4.4.2.1.4 Summary Quality ADS

This ADS consists of 1 ADSR containing the numbers of p,T and VMR retrievals terminated unsuccessful because of
- excess of allowed number of macro iterations
- excess of allowed number of micro iterations
- excess of allowed processing time

The detailed structure of this ADS is slightly different for the 2 forms of level 2 products. It can be found here 6.5.45. for the full level 2 product and here 6.5.54. for the NRT / meteo product.

2.4.4.2.1.5 Scan Geolocation ADS

This ADS contains 1 ADSR per scan providing geolocation information. It includes:

- The ZPD time of the sweep closest in time to the center of the scan. This time is used as time stamp for the scan.
- The WGS84 latitude and longitude of the tangent points of the first, last and sweep closest in time to the center of the scan.
- The altitude range of the scan.

The detailed structure of this ADS is the same for both forms of level 2 products. It can be found here 6.5.39. .

2.4.4.2.1.6 Structure ADS

This ADS provides the parameters which determine the size of the DSRs of the following MDSs and ADSs. A new ADSR is added every time one of these parameter change its value. Each ADSR contains:

- The number of sweeps per scan.
- The numbers of retrieved profile, continuum and offset values.
- Indicators for existence of p,T error propagation data.
- The numbers of microwindows.
- The numbers of spectral grid points.
- Offsets and size of first DSRs within the following MDSs and ADSs this ADSR refers to.

The detailed structure of this ADS can be found here 6.5.46. . It is the same for both forms of level 2 products, but within the NRT / meteo product several fields are not used.

2.4.4.2.1.7 Scan Information MDS

This MDS contains 1 MDSR per scan providing geolocation information of the individual sweeps and a subset of the relating retrieval results. It includes:

- The ZPD time of each sweep of the scan.
- The WGS84 latitude and longitude of the tangent points of each sweep of the scan.
- The altitudes of the tangent points of each sweep of the scan.
- Flags indicating success of p,T and VMR retrievals.
- The logical retrieval vectors for p,T and VMR retrievals.
- The corrected altitudes for each sweep.
- Retrieved pressure, temperature and VMR profiles.
- Concentration and vertical column density profiles.
- Variance data for height correction, pressure, temperature, VMR , concentration and vertical column density.

The detailed structure of this MDS is slightly different for the 2 forms of level 2 products. It can be found here for the full level 2 product and here for the NRT / meteo product.

2.4.4.2.1.8 PT Retrieval MDS

This MDS contains 1 MDSR per scan providing the following results of the p,T retrieval:

- The condition terminating the iterations.
- The last value of chi^2.
- The source of used initial guess data.
- Height correction and retrieved pressure and temperature profiles.
- Variance/covariance matrices for pressure, temperature and height correction.
- The pressure/temperature covariance data.

The detailed structure of this MDS is the same for both forms of level 2 products. It can be found here 6.5.48. .

2.4.4.2.1.9 VMR Retrieval MDSs

For each of the target species H_2O, N_2O, HNO_3, CH_4, O_3 and NO_2 1 VMR retrieval MDS is contained in the full level 2 product. The sequence of the species is given in the specific product header. The NRT / meteo product contains 2 of these MDSs covering O_3 and H_2O. Each of these MDSs contains 1 MDSR per scan providing the following results of the VMR retrieval:

- The condition terminating the iterations.
- The last value of chi^2.
- The source of used initial guess data.
- VMR, concentration and vertical column density profiles together with the relating variance/covariance matrices.
- The p,T error propagation variance/covariance matrix, if available.

The detailed structure of this MDS is the same for both forms of level 2 products. It can be found here 6.5.49. .

2.4.4.2.1.10 Continuum and Offset MDS

This MDS contains 1 MDSR per scan providing for p,T and VMR retrievals the results concerning continuum and offset fit. It includes:

- For each microwindow the fitted instrument offset and relating variance data.
- For all altitudes used for continuum fit the fitted or interpolated continuums together with the relating microwindows, grouping types and the covariance with fitted VMR, resp. fitted pressure and temperature.

This MDS is not contained in the NRT / meteo product. The detailed structure can be found here 6.5.47. .

2.4.4.2.1.11 PCD Information ADS

This ADS contains 1 ADSR per scan providing information on retrieval quality for p,T and

VMR retrievals. It includes:

- The numbers of iterations performed.
- The partial chi^2 depending on sweep and microwindow.
- The evolution of chi^2, lambda and retrieved parameters during macro iterations.
- Additional information produced by the processor in textual form.

This ADS is not contained in the NRT / meteo product. The detailed structure can be found here 6.5.43. .

2.4.4.2.1.12 MW Occupation Matrix ADS

This ADS provides information on the microwindows selected for p,T and VMR retrievals. A new ADSR is added every time the selection changes. It includes:

- For each sweep the labels of the selected microwindows (all retrievals).
- For each retrieval the logical retrieval vector.

The detailed structure of this ADS is the same for both forms of level 2 products. It can be found here 6.5.41. .

2.4.4.2.1.13 Residual Spectra ADS

This ADS provides information on the residual spectra. A new ADSR is added every time the microwindow selection changes. It includes for each retrieval:

- The mean values and standard deviations of residual spectra computed from all scans covered by current ADSR .
- The number of retrievals contributing to the current ADSR .
- The spectral mask relating to the current data.

This ADS is not contained in the NRT / meteo product. The detailed structure can be found here 6.5.44. .

2.4.4.2.1.14 Parameters ADS

This ADS provides information on instrument and processing parameters. It contains:

- The actual elevation angles for current scan.
- The pressure levels relating to the retrieved profiles.
- The allowed number of macro and micro iterations.

The detailed structure of this ADS is slightly different for the 2 forms of level 2 products. It can be found here 6.5.42. for the full level 2 product and here 6.5.53. for the NRT / meteo product.

2.4.4.2.2 Extraction of Profile Data from Level 2 Products

There are 2 ways to extract profile data from level 2 products. If neither covariance data nor continuum and offset data is requested, the data can be extracted from the Scan Information

MDS. Variance/covariance data for retrieved pressure, temperature and height correction can be extracted from the p,T retrieval MDS. Variance/covariance data for retrieved VMR, concentration and vertical column density can be extracted from the VMR retrieval MDSs. Continuum and offset data has to be extracted from the Continuum and Offset MDS.
Extraction of Profile Data from Scan Information MDS The Scan Information MDS contains a subset of the p,T and VMR retrieval results. Within this MDS all fields containing profile information are of size N^{SW}–6.5.46. . For sweeps not used for fit the logical retrieval vectors (lfit) contain 0 and the relating profile entries are set to NaN.
Extraction of p,T Retrieval Data For the extraction of the p,T retrieval data for the ith sweep, the ith entry of the logical retrieval vector for p,T retrieval (lfit) has to be checked. If it is 0, the ith sweep has been not been used for p,T retrieval and therefore the ith entries of the profiles of pressure, variance of pressure, corrected altitudes, variance of height correction, temperature and variance of temperature are set to NaN. Otherwise these entries contain the profile data related to the ith sweep as shown in table below.

Table 2.5

sweep index	tangent height, geolocation, time	lfit	pressure, temperature, corrected height variance of pressure, temperature and height correction
0	valid value	1	valid value
1	valid value	1	valid value
2	valid value	1	valid value
3	valid value	0	NaN
4	valid value	1	valid value
5	valid value	1	valid value
6	valid value	1	valid value
7	valid value	1	valid value
8	valid value	1	valid value
9	valid value	1	valid value
10	valid value	1	valid value
11	valid value	1	valid value
12	valid value	0	NaN
13	valid value	1	valid value
14	valid value	1	valid value
15	valid value	0	NaN

Extraction of VMR Retrieval Data For the extraction of the VMR retrieval data of the ith sweep, the ith entry of the relating logical retrieval vector (lfit) has to be checked. If it is 0, the ith sweep has been not been used for fit in species #1 VMR retrieval and therefore the ith entries of the profiles of VMR, variance of VMR, concentration, variance of concentration, vertical column density and variance of vertical column density are set to NaN. Otherwise these entries contain the profile data related to the ith sweep, as shown in the table below.

Relating altitude, pressure and temperature information can be extracted as described above.

Table 2.6

sweep index	lfit p,T	p,T retrieval profiles	lfit VMR	VMR, concentration, vertical column density variance of VMR, concentration and vertical column density
0	1	valid value	0	NaN
1	1	valid value	1	valid value
2	1	valid value	1	valid value
3	0	NaN	0	NaN
4	1	valid value	1	valid value
5	1	valid value	1	valid value
6	1	valid value	1	valid value
7	1	valid value	1	valid value
8	1	valid value	1	valid value
9	1	valid value	1	valid value
10	1	valid value	0	NaN
11	1	valid value	0	NaN
12	0	NaN	0	NaN
13	1	valid value	0	NaN
14	1	valid value	0	NaN
15	0	NaN	0	NaN

Extraction of Profile and VCM Data from p,T Retrieval MDS Within the p,T retrieval MDS 6.5.48. only the sweeps used for p,T retrieval are considered. Therefore the size of the fields containing profile information are of size N_{pT} 6.5.46. . For height correction N_{pT}-1 profile are used because no height correction is applied to lowest used sweep. Extraction of Profile Data For the extraction of pressure 6.5.48. , temperature 6.5.48. and height correction 6.5.48. profiles from the p,T retrieval MDS, the relating logical retrieval vector has to used to determine the profile indices relating to requested sweep indices, as shown in the example below.

Table 2.7

sweep index	lfit p,T	index on pressure and temperature profile	index on height corrections
0	1	0	0
1	1	1	1
2	1	2	2
3	0	-	-
4	1	3	3
5	1	4	4
6	1	5	5
7	1	6	6
8	1	7	7
9	1	8	8
10	1	9	9
11	1	10	10
12	0	-	-
13	1	11	11
14	1	12	-

15	0	-	-

Extraction of VCM Data The mapping between sweep indices and the indices on the variance/covariance matrices in the p,T retrieval MDS is the same as shown above.

For the symmetric variance covariance matrices for pressure 6.5.48. , temperature 6.5.48. and height correction 6.5.48. only the diagonal elements and the elements below are included in the MDS, as shown below.

Table 2.8

element[0,0]				
element[1,0]	element[1,1]			
element[2,0]	element[2,1]	element[2,2]		
...			...	
element[n,0]	element[n,1]	element[n,2]	...	element[n,n]

Extraction of Profile and VCM Data from VMR Retrieval MDS Within the VMR retrieval MDSs 6.5.49. only the sweeps used for relating VMR retrieval are considered. Therefore the size of the fields containing profile information are of size $N_{V(j)}$ 6.5.46. . Extraction of Profile Data For the extraction of VMR 6.5.49. , concentration 6.5.49. and vertical column density 6.5.49. profiles from the VMR retrieval MDSs, the relating logical retrieval vector has to used to determine the profile indices relating to requested sweep indices, as shown in the example below.

Table 2.9

sweep index	lfit VMR	index on VMR, concentration and vertical column density profile
0	0	-
1	1	0
2	1	1
3	0	-
4	1	2
5	1	3
6	1	4
7	1	5
8	1	6
9	1	7
10	0	-
11	0	-
12	0	-
13	0	-
14	0	-
15	0	-

Extraction of VCM Data The mapping between sweep indices and the indices on the variance/covariance matrices in the VMR retrieval MDSs is the same as shown above.

For the symmetric variance covariance matrices for VMR 6.5.48. , concentration 6.5.48. and vertical column density 6.5.48. only the diagonal elements and the elements below are included in the MDS, as shown above.
Extraction of Data from Continuum and Offset MDS Within the Continuum and Offset MDS the fitted continuum and offsets of all retrievals are reported. Extraction of Offset Data For each retrieval fields of size $N_{offset(pT)}$ 6.5.46. , respectively $N_{offset(V(i))}$ 6.5.46. are contained in the Continuum and Offset MDS containing the offset values 6.5.47. itself, the relating variance data 6.5.47. and the labels of the relating microwindows 6.5.47. . Extraction of Continuum Data For the extraction of continuum the parameters number of altitudes used for continuum fit ($N_{cgid(pT)}$ 6.5.46. , $N_{cgid(V(j))}$ 6.5.46.) and max. number of microwindows per height (N_{MWPT} 6.5.46. , $N_{MWV(j)}$ 6.5.46.) are needed. For each retrieval the indices of sweeps 6.5.47. used for continuum fit is given in the MDS.

For each of these sweeps the labels of the used microwindows 6.5.47. , the grouping types 6.5.47. of these microwindows and the continuum 6.5.47. at these microwindows is given. For all microwindows with grouping types 1 .. 4 additionally the variance of the fitted continuum 6.5.47. and the covariance with the fitted profile (i.e. for p,T retrieval covariance of continuum and pressure 6.5.47. and covariance of continuum and temperature 6.5.47. , for VMR retrieval covariance of continuum and VMR 6.5.47.) at this sweep is given. All of these fields are of size N_{MWPT} 6.5.46. , respectively $N_{MWV(j)}$ 6.5.46. with unused fields set to default values. The following table shows an example.

Table 2.10

sweep index	microwindow	grouping type	continuum	variance, covariance
10	PT__0001	3	valid value	valid values
	PT__0002	5	valid value	NaN [b]
	PT__0010	1	valid value	valid values
	blank [a]	-1 [a]	NaN [a]	NaN [a]
11	PT__0002	1	valid value	valid values
	PT__0010	2	valid value	valid values
	PT__0011	6	valid value	NaN [b]
	PT__0012	2	valid value	valid values
13	PT__0002	1	valid value	valid values
	PT__0012	1	valid value	valid values
	PT__0020	1	valid value	valid values
	blank [a]	-1 [a]	NaN [a]	NaN [a]
14	PT__0012	1	valid value	valid values
	PT__0020	1	valid value	valid values
	blank [a]	-1 [a]	NaN [a]	NaN [a]
	blank [a]	-1 [a]	NaN [a]	NaN [a]

a unused field
b relating continuum value is not fitted, but interpolated (grouping type > 4)

2.4.4.3 Appendix A: Mapping of temperature error on to the retrieved VMR profiles

At a generic iteration, the VMR profile y is obtained applying to the profile y_0 of the previous iteration the correction:

$$\mathbf{y} - \mathbf{y}_0 = \left(\mathbf{K}^T \mathbf{V}_n^{-1} \mathbf{K}\right)^{-1} \mathbf{K}^T \mathbf{V}_n^{-1} \mathbf{n} \equiv \mathbf{D}\mathbf{n} \qquad \text{eq 2.43}$$

where n is the residuals vector, $\mathbf{V}_n$ is the VCM of the observed spectra and K is the jacobian of the VMR retrieval.

An uncertainty $\Delta(\mathbf{p}, \mathbf{T})$ on the assumed tangent pressures and temperatures, translates into an error $\Delta\mathbf{n}$ on the simulated spectra and therefore into an error $\Delta\mathbf{y}$ on the retrieved profile equal to:

$$\Delta\mathbf{y} = \mathbf{D} \cdot \Delta\mathbf{n} = \mathbf{D} \cdot \mathbf{C} \cdot \Delta(\mathbf{p}, \mathbf{T}) \qquad \text{eq 2.44}$$

where C is the matrix accounting for p,T error propagation in the simulated spectra of VMR retrieval and contains the derivatives:

$$C_{i,j} = \frac{\partial S_i}{\partial \begin{pmatrix} P \\ T \end{pmatrix}_j} \qquad \text{eq 2.45}$$

The index 'i' identifies the fitted spectral points (as a function of frequency for all the microwindows and all the tangent altitudes) and the index 'j' identifies the retrieved tangent altitudes. In equation (A2) D is assumed locally independent on p,T (always true for small errors $\Delta(\mathbf{p}, \mathbf{T})$).

As the error on the retrieved p,T is described by a VCM $\mathbf{V}_{PT}$, the corresponding VCM $\mathbf{V}_y'$ relating to y and due to p,T error is given by:

$$\mathbf{V}_y' = \mathbf{D}\mathbf{C}\mathbf{V}_{PT}(\mathbf{D}\mathbf{C})^T \equiv \mathbf{E}\mathbf{V}_{PT}\mathbf{E}^T \qquad \text{eq 2.46}$$

where we have defined E = DC. E is the matrix transforming p,T error into VMR error.

Matrix E depends on:

- current atmospheric status (p,T and VMR)
- observation geometry
- set of adopted MWs in VMR retrieval (Occupation Matrix)

In MIPAS Level 2 processor each OM has a pT error propagation matrix E attached to it. Since OMs are tabulated for latitude bands, it is possible to use different E matrices for different latitude bands (of course this does not prevent from using the same OM throughout the whole orbit and different E matrices depending on latitude).

Matrix E and $\mathbf{V}_{PT}$ are both outputs of MIPAS Level 2 processor. The users should use Equ. (A4) to derive the VMR error component due pT error propagation.

The dependencies of the pT error propagation on latitude, atmospheric model and acquisition scenario are analyzed, quantified and discussed in [39] Ref. [1.57].

2.4.4.4 Appendix B: Algorithm for generation of the optimized microwindow databases

Microwindow selection is performed by an algorithm which simulates the propagation of random and systematic errors through a retrieval and attempts to maximise the information content Bennett, V. L., A. Dudhia and C. D. Rodgers Ref. [1.69] . The information content of a microwindow increases as the log of the determinant of the total covariance decreases, total covariance being the sum of the random and various systematic error covariances. Broadly speaking, 1 `bit' of information is equivalent to a factor 2 reduction in the uncertainty at one profile altitude.

Microwindows are created by first selecting a number of single measurements, identified by location in the spectral and tangent altitude grids, as starting points. Adjacent measurements are added to each until the information content no longer improves or a maximum width of $3cm^{-1}$ is reached. The best of these trial microwindows is selected, the retrieval covariance modified, and the process repeated for a new set of measurements as starting points. The procedure of growing microwindows also allows for measurements within microwindows to be `masked', i.e., excluded from the retrieval. This usually applies to measurements where the associated systematic errors such as the uncertainty in modelling a contaminant, outweigh any benefit in the reduction of the random error when considering the total covariance.

Initially, a set of typically 10 microwindows, or 10000 measurements (whichever occurs first) is selected based on the assumption that spectra for all MIPAS bands are available. Further microwindows are then selected to maximise information retrieved in situations where data

from different bnds may be unavailable. This set of 20-30 microwindows constitutes the database.

Occupation Matrices (OM) represent subsets of microwindows to be used under different retrieval circumstances, and these are constructed using the same approach: selecting the microwindows from the database (rather than growing new microwindows) in the sequence

which maximises the retrieved information. A number of these OMs are precomputed, corresponding to different band-availabilities, and associated with each of these is a single figure-of-merit representing the information content.

References: see Bennett, V. L., A. Dudhia and C. D. Rodgers Ref. [1.69]

2.4.4.5 Appendix C: Handling of initial guess profiles

For the analysis of a given scan, the retrieval code needs the following atmospheric profiles as input:

- Pressure and temperature profiles
- Continuum profiles for microwindows used in p,T retrieval
- H_2O VMR profile
- Continuum profiles for microwindows used in H_2O retrieval
- O_3 VMR profile
- Continuum profiles for microwindows used in O_3 retrieval
- HNO_3 VMR profile
- Continuum profiles for microwindows used in HNO_3 retrieval
- CH_4 VMR profile
- Continuum profiles for microwindows used in CH_4 retrieval
- N_2O VMR profile
- Continuum profiles for microwindows used in N_2O retrieval
- NO_2 VMR profile
- Continuum profiles for microwindows used in NO_2 retrieval
- VMR profiles for other contaminants.

These profiles are used in the different retrievals either as a first guess of the profiles that are going to be retrieved or as assumed profiles of the atmospheric model (profiles of interfering species and p,T profiles in the case of VMR retrievals).

For each of these profiles both an a-priori estimate and the result of the 'most recent measurement' (obtained either from the retrieval of the previous scans or from a previous retrieval of the same scan) are available. The a-priori estimate of a profile is obtained either from climatology or from the ECMWF.

On the light of the fact that in some cases the errors of the retrieved profiles may be very large (VMR retrieval at very low altitudes, continuum retrieval), using the 'most recently' retrieved profiles as initial guess for the retrieval may not be a good strategy. In MIPAS Level 2 processor, the initial guess / assumed profiles are obtained using the 'best estimate' of the profiles available at the time when the retrieval is started.

For pressure and temperature profiles the 'best estimate' coincides with the 'most recent measurement'. For continuum profiles the 'best estimate' coincides with their a-priori estimate. For all the other profiles, the 'best estimate' is obtained by calculating the optimal estimation (weighted average) between the most recently measured profiles and the a-priori ones.

The optimal estimation consists in weighting the retrieved profile, with its covariance matrix, with the a-priori profile, which is also characterized by a covariance matrix with eventually large diagonal values.

The optimal estimation of the profiles is determined not only at the beginning of each scan analysis, but also after each VMR retrieval, because the retrieved VMR profile is used as assumed profile in the subsequent retrievals (from the same scan).

2.5 Instrument specific topics

2.6 Auxiliary products

2.6.1 Level 1b

2.6.2 Level 2

Summary of input / output data files

The MIPAS Level 2 processing input / output data files are summarized in the following table.

Table 2.11 Summary of Level 2 Processing I/O Data

Level 2 I/O Data				
File No.	File Identifier	Description	Size [Bytes]	Update Period
Level 1 B Data Product (Input)				
	MIP_NL__1P	Level 1 B data product	303.1 M	100.6 min

Auxiliary Data (Input)				
	MIP_PS2_AX	Processing parameters data file	10 k	1 month
	MIP_MW2_AX	Microwindows data file	1.6 M	several months
	MIP_SP2_AX	Spectroscopic data file	200 M	several months
	MIP_IG2_AX	Initial guess profile data file	3 M	several months
	MIP_FM2_AX	Forward calculation results file	95 M	several months
	MIP_OM2_AX	Microwindows occupation matrices file	25 M	several months
	MIP_CS2_AX	Cross section lookup tables file	450 M	several months
	MIP_PI2_AX	A priori pointing information file	160 k	several months
Meteorology Data (Input)				
	AUX_ECF_AX	ECMWF meteorological forecast data	TBD	6 hours
	AUX_ECA_AX	ECMWF meteorological analysis data	TBD	6 hours
Annotation Data (referenced in Level 2 products)				
	MIP_NL__1P	Level 1 B input product		
	MIP_PS2_AX	Processing parameters data file		
	MIP_MW2_AX	Microwindows data file		
	MIP_SP2_AX	Spectroscopic data file		
	MIP_IG2_AX	Initial guess profile data file		
	MIP_FM2_AX	Forward calculation results file		
	MIP_OM2_AX	Microwindows occupation matrices file		
	MIP_CS2_AX	Cross section lookup tables file		
	MIP_PI2_AX	A priori pointing information file		
	deleted			
	AUX_ECF_AX	ECMWF meteorological forecast data		
	AUX_ECA_AX	ECMWF meteorological analysis data		
Level 2 Data Products (Output)				
	MIP_NL__2P	Level 2 data product	9 M	100.6 min
	MIP_NLE_2P	Level 2 NRT / Meteo product	1 M	100.6 min

Auxiliary data

The MIPAS Level 2 auxiliary data cover the following products:

- Processing parameters data file
- Microwindows data file
- Spectroscopic data file
- Initial guess profile data file
- Forward calculation results file
- Microwindows occupation matrices file
- Cross sections lookup tables file
- A priori pointing information file

The data fields for these products are presented in the following sections.

Processing parameters data file

Product ID: MIP_PS2_AX

This file contains a complete list of input parameters, settings and switches that control the execution of the Level 2 processor.

Microwindows data file

Product ID: MIP_MW2_AX

This file describes a set of spectral intervals to be extracted from the Level1B data for the subsequent retrieval steps. For each spectral interval (microwindow) the valid altitude range, information on spectral range of continuum, sensitivity and correlation parameters, NLTE quantifiers, NESR, and contributions to the systematic/random retrieval error is given.

Spectroscopic data file

Product ID: MIP_ SP2_AX

This input data is used in forward calculation for the simulation of atmospheric spectra. Spectroscopic data are provided for each microwindow as defined in the microwindows data file.

Initial guess profile data file

Product ID: MIP_IG2_AX

This product includes initial guess profiles of pressure, temperature, VMR and continuum for different latitudes.

Forward calculation results file

Product ID: MIP_FM2_AX

This file contains initial guess data copied from an initial guess data file and the results of

forward calculations based on this data.

Microwindow occupation matrices file

Product ID: MIP_OM2_AX

This files contains pre-computed occupation matrices for p,T and VMR retrievals for different latitude bands and a fixed altitude grid. Also occupation matrices to be used in cases of missing or corrupted spectral bands are contained.

Cross sections lookup table file

Product ID: MIP_CS2_AX

This file contains absorption cross section lookup tables for a set of microwindows.

A priori pointing information

Product ID: MIP_PI2_AX

This file contains pre-computed externally provided pointing covariance data.

ECMWF Meteo Products

The ECMWF Meteo Products contain meteorological data (geopotential profiles, relative humidity profiles, temperature profiles and ozone profiles (TBC), that is used to improve the initial guess data in p,T and VMR retrievals. A description of these products is given in [RD].

The S/W makes use of GRIB encoded data files for geopotential height, relative humidity profiles, temperature profiles and ozone profiles. The I/F to the GRIB files are provided by an ESTEC provided CFI.

Variations in Level 2 product size

The Level 2 product size estimate corresponds to a nominal measurement scenario, with 16sweep measurements per elevation scan at high spectral resolution, and a duration of ca. 71s per scan. Furthermore, it has been assumed that ca. 10% of the available measurement time is used for offset calibration measurements (see also [RD]) and that no other dedicated calibration measurements are performed. The corresponding measurement time available for scene measurements will allow to complete ca. 75 elevation scans per orbit.

It should be noted that the number of retrieved quantities typically varies linearly with the number of scene measurements in an individual elevation scan whereas the number of elevation scans per orbit is roughly inversely proportional to the number of height steps. As a consequence, no significant variations are expected in the size of the p, T and trace gas VMR or concentration profile data per orbit volume. However, the overall size of the data products

may vary significantly for scenarios with different height step numbers as the sizes of the covariance matrices typically vary with the square of the number of vertical grid points. In addition, some variations in product size will occur for different numbers of elevation scans per orbit, each contributing with a number of data set records in the MDS fields and with various annotation data. Moreover, some (minor) differences in product size may be expected between Level 2 NRT and Level 2 off-line data sets, depending on the specific algorithms used in the two processing chains. These algorithms may, for instance, use different gridding schemes to represent the p, T and VMR profile and covariance data.

2.7 Latency, throughput and data volume

2.8 Characterisation and calibration

2.8.1 Characterisation

Prior to launch several parameters of MIPAS had to be characterised on the ground. Some of these parameters were measured to verify the functionality and performance of the instrument. Other measurements were made to characterise the instrument and obtain sets of parameters that would later be used by some functions the level 1b processing such non-linearity correction and ILS retrieval.

The table below lists the system-level parameters characterised on the ground.

Table 2.12

Functional Characterisation				
Parameter	Testing conditions	Data product	Uncertainty	Remark
FOV mapping	128 um pinhole Hot source at 615 K	FOV alignment	4%	MIO at thermal extremes
ZPD centre	Nominal mode	Fringe count error	-	MIO at mean temperature

Analogue gain	OCB at 250 K and DSS CBA at 220 K and DSS	Adjustement of ZPD amplitude vs. gain	-	MIO at mean temperature
ODS and SPE check	Raw data mode Band D	ODS laser frequency SPE numerical filters	0.1 cm^{-1}	MIO at mean temperature
Characterisation parameters				
Parameters	Testing conditions	Data product	Uncertainty	Remark
Aliasing verification	CBA and OCB at 250 K	Rejection level of filters	0.1%	MIO at mean temperature
Band combination	Band C and D OCB at 230 K and DSS	SPE combination filters	-	MIO at mean temperature
High-resolution feature	CBA and OCB at 250 K and DSS	absence of feature < 0.25 cm^{-1}	30% of radiometric accuracy	MIO at mean temperature
Non-linearity	CBA at 210,222, 233, 242 and 250 K	Response vs. signal amplitude; non-linearity coefficients	0.2%	MIO at mean temperature
Radiometric	CBA and OCB at 220 K and DSS	gain and offset	30% of radiometric accuracy	MIO at mean temperature
Spectral characterisitics				
Parameters	Testing conditions	Data product	Uncertainty	Remark
Spectral stability	OCB at 300K Band D	Stability of spectral line during 165 sec	0.001 cm^{-1}	MIO at thermal extremes and mean temperature
Spectral resolution	Band D	FWHM of ILS	0.001 cm^{-1}	MIO at thermal extremes
Spectral linearity	OCB at 250K	Spectral position rms error	0.001 cm^{-1}	MIO at thermal extremes
ILS stability	OCB at 300K	ILS shape during 5 days	0.1 to 0.2%	MIO at thermal extremes and mean temperature
ILS morphology	OCB at 300K	ILS model parameters	1%	MIO at thermal extremes and mean temperature
Radiometric measurements				
Parameters	Testing conditions	Data product	Uncertainty	Remark
Dark NESR	DSS	Instrument noise	30% of radiometric accuracy	MIO at warmest temperature
NESR	OCB at 180, 207, 220, 230 and 250 K	Total noise	30% of radiometric accuracy	MIO at warmest temperature
Radiometric accuracy	OCB at 230 K, DSS	accuracy better than 2xNESR +x% of source radiance (x=5 (band A) to 1 (band D))	30% of radiometric accuracy	MIO at thermal extremes and mean temperature
Dynamic range	OCB at 180, 207, 220, 230 and 250 K	Adequate range up to 270 K	-	MIO at warmest temperature
Damage limit	OCB at 400 K	no damage verification	-	MIO at warmest temperature
Line of sight				
Parameters	Testing conditions	Data product	Uncertainty	Remark
LOS elevation and azimuth	50 um pinhole Band D	LOS algorithm verification Datation verification	-	MIO at mean temperature

2.8.2 Calibration

2.8.2.1 Level 1B

The following calibrations are considered necessary for MIPAS level 1b processing (see index)

2.8.2.1.1 Radiometric offset calibration

Offset calibration is performed by observation of cold space to determine the internal emission of MIPAS (which will be the major source for offset in the spectra). It has to be performed frequently to determine all variations of the instrument self-emission due to temperature variations. It is envisaged to perform an offset calibration after four elevation scan sequences (or every five minutes). This calibration measurement 1.1.3.4. takes about 20 s. It comprises several low-resolution interferometer sweeps that are co-added by the ground segment to reduce noise.

The offset measurements are corrected for detector non-linearity and for fringe count errors.

The algorithm that computes the radiometric offset is described here 2.4.3.1.1. .

2.8.2.1.2 Radiometric gain calibration

Gain calibration is performed by observation of the internal calibration blackbody 3.1.3.1.1.3. source to calibrate the instrument response throughout the spectral bands. Gain calibration also provides the information about phase distortions used for the phase correction of the interferograms during ground processing. It is planned to be performed much less frequently (once per day or less). It comprises a number (about 1,000) of blackbody-cold space measurements 1.1.3.4. performed at low resolution, which are coadded on ground to reduce the random noise. The temperature of the calibration blackbody is also downlinked to provide the basis for the conversion into an absolute radiance units.

The gain measurements are corrected for detector non-linearity and for fringe count errors.

The algorithm that computes the radiometric gain is described here 2.4.3.1.2. .

2.8.2.1.3 Line of sight

LOS calibration is required for the in-flight determination of the actual line-of-sight pointing biases and harmonic variations. This LOS-calibration is based on the observation of stars moving through the IFOV with the short wavelength channels. The actual time of star observation is correlated with the expected time as computed by the pointing information from the attitude and orbit control system (AOCS) of Envisat-1. Thus all biases and slow pointing variations between the star tracker package of Envisat-1 (providing the pointing reference for the AOCS) and the LOS of MIPAS are derived and used for pointing corrections.

The algorithm that performs the LOS calibration is described here 2.4.3.1.6. .

2.8.2.1.4 Spectral calibration

Spectral calibration means that the spectral axes of the radiometrically calibrated limb spectra will be recalibrated typically once per elevation scan. The calibration parameters will be retrieved from subsets of the atmospheric limb measurements, so that the routine scene data acquisition is not interrupted.

The goal of the spectral calibration is to correct the measured spectra for the Doppler shift caused by the relative motion of the satellite and the atmosphere. It also corrects shifts of the diode laser used to sample the interferograms 1.1.3.3. .

Spectral calibration is performed by comparing measured atmospheric spectra in selected spectral windows with theoretical spectra. The spectral lines and windows used are listed in the table below 2.13 . The spectral position of pre-selected lines are compared in both the observed spectra and theoretical spectra. The measured spectra are shifted in groups so that the spectral position of the compared lines matche the reference lines.

The algorithm that performs the spectral calibration is described here 2.4.3.1.3. .

2.8.2.1.5 Instrument line shape

The ILS is the instrumental response to a stimulus, in other words it is a function that describes how the instrument "sees" a spectral line of negligible width. The main contributor to the ILS is the maximum path difference between the two mirrors of the interferometers, the longer the MPD is, the thinner the ILS is. Other contributor to the ILS are the finite optical resolution of the instrument (blur) and misalignment of the optical components.

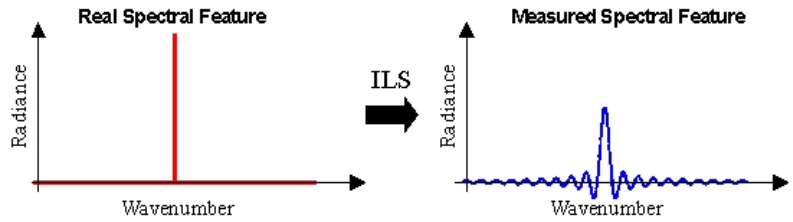

Figure 2.30

The ILS of the instrument is retrieved from the measurements by fitting the measured spectra to a theoretical spectrum built from the convolution a parameterised ILS model and known atmospheric spectral lines. The floating parameters of the model are determined by this fit.

The fitting method is an iterative simplex that stops when the squared difference between the observed and fitted line shape falls below a predefined threshold. The ILS retrieval is performed on recentered spectra and is thus independent of the spectral calibration. The spectral lines and windows used are listed in the table below:

Table 2.13 Reference lines and spectral windows used for spectral calibration and ILS retrieval

Band	Target gas	Peak position (cm^{-1})	Spectral interval (cm^{-1})	Tangent altitude (km)	No. of coadditions	Used for Spectral calibration	Used for ILS Retrieval
A	O_3	802.5074	802.40 - 802.62	30	1	yes	yes
AB	O_3	1125.2085	1125.10 - 1125.30	30	1	yes	no
B	H_2O	1409.9686	1409.85-1410.08	50	1	yes	yes
C	H_2O	1672.4750	1672.40 - 1672.55	50	1	yes	yes
D	H_2O	1966.2615	1966.00 - 1966.50	50	1	yes	yes

The ILS is retrieved from subsets of the routine scene data (as for spectral calibration), at a repetition rate of approximately once per week. It is included in the Level 1b product. It useful to track the evolution of the instrument (alignment, quality of the optical components, etc.). It can also be used during higher level processing to correct the measured spectra so as to remove the effect of the ILS in the measurements.

The ILS retrieval algorithm is described here 2.4.3.1.5. .

2.8.2.1.6 Radiometric calibration

The radiometric calibration is the series of operations that applies the offset and gain measurements to the scene measurements in order to obtain atmospheric spectra in units of spectral radiance.

In a first step, the offset interferogram is subtracted from the scene interferogram. The subtraction is performed only for a reduced number of data points centred around the ZPD position. This reduced range corresponds to a tenth of the spectral resolution used in acquiring deep space measurements. Due to the absence of fine spectral features in the deep space measurements, the offset interferogram is nearly zero outside that range.

In a second step the length of the corrected interferogram (scene minus offset) is extended to next higher power of two (2^N) by adding zeroes symmetrically on both ends. This operation is called "zero filling".

Next, the zero-filled offset-corrected scene interferogram is fast fourier transformed into a raw spectrum with arbitrary units. The prior zero-filling operation allows the use of a time efficient FFT algorithm. The gain interferogram are also zero-filled and FFT'ed. Next the spectral calibration 2.8.2.1.4. is applied to the resulting raw offset-corrected scene spectrum. This raw spectrum is vector of complex values: it has both a real and an imaginary

component.

The gain interferogram undergoes the same processing: offset subtraction, zero filling, FFT, spectral calibration.

The radiometric gain is obtained by dividing the theoretical spectral radiance of the calibration blackbody by the corrected gain raw spectrum. Since the gain spectrum is complex, the radiometric gain is also complex.

The last step of the radiometric calibration is the multiplication of the raw scene spectrum by the gain. The real part of this multiplication is the level 1b product: the calibrated atmospheric spectral radiance. The imaginary component, which should only contain noise, is used for quality verification and for computing the NESR of the measurement.

The application of the radiometric calibration is part of an algorithm described here 2.4.3.1.4. .

2.9 Data handling cookbook

Chapter 3

The MIPAS Instrument

3.1 Instrument description

3.1.1 Overview

MIPAS is a Fourier transform spectrometer for the detection of limb emission spectra in the middle and upper atmosphere. It observes a wide spectral interval throughout the mid infrared with high spectral resolution. Operating in a wavelength range from 4.15 microns to 14.6 microns, MIPAS detects and spectrally resolves a large number of emission features of atmospheric minor constituents playing a major role in atmospheric chemistry. Due to its

spectral resolution capabilities and low-noise performance, the detected features can be spectroscopically identified and used as input to suitable algorithms for extracting atmospheric concentration profiles of a number of target species.

MIPAS is a complex instrument made of several sub-systems. The figure below is a schematic view of MIPAS. It shows the major subsystems.

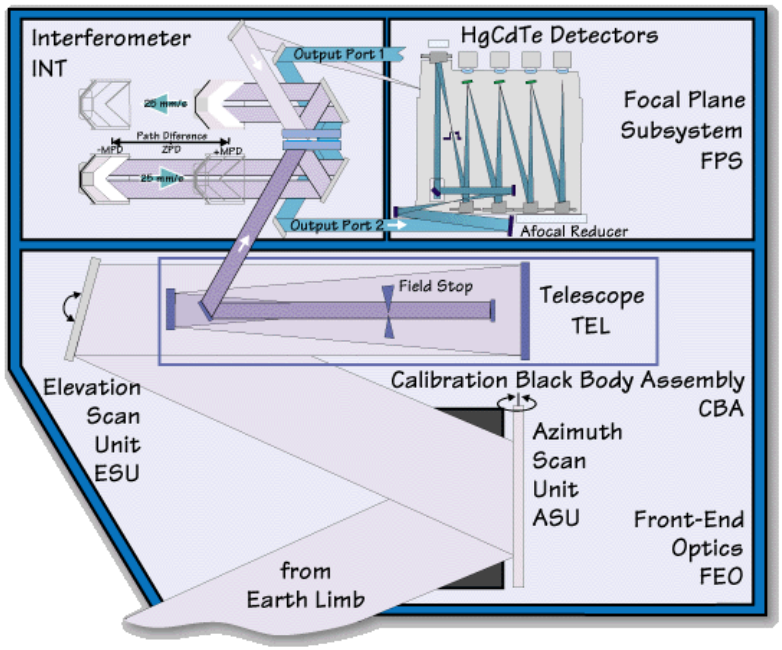

Figure 3.1 Schematic view of MIPAS

Radiation from the Earth limb enters the instrument (at the bottom of the figure). The exact location of the target is selected by rotating two mirrors in the front-end optics subsystem. The elevation scan mirror is used to select an altitude and the azimuth scan mirror is used to select an orientation with respect to the platform. The radiation is then directed to the input telescope and collimator. The collimator produces a collimated beam of radiation that is redirected to the interferometer. The interferometer is the heart of MIPAS. In the interferometer, the radiation beam is split in two parts by a beamsplitter. The two beam fractions are reflected back together to the beamsplitter by two retro-reflectors. When they return to the beamsplitter, the two beam are recombined and they interfere. By moving the retro-reflectors, the interference pattern is modified. The motion of the reflectors is controlled with a laser. The beamsplitter separates the recombined beam in two beams and each is directed to one output port. Behind the interferometer, the output beams are collected by a series of eight detectors (four per output port). The detectors are cooled by a

pair of synchronized Stirling cycle coolers. The detectors record the varying interference pattern. By post-processing of the recorded interferograms, the spectral distribution of the radiation can be obtained.

During the calibration sequence, the azimuth mirror is pointed to an internal calibration blackbody. This blackbody is a reference source that can be used to calibrate the measured signal.

The instrument control unit contains all the electronics to drive the front end optics mirrors (ESU and ASU) and the interferometer subsystems such as the laser diode and the cube corners actuators. It also contains modules used to perform basic processing of the acquired data before transferring it to the ENVISAT platform.

3.1.2 Payload description and position on the platform

The complete MIPAS instrument has a total mass of about 320 kg. Its power consumption is budgeted at 210 W. MIPAS is on a rear corner of the ENVISAT PLM between MERIS and AATSR. From this location and with the help of its pointing mirrors, MIPAS can measure the concentration profiles of various atmospheric constituents on a global scale .

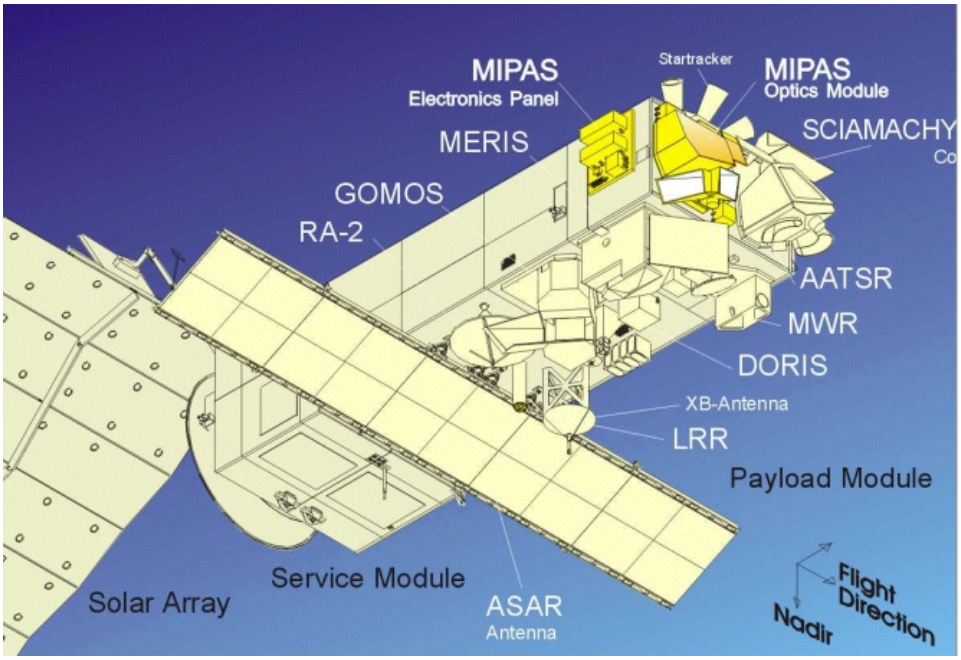

Figure 3.2 ENVISAT in flight

3.1.3 Subsystem description

The space segment of MIPAS is divided into two modules. These modules are further divided into the following subsystems and assemblies (see index)

3.1.3.1 MIPAS Optics (MIO) module

This module includes the Front End Optics 3.1.3.1.1. subsystem, the interferometer and the focal plane subsystem, mounted at the anti-sunward end of Envisat-1. The MIO, is about 1.36 m in the flight direction, 1.46 m high in the nadir direction and 0.74 m in the deep space direction. It has a mass of about 170 kg.

The outside of the MIO is covered in multi-layer insulation to minimize heating from the Sun and the Earth shine. MIPAS is an infrared sensor. It is necessary to reduce the amount of infrared radiation emitted by the instrument itself so that this radiation does not mask the infrared radiation of the atmosphere. To reduce the thermal self-emission of the optical components, the MIO is cooled using passive cooling. A large radiator is used to cool all optical components to about 210 K and two smaller radiators are used to cool the compressor of the Stirling cycle coolers of the detectors and to pre-cool the focal plane subsystem. All radiators are tilted away from nadir by 20 degrees top reduce the Earth shine and thus improve their efficiency.
Below the MIO are two baffles that reduce the amount of stray light that may enters MIPAS: one for the rear view and one for the side view. The baffle for the rear view extends sufficiently far from the first optical component to prevent the direct entry of sunlight when the instrument is observing the south pole region in summer. In this situation, the minimum angle between the Sun and the LOS of the instrument could be as small as 8 degrees. The size of the baffle is reduced on the side illuminated by the Sun to reduce heat input. Further reduction of the baffles' temperature is achieved by using a coating that is reflecting in the visible but absorbing in the thermal infrared.

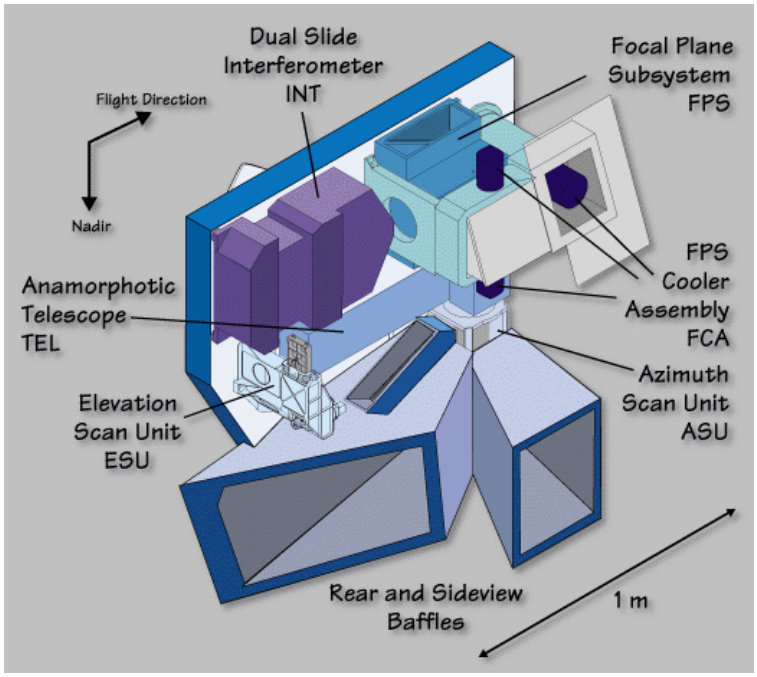

Figure 3.3 3-D view of the MIO

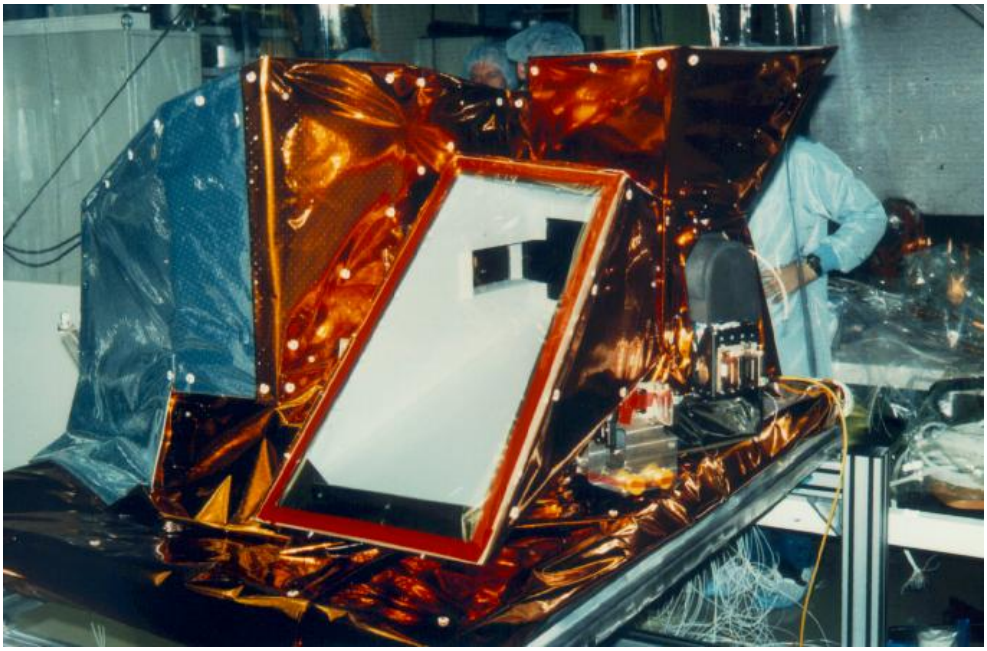

Figure 3.4 Picture of the MIO on its back from the rear side. Note the characters on the back.

3.1.3.1.1 Front End Optics (FEO) subsystem

This subsystem houses the azimuth scan unit and elevation scan unit, the anamorphic telescope and the internal calibration blackbody assembly.

3.1.3.1.1.1 Azimuth Scan Unit (ASU)

•

The azimuth scan unit allows the selection of the line of sight within the two field of view regions, and also to access an internal calibration blackbody source for gain calibration. A flat steering mirror is rotated about an axis parallel to nadir to direct the light into the instrument. This steering mirror has a dimension of about 295 mm in height and 109 mm in width and thus forms the largest optical component of MIPAS.

A second function of the ASU is the protection of the interior of the optics module from contamination; a shield is mounted behind the steering mirror and rotates with it. When the mirror is turned to an end stop, the shield closes the input aperture to the ASU and thus the ASU mirror from contamination during ground handling and the early flight phase.

3.1.3.1.1.2 Elevation Scan Unit (ESU)

•

The elevation scan unit determines the actual limb height of a particular measurement, and thus requires a very high pointing accuracy over a limited angular range. It comprises a flat steering mirror rotating about an axis that is orthogonal to nadir and flight direction. The angle covered by this mirror is less than 3 ° which is sufficient to reach limb heights between 5 km and 250 km; the high value will be used for measurements of cold space to determine the instrument self emission for offset calibration.

3.1.3.1.1.3 Calibration Blackbody Assembly (CBA)

•

This is a blackbody mounted in the azimuth scan unit is the calibration blackbody, used for the in-flight calibration of the instrument responsivity. To fill the IFOV, it needs a rather large clear aperture (55.165 mm^2). Its design is derived from the blackbody design for the along-track scanning radiometer (ATSR), presently flying on the ERS-1 and -2 satellites. Its emissivity is above 99.6 %, so that a high accuracy for the gain calibration becomes achievable. For precision gain calibration measurements, it can be heated to about 40 K above the ambient instrument temperature to increase its radiance emission. Its nominal temperature will then reach up to 250 K. The temperature of the calibration blackbody is monitored by a platinum resistance temperature (PRT) sensor.
The electrical signal of the PRT is included in the data packet downlinked to the ground station.

3.1.3.1.1.4 Receiving Telescope (TEL)

•

The front-end telescope collects the incident radiation to collimate it so as to match it to the input dimensions of the interferometer, and defines the IFOV of MIPAS. Driven by the demand for an atmospheric object size with a large edge ratio (30 km horizontal to 3 km vertical dimension), the overall volume of telescope and interferometer resulted in a design with a magnification of 6 in elevation and 1 in azimuth. The input aperture of the telescope is 55.165 mm^2, and thus the entrance aperture of the interferometer is 55.27 mm^2. A further reduction of the free aperture to 135.35 mm^2 by two Lyot stops is necessary to reduce the stray light contribution. A field stop in the focal plane of the front-end telescope defines the instrument IFOV. Thus, the view geometry of all following components is uniquely determined by this component and not by the position of the cold stops in front of the detector elements, thereby ensuring that all detection channels view the same atmospheric volume at the Earth's limb.

3.1.3.1.2 Interferometer (INT) subsystem

To meet the radiometric and spectrometric performance requirements, as well as the lifetime requirement of four years of continuous operation in space, a symmetrical dual slide interferometer with dual input and output ports has been selected. This provides highest detectable signal at the outputs, the least uncertainties in design, the highest degree of redundancy, and the most compact dimensions. It has a folded path to allow a more compact arrangement of the interferometer and to allow better compensation of the momentum generated by the cube corners during the reversal of their motion. The incident angle of the radiation onto the beamsplitter is 30 ° to reduce polarization effects by the beamsplitter. The MIPAS interferometer is over 0.58 m long and about 0.36 m wide, and has a mass of about 30 kg. It has the following major subassemblies: Interferometer Optics (INO), Interferometer Mechanism Assembly (IMA), and Optical-path Difference Sensor. Click here for details on

how the interferometer works 1.1.3.1. .

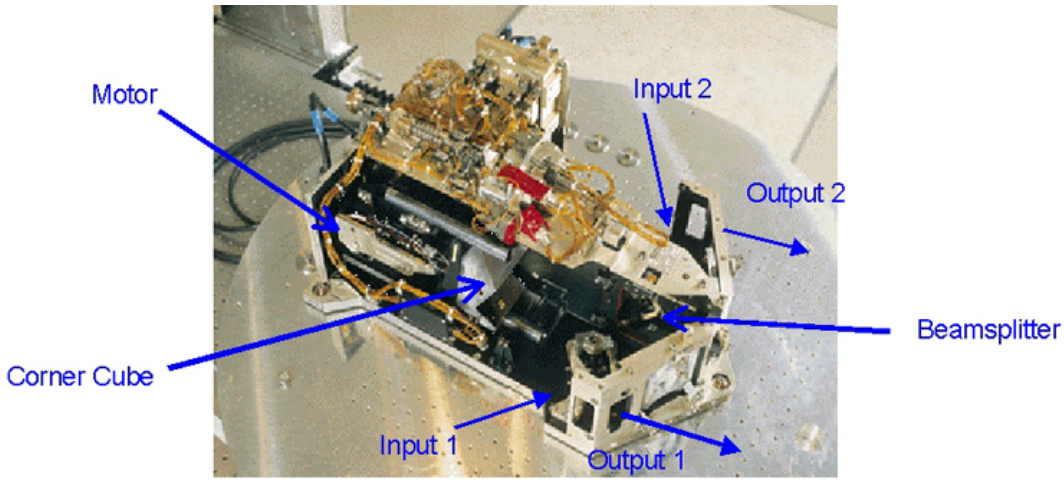

Figure 3.5 The MIPAS interferometer and its main parts

3.1.3.1.2.1 Interferometer optics (INO)

- The interferometer optics comprises the beamsplitter assembly, flat steering mirrors, and the cube corners on the slides. The beamsplitter coatings themselves are quite critical, as they have to provide a reflectance near 50 % throughout the broad spectral range. More difficult to manufacture are the broadband antireflection coatings on the other surfaces that are essential to reduce undesired interferometer effects that would modulate the transmission of the substrate and could result in ghost spectra. The beamsplitter assembly also has to compensate the phase delays caused by the varying refractive index throughout the spectral range. This is done with a second substrate of same thickness as the beamsplitter itself and mounted with a narrow gap to the beamsplitter coatings. Both substrates have a slight wedge angle to reduce the residual Etalon effects.

3.1.3.1.2.2 Interferometer mechanism assembly (IMA)

The two identical interferometer drive units perform the actual translation of the cube corners. Linear motors behind the cube corners generate the drive force. The slides are guided by mechanical bearings. The lifetime requirement of four years' continuous operation corresponds to about 20 million motion cycles for each of the bearings. Lifetime tests have

shown that dry lubricated ballbearings operating with a light preload can well achieve this lifetime. The difference velocity between the two slides has to be controlled with less than 1% rms error. A drive control loop processes the inputs from linear optical encoders in each of the drive arms for a coarse control and for centering of the slides, and from a built-in laser interferometer (called the optical-path difference sensor or ODS) for fine velocity control. The laser interferometer is also required to trigger the sampling of the detector output at very precise intervals of optical path values.

3.1.3.1.2.3 Optical-path difference sensor (ODS)

- The built-in laser interferometer makes use of a single-mode 1.3 micron diode laser which is located in the optics module near the Stirling coolers. The output from the diode laser is guided by a single mode polarizing optical fibre to the interferometer. Although the individual components are proven in many communication systems, their use in a spaceborne instrument with operation over a wide temperature range is new and requires space qualification. The 1.3 micron radiation from the ODS laser and its fibre optics are circularly polarised and injected to the interferometer via dedicated filter coatings on the beamsplitter. The circular polarisation allows to retrieve both sine- and cosine components of the superimposed beams, and thus to determine the direction of the cube corner motion. This direction information will be important as the interference fringes of the optical path difference system will provide an absolute position reference between two gain calibration sequences, that must be accurately maintained. The laser diode is stabilised in temperature to limits its frequency drift to less than 50 MHz for periods of 200 seconds. No absolute frequency control is used since the spectra acquired by MIPAS can easily be spectrally calibrated using known atmospheric lines.

3.1.3.1.3 Focal Plane Subsystem (FPS)

The two output beams from the interferometer are reduced in size by two small off-axis Newton telescopes, and directed into the cold focal plane subsystem, which houses the signal detectors with their interfaces to the active coolers, as well as the associated optics required for spectral separation and beam shaping. It is smaller than the interferometer (0.36 m wide and 0.45 m high, including the precooler radiator on top) and has a mass of 16 kg.

To achieve the best radiometric sensitivity, a set of four detectors in each output port (thus a total of eight detectors) are used, each optimized for highest sensitivity in a spectral band. A set of beamsplitters and steering mirrors separate the input from the two interferometer ports to the different spectral bands, and the optics required to illuminate each detector element. All optical elements are mounted and aligned in a very tight package. All optics and the detectors are cooled to 70 K to reduce their thermal emission. Cooling is performed by a pair of active Stirling cycle coolers. Thus, although the focal plane subsystem is conceptually a simple design, the numerous interfaces between the optics, the detectors and the coolers under the constraints of good thermal insulation and high alignment stability of the optical components result in very demanding requirements. The focal plane subsystem

has the following elements: detector/preamplifier unit (DPU) and focal-plane cooler assembly (FCA) (see below).

3.1.3.1.3.1 Detector/preamplifier unit (DPU)

To achieve the specified radiometric sensitivity, detectors have to be optimized for a specific spectral band. An analysis has shown that four spectral bands in each interferometer output port are required to achieve the low instrument noise contribution and to provide some redundancy at the long wavelength region. Thus a total of eight detector elements are needed in MIPAS. In the long wave spectral region (14.6 to about 7 microns), only photoconductive HgCdTe detectors (PC-CMT) are able to meet the specifications on low noise contribution and electronics bandwidth. At the shorter wavelengths (7 to 4 microns), photovoltaic HgCdTe detectors (PV-CMT) are the best choice. The detector elements are cooled to about 70 K to reduce their internal noise contribution. The preamplifiers are individually optimized for each detector to fulfill stringent requirements on noise, phase distortions and linearity. The cold part of the preamplifiers are mounted in the detector housing, while final amplification is performed in an externally mounted package at room temperature.

3.1.3.1.3.2 FPS Cooler Assembly (FCA)

•

The complete inner structure of the focal plane subsystem (housing, optics, detectors, and preamplifiers) is cooled to 70 K. Passive cooling has been considered but would require a rather large cooler, while active coolers allow to reach these temperatures under all operating conditions. Stirling cycle coolers with a performance that satisfies the cooling requirements of MIPAS (500 mW heat lift at 70 K temperature) are used in a twin-cooler arrangement, comprising two identical compressor and displacer units that operate synchronously to compensate most vibrations from the oscillating parts.

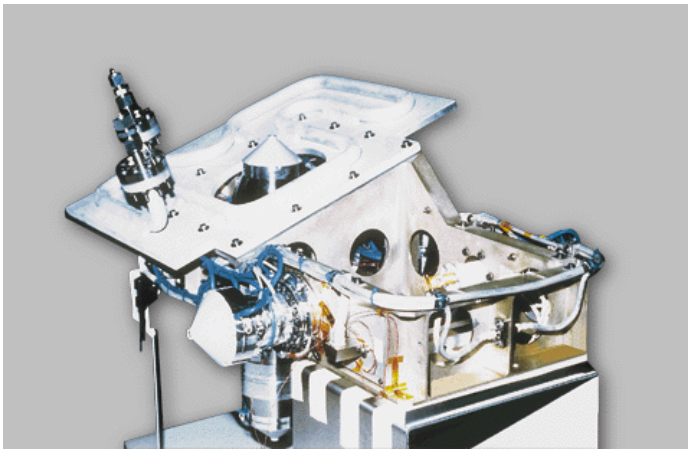

Figure 3.6 Picture of the FPS Cooler Assembly

3.1.3.2 MIPAS Electronics (MIE) module

The MIE comprises the electronics support plate (ESP), the instrument control electronics (ICE) boxes, the MIPAS power distribution unit (MPD), the digital bus unit (DBU) and the signal processing electronics subsystem (SPE). Most of the MIE is located on the rear-looking side of the instrument. Some elements of the MIE (SPE, PAW and FCE) are on the deep space side of the instrument.

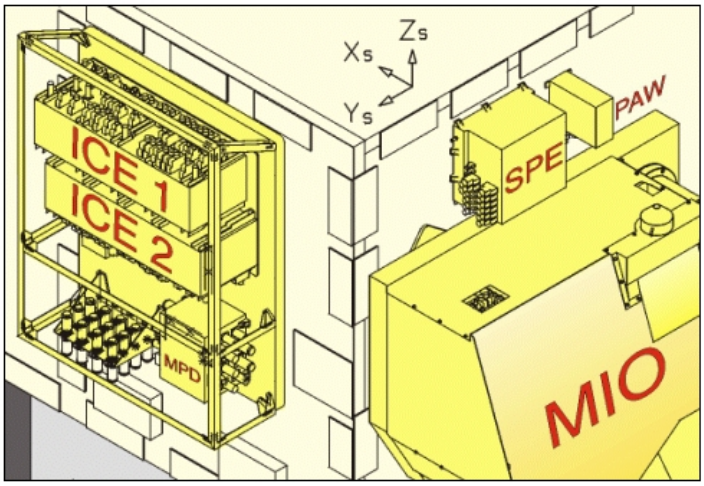

Figure 3.7 View of some MIE modules mounted on ENVISAT

3.1.3.2.1 Electronics Support Plate (ESP)

The plate is the support on which several of the elements of the MIE are attached. The ESP is located on the rear-looking side of the instrument.

3.1.3.2.2 Instrument Control Electronics (ICE)

The instrument control electronics ICE contains all electronics modules to supervise and to execute macrocommands for MIPAS, and it also houses the plug-in modules to drive the FEO and INT subsystems. The Stirling coolers of the FPS are controlled by a dedicated electronics box. There are two ICE boxes (ICE 1 and ICE 2) for redundancy. Both ICE boxes are attached to the ESP and placed on the rearward looking side of the instrument.

3.1.3.2.3 MIPAS Power Distribution Unit (MPD)

This task of this unit is to distribute power from ENVISAT to the various electronical and mechanical components of MIPAS. It is located below the ICE on the ESP.

3.1.3.2.4 Signal Processor Electronics (SPE)

The onboard signal processing electronics (SPE) is in charge of performing the housekeeping and the first processing of the raw data collected by the MIPAS instrument. It is located on the deep-space side of the instrument over the MIO. In details, it performs the following functions:

- analogue anti-alias filtering of the detector outputs
- digitization (16 bit, 77 kHz) of each signal
- digital filtering to reduce bandwidth
- decimation to reduce the data rate
- combination of some detector outputs, if appropriate, downsampling, word length reduction, and data compressing to reduce the data rate
- combination of all output data, formatting and transmission (nominal data rate is 550 kbit/s) to the platform data handling and transmission interface.

Onboard decimation is used to reduce the data rate. Digital filtering and decimation can be disabled by telecommand. However, if they are disabled, the data rate increases to 8 Mbit/s which can be used only for a short time.

During the formatting of the data stream, the word length of the interferogram data is

reduced. As the full dynamic range of ADC is used only near the zero path difference points, the remainder of the interferograms can be coded on a much smaller number of bits which significantly reduce the data rate.

The interferograms and pointing data are downlinked to ground, where the phase correction, anodisation, retransformation, and radiometric/spectral calibration will be performed to yield the atmospheric spectra. Further processing of these spectra to derive concentration profiles of atmospheric constituents will also be performed by the ground segment.

3.1.3.2.5 Detector Preamplifier (PAW)

•

The detector preamplifiers are responsible for increasing the signal of the detectors. They are individually optimized for each detector to improve the signal to noise ratio and the linearity and reduce phase distortion. The cold part of the preamplifiers is mounted in the detector housing and the final amplification is performed by the PAW (preamplifier warm) which is located close to the FPS above the MIO and beside the SPE. The preamplifiers gain is programmable by telecommand. However, once it is adjusted to achieve the full dynamic range of the ADC, it remains constant during the interferometer sweep and elevation scans.

3.1.3.2.6 Focal plane cooler drive electronics (FCE)

•

The FCE is responsible for controlling the two synchronised Stirling coolers that keep the detectors at 70 K.

3.2 Instrument characteristics and performances

This section described the main specification of the instrument as determined by the pre-flight characterisation campaigns. This is followed by a section on the in-flight verification plan.

3.2.1 Preflight characteristics and expected performances

3.2.1.1 Spectral

3.2.1.2 Spatial

3.2.1.3 Radiometric

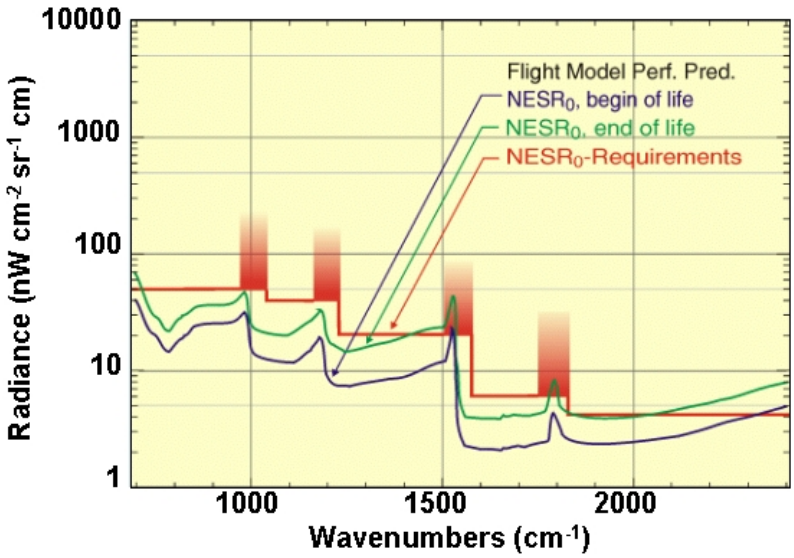

Figure 3.8 Instrument noise (dark noise) predictions (green and blue) and requirements (red)

3.2.1.4 Pointing

3.2.1.5 Stability

3.2.1.6 Summary

This table contains a list of the performance and characteristics of MIPAS

Table 3.1

Performance	Expected value	Notes
Mass	320 kg	
Volume		
Electrical power consumption	< 210 W	During operation mode
Instrument temperature	210 K	
Detector temperature	70 K	
Spectral range, Band A	685 - 970 cm^{-1}	
Spectral range, Band AB	1020 - 1170 cm^{-1}	
Spectral range, Band B	1215 - 1500 cm^{-1}	
Spectral range, Band C	1570 - 1750 cm^{-1}	
Spectral range, Band D	1820 - 2410 cm^{-1}	
Spectral stability	0.001 cm^{-1}	During 165 seconds
Spectral resolution	< 0.035 cm^{-1}	Defined as the FWHM of the ILS
Spectral bin width	0.025 cm^{-1}	0.5 / MPD
Maximum optical path difference	20 cm	
Mean dark NESR, Band A	50 nW cm^{-2} sr^{-1} cm	NESR due to instrument only
Mean dark NESR, Band AB	40 nW cm^{-2} sr^{-1} cm	NESR due to instrument only
Mean dark NESR, Band B	20 nW m^{-2} sr^{-1} cm	NESR due to instrument only
Mean dark NESR, Band C	6 nW cm^{-2} sr^{-1} cm	NESR due to instrument only
Mean dark NESR, Band D	4 nW cm^{-2} sr^{-1} cm	NESR due to instrument only
Radiometric accuracy, Band A		
Radiometric accuracy, Band AB		
Radiometric accuracy, Band B		
Radiometric accuracy, Band C		
Radiometric accuracy, Band D		
LOS uncertainty		
LOS stability		
Elevation scan range	5 to 150 km	Tangential height
Azimuth scan range	80 -110 and 160-195 deg.	w/r to flight direction
Operation period	continuous	
Coverage	global coverage	

3.3 Inflight performance verification

Instrument Characteristics and Performance This section described the main specification of the instrument as determined by the pre-flight characterisation campaigns. This is followed

by a section on the in-flight verification plan. Pre-flight characteristics and expected performance Spectral Spatial Pointing Radiometric

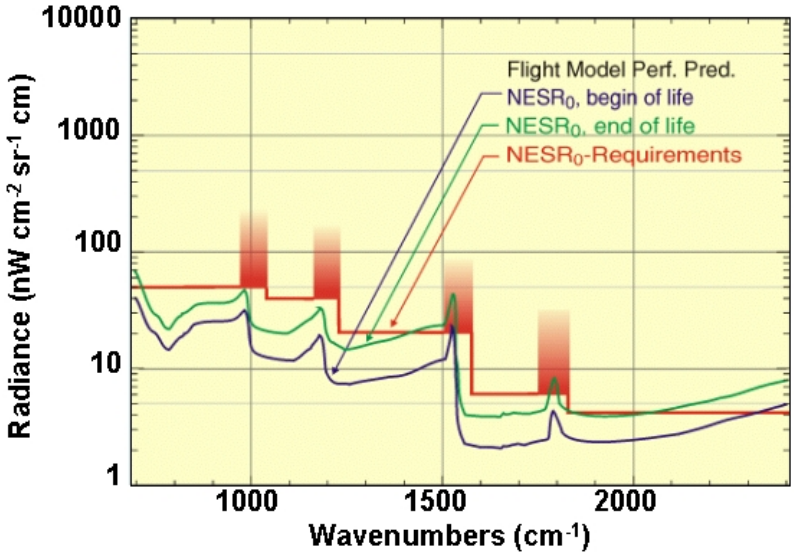

Figure 3.9 Instrument noise (dark noise) predictions (green and blue) and requirements (red)

Stability Summary

Table 3.2 This table contains a list of the performance and characteristics of MIPAS

Performance	Expected value	Notes
Mass	320 kg	
Volume		
Electrical power consumption	< 210 W	During operation mode
Instrument temperature	210 K	
Detector temperature	70 K	
Spectral range, Band A	685 - 970 cm^{-1}	
Spectral range, Band AB	1020 - 1170 cm^{-1}	
Spectral range, Band B	1215 - 1500 cm^{-1}	
Spectral range, Band C	1570 - 1750 cm^{-1}	
Spectral range, Band D	1820 - 2410 cm^{-1}	
Spectral stability	0.001 cm^{-1}	During 165 seconds
Spectral resolution	< 0.035 cm^{-1}	Defined as the FWHM of the ILS
Spectral bin width	0.025 cm^{-1}	0.5 / MPD
Maximum optical path difference	20 cm	
Mean dark NESR, Band A	50 nW cm^{-2} sr^{-1} cm	NESR due to instrument only
Mean dark NESR, Band AB	40 nW cm^{-2} sr^{-1} cm	NESR due to instrument only
Mean dark NESR, Band B	20 nW m^{-2} sr^{-1} cm	NESR due to instrument only
Mean dark NESR, Band C	6 nW cm^{-2} sr^{-1} cm	NESR due to instrument only
Mean dark NESR, Band D	4 nW cm^{-2} sr^{-1} cm	NESR due to instrument only
Radiometric accuracy, Band A		
Radiometric accuracy, Band AB		
Radiometric accuracy, Band B		

Radiometric accuracy, Band C		
Radiometric accuracy, Band D		
LOS uncertainty		
LOS stability		
Elevation scan range	5 to 150 km	Tangential height
Azimuth scan range	80 -110 and 160-195 deg.	w/r to flight direction
Operation period	continuous	
Coverage	global coverage	

In-flight performance validation

Chapter 4

Frequently Asked Questions

Work in progress

Chapter 5

Glossary

5.1 List of acronyms

AILS: Apodized Instrument Line Shape (i.e. Instrument Line Shape after apodization)

AATSR: Advanced Along Track Scanning Radiometer

ADC: Analog to Digital Converter

ADS: Annotated Data Set

ADSR: Annotated Data Set Record

AOCS: Attitude and Orbit Control System

ASU: Azimuth Scan Unit

ATSR: Along-Track Scanning Radiometer

CBA: Calibration Blackbody Assembly 3.1.

CBB: Calibration Black Body 3.1.

CCM: Cross-Correlation Method

DS: Deep Space

DSD: Data Set Descriptors 2.4.3.2.

DSR: Data Set Record

DSS: Deep Space Simulator

ECMWF: European Center for Medium range Weather Forecast

ENVISAT: Environmental satellite

ERS: European Remote Satellite

ESP:Electronics Support Plate 3.1.

ESU: Elevation Scan Unit 3.1.

FCA: FPS Cooler Assembly 3.1.

FCE: Focal-plane Cooler Electronics

FCE: Fringe Count Error 2.4.3.1.9.

FEO: Front End Optics 3.1.

FFT: Fast Fourier Transform

FOV: Field of View

FPS: Focal Plane Subsystem 3.1.

FTS: Fourier Transform Spectrometer 1.1.4.1.1.

FWHM: Full Width at Half Maximum

GADS: Global Annotated Data Set

GOMOS: Global Ozone Monitoring by Occultation of Stars

ICE: Instrument Control Electronics 3.1.

IFFT: Inverse Fast Fourier Transform

IFOV: Instantaneous Field of View

IGM: Interferogram

ILS: Instrumental Line Shape (see also here)

IMK: Institute for Meterology and Climate Research (Karlsruhe, Germany)

INT: Interferometer 3.1.

LBL: Line-by-line (method for computing absorption cross-sections)

LISA: Limb Sounder of the Atmosphere

LOS: Line Of Sight

LTE: Local Termodynamic Equilibrium

LUT: Look-Up-Table

MDS: Measurement Data Set

MDSR: Measurement Data Set Record

MERIS: MEdium Resolution Imaging Specrometer

MIE: MIPAS Electronics module 3.1.

MIO: MIPAS Optical module 3.1.

MIPAS: Michelson Interferometer for Passive Atmospheric Sounding

MPD: Maximum Path Difference 5.3.2.

MPD: MIPAS Power Distribution unit

MPH: Main Product Header 2.4.3.2.

MW: Microwindow

NESR: Noise Equivalent Spectral Radiance

NL: Non Linearity 2.4.3.1.10.

NRT: Near Real Time

OCB: Blackbody Optical Calibration facility

OCF: Optical Calibration Facility

ODS: Optical-path Difference Sensor 3.1.

OFM: Optimized Forward Model

OM: Occupation Matrix

OPD: Optical Path Difference

ORM: Optimized Retrieval Model

PAW: PreAmplifier Warm 3.1.

PC: PhotoConductive

PDS: Payload Data Segment

PFM: Peak Finding Method

PLM: Payload Module

PRT: Platinum Resistance Thermometer

PV: PhotoVoltaic

RAM: Random Access Memory

RFM: Reference Forward Model

RMS: Root Mean Squared

RSL: Radiometrically and Spectrally and Locally calibrated

SCIAMACHY: Scanning Imaging Absoprtion Spectrometer for Atmopsheric Chartography

SNR: Signal to Noise Ratio

SPC: Spectrum

SPE: Signal processing electronics 3.1.

SPH: Specific Product Header 2.4.3.2.

UTC: Universial Time Coordinated

VCM: Variance Covariance Matrix

VMR: Volume Mixing Ratio

WGS84: World Geodetic System 1984

ZPD: Zero Path Difference

5.2 Alphabetical index of technical terms

A - B - C - D - E - F - G - H - I - J - K - L - M - N - O - P - Q - R - S - T - U - V - W - X - Y - Z

A
Altitude range

Anamorphic telescope

Atmospheric continuum

Auxiliary data
B Baffle

Bands

Beamsplitter

Blackbody
C Calibration

Coaddition

Corner cube retro-reflectors
D Decimation

Doppler effect

Doppler shift
E Elevation Scan

Emissivity

Exitance
F Flux
G Gain
H Horizontal spacing
I Instrumental line shape

Intensity

Interference

Interferogram

Irradiance

Irregular grid
L Level 0 data

Level 1a data

Level 1b data

Level 2 data

Limb scan

Limb scanning sequence

Limb view
M Maximum path difference

Measurement data

Microwindow
N Nadir

Noise Equivalent Spectral Radiance

Nominal scan
O Observational data
R Radiance

Radiometric calibration

Radiometric quantity

Radiometry

Retrieval grid
S Scan

Signal to noise ratio

Sinc function eq. 5.3

Special event scan

Spectral bands

Spectral bindwidth

Spectral calibration

Spectral interval

Spectral resolution

Spectroradiometer

Spectrum

Stirling cycle

Sweep
T Tangent point

Tangent pressure
V Vertical spacing
W Wavenumber
Z Zero level calibration

Zero Path Difference

ZPD time

5.3 Glossaries of technical terms

Technical terms used throughout the handbook are explained in the technical glossaries. These glossaries are regrouped by subject. There is also an alphabetical index of all the technical terms of these glossaries and an alphabetical index of acronyms.

- Alphabetical index of acronyms 5.1.
- Alphabetical index of technical terms 5.2.
- Glossaries of technical terms by subject:

- Data processing terms 5.3.1.
- Miscellaneous hardware and optical terms 5.3.3.
- Pointing and geolocation terms 5.3.4.
- Spectrometry and radiometry terms 5.3.2.
- Level 2 processing terms 5.3.5.

5.3.1 Data Processing

Auxiliary data: Auxiliary data are all data to be provided by an instrument or an external source to allow full interpretation and evaluation of its observational data.
Coaddition: Coaddition is synonym of averaging.
Level 0 data: MIPAS Level 0 data is a raw interferogram with corresponding ancillary data. Level 0 data typically covers one complete orbit corresponding to a data stream of about 100 minutes. Level 0 data comes directly from the instrument.
Level 1a data: MIPAS Level 1a data is an intermediary data set. It consists of reconstructed interferograms. Level 1 a data are not archived.
Level 1b data: MIPAS Level 1b data is a radiance spectrum that is geolocated, radiometrically calibrated, spectrally calibrated, corrected for spike, corrected for non-linearity and fringe count errors, and annotated with quality indicators.
Level 2 data: MIPAS Level 2 data include geolocated geophysical parameters retrieved from the atmospheric radiance spectra. Level 2 data includes: atmospheric pressure at tangent altitudes, kinetic temperature, tangent height correction, volume mixing ratio of O_3, H_2O, HNO_3, CH_4, and N_2O and variance / covariance matrices for the retrieved profile data.
Measurement data: Measurement data are all processed observational data and auxiliary data delivered by the instrument to the PPF Data Handling Assembly.
Observational data: Observational data are all raw sensor data acquired by the instrument after digitization.

5.3.2 Spectrometry and radiometry

Bands: MIPAS detectors are combined in five spectral bands. The table below gives the detectors configuration and the spectral range of these bands.

Table 5.1

Band	Detectors	Spectral range (cm^{-1})
A	A1 and A2	685 - 970
AB	B1	1020 - 1170
B	B2	1215 - 1500
C	C1 and C2	1570 - 1750
D	D1 and D2	1820 - 2410

Beamsplitter:
In MIPAS, the beamsplitter is a plate of transparent material with optical coatings designed to reflect 50% of the incoming infrared radiation and let the remaining fraction goes through. In other words, it is a semi-transparent mirror.
Blackbody: An ideal body that completely absorbs all radiant energy striking it and, therefore, appears perfectly black at all wavelengths. The radiation emitted by such a body when heated is referred to as blackbody radiation and is given by the Planck's equation. Black body radiation is only function of the temperature of the black body emitting it. Almost ideal blackbodies are often used as reference sources in infrared radiometry.
Calibration: Radiometric calibration is the process by which physical units are attributed to the raw spectrum derived from the measured interferograms. The radiometric calibration is applied as follow:

$$L = G\,x \qquad \text{eq 5.1}$$

$$\text{FFT}\{I - I_o\} = G\,x\,(S - S_o)$$

where L is the calibrated radiance, G is the radiometric gain, S is the raw spectrum to calibrate and I is its correspondin interferogram, I_o is the interferogram acquired while looking at the deep space (offset measurement 1.1.3.5.) and S_o is its corresponding raw spectrum.

Click here for details.

Spectral calibration is the process by which the wavenumber of every point of the spectrum are validated and corrected if necessary. Spectral calibration is done by verifying the spectral position of reference atmospheric lines. Click here for details.

Cube corner retro-reflectors:
A cube corner retro-reflector is made of three perpendicular flat mirrors. Any ray of light that strikes the inside of the cube corner is reflected in the same direction that it came.
Decimation: The act of systematically rejecting points at given intervals in the interferogram. Decimation is used to reduce the data rate. The decimation factor is the integer ratio of the initial sampling frequency to the new one. Decimation factors are programable. The following table list the nominal decimation factors for the bands of MIPAS:

Table 5.2

Band	Detectors	Decimation factor
A	A1 and A2	21
AB	B1	38
B	B2	25
C	C1 and C2	31
D	D1 and D2	11

Doppler shift: A spectral shift of the observed radiation as a result of the Doppler effect. The Doppler effect is due to a relative motion between the source and the observer. The radiation emitted from a source that moves away from an observer appears to be of lower frequency than the radiation emitted from a stationary source. The radiation emitted from a source moving toward the observer appears to be of a higher frequency than that from a stationary source. For MIPAS, the Doppler shift is caused by the relative motion between ENVISAT and the atmosphere.

The random relative motion of the atmospheric molecules causes a broadening of the atmospheric spectral lines, called Doppler broadening. Since the relative motion of the atmospheric molecules depends on pressure and temperature, the importance of the Doppler broadening contains information about the altitude and the temperature of the air.
Gain In MIPAS 5.1. the radiometric gain, G, is computed as follow:

$$G = L_{bb} / (\qquad \text{eq 5.2}$$

FFT$\{I_{bb} - I_o\}) = L_{bb} / (S_{bb} - S_o)$

where L_{bb} is the theoretical radiance of the calibration blackbody. I_{bb} is the interfeogram acquired while looking at the calibration blackbody (gain measurement), I_o is the correspomding raw spectrum, Io is the interferogram acquired while looking at the deep space (offset measurement 1.1.3.5.) and I_o is the corresponding raw spectrum. See radiometric calibration.
Emissivity: The ratio of an object's radiance to that emitted by a blackbody radiator at the same temperature and at the same wavelength. A perfect blackbody has an emissivity of 1.
Exitance: Exitance is the amount of radiant flux emitted by a source per unit source area. It is the surface density of power on a source. It depends only on the source. For example a spherical source with a radius of 1 cm that emits a radiant flux of 10 W has an exitance of 10 W divided by the surface (4 pi times 1 cm^2) or 25000 W m^{-2}.

Flux:
Radiant flux (also called radiant power) is the amount of energy emitted by a source or received by a detector per unit time. For example if a source emits 100 Joules of radiant energy in 10 seconds, its radiant flux is 10 Watt.
Instrumental line shape: The instrumental line shape (or ILS) is the unapodised instrumental

response to a stimulus of negligible spectral width. The ILS varies as a function of the wavenumber. The ILS also determines the spectral resolution of the instrument.

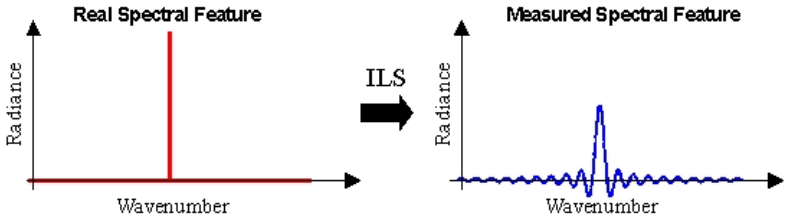

Figure 5.1

Intensity:
Intensity is the amount of radiant flux radiating in a given direction per unit solid angle. For example an isotropic source that emits a radiant flux of 10 Watt has an intensity of 10 W divided by the solid angle of sphere (4 pi steradians) or 0.8 W sr^{-1} in any direction and at any distance from the source.

Interference:
The additive process whereby the amplitudes of two or more overlapping radiation beams are systematically attenuated and reinforced.

Interferogram:
Photographic or electronic recording of an interference pattern.

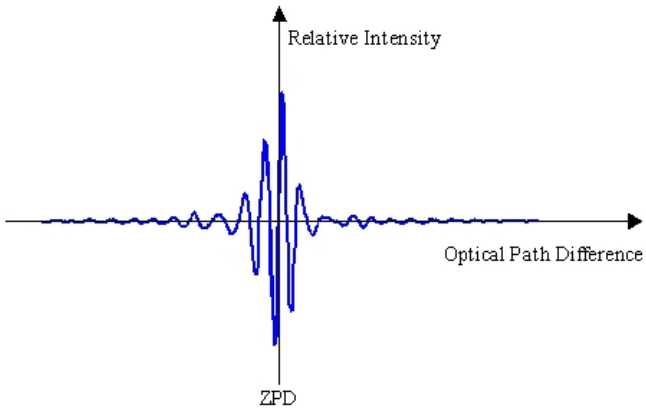

Figure 5.2

A typical interferogram

Click here to see a simulated inteferogram of MIPAS.

Irradiance:
Irradiance is the amount of radiant flux received by a surface perpendicular to the incident radiation per unit area of the surface.

Maximum path difference:
Maximum path difference (MPD) is the maximum distance between a mirror and ZPD. It is half the maximum effective distance between the two mirrors of the interferometer. For MIPAS, the MPD is 20 cm.
Noise Equivalent Spectral Radiance: The noise equivalent spectral radiance (NESR) is the rms noise of a given measurement expressed in unit of radiance.
Radiance: Radiance is the amount of radiant flux propagating in a given direction per unit area and unit solid angle. It is the most general radiometric quantity. It is used to describe both emitted and received radiation.

Radiometric quantity:
The various quantities used in radiometry to quantify radiation. The usual radiometric quantities, the symbols used in this document to describe them and their SI units are given in the following table:

Table 5.3

Radiometric quantity	Symbol	Units
Energy	Q	J
Power, flux	F	W
Exitance	M	$W\ m^{-2}$
Irradiance	E	$W\ m^{-2}$
Intensity	I	$W\ sr^{-1}$
Radiance	L	$W\ m^{-2}\ sr^{-1}$

Spectral radiometric quantity are given per unit wavelength or per unit wavenumber.

Radiometry:
The science interested by the detection, measurement and quantification of electro-magnetic radiation in terms of energy.
Signal to noise ratio: Signal to noise ratio is the signal divided by the noise, both quantities being given in the same units. It gives the relative importance of the measured signal compared to the noise in the measurement.

Spectral binwidth:
The spectral binwidth or spectral interval is the difference along the spectral axis between two consecutive points in a spectra. This is to be distinguished from the spectral resolution. The spectral interval in wavenumber units of spectra generated by a given Fourier transform spectrometers is a constant and is given by 0.5 / MPD.

Spectral resolution:
Spectral resolution determines the ability of the instrument to distinguish closely spaced spectral features. An instrument cannot distinguish two spectral features that are closer than its spectral resolution. Spectral resolution is usually determined by the full width at half maximum of the instrumental line shape.Spectral resolution is often confused with spectral bindwidth.
Spectroradiometer: An instrument that is calibrated so as to measure radiation (energy) amplitude as a function of wavelength.
Spectrum: A curve that shows a spectral radiometric quantity as a function of wavelength (or wavenumber).

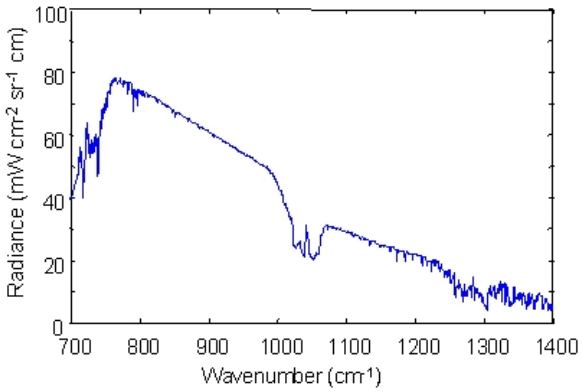

Figure 5.3

A typical atmospheric spectrum
Click here to see a simulated MIPAS spectrum.
Sweep: Recording for a single interferogram. A sweep can be forward or reverse. The adjective forward or reverse are attributed to the sweep depending on the direction of motion of one of the cube corner of the interferometer.

Wavenumber:
In spectroscopy, the wavenumber is the inverse of the wavelength. In infrared spectroscopy it is customary to express the wavenumber in cm^{-1}. Wavenumbers are preferred to wavelengths in Fourier transform spectroscopy because the spectra measured by such instruments are of constant step size (along the spectral axis) when expressed in wavenumbers.
Zero Path Difference: The expression "Zero path difference" or ZPD is used to describe the

location of the moving mirrors such that the two arms of the interferometer are of equal optical path length. At ZPD, the interference is constructive for every wavelengths and the interferogram is at its absolute maximum in one of the output port (and thus at its absolute minimum in the other output port).

5.3.3 Miscellaneous hardware and optical terms

Anamorphic telescope:
A telescope, usually having one or more cylindrical surfaces, used to produce distorted images and later to restore them to true form.

Baffle:
An opaque shielding device designed to reduce the effect of stray light on an optical system.

Stirling cycle:
The Stirling cycle is a thermodynamical cycle named after its inventor, a Scottish minister. It comprises in succession an isothermal expansion of a fluid, a constant-volume cooling, an isothermal compression, and a constant-volume heating. Stirling cycle coolers are mechanical coolers that use the Stirling cycle.

5.3.4 Pointing

Altitude range: The altitude range is delimited by the first and last measurement of the same elevation scan.
Elevation Scan: An elevation scan include all the measurements made by varying the angle of the elevation mirror while the azimuth mirror remains at a fixed angle. See pointing 1.1.4.2. for more information.
Horizontal spacing: The distance along-track between two measurements at the same altitude.
Nadir: In a remote sensing system, nadir refers to the point on the ground located vertically below the center of the system.
Nominal scan: A nominal scan is a elevation scan that acquired in nominal mode 1.1.4.2. . Other type of scans are called "special event scans".
Special event scan: Any scene measurement scan that is not a nominal scan.
Tangent point: The point where the line of sight of MIPAS intercept a line that is

perpendicular to the Earth geoid.

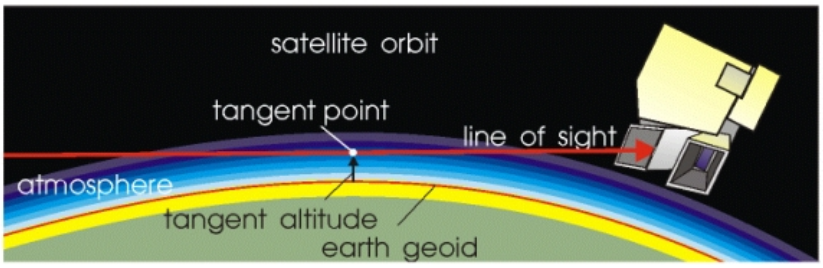

Figure 5.4

Vertical spacing: The distance between two consecutive measurements in the same elevation scan.
ZPD time: The ZPD time is the UTC time at the moment when there is no optical path difference between the two mirrors of the interferometer. It is used as reference time for time tagging the sweeps and the scans.

5.3.5 Level 2 processing

Atmospheric continuum:

Is the atmospheric radiation originated from the wings of far lines that are not properly modelled by the Voigt line-profile. See [4] for more information on atmospheric continuum.

Irregular grid:

Is the "minimum" set of spectral points actually required to reconstruct the high-resolution atmospheric emission spectrum. A more exhaustive definition is in the section dealing with the dependence of the radiative transfer on spectral frequency.

Limb Scan:

"Limb - Scan" has the same meaning of "elevation scan". It indicates a scan of the atmospheric limb, made by varying the angle of the elevation mirror while the azimuth mirror remains at a fixed angle. See pointing for more information.

Limb Scanning sequence:

Is the same as "Limb - Scan" and as "elevation scan"

Limb view:

Corresponds to the acquisition of an interferogram (and therefore of a spectrum). While the interferogram is acquired, the input telescope of MIPAS (including elevation mirror and azimuth mirror) views at a fixed atmospheric parcel in the limb. A limb-scan is constituted of sveral limb-views (16 limb-views in the standard scan).

Microwindow

Narrow spectral interval (less than 3 cm^{-1} width) containing major information on the target parameters to be retrieved.

Retrieval grid

Set of altitudes in correspondence of which a given atmospheric distribution is retrieved (see also "Retrieval vertical grid 2.4.4.1.3.4.4. "

sinc function: eq 5.3

The definition of the sinc function is:

$$\mathrm{sinc}(x) \equiv \frac{\sin(x)}{x}$$

Tangent pressure:

Pressure in correspondence of the tangent point of a particular limb observation angle.

Zero-level calibration:

Residual additive offset (on the spectra) that could remain uncorrected from Level 1b 2.4.3.2. processing. In the retrieval algorithm this offset is assumed as limb-view 5.3.5. independent and microwindow dependent and it is retrieved.

5.4 References

See Further Reading 1.3. section.

Chapter 6

MIPAS Data Formats Products

6.1 Level 2 Products

Table 6.1

6.1.1 MIP_NL__2P: MIPAS Temperature , Pressure and Atmospheric Constituents Profiles

Table 6.2

MIP_NL__2P

MIPAS Temperature , Pressure and Atmospheric Constituents Profiles

File Structure

Data Sets 18

MPH 6.5.1.	Envisat MPH
SPH 6.5.50.	Level 2 product SPH
SUMMARY QUALITY ADS 6.5.45.	Summary Quality ADS
SCAN GEOLOCATION ADS 6.5.39.	Scan Geolocation ADS
DATASET STRUCTURE ADS 6.5.46.	Structure ADS
SCAN INFORMATION MDS 6.5.40.	Scan Information MDS
PT RETRIEVAL MDS 6.5.48.	P, T, and Height Correction Profiles MDS
H2O RETRIEVAL MDS 6.5.49.	H2O Target Species MDS
N2O RETRIEVAL MDS 6.5.49.	H2O Target Species MDS
HNO3 RETRIEVAL MDS 6.5.49.	H2O Target Species MDS
CH4 RETRIEVAL MDS 6.5.49.	H2O Target Species MDS
O3 RETRIEVAL MDS 6.5.49.	H2O Target Species MDS
NO2 RETRIEVAL MDS 6.5.49.	H2O Target Species MDS
CONTINUUM AND OFFSET MDS 6.5.47.	Continuum Contribution and Radiance Offset MDS
PCD INFORMATION ADS 6.5.43.	PCD Information of Individual Scans ADS
MICROWINDOW OCCUPATION ADS 6.5.41.	Microwindows Occupation Matrices ADS
RESIDUAL SPECTRA ADS 6.5.44.	Residual Spectra , mean values and standard deviation data ADS
PROCESSING PARAMETERS ADS 6.5.42.	Instrument and Processing Parameters ADS

Format Version 114.0

6.1.2 MIP_NLE_2P: MIPAS Extracted Temperature , Pressure and Atmospheric Constituents Profiles

MIPAS Extracted Temperature , Pressure and Atmospheric Constituents Profiles

File Structure

Data Sets 11

MPH 6.5.1.	Main Product Header
SPH 6.5.55.	MIP_NLE_2P SPH
SUMMARY QUALITY ADS 6.5.54.	Summary Quality ADS
SCAN GEOLOCATION ADS 6.5.39.	Scan Geolocation ADS
DATASET STRUCTURE ADS 6.5.46.	Structure ADS
SCAN INFORMATION MDS 6.5.51.	Scan information MDS
PT RETRIEVAL MDS 6.5.48.	P T and Height Correction Profiles MDS
O3 RETRIEVAL MDS 6.5.49.	O3 Target Species MDS
H2O RETRIEVAL MDS 6.5.49.	H2O Target Species MDS
MICROWINDOW OCCUPATION ADS 6.5.52.	Microwindows occupation matrices for p T and trace gas retrievals
PROCESSING PARAMETERS ADS 6.5.53.	Instrument and Processing Parameters ADS

Format Version DDT v100.3a EV 2.0.1 (08/03/2002)

6.2 Level 1 Products

Table 6.3

6.2.1 MIP_NL__1P: MIPAS Geolocated and Calibrated Spectra

Table 6.4

MIP_NL__1P

MIPAS Geolocated and Calibrated Spectra

File Structure

Data Sets 13

MPH 6.5.1.	Envisat MPH
SPH 6.5.38.	Mipas Level 1B SPH
SUMMARY QUALITY ADS 6.5.35.	Summary Quality ADS
GEOLOCATION ADS 6.5.32.	Geolocation ADS (LADS)
STRUCTURE ADS 6.5.36.	Structure ADS
MIPAS LEVEL-1B MDS 6.5.37.	Calibrated Spectra MDS
SCAN INFORMATION ADS 6.5.33.	Scan Information ADS
OFFSET CALIBRATION ADS 6.5.34.	Offset Calibration ADS
GAIN CALIBRATION ADS#1 6.5.30.	Gain Calibration ADS #1
GAIN CALIBRATION ADS#2 6.5.31.	Gain Calibration ADS #2
ILS/SPECTRAL CAL GADS 6.5.10.	ILS Calibration GADS
LOS CALIBRATION GADS 6.5.7.	LOS calibration GADS
PROCESS PARAMETERS GADS 6.5.63.	1 MDSR per MDS

Format Version 114.0

6.3 Level 0 Products

Table 6.5

6.3.1 MIP_LS__0P: MIPAS Line of Sight (LOS) Level 0

Table 6.6

MIP_LS__0P

MIPAS Line of Sight (LOS) Level 0

File Structure

Data Sets	3

MPH 6.5.1.	Envisat MPH

SPH 6.5.3.	Level 0 SPH
MIPAS_SOURCE_PACKETS 6.5.2.	Level 0 MDSR

Format Version 114.0

6.3.2 MIP_NL__0P: MIPAS Nominal Level 0

Table 6.7

MIP_NL__0P

MIPAS Nominal Level 0

File Structure

Data Sets 3

MPH 6.5.1.	Envisat MPH
SPH 6.5.3.	Level 0 SPH
MIPAS_SOURCE_PACKETS 6.5.2.	Level 0 MDSR

Format Version 114.0

6.3.3 MIP_RW__0P: MIPAS Raw Data and SPE Self Test Mode

Table 6.8

MIP_RW__0P

MIPAS Raw Data and SPE Self Test Mode

File Structure

Data Sets 3

MPH 6.5.1.	Envisat MPH
SPH 6.5.3.	Level 0 SPH
MIPAS_SOURCE_PACKETS 6.5.2.	Level 0 MDSR

Format Version 114.0

6.4 Auxilliary Products

Table 6.9

6.4.1 MIP_CA1_AX: Instrument characterization data

Table 6.10

MIP_CA1_AX

Instrument characterization data

File Structure

Data Sets 3

MPH 6.5.1.	Envisat MPH
SPH	Auxiliary data SPH with N=1 DSDs:DSD (M) pointing to the MDS
MIPAS_INST_CHARACTERIZATION 6.5.4.	1 MDSR per MDS

Format Version 114.0

6.4.2 MIP_CG1_AX: MIPAS Gain calibration

Table 6.11

MIP_CG1_AX

MIPAS Gain calibration

File Structure

Data Sets 4

MPH 6.5.1.	Envisat MPH
SPH	Auxiliary data SPH with N=1 DSDs:DSD (M) pointing to the MDS
MIPAS_GAIN_VECTORS 6.5.5.	MDS1 -- 1 mdsr forward sweep, 1 mdsr reverse sweep
MIPAS_GAIN_STATISTICS 6.5.6.	MDS2 -- 1 mdsr forward sweep, 1 mdsr reverse

Format Version 114.0

6.4.3 MIP_CL1_AX: Line of sight calibration

Table 6.12

MIP_CL1_AX

Line of sight calibration

File Structure

Data Sets 3

MPH 6.5.1.	Envisat MPH
SPH	Auxiliary data SPH with N=1 DSDs:DSD (M) pointing to the MDS
LOS CALIBRATION GADS 6.5.7.	LOS calibration GADS

Format Version 114.0

6.4.4 MIP_CO1_AX: MIPAS offset validation

Table 6.13

MIP_CO1_AX

MIPAS offset validation

File Structure

Data Sets 4

MPH 6.5.1.	Envisat MPH
SPH	Auxiliary data SPH with N=1 DSDs:DSD (M) pointing to the MDS
MIPAS_OFFSET_VECTORS 6.5.8.	2 MDSRs per MDS, 1 forward sweep, 1 reverse sweep
MIPAS_OFFSET_STATISTICS 6.5.9.	2 MDSR per MDS,1 forward sweep, 1 reverse sweep

Format Version 114.0

6.4.5 MIP_CS1_AX: MIPAS ILS and Spectral calibration

Table 6.14

MIP_CS1_AX

MIPAS ILS and Spectral calibration

File Structure

Data Sets 3

MPH 6.5.1.	Envisat MPH
SPH	Auxiliary data SPH with N=1 DSDs:DSD (M) pointing to the MDS
ILS/SPECTRAL CAL GADS 6.5.10.	ILS Calibration GADS

Format Version 114.0

6.4.6 MIP_CS2_AX: Cross Sections Lookup Table

Table 6.15

MIP_CS2_AX

Cross Sections Lookup Table

File Structure

Data Sets 17

MPH 6.5.1.	Envisat MPH
SPH	Auxiliary data SPH with N=1 DSDs:DSD (M) pointing to the MDS

LOOKUP TABLES GENERAL DATA 6.5.12.	GADS General
PT MICROWINDOWS LUT ADS 6.5.11.	VMR #6 retrieval microwindows ADS
H2O MICROWINDOWS LUT ADS 6.5.11.	VMR #6 retrieval microwindows ADS
N2O MICROWINDOWS LUT ADS 6.5.11.	VMR #6 retrieval microwindows ADS
HNO3 MICROWINDOWS LUT ADS 6.5.11.	VMR #6 retrieval microwindows ADS
CH4 MICROWINDOWS LUT ADS 6.5.11.	VMR #6 retrieval microwindows ADS
O3 MICROWINDOWS LUT ADS 6.5.11.	VMR #6 retrieval microwindows ADS
NO2 MICROWINDOWS LUT ADS 6.5.11.	VMR #6 retrieval microwindows ADS
PT MICROWINDOWS LUT MDS 6.5.13.	LUTs for VMR#6 retrieval microwindows MDS
H2O MICROWINDOWS LUT MDS 6.5.13.	LUTs for VMR#6 retrieval microwindows MDS
N2O MICROWINDOWS LUT MDS 6.5.13.	LUTs for VMR#6 retrieval microwindows MDS
HNO3 MICROWINDOWS LUT MDS 6.5.13.	LUTs for VMR#6 retrieval microwindows MDS
CH4 MICROWINDOWS LUT MDS 6.5.13.	LUTs for VMR#6 retrieval microwindows MDS
O3 MICROWINDOWS LUT MDS 6.5.13.	LUTs for VMR#6 retrieval microwindows MDS
NO2 MICROWINDOWS LUT MDS 6.5.13.	LUTs for VMR#6 retrieval microwindows MDS

Format Version 114.0

6.4.7 MIP_FM2_AX: Forward Calculation Results

Table 6.16

MIP_FM2_AX

Forward Calculation Results

File Structure

Data Sets 19

MPH 6.5.1.	Envisat MPH
SPH	Auxiliary data SPH with N=1 DSDs:DSD (M) pointing to the MDS
INITIAL GUESS GENERAL DATA 6.5.20.	General GADS
PRESSURE PROFILES MDS 6.5.22.	Pressure profiles MDS
TEMPERATURE PROFILES MDS 6.5.23.	Temperature profiles MDS
VMR PROFILES MDS 6.5.24.	VMR profiles MDS
PT MW CONTINUUM PROF MDS 6.5.21.	VMR #6 Cont. profiles MDS
H2O MW CONTINUUM PROF MDS 6.5.21.	VMR #6 Cont. profiles MDS
N2O MW CONTINUUM PROF MDS 6.5.21.	VMR #6 Cont. profiles MDS
HNO3 MW CONTINUUM PROF MDS 6.5.21.	VMR #6 Cont. profiles MDS
CH4 MW CONTINUUM PROF MDS 6.5.21.	VMR #6 Cont. profiles MDS
O3 MW CONTINUUM PROF MDS 6.5.21.	VMR #6 Cont. profiles MDS
NO2 MW CONTINUUM PROF MDS 6.5.21.	VMR #6 Cont. profiles MDS
FORWARD MODEL GENERAL DATA 6.5.16.	General data
MW OCCUPATION MATRIX ADS 6.5.15.	Data depending on occupation matrix location ADS
MW GROUPING ADS 6.5.14.	Microwindow grouping data ADS
SIMULATED SPECTRA MDS 6.5.18.	Computed spectra MDS
FITTED PARAMETERS MDS 6.5.19.	Values of unknown parameters MDS

JACOBI MATRICES MDS 6.5.17.	Jacobian matrices MDS

Format Version 114.0

6.4.8 MIP_IG2_AX: Initial Guess Profile data

Table 6.17

MIP_IG2_AX

Initial Guess Profile data

File Structure

Data Sets 13

MPH 6.5.1.	Envisat MPH
SPH	Auxiliary data SPH with N=1 DSDs:DSD (M) pointing to the MDS
INITIAL GUESS GENERAL DATA 6.5.20.	General GADS
PRESSURE PROFILES MDS 6.5.22.	Pressure profiles MDS
TEMPERATURE PROFILES MDS 6.5.23.	Temperature profiles MDS
VMR PROFILES MDS 6.5.24.	VMR profiles MDS
PT MW CONTINUUM PROF MDS 6.5.21.	VMR #6 Cont. profiles MDS
H2O MW CONTINUUM PROF MDS 6.5.21.	VMR #6 Cont. profiles MDS
N2O MW CONTINUUM PROF MDS 6.5.21.	VMR #6 Cont. profiles MDS
HNO3 MW CONTINUUM PROF MDS 6.5.21.	VMR #6 Cont. profiles MDS
CH4 MW CONTINUUM PROF MDS 6.5.21.	VMR #6 Cont. profiles MDS
O3 MW CONTINUUM PROF MDS 6.5.21.	VMR #6 Cont. profiles MDS
NO2 MW CONTINUUM PROF MDS 6.5.21.	VMR #6 Cont. profiles MDS

Format Version 114.0

6.4.9 MIP_MW1_AX: Level 1B Microwindow dictionary

Table 6.18

MIP_MW1_AX

Level 1B Microwindow dictionary

File Structure

Data Sets 3

MPH 6.5.1.	Envisat MPH
SPH	Auxiliary data SPH with N=1 DSDs:DSD (M) pointing to the MDS
MIPAS_MICROWINDOW_DICTIONARY 6.5.25.	1 MDSR per MDS

Format Version 114.0

6.4.10 MIP_MW2_AX: Level 2 Microwindows data

Table 6.19

MIP_MW2_AX

Level 2 Microwindows data

File Structure

Data Sets 16

MPH 6.5.1.	Envisat MPH
SPH	Auxiliary data SPH with N=1 DSDs:DSD (M) pointing to the MDS
PT MICROWINDOWS ADS 6.5.26.	P,T retrieval microwindows ADS
H2O MICROWINDOWS ADS 6.5.27.	VMR #6 retrieval microwindows ADS
N2O MICROWINDOWS ADS 6.5.27.	VMR #6 retrieval microwindows ADS
HNO3 MICROWINDOWS ADS 6.5.27.	VMR #6 retrieval microwindows ADS
CH4 MICROWINDOWS ADS 6.5.27.	VMR #6 retrieval microwindows ADS
O3 MICROWINDOWS ADS 6.5.27.	VMR #6 retrieval microwindows ADS
NO2 MICROWINDOWS ADS 6.5.27.	VMR #6 retrieval microwindows ADS
PT MICROWINDOWS MDS 6.5.28.	DSD for MDS containing p,T retrieval microwindows data
H2O MICROWINDOWS MDS 6.5.29.	DSD#6 for MDS containing VMR retrieval microwindows data
N2O MICROWINDOWS MDS 6.5.29.	DSD#6 for MDS containing VMR retrieval microwindows data
HNO3 MICROWINDOWS MDS 6.5.29.	DSD#6 for MDS containing VMR retrieval microwindows data
CH4 MICROWINDOWS MDS 6.5.29.	DSD#6 for MDS containing VMR retrieval microwindows data
O3 MICROWINDOWS MDS 6.5.29.	DSD#6 for MDS containing VMR retrieval microwindows data
NO2 MICROWINDOWS MDS 6.5.29.	DSD#6 for MDS containing VMR retrieval microwindows data

Format Version 114.0

6.4.11 MIP_OM2_AX: Microwindow Occupation Matrix

Table 6.20

MIP_OM2_AX

Microwindow Occupation Matrix

File Structure

Data Sets 24

MPH 6.5.1.	Envisat MPH
SPH	Auxiliary data SPH with N=1 DSDs:DSD (M) pointing to the MDS
OCC MATRIX GENERAL DATA 6.5.58.	General GADS
PT OCC MATRIX PRIORITY ADS 6.5.57.	Priority of VMR#6 retrieval occupation matices
H2O OCC MATRIX PRIORITY ADS 6.5.57.	Priority of VMR#6 retrieval occupation matices
N2O OCC MATRIX PRIORITY ADS 6.5.57.	Priority of VMR#6 retrieval occupation matices
HNO3 OCC MATRIX PRIORITY ADS 6.5.57.	Priority of VMR#6 retrieval occupation matices
CH4 OCC MATRIX PRIORITY ADS 6.5.57.	Priority of VMR#6 retrieval occupation matices
O3 OCC MATRIX PRIORITY ADS 6.5.57.	Priority of VMR#6 retrieval occupation matices
NO2 OCC MATRIX PRIORITY ADS 6.5.57.	Priority of VMR#6 retrieval occupation matices
PT OCCUPATION MATRICES ADS 6.5.56.	VMR #6 occupation matrices ADS
H2O OCCUPATION MATRICES ADS 6.5.56.	VMR #6 occupation matrices ADS
N2O OCCUPATION MATRICES ADS 6.5.56.	VMR #6 occupation matrices ADS
HNO3 OCCUPATION MATRICES ADS 6.5.56.	VMR #6 occupation matrices ADS
CH4 OCCUPATION MATRICES ADS 6.5.56.	VMR #6 occupation matrices ADS
O3 OCCUPATION MATRICES ADS 6.5.56.	VMR #6 occupation matrices ADS
PT OCCUPATION MATRICES MDS 6.5.59.	Occupation matrices for p,T retrieval MDS
NO2 OCCUPATION MATRICES ADS 6.5.56.	VMR #6 occupation matrices ADS
H2O OCCUPATION MATRICES MDS 6.5.60.	Occupation matrices for vmr#6 retrieval MDS
N2O OCCUPATION MATRICES MDS 6.5.60.	Occupation matrices for vmr#6 retrieval MDS
HNO3 OCCUPATION MATRICES MDS 6.5.60.	Occupation matrices for vmr#6 retrieval MDS
CH4 OCCUPATION MATRICES MDS 6.5.60.	Occupation matrices for vmr#6 retrieval MDS
O3 OCCUPATION MATRICES MDS 6.5.60.	Occupation matrices for vmr#6 retrieval MDS
NO2 OCCUPATION MATRICES MDS 6.5.60.	Occupation matrices for vmr#6 retrieval MDS

Format Version 114.0

6.4.12 MIP_PI2_AX: A Priori Pointing Information

Table 6.21

MIP_PI2_AX

A Priori Pointing Information

File Structure

Data Sets 4

MPH 6.5.1.	Envisat MPH
SPH	Auxiliary data SPH with N=1 DSDs:DSD (M) pointing to the MDS
POINTING GENERAL DATA 6.5.61.	General GADS
LOS VCM MATRICES MDS 6.5.62.	Inverse LOS VCM matrices MDS

Format Version 114.0

6.4.13 MIP_PS1_AX: Level 1B Processing Parameters

Table 6.22

MIP_PS1_AX

Level 1B Processing Parameters

File Structure

Data Sets 3

MPH 6.5.1.	Envisat MPH

SPH	Auxiliary data SPH with N=1 DSDs:DSD (M) pointing to the MDS
PROCESS PARAMETERS GADS 6.5.63.	1 MDSR per MDS

Format Version 114.0

6.4.14 MIP_PS2_AX: Level 2 Processing Parameters

Table 6.23

MIP_PS2_AX

Level 2 Processing Parameters

File Structure

Data Sets 5

MPH 6.5.1.	Envisat MPH
SPH	Auxiliary data SPH with N=1 DSDs:DSD (M) pointing to the MDS
SETTINGS FOR FRAMEWORK 6.5.64.	Framework Parameters GADS
SETTINGS FOR PT RETRIEVAL 6.5.65.	P, t, Retrieval GADS
SETTINGS FOR VMR RETRIEVALS 6.5.66.	VMR Retrieval Parameters GADS

Format Version 114.0

6.4.15 MIP_SP2_AX: Spectroscopic data

Spectroscopic data

File Structure

Data Sets 10

MPH 6.5.1.	Main Product Header
SPH	Auxiliary data SPH with 8 DSDs.
PT MICROWINDOWS ADS 6.5.67.	P T Retrieval MW ADS

H2O MICROWINDOWS ADS 6.5.67.	VMR Retrieval MW ADS for species #1
N2O MICROWINDOWS ADS 6.5.67.	VMR Retrieval MW ADS for species #2
HNO3 MICROWINDOWS ADS 6.5.67.	VMR Retrieval MW ADS for species #3
CH4 MICROWINDOWS ADS 6.5.67.	VMR Retrieval MW ADS for species #4
O3 MICROWINDOWS ADS 6.5.67.	VMR Retrieval MW ADS for species #5
NO2 MICROWINDOWS ADS 6.5.67.	VMR Retrieval MW ADS for species #6
SPECTROSCOPIC LINES MDS 6.5.68.	Spectral Lines MDS

Format Version DDT v100.3a EV 2.0.1 (08/03/2002)

6.5 Records

6.5.1 Main Product Header

Table 6.24 Main Product Header

Envisat MPH

#	Description	Units	Count	Type	Size
Data Record					
0	product_name_title PRODUCT=	keyword	1	AsciiString	8 byte(s)
1	quote_1 quotation mark (""")	ascii	1	AsciiString	1 byte(s)
2	product Product File name	ascii	1	AsciiString	62 byte(s)
3	quote_2 quotation mark (""")	ascii	1	AsciiString	1 byte(s)
4	newline_char_1 newline character	terminator	1	AsciiString	1 byte(s)
5	processing_stage_title PROC_STAGE=	keyword	1	AsciiString	11 byte(s)
6	proc_stage Processing Stage FlagN = Near Real Time, T = test product, V= fully validated (fully consolidated) product, S = special product. Letters between N and V (with the exception of T and S) indicate steps in the consolidation process, with letters closer to V	ascii	1	AsciiString	1 byte(s)
7	newline_char_2 newline character	terminator	1	AsciiString	1 byte(s)
8	reference_doc_title REF_DOC=	keyword	1	AsciiString	8 byte(s)

#	Description	Units	Count	Type	Size
9	quote_3 quotation mark (""")	ascii	1	AsciiString	1 byte(s)
10	ref_doc Reference Document Describing Product AA-BB-CCC-DD-EEEE_V/I?? (23 characters, including blank space characters) where AA-BB-CCC-DD-EEEE is the ESA standard document no. and V/I is the Version / Issue. If the reference document is the Products Specifications PO-RS-MDA-GS-2009, the version and revision have to refer to the volume 1 of the document, where the status (version/revision) of all volumes can be found. If not used, set to ???????????????????????	ascii	1	AsciiString	23 byte(s)
11	quote_4 quotation mark (""")	ascii	1	AsciiString	1 byte(s)
12	newline_char_3 newline character	terminator	1	AsciiString	1 byte(s)
13	spare_1 Spare	-	1	SpareField	41 byte(s)
14	acquisition_station_id_title ACQUISITION_STATION=	keyword	1	AsciiString	20 byte(s)
15	quote_5 quotation mark (""")	ascii	1	AsciiString	1 byte(s)
16	acquisition_station Acquisition Station ID (up to 3 codes) If not used, set to ???????????????????	ascii	1	AsciiString	20 byte(s)
17	quote_6 quotation mark (""")	ascii	1	AsciiString	1 byte(s)
18	newline_char_5 newline character	terminator	1	AsciiString	1 byte(s)
19	processing_center_title PROC_CENTER=	keyword	1	AsciiString	12 byte(s)
20	quote_7 quotation mark (""")	ascii	1	AsciiString	1 byte(s)
21	proc_center Processing Center ID which generated current product If not used, set to ??????	ascii	1	AsciiString	6 byte(s)
22	quote_8 quotation mark (""")	ascii	1	AsciiString	1 byte(s)
23	newline_char_6 newline character	terminator	1	AsciiString	1 byte(s)
24	processing_time_title PROC_TIME=	keyword	1	AsciiString	10 byte(s)
25	quote_9 quotation mark (""")	ascii	1	AsciiString	1 byte(s)
26	proc_time UTC Time of Processing (product generation time)UTC Time format. If not used, set to ??????????????????????????????.	UTC	1	UtcExternal	27 byte(s)
27	quote_10 quotation mark (""")	ascii	1	AsciiString	1 byte(s)
28	newline_char_7 newline character	terminator	1	AsciiString	1 byte(s)
29	software_version_title SOFTWARE_VER=	keyword	1	AsciiString	13 byte(s)
30	quote_11 quotation mark (""")	ascii	1	AsciiString	1 byte(s)
31	software_ver Software Version number of processing softwareFormat: Name of processor (up to 10 characters)/ version number (4 characters) -- left justified (any blanks added at end). If not used, set to ??????????????.e.g. MIPAS/2.31????	ascii	1	AsciiString	14 byte(s)
32	quote_12 quotation mark (""")	ascii	1	AsciiString	1 byte(s)
33	newline_char_8 newline character	terminator	1	AsciiString	1 byte(s)
34	spare_2 Spare	-	1	SpareField	41 byte(s)
35	sensing_start_title SENSING_START=	keyword	1	AsciiString	14 byte(s)
36	quote_13 quotation mark (""")	ascii	1	AsciiString	1 byte(s)
37	sensing_start UTC start time of data sensing (first measurement in first data record) UTC Time format. If not used, set to ??????????????????????????????.	UTC	1	UtcExternal	27 byte(s)
38	quote_14 quotation mark (""")	ascii	1	AsciiString	1 byte(s)
39	newline_char_10 newline character	terminator	1	AsciiString	1 byte(s)
40	sensing_stop_title	keyword	1	AsciiString	13 byte(s)

#	Description	Units	Count	Type	Size
	SENSING_STOP=				
41	quote_15 quotation mark (""")	ascii	1	AsciiString	1 byte(s)
42	sensing_stop UTC stop time of data sensing (last measurements last data record) UTC Time format. If not used, set to ????????????????????????????.	UTC	1	UtcExternal	27 byte(s)
43	quote_16 quotation mark (""")	ascii	1	AsciiString	1 byte(s)
44	newline_char_11 newline character	terminator	1	AsciiString	1 byte(s)
45	spare_3 Spare	-	1	SpareField	41 byte(s)
46	phase_title PHASE=	keyword	1	AsciiString	6 byte(s)
47	phase Phasephase letter. If not used, set to X.	ascii	1	AsciiString	1 byte(s)
48	newline_char_13 newline character	terminator	1	AsciiString	1 byte(s)
49	cycle_title CYCLE=	keyword	1	AsciiString	6 byte(s)
50	cycle CycleCycle number. If not used, set to +000.	-	1	AsciiIntegerAuc	4 byte(s)
51	newline_char_14 newline character	terminator	1	AsciiString	1 byte(s)
52	relative_orbit_title REL_ORBIT=	keyword	1	AsciiString	10 byte(s)
53	rel_orbit Start relative orbit number If not used, set to +00000	-	1	As	6 byte(s)
54	newline_char_15 newline character	terminator	1	AsciiString	1 byte(s)
55	absolute_orbit_title ABS_ORBIT=	keyword	1	AsciiString	10 byte(s)
56	abs_orbit Start absolute orbit number.If not used, set to +00000.	-	1	As	6 byte(s)
57	newline_char_16 newline character	terminator	1	AsciiString	1 byte(s)
58	state_vector_time_title STATE_VECTOR_TIME=	keyword	1	AsciiString	18 byte(s)
59	quote_17 quotation mark (""")	ascii	1	AsciiString	1 byte(s)
60	state_vector_time UTC of ENVISAT state vector. UTC time format. If not used, set to ????????????????????????????.	UTC	1	UtcExternal	27 byte(s)
61	quote_18 quotation mark (""")	ascii	1	AsciiString	1 byte(s)
62	newline_char_17 newline character	terminator	1	AsciiString	1 byte(s)
63	delta_ut1_title DELTA_UT1=	keyword	1	AsciiString	10 byte(s)
64	delta_ut1 DUT1=UT1-UTC. If not used, set to +.000000.	s	1	Ado06	8 byte(s)
65	delta_ut1_units <s>	units	1	AsciiString	3 byte(s)
66	newline_char_18 newline character	terminator	1	AsciiString	1 byte(s)
67	x_position_title X_POSITION=	keyword	1	AsciiString	11 byte(s)
68	x_position X Position in Earth-Fixed reference. If not used, set to +0000000.000.	m	1	Ado73	12 byte(s)
69	x_position_units <m>	units	1	AsciiString	3 byte(s)
70	newline_char_19 newline character	terminator	1	AsciiString	1 byte(s)
71	y_position_title Y_POSITION=	keyword	1	AsciiString	11 byte(s)
72	y_position Y Position in Earth-Fixed reference. If not used, set to +0000000.000.	m	1	Ado73	12 byte(s)
73	y_position_units <m>	units	1	AsciiString	3 byte(s)
74	newline_char_20 newline character	terminator	1	AsciiString	1 byte(s)

#	Description	Units	Count	Type	Size
75	z_position_title Z_POSITION=	keyword	1	AsciiString	11 byte(s)
76	z_position Z Position in Earth-Fixed reference. If not used, set to +0000000.000.	m	1	Ado73	12 byte(s)
77	z_position_units <m>	units	1	AsciiString	3 byte(s)
78	newline_char_21 newline character	terminator	1	AsciiString	1 byte(s)
79	x_velocity_title X_VELOCITY=	keyword	1	AsciiString	11 byte(s)
80	x_velocity X velocity in Earth fixed reference. If not used, set to +0000.000000.	m/s	1	Ado46	12 byte(s)
81	x_velocity_units <m/s>	units	1	AsciiString	5 byte(s)
82	newline_char_22 newline character	terminator	1	AsciiString	1 byte(s)
83	y_velocity_title Y_VELOCITY=	keyword	1	AsciiString	11 byte(s)
84	y_velocity Y velocity in Earth fixed reference. If not used, set to +0000.000000.	m/s	1	Ado46	12 byte(s)
85	y_velocity_units <m/s>	units	1	AsciiString	5 byte(s)
86	newline_char_23 newline character	terminator	1	AsciiString	1 byte(s)
87	z_velocity_title Z_VELOCITY=	keyword	1	AsciiString	11 byte(s)
88	z_velocity Z velocity in Earth fixed reference. If not used, set to +0000.000000.	m/s	1	Ado46	12 byte(s)
89	z_velocity_units <m/s>	units	1	AsciiString	5 byte(s)
90	newline_char_24 newline character	terminator	1	AsciiString	1 byte(s)
91	vector_source_title VECTOR_SOURCE=	keyword	1	AsciiString	14 byte(s)
92	quote_19 quotation mark (""")	ascii	1	AsciiString	1 byte(s)
93	vector_source Source of Orbit Vectors	ascii	1	AsciiString	2 byte(s)
94	quote_20 quotation mark (""")	ascii	1	AsciiString	1 byte(s)
95	newline_char_25 newline character	terminator	1	AsciiString	1 byte(s)
96	spare_4 Spare	-	1	SpareField	41 byte(s)
97	utc_sbt_time_title UTC_SBT_TIME=	keyword	1	AsciiString	13 byte(s)
98	quote_21 quotation mark (""")	ascii	1	AsciiString	1 byte(s)
99	utc_sbt_time UTC time corresponding to SBT below(currently defined to be given at the time of the ascending node state vector). If not used, set to ??????????????????????????????.	UTC	1	UtcExternal	27 byte(s)
100	quote_22 quotation mark (""")	ascii	1	AsciiString	1 byte(s)
101	newline_char_28 newline character	terminator	1	AsciiString	1 byte(s)
102	sat_binary_time_title SAT_BINARY_TIME=	keyword	1	AsciiString	16 byte(s)
103	sat_binary_time Satellite Binary Time (SBT) 32bit integer time of satellite clock. Its value is unsigned (=>0). If not used, set to +0000000000.	-	1	AsciiIntegerAul	11 byte(s)
104	newline_char_29 newline character	terminator	1	AsciiString	1 byte(s)
105	clock_step_title CLOCK_STEP=	keyword	1	AsciiString	11 byte(s)
106	clock_step Clock Step Sizeclock step in picoseconds. Its value is unsigned (=>0). If not used, set to +0000000000.	psec.	1	AsciiIntegerAul	11 byte(s)
107	clock_step_units <ps>	units	1	AsciiString	4 byte(s)
108	newline_char_30	terminator	1	AsciiString	1 byte(s)

#	Description	Units	Count	Type	Size
	newline character				
109	spare_5 Spare	-	1	SpareField	33 byte(s)
110	leap_utc_title LEAP_UTC=	keyword	1	AsciiString	9 byte(s)
111	quote_23 quotation mark (""")	ascii	1	AsciiString	1 byte(s)
112	leap_utc UTC time of the occurrence of the Leap SecondSet to ?????????????????????????? if not used.	UTC	1	UtcExternal	27 byte(s)
113	quote_24 quotation mark (""")	ascii	1	AsciiString	1 byte(s)
114	newline_char_302 newline character	terminator	1	AsciiString	1 byte(s)
115	leap_sign_title LEAP_SIGN=	keyword	1	AsciiString	10 byte(s)
116	leap_sign Leap second sign(+001 if positive Leap Second, -001 if negative)Set to +000 if not used.	s	1	Ac	4 byte(s)
117	newline_char_303 newline character	terminator	1	AsciiString	1 byte(s)
118	leap_err_title LEAP_ERR=	keyword	1	AsciiString	9 byte(s)
119	leap_err Leap second errorif leap second occurs within processing segment = 1, otherwise = 0If not used, set to 0.	ascii	1	AsciiString	1 byte(s)
120	newline_char_304 newline character	terminator	1	AsciiString	1 byte(s)
121	spare_6 Spare	-	1	SpareField	41 byte(s)
122	product_err_title PRODUCT_ERR=	keyword	1	AsciiString	12 byte(s)
123	product_err 1 or 0. If 1, errors have been reported in the product. User should then refer to the SPH or Summary Quality ADS of the product for details of the error condition. If not used, set to 0.	ascii	1	AsciiString	1 byte(s)
124	newline_char_33 newline character	terminator	1	AsciiString	1 byte(s)
125	total_size_title TOT_SIZE=	keyword	1	AsciiString	9 byte(s)
126	tot_size Total Size Of Product (# bytes DSR + SPH+ MPH)	bytes	1	Ad	21 byte(s)
127	total_size_units <bytes>	units	1	AsciiString	7 byte(s)
128	newline_char_34 newline character	terminator	1	AsciiString	1 byte(s)
129	sph_size_title SPH_SIZE=	keyword	1	AsciiString	9 byte(s)
130	sph_size Length Of SPH(# bytes in SPH)	bytes	1	Al	11 byte(s)
131	sph_size_units <bytes>	units	1	AsciiString	7 byte(s)
132	newline_char_35 newline character	terminator	1	AsciiString	1 byte(s)
133	number_of_dsd_title NUM_DSD=	keyword	1	AsciiString	8 byte(s)
134	num_dsd Number of DSDs(# DSDs)	-	1	Al	11 byte(s)
135	newline_char_36 newline character	terminator	1	AsciiString	1 byte(s)
136	size_of_dsd_title DSD_SIZE=	keyword	1	AsciiString	9 byte(s)
137	dsd_size Length of Each DSD(# bytes for each DSD, all DSDs shall have the same length)	-	1	Al	11 byte(s)
138	size_of_dsd_units <bytes>	units	1	AsciiString	7 byte(s)
139	newline_char_37 newline character	terminator	1	AsciiString	1 byte(s)
140	number_of_ds_att_title NUM_DATA_SETS=	keyword	1	AsciiString	14 byte(s)
141	num_data_sets Number of DSs attached(not all DSDs have a DS attached)	-	1	Al	11 byte(s)

#	Description	Units	Count	Type	Size
142	newline_char_38 newline character	terminator	1	AsciiString	1 byte(s)
143	spare_7 Spare	-	1	SpareField	41 byte(s)

Record Length : 1247

DS_NAME : Envisat MPH

Format Version 114.0

6.5.2 Level 0 MDSR

Table 6.25 Level 0 MDSR

Level 0 MDSR

#	Description	Units	Count	Type	Size
Data Record					
0	dsr_time MJD of sensing time as extracted from Aisp	MJD	1	mjd	12 byte(s)
1	gsrt Ground station reference time	MJD	1	mjd	12 byte(s)
2	isp_length Length of the isp = length of the source packet - 7 bytes	bytes	1	us	2 byte(s)
3	crc_errs Number of VCDUs in the isp which contain a CRC error	VCDU	1	us	2 byte(s)
4	rs_errs Number of VCDUs in the isp for which an RS correction was performed	VCDU	1	us	2 byte(s)
5	spare_1 spare	-	1	SpareField	2 byte(s)
6	source_packet downlinked source packet	-	1	source_packetStruct	-1.0 byte(s)
	a: Isp_Fields Instrument Source Packet	-		uc	1 byte(s)

Record Length : 31

DS_NAME : Level 0 MDSR

Format Version 114.0

6.5.3 Level 0 SPH

Table 6.26 Level 0 SPH

Level 0 SPH

#	Description	Units	Count	Type	Size
Data Record					
0	sph_descriptor_title SPH_DESCRIPTOR=	keyword	1	AsciiString	15 byte(s)
1	quote_1 quotation mark (""")	ascii	1	AsciiString	1 byte(s)
2	sph_descriptor SPH descriptor ASCII string describing the product	ascii	1	AsciiString	28 byte(s)
3	quote_2 quotation mark (""")	ascii	1	AsciiString	1 byte(s)
4	newline_char_1 newline character	terminator	1	AsciiString	1 byte(s)
5	start_lat_title START_LAT=	keyword	1	AsciiString	10 byte(s)
6	start_lat WGS84 latitude of first satellite nadir point at the sensing start time of the MPH A negative value denotes south latitude; a positive value denotes north latitude.	(1e-6) degrees	1	AsciiGeoCoordinate	11 byte(s)
7	start_lat_units <10-6degN>	units	1	AsciiString	10 byte(s)
8	newline_char_2 newline character	terminator	1	AsciiString	1 byte(s)
9	start_long_title START_LONG=	keyword	1	AsciiString	11 byte(s)
10	start_long WGS84 longitude of first satellite nadir point at the sensing start time of the MPH A positive value denotes east of Greenwich; a negative value denotes west of Greenwich.	(1e-6) degrees	1	AsciiGeoCoordinate	11 byte(s)
11	start_long_units <10-6degE>	units	1	AsciiString	10 byte(s)
12	newline_char_3 newline character	terminator	1	AsciiString	1 byte(s)
13	stop_lat_title STOP_LAT=	keyword	1	AsciiString	9 byte(s)
14	stop_lat WGS84 latitude of first satellite nadir point at the sensing stop time of the MPH A negative value denotes south latitude; a positive value denotes north latitude.	(1e-6) degrees	1	AsciiGeoCoordinate	11 byte(s)
15	stop_lat_units <10-6degN>	units	1	AsciiString	10 byte(s)
16	newline_char_4 newline character	terminator	1	AsciiString	1 byte(s)
17	stop_long_title STOP_LONG=	keyword	1	AsciiString	10 byte(s)
18	stop_long	(1e-6) degrees	1	AsciiGeoCoordinate	11 byte(s)

#	Description	Units	Count	Type	Size
	WGS84 longitude of first satellite nadir point at the sensing stop time of the MPH A positive value denotes east of Greenwich; a negative value denotes west of Greenwich.				
19	stop_long_units <10-6degE>	units	1	AsciiString	10 byte(s)
20	newline_char_5 newline character	terminator	1	AsciiString	1 byte(s)
21	sat_track_title SAT_TRACK=	keyword	1	AsciiString	10 byte(s)
22	sat_track Sub-satellite track heading at the sensing start time in the MPH.	degrees	1	Afl	15 byte(s)
23	sat_track_units <deg>	units	1	AsciiString	5 byte(s)
24	newline_char_6 newline character	terminator	1	AsciiString	1 byte(s)
25	spare_1 Spare	-	1	SpareField	51 byte(s)
26	isp_errors_sig_title ISP_ERRORS_SIGNIFICANT=	keyword	1	AsciiString	23 byte(s)
27	isp_errors_significant 1 or 0.1 if number of ISPs with CRC errors exceeds threshold	ascii	1	AsciiString	1 byte(s)
28	newline_char_8 newline character	terminator	1	AsciiString	1 byte(s)
29	missing_isps_sig_title MISSING_ISPS_SIGNIFICANT=	keyword	1	AsciiString	25 byte(s)
30	missing_isps_significant 1 or 0.1 if number of missing ISPs exceeds threshold	ascii	1	AsciiString	1 byte(s)
31	newline_char_9 newline character	terminator	1	AsciiString	1 byte(s)
32	isp_discard_sig_title ISP_DISCARDED_SIGNIFICANT=	keyword	1	AsciiString	26 byte(s)
33	isp_discarded_significant 1 or 0.1 if number of ISPs discarded by the PF-HS exceeds threshold	ascii	1	AsciiString	1 byte(s)
34	newline_char_10 newline character	terminator	1	AsciiString	1 byte(s)
35	rs_sig_title RS_SIGNIFICANT=	keyword	1	AsciiString	15 byte(s)
36	rs_significant 1 or 0.1 if number of ISPs with Reed Solomon corrections exceeds threshold	ascii	1	AsciiString	1 byte(s)
37	newline_char_11 newline character	terminator	1	AsciiString	1 byte(s)
38	spare_2 Spare	-	1	SpareField	51 byte(s)
39	num_err_isps_title NUM_ERROR_ISPS=	keyword	1	AsciiString	15 byte(s)
40	num_error_isps Number of ISPs containing CRC errors as reported by the FEP	ISPs	1	AI	11 byte(s)
41	newline_char_13 newline character	terminator	1	AsciiString	1 byte(s)
42	err_isp_thresh_title ERROR_ISPS_THRESH=	keyword	1	AsciiString	18 byte(s)
43	error_isps_thresh Threshold at which number of ISPs containing CRC errors is considered significant	percent	1	Afl	15 byte(s)
44	err_isp_thresh_units <%>	units	1	AsciiString	3 byte(s)
45	newline_char_14 newline character	terminator	1	AsciiString	1 byte(s)
46	num_missing_isps_title NUM_MISSING_ISPS=	keyword	1	AsciiString	17 byte(s)
47	num_missing_isps Number of missing ISPs	ISPs	1	AI	11 byte(s)
48	newline_char_15 newline character	terminator	1	AsciiString	1 byte(s)
49	missing_isps_thresh_title MISSING_ISPS_THRESH=	keyword	1	AsciiString	20 byte(s)
50	missing_isps_thresh Threshold at which number of ISPs missing is considered significant	percent	1	Afl	15 byte(s)
51	missing_isps_thresh_units <%>	units	1	AsciiString	3 byte(s)
52	newline_char_16	terminator	1	AsciiString	1 byte(s)

#	Description	Units	Count	Type	Size
	newline character				
53	num_discard_title NUM_DISCARDED_ISPS=	keyword	1	AsciiString	19 byte(s)
54	num_discarded_isps Number of ISPs discarded by PF-HS	ISPs	1	Al	11 byte(s)
55	newline_char_17 newline character	terminator	1	AsciiString	1 byte(s)
56	discard_thresh_title DISCARDED_ISPS_THRESH=	keyword	1	AsciiString	22 byte(s)
57	discarded_isps_thresh Threshold at which number of ISPs discarded by PF-HS is considered significant	percent	1	Afl	15 byte(s)
58	discard_thresh_units <%>	units	1	AsciiString	3 byte(s)
59	newline_char_18 newline character	terminator	1	AsciiString	1 byte(s)
60	num_rs_title NUM_RS_ISPS=	keyword	1	AsciiString	12 byte(s)
61	num_rs_isps Number of ISPs with Reed Solomon corrections	ISPs	1	Al	11 byte(s)
62	newline_char_19 newline character	terminator	1	AsciiString	1 byte(s)
63	rs_thresh_title RS_THRESH=	keyword	1	AsciiString	10 byte(s)
64	rs_thresh Threshold at which number of ISPs discarded by PF-HS is considered significant	percent	1	Afl	15 byte(s)
65	rs_thresh_units <%>	units	1	AsciiString	3 byte(s)
66	newline_char_20 newline character	terminator	1	AsciiString	1 byte(s)
67	spare_3 Spare	-	1	SpareField	101 byte(s)
68	tx_polar_title TX_RX_POLAR=	keyword	1	AsciiString	12 byte(s)
69	quote_3 quotation mark (""")	ascii	1	AsciiString	1 byte(s)
70	tx_rx_polar Transmitter/receiver polarization (used for ASAR only) for non-ASAR products	ascii	1	AsciiString	5 byte(s)
71	quote_4 quotation mark (""")	ascii	1	AsciiString	1 byte(s)
72	newline_char_22 newline character	terminator	1	AsciiString	1 byte(s)
73	swath_title SWATH=	keyword	1	AsciiString	6 byte(s)
74	quote_5 quotation mark (""")	ascii	1	AsciiString	1 byte(s)
75	swath Swath number (used for ASAR only) for non-ASAR products	ascii	1	AsciiString	3 byte(s)
76	quote_6 quotation mark (""")	ascii	1	AsciiString	1 byte(s)
77	newline_char_23 newline character	terminator	1	AsciiString	1 byte(s)
78	spare_4 Spare	-	1	SpareField	42 byte(s)
79	dsd_spare_5 DSD Spare	-	1	dsd_sp	0 byte(s)

Record Length : 836

DS_NAME : Level 0 SPH

Format Version 114.0

6.5.4 1 MDSR per MDS

Table 6.27 1 MDSR per MDS

1 MDSR per MDS

#	Description	Units	Count	Type	Size
Data Record					
0	dsr_time Creation Time	MJD	1	mjd	12 byte(s)
1	quality_flag Quality indicator (PCD)"""0""" non-corrupted,"""-1""" = corrupted, default values filled in	flag	1	BooleanFlag	1 byte(s)
2	therm_time Thermistor time (UTC).Last modification time of file section using UTC time format	UTC	1	UtcExternal	27 byte(s)
3	feo_coef FEOA fifth order polynomial relates each thermistor (or a set of) reading (ADC count) to the actual temperature (Kelvin) which leads to a set of 6 coefficients. The units of coefficients are K, K/ADC count, K/(ADC count)2, K/(ADC count)3, K/(ADC count)4,	-	6	db	6*8 byte(s)
4	inst_coef InstrumentA fifth order polynomial relates each thermistor (or a set of) reading (ADC count) to the actual temperature (Kelvin) which leads to a set of 6 coefficients. The units of coefficients are K, K/ADC count, K/(ADC count)2, K/(ADC count)3, K/(ADC co	-	6	db	6*8 byte(s)
5	cbe_coef CBEA fifth order polynomial relates each thermistor (or a set of) reading (ADC count) to the actual temperature (Kelvin) which leads to a set of 6 coefficients. The units of coefficients are K, K/ADC count, K/(ADC count)2, K/(ADC count)3, K/(ADC count)4,	-	6	db	6*8 byte(s)
6	dpu_1_coef DPU/DTU range 1A fifth order polynomial relates each thermistor (or a set of) reading (ADC count) to the actual temperature (Kelvin) which leads to a set of 6 coefficients. The units of coefficients are K, K/ADC count, K/(ADC count)2, K/(ADC count)3, K/(A	-	6	db	6*8 byte(s)
7	dpu_2_coef DPU/DTU range 2A fifth order polynomial relates each thermistor (or a set of) reading (ADC count) to the actual temperature (Kelvin) which leads to a set of 6 coefficients. The units of coefficients are K, K/ADC count, K/(ADC count)2, K/(ADC count)3, K/(A	-	6	db	6*8 byte(s)
8	spe_coef SPEA fifth order polynomial relates each thermistor (or a set of) reading (ADC count) to the actual temperature (Kelvin) which leads to a set of 6 coefficients. The units of coefficients are K, K/ADC count, K/(ADC count)2, K/(ADC count)3, K/(ADC count)4,	-	6	db	6*8 byte(s)
9	paw_coef PAWA fifth order polynomial relates each thermistor (or a set of) reading (ADC count) to the actual temperature (Kelvin) which leads to a set of 6 coefficients. The units of coefficients are K, K/ADC count, K/(ADC count)2, K/(ADC count)3, K/(ADC count)4,	-	6	db	6*8 byte(s)
10	spare_1 Spare	-	1	SpareField	50 byte(s)
11	nonlin_time Non-linearity r time. Last modification time of file section using UTC time format.	UTC	1	UtcExternal	27 byte(s)
12	detector_coef Detector responsivity coefficients with ASCM approach (relates responsivity to a """digitized""" incident flux). A third order polynomial (4 values from zero order term to third order term) for detectors A1, A2, B1 and B2 respectively.	-	4*4*2	db	4*4*2*8 byte(s)

#	Description	Units	Count	Type	Size
13	photon_flux_min Photon flux min associated with the fit coefficients	-	4	db	4*8 byte(s)
14	photon_flux_max Photon flux max associated with the fit coefficients	-	4	db	4*8 byte(s)
15	spare_2 Spare	-	1	SpareField	32 byte(s)
16	spare_3 Spare	-	1	SpareField	50 byte(s)
17	equal_time Equalization time (UTC)Last modification time of file section using UTC time format	UTC	1	UtcExternal	27 byte(s)
18	output_port Output port to equalize channel A.'0' means no equalization, '1' means channel A1 and '2' means channel A2	-	1	uc	1 byte(s)
19	num_coef Number of coefficients (N=32 TBD)The number of coefficients is expected to be between 2 and 32, may be set to zero if field 17 is zero.	-	1	us	2 byte(s)
20	coef Complex coefficients	-		db	8 byte(s)
21	spare_4 Spare	-	1	SpareField	50 byte(s)
22	bb_time Blackbody time (UTC)Last modification time of file section using UTC time format	UTC	1	UtcExternal	27 byte(s)
23	corr_factor Correction factors(size TBD)	-	1	db	8 byte(s)
24	element_loc Base area element locations	m	8	db	8*8 byte(s)
25	prt_loc Base area PRT locations	m	3	db	3*8 byte(s)
26	view_factor View factors	-	3	db	3*8 byte(s)
27	emis_star_freq Start wavenumber of grid on which surface emissivity data are represented	cm-1	1	fl	4 byte(s)
28	emis_step Wavenumber increment of grid on which surface emissivity data are represented	cm-1	1	fl	4 byte(s)
29	emis_num Number of Data points in grid for surface emissivity (G).	-	1	us	2 byte(s)
30	surf_emiss Surface emissivity vs wavenumber	-		db	8 byte(s)
31	start_freq_grid Start wavenumber of grid on which effective emissivity data are represented.	cm-1	1	fl	4 byte(s)
32	freq_inc_grid Wavenumber increment of grid on which effective emissivity data are represented.	cm-1	1	fl	4 byte(s)
33	num_data_pt_grid Number of data points in grid for effective emissivity (H)	-	1	us	2 byte(s)
34	eff_emiss Effective emissivity vs wavenumber	-		db	8 byte(s)
35	prt_res PRT resistance values (high & low)	-	10	db	10*8 byte(s)
36	dig_prt_coef Digital to PRT resistanceA second order polynomial relates digital reading (from the CBB PRT) to resistance values which leads to a set of 3 coefficients. The units of the coefficients are ohm, ohm/ADC count, ohm/(ADC count)2.	-	15	db	15*8 byte(s)
37	prt_temp_coef PRT resistance to temperatureA second order polynomial relates PRT resistance values to actual temperature (Kelvin) which leads to a set of 3 coefficients. The units of coefficients are K, K/ohm, K/ohm2	-	15	db	15*8 byte(s)
38	spare_5 Spare	-	1	SpareField	30 byte(s)
39	dtu_time DTU time (UTC)Last modification time of file section using UTC time format	UTC	1	UtcExternal	27 byte(s)
40	dectector_coef Detector responsivity vs temperatureA third order polynomial relates detector (for all 8) responsivity to DTU temperature which leads to a set of 4 coefficients. The units of coefficients are no units, K-1, K-2, K-3	-	32	db	32*8 byte(s)
41	temp_scale_fact Responsivity scaling factor (kR)	-	1	db	8 byte(s)
42	spare_6 Spare	-	1	SpareField	42 byte(s)
43	spe_time SPE time (UTC)Last modification time of file section using UTC time format	UTC	1	UtcExternal	27 byte(s)
44	spe_gain	-	480	db	480*8 byte(s)

#	Description	Units	Count	Type	Size
	Gain vs temperature and frequency (size TBD)				
45	spe_phase Phase vs temperature and frequency (size TBD)	-	480	db	480*8 byte(s)
46	spare_7 Spare	-	1	SpareField	50 byte(s)
47	paw_time PAW time (UTC)Last modification time of file section using UTC time format	UTC	1	UtcExternal	27 byte(s)
48	paw_gain_setting Gain vs setting	-	64	db	64*8 byte(s)
49	paw_gain_temp Gain vs temperature	-	10	db	10*8 byte(s)
50	azi_offset Azimuth offset	degrees	1	db	8 byte(s)
51	spare_8 Spare	-	1	SpareField	42 byte(s)

Record Length : 10187

DS_NAME : 1 MDSR per MDS

Format Version 114.0

6.5.5 MDS1 -- 1 mdsr forward sweep 1 mdsr reverse sweep

Table 6.28 MDS1 -- 1 mdsr forward sweep 1 mdsr reverse sweep

MDS1 -- 1 mdsr forward sweep, 1 mdsr reverse sweep

#	Description	Units	Count	Type	Size
Data Record					
0	dsr_time ZPD crossing time of the first sweep coadded in gain for the given direction	MJD	1	mjd	12 byte(s)
1	quality_flag Quality indicator (PCD), summarize PCD information per band	flag	1	BooleanFlag	1 byte(s)
2	min_max_adc IGM average min/max at ADC for each detector(IGM min at ADC for detectors A1, A2,..,D2 followed by IGM max at ADC for detectors A1, A2,..,D2)	-	16	ss	16*2 byte(s)
3	prt_avg_temp PRT average temperatures	Kelvin	5	db	5*8 byte(s)
4	spare_1 spare	-	1	SpareField	8 byte(s)
5	num_bb_coadded Number of blackbody igms coadded	-	1	us	2 byte(s)
6	num_bb_corr Number of blackbody igms corrupted and not coadded	-	1	us	2 byte(s)

#	Description	Units	Count	Type	Size
7	num_ds_coadded Number of deep space igms coadded	-	1	us	2 byte(s)
8	num_ds_corr Number of deep space igms corrupted and not coadded	-	1	us	2 byte(s)
9	fringe_count_err Finge count error after current gain measurement wrt previous gain	-	1	ss	2 byte(s)
10	feo_elem_temp FEO Element temperature	-	3	db	3*8 byte(s)
11	sweep_dir Sweep direction, """"F"""" forward and """"R"""" reverse	-	1	uc	1 byte(s)
12	band_valid Band Validity PCD for latest gain measurement. (5 values for bands A, AB, B, C, and D) """"0"""" non-corrupted,""""4"""" invalid due to radiometric accuracy verification	-	5	uc	5*1 byte(s)
13	det_nonlin_ds Detector non-linearity flux validity. (4 values, for detectors A1, A2, AB and B),""""0"""" = flux value is valid, """"1"""" = flux > upper threshold or < lower threshold for at least 1 DS	-	4	uc	4*1 byte(s)
14	det_nonlin_bb Detector non-linearity flux validity. (4 values, for detectors A1, A2, AB and B),""""0"""" = flux value is valid, """"1"""" = flux > upper threshold or < lower threshold for at least 1 BB	-	4	uc	4*1 byte(s)
15	spare_2 Spare	-	1	SpareField	11 byte(s)
16	band_info_a band A information	-	1	band_info_aStruct	262.0 byte(s)

a	deci_fac Decimation factor for current band	-	1	us	2 byte(s)
b	num_spikes Number of detected/corrected spikes	-	1	ul	4 byte(s)
c	igm_id Sweep ID of igms containing spikes (room for 10 values, unused entries set to zero)	-	10	us	10*2 byte(s)
d	spike_pos Spike positions in the interferogram (room for 10 values, unused entries set to zero)	-	10	ul	10*4 byte(s)
e	spike_amp Spike amplitudes (room for 10 complex values, each i followed by q. Unused entries set to zero). Spikes occured at positions described by the corresponding entry in previous fields.	-	10*2	db	10*2*8 byte(s)
f	remain_spikes Number of remaining detected/corrected spikes	-	1	ul	4 byte(s)
g	average_remain_spikes Average amplitudes of remaining detected/corrected spikes	-	2	db	2*8 byte(s)
h	num_band_points Number of points in band (NA)	-	1	ul	4 byte(s)
i	wavenumber_first Wavenumber of first point in band	cm-1	1	db	8 byte(s)
j	wavenumber_last Wavenumber of last point in band	cm-1	1	db	8 byte(s)
k	complex_points Complex data points (N*2)	-		fl	4 byte(s)

17	band_info_ab band AB information	-	1	band_info_abStruct	262.0 byte(s)

a	deci_fac Decimation factor for current band	-	1	us	2 byte(s)

#	Description			Units	Count	Type	Size
	b	num_spikes Number of detected/corrected spikes	-	1		ul	4 byte(s)
	c	igm_id Sweep ID of igms containing spikes (room for 10 values, unused entries set to zero)	-	10		us	10*2 byte(s)
	d	spike_pos Spike positions in the interferogram (room for 10 values, unused entries set to zero)	-	10		ul	10*4 byte(s)
	e	spike_amp Spike amplitudes (room for 10 complex values, each i followed by q. Unused entries set to zero). Spikes occured at positions described by the corresponding entry in previous fields.	-	10*2		db	10*2*8 byte(s)
	f	remain_spikes Number of remaining detected/corrected spikes	-	1		ul	4 byte(s)
	g	average_remain_spikes Average amplitudes of remaining detected/corrected spikes	-	2		db	2*8 byte(s)
	h	num_band_points Number of points in band (NA)	-	1		ul	4 byte(s)
	i	wavenumber_first Wavenumber of first point in band	cm-1	1		db	8 byte(s)
	j	wavenumber_last Wavenumber of last point in band	cm-1	1		db	8 byte(s)
	k	complex_points Complex data points (N*2)	-			fl	4 byte(s)
18	band_info_b band B information		-	1		band_info_bStruct	262.0 byte(s)
	a	deci_fac Decimation factor for current band	-	1		us	2 byte(s)
	b	num_spikes Number of detected/corrected spikes	-	1		ul	4 byte(s)
	c	igm_id Sweep ID of igms containing spikes (room for 10 values, unused entries set to zero)	-	10		us	10*2 byte(s)
	d	spike_pos Spike positions in the interferogram (room for 10 values, unused entries set to zero)	-	10		ul	10*4 byte(s)
	e	spike_amp Spike amplitudes (room for 10 complex values, each i followed by q. Unused entries set to zero). Spikes occured at positions described by the corresponding entry in previous fields.	-	10*2		db	10*2*8 byte(s)
	f	remain_spikes Number of remaining detected/corrected spikes	-	1		ul	4 byte(s)
	g	average_remain_spikes Average amplitudes of remaining detected/corrected spikes	-	2		db	2*8 byte(s)
	h	num_band_points Number of points in band (NA)	-	1		ul	4 byte(s)
	i	wavenumber_first	cm-1	1		db	8 byte(s)

#	Description		Units	Count	Type	Size
		Wavenumber of first point in band				
	j	wavenumber_last Wavenumber of last point in band	cm-1	1	db	8 byte(s)
	k	complex_points Complex data points (N*2)	-		fl	4 byte(s)
19	band_info_c band C information		-	1	band_info_cStruct	262.0 byte(s)
	a	deci_fac Decimation factor for current band	-	1	us	2 byte(s)
	b	num_spikes Number of detected/corrected spikes	-	1	ul	4 byte(s)
	c	igm_id Sweep ID of igms containing spikes (room for 10 values, unused entries set to zero)	-	10	us	10*2 byte(s)
	d	spike_pos Spike positions in the interferogram (room for 10 values, unused entries set to zero)	-	10	ul	10*4 byte(s)
	e	spike_amp Spike amplitudes (room for 10 complex values, each i followed by q. Unused entries set to zero). Spikes occured at positions described by the corresponding entry in previous fields.	-	10*2	db	10*2*8 byte(s)
	f	remain_spikes Number of remaining detected/corrected spikes	-	1	ul	4 byte(s)
	g	average_remain_spikes Average amplitudes of remaining detected/corrected spikes	-	2	db	2*8 byte(s)
	h	num_band_points Number of points in band (NA)	-	1	ul	4 byte(s)
	i	wavenumber_first Wavenumber of first point in band	cm-1	1	db	8 byte(s)
	j	wavenumber_last Wavenumber of last point in band	cm-1	1	db	8 byte(s)
	k	complex_points Complex data points (N*2)	-		fl	4 byte(s)
20	band_info_d band D information		-	1	band_info_dStruct	262.0 byte(s)
	a	deci_fac Decimation factor for current band	-	1	us	2 byte(s)
	b	num_spikes Number of detected/corrected spikes	-	1	ul	4 byte(s)
	c	igm_id Sweep ID of igms containing spikes (room for 10 values, unused entries set to zero)	-	10	us	10*2 byte(s)
	d	spike_pos Spike positions in the interferogram (room for 10 values, unused entries set to zero)	-	10	ul	10*4 byte(s)
	e	spike_amp Spike amplitudes (room	-	10*2	db	10*2*8 byte(s)

#	Description		Units	Count	Type	Size
		for 10 complex values, each i followed by q. Unused entries set to zero). Spikes occured at positions described by the corresponding entry in previous fields.				
	f	remain_spikes Number of remaining detected/corrected spikes	-	1	ul	4 byte(s)
	g	average_remain_spikes Average amplitudes of remaining detected/corrected spikes	-	2	db	2*8 byte(s)
	h	num_band_points Number of points in band (NA)	-	1	ul	4 byte(s)
	i	wavenumber_first Wavenumber of first point in band	cm-1	1	db	8 byte(s)
	j	wavenumber_last Wavenumber of last point in band	cm-1	1	db	8 byte(s)
	k	complex_points Complex data points (N*2)	-		fl	4 byte(s)

Record Length : 1462

DS_NAME : MDS1 -- 1 mdsr forward sweep, 1 mdsr reverse sweep

Format Version 114.0

6.5.6 MDS2 -- 1 mdsr forward sweep 1 mdsr reverse

Table 6.29 MDS2 -- 1 mdsr forward sweep 1 mdsr reverse

MDS2 -- 1 mdsr forward sweep, 1 mdsr reverse

#	Description	Units	Count	Type	Size
	Data Record				
0	dsr_time Time of creation	MJD	1	mjd	12 byte(s)
1	quality_flag Quality indicator (PCD)"""0""" non-corrupted, """1""" corrupted due to the instrument, """2""" corrupted due to the transmission and """4""" corrupted due to the observational validation, -1 = empty	flag	1	BooleanFlag	1 byte(s)
2	num_statistics Number cumulated in statistics, one value per band (A, AB, B, C, D)	-	5	ul	5*4 byte(s)

#	Description	Units	Count	Type	Size
3	sweep_dir Sweep direction, """"F"""" forward and """"R"""" reverse	-	1	uc	1 byte(s)
4	spare_1 Spare	-	1	SpareField	34 byte(s)
5	band_info_a information for band A	-	1	band_info_aStruct	12.0 byte(s)

a	num_points Number of points in band (MA)	-	1	ul	4 byte(s)
b	wavenumber_first Wavenumber of first point in band	cm-1	1	db	8 byte(s)
c	wavenumber_last Wavenumber of last point in band	cm-1	1	db	8 byte(s)
d	mean Mean data points (M points)	W/(cm2.sr.cm-1)		fl	4 byte(s)
e	std_dev Standard deviation data points (M points)	W/(cm2.sr.cm-1)		fl	4 byte(s)

#	Description	Units	Count	Type	Size
6	band_info_ab information for band AB	-	1	band_info_abStruct	12.0 byte(s)

a	num_points Number of points in band (MA)	-	1	ul	4 byte(s)
b	wavenumber_first Wavenumber of first point in band	cm-1	1	db	8 byte(s)
c	wavenumber_last Wavenumber of last point in band	cm-1	1	db	8 byte(s)
d	mean Mean data points (M points)	W/(cm2.sr.cm-1)		fl	4 byte(s)
e	std_dev Standard deviation data points (M points)	W/(cm2.sr.cm-1)		fl	4 byte(s)

#	Description	Units	Count	Type	Size
7	band_info_b information for band B	-	1	band_info_bStruct	12.0 byte(s)

a	num_points Number of points in band (MA)	-	1	ul	4 byte(s)
b	wavenumber_first Wavenumber of first point in band	cm-1	1	db	8 byte(s)
c	wavenumber_last Wavenumber of last point in band	cm-1	1	db	8 byte(s)
d	mean Mean data points (M points)	W/(cm2.sr.cm-1)		fl	4 byte(s)
e	std_dev Standard deviation data points (M points)	W/(cm2.sr.cm-1)		fl	4 byte(s)

#	Description	Units	Count	Type	Size
8	band_info_c information for band C	-	1	band_info_cStruct	12.0 byte(s)

a	num_points Number of points in band (MA)	-	1	ul	4 byte(s)
b	wavenumber_first Wavenumber of first point in band	cm-1	1	db	8 byte(s)
c	wavenumber_last Wavenumber of last point in band	cm-1	1	db	8 byte(s)

#	Description	Units	Count	Type	Size
	d: mean — Mean data points (M points)	W/(cm2.sr.cm-1)		fl	4 byte(s)
	e: std_dev — Standard deviation data points (M points)	W/(cm2.sr.cm-1)		fl	4 byte(s)
9	band_info_d — information for band D	-	1	band_info_dStruct	12.0 byte(s)
	a: num_points — Number of points in band (MA)	-	1	ul	4 byte(s)
	b: wavenumber_first — Wavenumber of first point in band	cm-1	1	db	8 byte(s)
	c: wavenumber_last — Wavenumber of last point in band	cm-1	1	db	8 byte(s)
	d: mean — Mean data points (M points)	W/(cm2.sr.cm-1)		fl	4 byte(s)
	e: std_dev — Standard deviation data points (M points)	W/(cm2.sr.cm-1)		fl	4 byte(s)

Record Length : 128

DS_NAME : MDS2 -- 1 mdsr forward sweep, 1 mdsr reverse

Format Version 114.0

6.5.7 LOS calibration GADS

Table 6.30 LOS calibration GADS

LOS calibration GADS

#	Description	Units	Count	Type	Size
Data Record					
0	dsr_time — Time of creation	MJD	1	mjd	12 byte(s)
1	quality_flag — Quality indicator (PCD)"""0""" non-corrupted,"""-1""" = corrupted, default values filled in	flag	1	BooleanFlag	1 byte(s)
2	freq_err_x — Angular frequency of first order harmonic pointing error related to x-axis (pitch)	degrees/second	1	db	8 byte(s)

#	Description	Units	Count	Type	Size
3	freq_err_y Angular frequency of first order harmonic pointing error related to y-axis (roll)	degrees/second	1	db	8 byte(s)
4	bias_x Estimated bias of pointing related to x-axis (pitch)	degrees	1	db	8 byte(s)
5	amp_err_x Estimated amplitude of first order harmonic pointing error related to x-axis (pitch)	degrees	1	db	8 byte(s)
6	phs_err_x Estimated phase of first order harmonic pointing error related to x-axis (pitch)	degrees	1	db	8 byte(s)
7	bias_y Estimated bias of pointing related to y-axis (roll)	degrees	1	db	8 byte(s)
8	amp_err_y Estimated amplitude of first order harmonic pointing error related to y-axis (roll)	degrees	1	db	8 byte(s)
9	phs_err_y Estimated phase of first order harmonic pointing error related to y-axis (roll)	degrees	1	db	8 byte(s)
10	var_bias_x Variance of estimated bias of pointing related to x-axis (pitch)	degrees2	1	db	8 byte(s)
11	var_amp_x Variance of estimated amplitude of first order harmonic pointing error related to x-axis (pitch)	degrees2	1	db	8 byte(s)
12	var_phs_x Variance of estimated phase of first order harmonic pointing error related to x-axis (pitch)	degrees2	1	db	8 byte(s)
13	var_bias_y Variance of estimated bias of pointing related to y-axis (roll)	degrees2	1	db	8 byte(s)
14	var_amp_y Variance of estimated amplitude of first order harmonic pointing error related to y-axis (roll)	degrees2	1	db	8 byte(s)
15	var_phs_y Variance of estimated phase of first order harmonic pointing error related to y-axis (roll)	degrees2	1	db	8 byte(s)
16	min_fit Minimum function value for fit	-	1	db	8 byte(s)
17	num_orb Number of orbits averaged	-	1	ul	4 byte(s)
18	search_interval Search interval defined as a radius about expected position used for peak find algorithm	sec	1	db	8 byte(s)
19	spare_1 Spare	-	1	SpareField	30 byte(s)

Record Length : 175

DS_NAME : LOS calibration GADS

Format Version 114.0

6.5.8 2 MDSRs per MDS 1 forward sweep 1 reverse sweep

Table 6.31 2 MDSRs per MDS 1 forward sweep 1 reverse sweep

2 MDSRs per MDS, 1 forward sweep, 1 reverse sweep

#	Description	Units	Count	Type	Size
Data Record					
0	zpd_time ZPD time of first deep space sweep used to generate current offset data	MJD	1	mjd	12 byte(s)
1	quality_flag Quality indicator (PCD)."""0""" non-corrupted,"""-1""" = corrupted, default values filled in	flag	1	BooleanFlag	1 byte(s)
2	sweep_dir Sweep direction, """F""" forward and """R""" reverse	-	1	uc	1 byte(s)
3	spare_1 Spare	-	1	SpareField	50 byte(s)
4	band_a band A information	-	1	band_aStruct	18.0 byte(s)

a	deci_fac_curr_band Decimation factor for current band	-	1	us	2 byte(s)
b	num_points Number of points in band (NA)	-	1	ul	4 byte(s)
c	first_wavenum Wavenumber of first point in band	cm-1	1	db	8 byte(s)
d	last_wavenum Wavenumber of last point in band	cm-1	1	db	8 byte(s)
e	data_point Complex data points (N*2 floats)	-		fl	4 byte(s)

5	band_ab band AB information	-	1	band_abStruct	18.0 byte(s)

a	deci_fac_curr_band Decimation factor for current band	-	1	us	2 byte(s)
b	num_points Number of points in band (NA)	-	1	ul	4 byte(s)
c	first_wavenum Wavenumber of first point in band	cm-1	1	db	8 byte(s)
d	last_wavenum Wavenumber of last point in band	cm-1	1	db	8 byte(s)
e	data_point Complex data points (N*2 floats)	-		fl	4 byte(s)

6	band_b band B information	-	1	band_bStruct	18.0 byte(s)

a	deci_fac_curr_band Decimation factor for current band	-	1	us	2 byte(s)
b	num_points Number of points in band (NA)	-	1	ul	4 byte(s)
c	first_wavenum Wavenumber of first point in band	cm-1	1	db	8 byte(s)
d	last_wavenum Wavenumber of last point	cm-1	1	db	8 byte(s)

#	Description			Units	Count	Type	Size
		in band					
	e	data_point Complex data points (N*2 floats)	-			fl	4 byte(s)
7	band_c band C information			-	1	band_cStruct	18.0 byte(s)
	a	deci_fac_curr_band Decimation factor for current band	-	1		us	2 byte(s)
	b	num_points Number of points in band (NA)	-	1		ul	4 byte(s)
	c	first_wavenum Wavenumber of first point in band	cm-1	1		db	8 byte(s)
	d	last_wavenum Wavenumber of last point in band	cm-1	1		db	8 byte(s)
	e	data_point Complex data points (N*2 floats)	-			fl	4 byte(s)
8	band_d band D information			-	1	band_dStruct	18.0 byte(s)
	a	deci_fac_curr_band Decimation factor for current band	-	1		us	2 byte(s)
	b	num_points Number of points in band (NA)	-	1		ul	4 byte(s)
	c	first_wavenum Wavenumber of first point in band	cm-1	1		db	8 byte(s)
	d	last_wavenum Wavenumber of last point in band	cm-1	1		db	8 byte(s)
	e	data_point Complex data points (N*2 floats)	-			fl	4 byte(s)

Record Length : 154

DS_NAME : 2 MDSRs per MDS, 1 forward sweep, 1 reverse sweep

Format Version 114.0

6.5.9 2 MDSR per MDS 1 forward sweep 1 reverse sweep

Table 6.32 2 MDSR per MDS 1 forward sweep 1 reverse sweep

2 MDSR per MDS,1 forward sweep, 1 reverse sweep

#	Description	Units	Count	Type	Size
Data Record					
0	zpd_time ZPD time of first deep space sweep used to generate current offset validation data.	MJD	1	mjd	12 byte(s)
1	quality_flag Quality indicator (PCD)"""0""" non-corrupted,"""-1""" = corrupted, default values filled in	flag	1	BooleanFlag	1 byte(s)
2	num_cumulated Number cumulated in statistics	-	5	ul	5*4 byte(s)
3	sweep_dir Sweep direction, """F""" forward and """R""" reverse	-	1	uc	1 byte(s)
4	spare_1 Spare	-	1	SpareField	34 byte(s)
5	band_a info for band A	-	1	band_aStruct	12.0 byte(s)

a	num_points Number of points in band (M)	-	1	ul	4 byte(s)
b	first_wavenum Wavenumber of first point in band	cm-1	1	db	8 byte(s)
c	last_wavenum Wavenumber of last point in band	cm-1	1	db	8 byte(s)
d	mean Mean data points (M points)	W/(cm2.sr.cm-1)		fl	4 byte(s)
e	std_dev Standard Deviation data points (M points)	W/(cm2.sr.cm-1)		fl	4 byte(s)

#	Description	Units	Count	Type	Size
6	band_ab info for band AB	-	1	band_abStruct	12.0 byte(s)

a	num_points Number of points in band (M)	-	1	ul	4 byte(s)
b	first_wavenum Wavenumber of first point in band	cm-1	1	db	8 byte(s)
c	last_wavenum Wavenumber of last point in band	cm-1	1	db	8 byte(s)
d	mean Mean data points (M points)	W/(cm2.sr.cm-1)		fl	4 byte(s)
e	std_dev Standard Deviation data points (M points)	W/(cm2.sr.cm-1)		fl	4 byte(s)

#	Description	Units	Count	Type	Size
7	band_b info for band B	-	1	band_bStruct	12.0 byte(s)

a	num_points Number of points in band (M)	-	1	ul	4 byte(s)
b	first_wavenum Wavenumber of first point in band	cm-1	1	db	8 byte(s)
c	last_wavenum Wavenumber of last point	cm-1	1	db	8 byte(s)

#	Description			Units	Count	Type	Size
		in band					
	d	mean Mean data points (M points)	W/(cm2.sr.cm-1)			fl	4 byte(s)
	e	std_dev Standard Deviation data points (M points)	W/(cm2.sr.cm-1)			fl	4 byte(s)
8	band_c info for band C			-	1	band_cStruct	12.0 byte(s)
	a	num_points Number of points in band (M)	-	1		ul	4 byte(s)
	b	first_wavenum Wavenumber of first point in band	cm-1	1		db	8 byte(s)
	c	last_wavenum Wavenumber of last point in band	cm-1	1		db	8 byte(s)
	d	mean Mean data points (M points)	W/(cm2.sr.cm-1)			fl	4 byte(s)
	e	std_dev Standard Deviation data points (M points)	W/(cm2.sr.cm-1)			fl	4 byte(s)
9	band_d info for band D			-	1	band_dStruct	12.0 byte(s)
	a	num_points Number of points in band (M)	-	1		ul	4 byte(s)
	b	first_wavenum Wavenumber of first point in band	cm-1	1		db	8 byte(s)
	c	last_wavenum Wavenumber of last point in band	cm-1	1		db	8 byte(s)
	d	mean Mean data points (M points)	W/(cm2.sr.cm-1)			fl	4 byte(s)
	e	std_dev Standard Deviation data points (M points)	W/(cm2.sr.cm-1)			fl	4 byte(s)

Record Length : 128

DS_NAME : 2 MDSR per MDS,1 forward sweep, 1 reverse sweep

Format Version 114.0

6.5.10 ILS Calibration GADS

Table 6.33 ILS Calibration GADS

ILS Calibration GADS

#	Description	Units	Count	Type	Size
Data Record					
0	dsr_time Time of creation	MJD	1	mjd	12 byte(s)
1	quality_flag Quality indicator (PCD)"""0""" non-corrupted,"""-1""" = empty	flag	1	BooleanFlag	1 byte(s)
2	ils_time ILS retrieval time. ZPD time of first scene sweep used for ILS retrieval.	MJD	1	mjd	12 byte(s)
3	quality_flag_2_flag Quality indicator (PCD) "0" non-corrupted,"-1" = corrupted, default values filled in	flag	1	BooleanFlag	1 byte(s)
4	prod_ref_1 Level 1B product filename containing the scene measurements usedWith the reference to the level 1B product file and sweep ID, it is possible to identify unambiguously the scene measurement that has been used for the actual spectral calibration. The refere	-	62	uc	62*1 byte(s)
5	num_ils Number of ILS retrieved (R)	-	1	us	2 byte(s)
6	spare_1 Spare	-	1	SpareField	50 byte(s)
7	ils_data ILS parameters (R ils parameters)	-		ils_dataStruct	-24.0 byte(s)

a	micro_id Microwindow ID	-	8	uc	8*1 byte(s)
b	wavenumber Exact wavenumber of spectral lineThe wavenumber at which the ILS or peak has been computed in a given microwindow is also given, corresponding to the reference line position used in auxiliary data.	cm-1	1	db	8 byte(s)
c	num_coadded Number of coadded scene measurements (N)	-	1	us	2 byte(s)
d	seq_id Sequential ID of scene measurements coadded (N us)	-		us	2 byte(s)
e	param_1 ILS modeling parameter: retroreflector linear shear along Z, vs. OPDThe computed ILS itself is not stored, but instead are stored the two generating parameters that can be used to generate the corresponding ILS at a given wavenumber	cm	1	fl	4 byte(s)
f	param_2 ILS modeling parameter: systematic IR misalignment along YThe computed ILS itself is not stored, but instead are stored the two generating parameters that can be used to generate the corresponding ILS at a given wavenumber	rad	1	fl	4 byte(s)

8	spectral_time Spectral calibration time . ZPD time of first scene sweep used for spectral calibration.	MJD	1	mjd	12 byte(s)
9	quality_flag_3_flag Quality indicator (PCD)	flag	1	BooleanFlag	1 byte(s)

#	Description	Units	Count	Type	Size
	"0" non-corrupted, "-1" = empty				
10	prod_ref_2 Level 1B product filename containing the scene measurements used With the reference to the level 1B product file and sweep ID, it is possible to identify unambiguously the scene measurement that has been used for the actual spectral calibration.	-	62	uc	62*1 byte(s)
11	corr_factor Linear spectral correction factor (Ksc). Linear correction factor(same for all the bands). Doppler effect is treated separately and removed from scene spectra before spectral calibration.	-	1	db	8 byte(s)
12	std_dev_corr_fac Standard deviation of correction factor	-	1	db	8 byte(s)
13	spare_2 Spare	-	1	SpareField	24 byte(s)
14	num_peaks Number of peak fitted (S)	-	1	us	2 byte(s)
15	spare_3 Spare	-	1	SpareField	50 byte(s)
16	peak_data Information about the spectral lines used for the spectral calibration	-		peak_dataStruct	-32.0 byte(s)

a	mcro_id Microwindow ID	-	8	uc	8*1 byte(s)
b	wavenumber Exact wavenumber of spectral line.	cm-1	1	db	8 byte(s)
c	dect_freq_shift Detected frequency shift	cm-1	1	db	8 byte(s)
d	correl_coeff Correlation Coefficient	-	1	db	8 byte(s)
e	num_coadded Number of coadded scene measurements (M)	-	1	us	2 byte(s)
f	seq_id Sequential ID of scene measurements coadded (M us)	-		us	2 byte(s)

Record Length : 251

DS_NAME : ILS Calibration GADS

Format Version 114.0

6.5.11 P T retrieval microwindows ADS

Table 6.34 P T retrieval microwindows ADS

VMR #6 retrieval microwindows ADS

#	Description	Units	Count	Type	Size
Data Record					
0	dsr_time Time of creation	MJD	1	mjd	12 byte(s)
1	attach_flag Attachment flag (Always set to zero for this ADS)	flag	1	BooleanFlag	1 byte(s)
2	mw_label label of microwindow 8 character string	ascii	1	AsciiString	8 byte(s)
3	nlut Number of LUTs included for this microwindow [NLUT]	-	1	us	2 byte(s)
4	dsr_offset Offset of DSR within the corresponding LUT Retrieval Microwindows MDS containing LUT for absorber #i, i = 1, ..., Ngas	-		sl	4 byte(s)

Record Length : 19

DS_NAME : VMR #6 retrieval microwindows ADS

Format Version 114.0

6.5.12 GADS General

Table 6.35 GADS General

GADS General

#	Description	Units	Count	Type	Size
Data Record					
0	dsr_time Time of creation	MJD	1	mjd	12 byte(s)
1	npt Number of p,T microwindows[NpT]	-	1	us	2 byte(s)
2	nvmr Number of species #i VMR microwindows, i = 1,...,6 [NV(i)]	-	6	us	6*2 byte(s)
3	ngas Number of absorbers for which lookup tables are included [Ngas]	-	1	us	2 byte(s)
4	hitran_code HITRAN code of included absorber #1, i = 1, ..., #Ngas	-		us	2 byte(s)

Record Length : 26

DS_NAME : GADS General

Format Version 114.0

6.5.13 LUTs for p T retrieval microwindows MDS

Table 6.36 LUTs for p T retrieval microwindows MDS

LUTs for VMR#6 retrieval microwindows MDS

#	Description	Units	Count	Type	Size
Data Record					
0	dsr_time Time of creation	MJD	1	mjd	12 byte(s)
1	dsr_length Length of this DSR in bytes	bytes	1	ul	4 byte(s)
2	quality_flag Quality indicator (PCD)	flag	1	BooleanFlag	1 byte(s)
3	hitran_code HITRAN code of gas	-	1	us	2 byte(s)
4	tab_code Tabulation code	-	1	us	2 byte(s)
5	nbv Number of base vectors [Nbv]	-	1	ul	4 byte(s)
6	np Number of -ln(pressure) tabulation points [Np]	-	1	ul	4 byte(s)
7	low_press Lowest -ln(pressure) point	hPa	1	fl	4 byte(s)
8	space_press Spacing of -ln(pressure) tabulation	-	1	fl	4 byte(s)
9	nt Number of temperature tabulation points [NT]	-	1	ul	4 byte(s)
10	low_temp Lowest temperature point	K	1	fl	4 byte(s)
11	space_temp Spacing of temperaturetabulation	K	1	fl	4 byte(s)
12	nwn Number of wavenumber points [Nwn]	-	1	ul	4 byte(s)
13	wvn_first wavenumber of first point	cm-1	1	fl	4 byte(s)
14	space_wvn Spacing between wavenumber points	cm-1	1	fl	4 byte(s)
15	u_matrix U-Matrix	-		fl	4 byte(s)
16	k_matrices K-Matrices	cm2/molec		fl	4 byte(s)

Record Length : 53

DS_NAME : LUTs for VMR#6 retrieval microwindows MDS

Format Version 114.0

6.5.14 Microwindow grouping data ADS

Table 6.37 Microwindow grouping data ADS

Microwindow grouping data ADS

#	Description	Units	Count	Type	Size
Data Record					
0	dsr_time Time of creation	MJD	1	mjd	12 byte(s)
1	dsr_length Length of this DSR in bytes	bytes	1	ul	4 byte(s)
2	attach_flag Attachment flag (Always set to zero for this ADS)	flag	1	BooleanFlag	1 byte(s)
3	noffset Index of highest considered geometry for continuum fit	-	1	us	2 byte(s)
4	ngeo_cont Number of geometries used for continuum fit [Ngeo,cont]	-	1	us	2 byte(s)
5	cont_occ Continuum occupation matrix	-		us	2 byte(s)
6	occ_close Occupation matrix of close to close microwindows	-		us	2 byte(s)
7	group_type Types of grouping for continuum fit	-		us	2 byte(s)
8	nmw_cont Number of microwindows considered for continuum fit at geometries used for continuum fit [NMW,cont(i), i = 1, ... ,Ngeo,cont]	-		us	2 byte(s)
9	tot_mw total number of microwindows selected at geometries used for continuum fit [NMW,geo(i),i = 1, ... ,Ngeo,cont]	-		us	2 byte(s)
10	rel_ind_info Relative index of microwindows considered for continuum fit (one at each geometry used for continuum fit)	-		us	2 byte(s)
11	prog_enum_info Progressive enumeration of microwindows considered for continuum fit (one at each geometry used for continuum fit)	-		us	2 byte(s)
12	abs_ind_info Absolute index of all microwindows selected (one at each geometry used for continuum fit)	-		us	2 byte(s)
13	num_interp_info Number of continuum values to be interpolated (one at each geometry used for continuum fit)	-		us	2 byte(s)
14	nholedmw Total number of ?holed? microwindows [NholedMW]	-	1	us	2 byte(s)
15	tot_holes Total number of holes in occupation matrix	-	1	us	2 byte(s)
16	num_holes Number of holes in each holed microwindow [Nholes (i),i=1, ..., NholedMW]	-		us	2 byte(s)
17	ind_holes Indices of holed microwindow [Iholes (i),i=1, ..., NholedMW]	-		us	2 byte(s)

#	Description	Units	Count	Type	Size
18	ind_geom_info Indices of geometries containing holes (one for each holed microwindow)	-		us	2 byte(s)
19	ncc Number of geometries containing at least one close to close microwindow pair [NCC]	-	1	us	2 byte(s)
20	ncc_geo Number of close to close microwindows for each geometry containing close to close microwindow pairs [NCC,geo (i),i = 1, ..., NCC]	-		us	2 byte(s)
21	ind_geo_close Indices of geometries containing close to close microwindow-pairs	-		us	2 byte(s)
22	ind_parent_info Indices of parent windows for each close to close microwindow pair contained for geometry containing close to close microwindow pairs (one for each geometry containing close to close microwindow pairs)	-		us	2 byte(s)
23	ind_high_low Indices of highest and lowest geometry where microwindow #i is selected,i = 1, ..., Nmw(1)	-		us	2 byte(s)

Record Length : N/A

DS_NAME : Microwindow grouping data ADS

Format Version 114.0

6.5.15 Data depending on occupation matrix location ADS

Table 6.38 Data depending on occupation matrix location ADS

Data depending on occupation matrix location ADS

#	Description	Units	Count	Type	Size
Data Record					
0	dsr_time Time of creation	MJD	1	mjd	12 byte(s)
1	dsr_length Length of this DSR in bytes	bytes	1	ul	4 byte(s)
2	attach_flag Attachment flag (Always set to zero for this ADS)	flag	1	BooleanFlag	1 byte(s)
3	occ_label Label of occupation matrix used for latitude #m. 10 character string	ascii	1	AsciiString	10 byte(s)
4	nmw Number of p,T retrieval MWs used at latitude #m [Nmw(m)]	-	1	us	2 byte(s)
5	mw_pt p,T retrieval microwindows used for forward calculations each is an 8 character string	ascii	1	AsciiString	1 byte(s)
6	mw_occ	-		us	2 byte(s)

#	Description	Units	Count	Type	Size
	Microwindow occupation matrix				
7	nsp Number of spectral data points in p,T MW #i,i = 1,...,Nmw(m) [Nsp(m, i)]	-		us	2 byte(s)
8	n_param_levels Number of parameter levels for latitude #m [Npar(m)]	-	1	us	2 byte(s)
9	n_fit_cont_val Number of fitted continuum values for latitude #m [Ncont(m)]	-	1	us	2 byte(s)
10	n_fit_offset_val Number of fitted offset values for latitude #m [Noffset(m)]	-	1	us	2 byte(s)
11	nsim Number of simulations for latitude #m [Nsim(m)]	-	1	us	2 byte(s)
12	alt_grid Altitude grid for simulation #i, i = 1, ..., Nsim(m)	-		fl	4 byte(s)
13	ads2_off Offset of DSR within Data for Continuum and Offset Fit ADS containing data relevant for continuum and offset fit	-		sl	4 byte(s)
14	mds11_off Offset of DSR within Values for Unknowm Parameters MDS containing pressure and temperature profile for simulation #i, i = 1, ..., Nsim(m)	-		sl	4 byte(s)
15	mds10_off Offset of DSR within Spectra MDS containing spectrum for microwindow #k at geometry #j for simulation #i, i = 1, ..., Nsim(m), j = 1, ..., Ngeo, k = 1, ..., NpT,fwd,	-		sl	4 byte(s)
16	mds12_off Offset of DSR within Jacobian Matrices MDS containing rows of jacobian matrix for microwindow #k at geometry #j for simulation #i, i = 1, ..., Nsim(m), j = 1, ..., Ngeo, k = 1, ..., NpT,fwd	-		sl	4 byte(s)

Record Length : 14

DS_NAME : Data depending on occupation matrix location ADS

Format Version 114.0

6.5.16 General data

Table 6.39 General data

General data

#	Description	Units	Count	Type	Size
	Data Record				
0	dsr_time Time of creation	MJD	1	mjd	12 byte(s)
1	ngeo Number of simulated LOS geometries [Ngeo]	-	1	us	2 byte(s)
2	fit_flag Flag indicating fitting of continuum and offsets at contained forward calculations	flag	1	us	2 byte(s)

Record Length : 16

DS_NAME : General data

Format Version 114.0

6.5.17 Jacobian matrices MDS

Table 6.40 Jacobian matrices MDS

Jacobian matrices MDS

#	Description	Units	Count	Type	Size
Data Record					
0	dsr_time Time of creation	MJD	1	mjd	12 byte(s)
1	dsr_length Length of this DSR in bytes	bytes	1	ul	4 byte(s)
2	quality_flag Quality Indicator (-1 for blank MDSR, 0 otherwise)	flag	1	BooleanFlag	1 byte(s)
3	deriv_info Derivative information	-		deriv_infoStruct	16.0 byte(s)
	a — deriv_press Derivatives w.r.t. pressure	-		fl	4 byte(s)
	b — deriv_temp Derivatives w.r.t. temperature	-		fl	4 byte(s)
	c — deriv_cont Derivatives w.r.t. continuum	-		fl	4 byte(s)
	d — deriv_off Derivatives w.r.t. offset	-		fl	4 byte(s)

Record Length : 33

DS_NAME : Jacobian matrices MDS

Format Version 114.0

6.5.18 Computed spectra MDS

Table 6.41 Computed spectra MDS

Computed spectra MDS

#	Description	Units	Count	Type	Size
Data Record					
0	dsr_time Time of creation	MJD	1	mjd	12 byte(s)
1	dsr_length Length of this DSR in bytes	bytes	1	ul	4 byte(s)
2	quality_flag Quality Indicator (-1 for blank MDSR, 0 otherwise)	flag	1	BooleanFlag	1 byte(s)
3	spectrum Spectrum for MW	-		fl	4 byte(s)

Record Length : 13

DS_NAME : Computed spectra MDS

Format Version 114.0

6.5.19 Values of unknown parameters MDS

Table 6.42 Values of unknown parameters MDS

Values of unknown parameters MDS

#	Description	Units	Count	Type	Size
Data Record					
0	dsr_time Time of creation	MJD	1	mjd	12 byte(s)
1	dsr_length Length of this DSR in bytes	bytes	1	ul	4 byte(s)
2	quality_flag Quality indicator (always set to zero)	flag	1	BooleanFlag	1 byte(s)
3	press_prof Pressure profile	-		fl	4 byte(s)
4	temp_prof Temperature profile	-		fl	4 byte(s)
5	cont_val Continuum values	-		fl	4 byte(s)
6	offset_val Offset values	-		fl	4 byte(s)

Record Length : 1

DS_NAME : Values of unknown parameters MDS

Format Version 114.0

6.5.20 GADS General (same format as for MIP_IG2_AX)

Table 6.43 GADS General (same format as for MIP_IG2_AX)

General GADS

#	Description	Units	Count	Type	Size
Data Record					
0	dsr_time Time of creation	MJD	1	mjd	12 byte(s)
1	num_lat_bands Number of latitude bands for which data is contained [Nlat]	-	1	us	2 byte(s)
2	lat_bands Vector of latitude bands	deg		fl	4 byte(s)
3	num_elem Number of elements in altitude grid [Nalt]	-	1	us	2 byte(s)
4	alt_grid Altitude grid	km		fl	4 byte(s)
5	num_gas Number of gases contained [Ngas]	-	1	us	2 byte(s)
6	hitran_code HITRAN codes of gases	-		ul	4 byte(s)
7	gas_name Names of gasesEach is a 16 character string	ascii	1	AsciiString	1 byte(s)

#	Description	Units	Count	Type	Size
8	num_pt_mw Number of p,T microwindows [NpT]	-	1	us	2 byte(s)
9	mw p,T retrieval microwindow labels each is an 8 character string	ascii	1	AsciiString	1 byte(s)
10	num_vmr_mw Number of species #i VMR microwindows, i = 1,...,6 [NV(i)]	-	6	us	6*2 byte(s)
11	vmr1_mw Species #1 VMR retrieval microwindow label. Each is an 8 character string	-		vmr1_mwStruct	-8.0 byte(s)
	a: label Microwindow Label; ascii; 1; AsciiString; 8 byte(s)				
12	vmr2_mw Species #2 VMR retrieval microwindow label. Each is an 8 character string	-		vmr2_mwStruct	-8.0 byte(s)
	a: label Microwindow Label; ascii; 1; AsciiString; 8 byte(s)				
13	vmr3_mw Species #3 VMR retrieval microwindow label. Each is an 8 character string	-		vmr3_mwStruct	-8.0 byte(s)
	a: label Microwindow Label; ascii; 1; AsciiString; 8 byte(s)				
14	vmr4_mw Species #4 VMR retrieval microwindow label. Each is an 8 character string	-		vmr4_mwStruct	-8.0 byte(s)
	a: label Microwindow Label; ascii; 1; AsciiString; 8 byte(s)				
15	vmr5_mw Species #5 VMR retrieval microwindow label. Each is an 8 character string	-		vmr5_mwStruct	-8.0 byte(s)
	a: label Microwindow Label; ascii; 1; AsciiString; 8 byte(s)				
16	vmr6_mw Species #6 VMR retrieval microwindow label. Each is an 8 character string	-		vmr6_mwStruct	-8.0 byte(s)
	a: label Microwindow Label; ascii; 1; AsciiString; 8 byte(s)				

Record Length : N/A

DS_NAME : General GADS

Format Version 114.0

6.5.21 P T continuum profiles MDS (same format as for MIP_IG2_AX)

Table 6.44 P T continuum profiles MDS (same format as for MIP_IG2_AX)

VMR #6 Cont. profiles MDS

#	Description	Units	Count	Type	Size
Data Record					
0	dsr_time Time of creation	MJD	1	mjd	12 byte(s)
1	quality_flag Quality indicator (always set to zero)	flag	1	BooleanFlag	1 byte(s)
2	prof_cont Continuum profiles for p,T retrieval microwindows	cm2		prof_contStruct	4.0 byte(s)
	a: cont_profile Continuum profile — cm2 — fl — 4 byte(s)				

Record Length : 17

DS_NAME : VMR #6 Cont. profiles MDS

Format Version 114.0

6.5.22 Pressure profile MDS (same format as for MIP_IG2_AX)

Table 6.45 Pressure profile MDS (same format as for MIP_IG2_AX)

Pressure profiles MDS

#	Description	Units	Count	Type	Size
Data Record					
0	dsr_time Time of creation	MJD	1	mjd	12 byte(s)

#	Description	Units	Count	Type	Size
1	quality_flag Quality indicator (always set to zero)	flag	1	BooleanFlag	1 byte(s)
2	press_prof Pressure profile	hPa		fl	4 byte(s)

Record Length : 9

DS_NAME : Pressure profiles MDS

Format Version 114.0

6.5.23 Temperature profiles MDS (same format as for MIP_IG2_AX)

Table 6.46 Temperature profiles MDS (same format as for MIP_IG2_AX)

Temperature profiles MDS

#	Description	Units	Count	Type	Size
Data Record					
0	dsr_time Time of creation	MJD	1	mjd	12 byte(s)
1	quality_flag Quality indicator (always set to zero)	flag	1	BooleanFlag	1 byte(s)
2	temp_prof Temperature profile	K		fl	4 byte(s)

Record Length : 9

DS_NAME : Temperature profiles MDS

Format Version 114.0

6.5.24 VMR profiles MDS (same format as for MIP_IG2_AX)

Table 6.47 VMR profiles MDS (same format as for MIP_IG2_AX)

VMR profiles MDS

#	Description	Units	Count	Type	Size
Data Record					
0	dsr_time Time of creation	MJD	1	mjd	12 byte(s)
1	quality_flag Quality indicator (always set to zero)	flag	1	BooleanFlag	1 byte(s)
2	prof Profiles	-		profStruct	4.0 byte(s)
	a: vmr_profile VMR profile	ppm		fl	4 byte(s)

Record Length : 17

DS_NAME : VMR profiles MDS

Format Version 114.0

6.5.25 1 MDSR per MDS

Table 6.48 1 MDSR per MDS

1 MDSR per MDS

#	Description	Units	Count	Type	Size
Data Record					
0	dsr_time Time of creation	MJD	1	mjd	12 byte(s)

#	Description	Units	Count	Type	Size
1	quality_flag Quality indicator (PCD)"""""()""""" non-corrupted,"""""-1""""" = corrupted, default values filled in	flag	1	BooleanFlag	1 byte(s)
2	num_microwindows Total number in file (N)	-	1	ul	4 byte(s)
3	microwindow_info Microwindow descriptions	-		microwindow_infoStruct	-71.0 byte(s)

a	micro_id ID: The spectral line is referenced by its 8 character id	-	8	uc	8*1 byte(s)
b	active_flag Active: Set to 'A' if the microwindow is active or set to 'N' if it is not active.	flag	1	BooleanFlag	1 byte(s)
c	utility_flag Utility: Set to 'S' if the microwindow is used for spectral calibration or set to 'I' if it is used for ILS retrieval.	flag	1	BooleanFlag	1 byte(s)
d	peak_pos Peak position	cm-1	1	db	8 byte(s)
e	left_limit Microwindow left limit	cm-1	1	db	8 byte(s)
f	right_limit Microwindow right limit	cm-1	1	db	8 byte(s)
g	altitude Altitude	km	1	db	8 byte(s)
h	peak_hght Peak height	W/(cm2.sr.cm-1)	1	db	8 byte(s)
i	peak_width Peak width (HWHM)	cm-1	1	db	8 byte(s)
j	math_model Mathematical model	-	1	uc	1 byte(s)
k	num_coadd Number of necessary coadditions	-	1	ul	4 byte(s)
l	valid_thresh Validity threshold	-	1	db	8 byte(s)

Record Length : N/A

DS_NAME : 1 MDSR per MDS

Format Version 114.0

6.5.26 P T retrieval microwindows ADS

Table 6.49 P T retrieval microwindows ADS

P,T retrieval microwindows ADS

#	Description	Units	Count	Type	Size
Data Record					
0	dsr_time Time of creation	MJD	1	mjd	12 byte(s)
1	attach_flag Attachment flag	flag	1	BooleanFlag	1 byte(s)
2	height_trop_p_t Height of tropopause for p,T retrieval microwindows	km	1	db	8 byte(s)
3	npt Number of p,T retrieval microwindows	-	1	us	2 byte(s)
4	lab_p_t_mw Label of p,T microwindow #i, i = 1, ..., Npt. Each is an 8 character string	-		lab_p_t_mwStruct	-8.0 byte(s)
	a: label Microwindow Label — ascii — 1 — AsciiString — 8 byte(s)				
5	offset_dsr_mds_1_data Offset of DSR within MDS#1 containing data for p,T microwindow #i, i = 1, ..., Npt	-		ul	4 byte(s)

Record Length : 11

DS_NAME : P,T retrieval microwindows ADS

Format Version 114.0

6.5.27 VMR #1 retrieval microwindows ADS

Table 6.50 VMR #1 retrieval microwindows ADS

VMR #6 retrieval microwindows ADS

#	Description	Units	Count	Type	Size
Data Record					
0	dsr_time Time of creation	MJD	1	mjd	12 byte(s)
1	attach_flag Attachment flag	flag	1	BooleanFlag	1 byte(s)
2	height_trop_vmr	km	1	db	8 byte(s)

#	Description	Units	Count	Type	Size
	Height of tropopause for species#n VMR retrieval microwindows				
3	num_species_vmr Number of species#n VMR retrieval microwindows	-	1	us	2 byte(s)
4	lab_species_vmr_mw Label of species#n VMR microwindow #i, i = 1, ..., Nv(n). Each is an 8 character string	ascii		lab_species_vmr_mwStruct	-8.0 byte(s)
	a: label, Microwindow Label; ascii; 1; AsciiString; 8 byte(s)				
5	offset_dsr_mds Offset of DSR within MDS#(n+1) containing data for species#n VMR microwindow #i, i = 1, ..., Nv(n)	-		ul	4 byte(s)

Record Length : 11

DS_NAME : VMR #6 retrieval microwindows ADS

Format Version 114.0

6.5.28 DSD for MDS containing p T retrieval microwindows data

Table 6.51 DSD for MDS containing p T retrieval microwindows data

DSD for MDS containing p,T retrieval microwindows data

#	Description	Units	Count	Type	Size
	Data Record				
0	dsr_time Time of creation	MJD	1	mjd	12 byte(s)
1	dsr_length DSR length	-	1	ul	4 byte(s)
2	quality_flag Quality indicator (PCD)	flag	1	BooleanFlag	1 byte(s)
3	microwindow_id Microwindow identifier	-	1	microwindow_idStruct	8.0 byte(s)
	a: label, Microwindow Label; ascii; 1; AsciiString; 8 byte(s)				
4	lowest_wavenumber Lowest wavenumber	cm-1	1	db	8 byte(s)

#	Description	Units	Count	Type	Size
5	highest_wavenumber Highest wavenumber	cm-1	1	db	8 byte(s)
6	wavenumber_grid_spacing Spacing of wavenumber grid	cm-1	1	db	8 byte(s)
7	num_wavenumber_grid_points Number of wavenumber grid points	-	1	us	2 byte(s)
8	lowest_lat_mw Lowest latitude where MW is valid	deg	1	db	8 byte(s)
9	highest_lat_mw Highest latitude where MW is valid	deg	1	db	8 byte(s)
10	num_altitudes Number of altitudes	-	1	us	2 byte(s)
11	tangent_altitude Tangent altitude #i, i = 1, ..., Nalt	km		db	8 byte(s)
12	linear_cont_alt Lower and upper border of region of linear continuum for altitude #i, i = 1, ..., Nalt	km		db	8 byte(s)
13	spacing_fine_grid Spacing of fine grid	cm-1	1	db	8 byte(s)
14	num_fine_grid_points Number of fine grid points for irregular grid	-	1	us	2 byte(s)
15	wavenumber_first_fine_grid Wavenumber of first fine grid point	cm-1	1	db	8 byte(s)
16	bitvector_compressed_grid Bitvector indicating fine grid points to be used for compressed grid	-		uc	1 byte(s)
17	num_compressed_grid_points Number of compressed grid points	-	1	us	2 byte(s)
18	interpolation_flag Flag indicating interpolation method	flag	1	us	2 byte(s)
19	num_gases Number of gases	-	1	us	2 byte(s)
20	hitran_codes_gases HITRAN codes of gases	-		us	2 byte(s)
21	num_spectral_masks Number of spectral masks	-	1	us	2 byte(s)
22	lower_alt_border Lower altitude border for mask #i, i = 1, ..., Nm	km		db	8 byte(s)
23	upper_alt_border_mask Upper altitude border for mask #i, i = 1, ..., Nm	km		db	8 byte(s)
24	spectral_mask Spectral mask # m	-		uc	1 byte(s)

Record Length : 59

DS_NAME : DSD for MDS containing p,T retrieval microwindows data

Format Version 114.0

6.5.29 DSD#1 for MDS containing VMR retrieval microwindows data

Table 6.52 DSD#1 for MDS containing VMR retrieval microwindows data

DSD#6 for MDS containing VMR retrieval microwindows data

#	Description	Units	Count	Type	Size
Data Record					
0	dsr_time Time of creation	MJD	1	mjd	12 byte(s)
1	dsr_length DSR length	-	1	ul	4 byte(s)
2	quality_flag Quality indicator (PCD)	flag	1	BooleanFlag	1 byte(s)
3	microwindow_id Microwindow identifier	-	1	microwindow_idStruct	8.0 byte(s)
	a: label, Microwindow Label; ascii; 1; AsciiString; 8 byte(s)				
4	lowest_wavenumber Lowest wavenumber	cm-1	1	db	8 byte(s)
5	highest_wavenumber Highest wavenumber	cm-1	1	db	8 byte(s)
6	wavenumber_grid_spacing Spacing of wavenumber grid	cm-1	1	db	8 byte(s)
7	num_wavenumber_grid_points Number of wavenumber grid points	-	1	us	2 byte(s)
8	lowest_lat_mw Lowest latitude where MW is valid	deg	1	db	8 byte(s)
9	highest_lat_mw Highest latitude where MW is valid	deg	1	db	8 byte(s)
10	num_altitudes Number of altitudes	-	1	us	2 byte(s)
11	tangent_altitude Tangent altitude #i, i = 1, ..., Nalt	km		db	8 byte(s)
12	linear_cont_alt Lower and upper border of region of linear continuum for altitude #i, i = 1, ..., Nalt	km		db	8 byte(s)
13	spacing_fine_grid Spacing of fine grid	cm-1	1	db	8 byte(s)
14	num_fine_grid_points Number of fine grid points for irregular grid	-	1	us	2 byte(s)
15	wavenumber_first_fine_grid Wavenumber of first fine grid point	cm-1	1	db	8 byte(s)
16	bitvector_compressed_grid Bitvector indicating fine grid points to be used for compressed grid	-		uc	1 byte(s)
17	num_compressed_grid_points Number of compressed grid points	-	1	us	2 byte(s)
18	interpolation_flag Flag indicating interpolation method	flag	1	us	2 byte(s)
19	num_gases Number of gases	-	1	us	2 byte(s)
20	hitran_codes_gases HITRAN codes of gases	-		us	2 byte(s)
21	num_spectral_masks Number of spectral masks	-	1	us	2 byte(s)
22	lower_alt_border Lower altitude border for mask #i, i = 1, ..., Nm	km		db	8 byte(s)
23	upper_alt_border_mask Upper altitude border for mask #i, i = 1, ..., Nm	km		db	8 byte(s)
24	spectral_mask Spectral mask # m	-		uc	1 byte(s)

Record Length : 59

DS_NAME : DSD#6 for MDS containing VMR retrieval microwindows data

Format Version 114.0

6.5.30 Gain Calibration ADS #1

Table 6.53 Gain Calibration ADS #1

Gain Calibration ADS #1

#	Description	Units	Count	Type	Size
Data Record					
0	dsr_time Start time (MJD)(this time corresponds to the ZPD crossing time of the first sweep of the scan for which the data is valid or used)	MJD	1	mjd	12 byte(s)
1	attach_flag Attachment flag (always set to zero for this ADSR)	flag	1	BooleanFlag	1 byte(s)
2	create_time ZPD crossing time of the first sweep coadded in gain for the given direction	MJD	1	mjd	12 byte(s)
3	quality_flag Quality indicator (PCD), summarize PCD information per band	flag	1	BooleanFlag	1 byte(s)
4	min_max_adc Interferogram average min/max at ADC for each detector (IGM min at ADC for detectors A1, A2,...,D2 followed by IGM max at ADC for detectors A1, A2,...,D2) Used by non-linearity correction algorithm	-	16	ss	16*2 byte(s)
5	prt_avg_temp Platinum Resistance Temperature (PRT) sensor average temperatures Temperature of internal calibration blackbody	Kelvin	5	db	5*8 byte(s)
6	spare_1 spare	-	1	SpareField	8 byte(s)
7	num_bb_coadded Number of coadded internal calibration blackbody interferograms	-	1	us	2 byte(s)
8	num_bb_corr Number of blackbody interferograms corrupted and not coadded	-	1	us	2 byte(s)
9	num_ds_coadded Number of deep space interferograms coadded	-	1	us	2 byte(s)
10	num_ds_corr Number of deep space interferograms corrupted and not coadded	-	1	us	2 byte(s)
11	fringe_count_err Finge count error after current gain measurement wrt previous gain	-	1	ss	2 byte(s)
12	feo_elem_temp Front End Optics (FEO) Element temperature	-	3	db	3*8 byte(s)
13	sweep_dir Sweep direction, """"F"""" forward and """"R"""" reverse	-	1	uc	1 byte(s)
14	band_valid Band Validity PCD for latest gain measurement. (5 values for bands A, AB, B, C, and D) """"0"""" non-corrupted,""""4"""" invalid due to radiometric accuracy verification	-	5	uc	5*1 byte(s)
15	det_nonlin_ds Detector non-linearity flux validity. (4 values, for detectors A1, A2, AB and B),""""0"""" = flux value is valid, """"1"""" = flux > upper threshold or < lower	-	4	uc	4*1 byte(s)

#	Description	Units	Count	Type	Size
	threshold for at least 1 DS				
16	det_nonlin_bb Detector non-linearity flux validity. (4 values, for detectors A1, A2, AB and B),"""0""" = flux value is valid, """1""" = flux > upper threshold or < lower threshold for at least 1 BB	-	4	uc	4*1 byte(s)
17	spare_2 Spare	-	1	SpareField	11 byte(s)
18	band_info_a band A information	-	1	band_info_aStruct	262.0 byte(s)

a	deci_fac Decimation factor for current band	-	1	us	2 byte(s)
b	num_spikes Number of detected/corrected spikes	-	1	ul	4 byte(s)
c	igm_id Sweep ID of igms containing spikes (room for 10 values, unused entries set to zero)	-	10	us	10*2 byte(s)
d	spike_pos Spike positions in the interferogram (room for 10 values, unused entries set to zero)	-	10	ul	10*4 byte(s)
e	spike_amp Spike amplitudes (room for 10 complex values, each i followed by q. Unused entries set to zero). Spikes occured at positions described by the corresponding entry in previous fields.	-	10*2	db	10*2*8 byte(s)
f	remain_spikes Number of remaining detected/corrected spikes	-	1	ul	4 byte(s)
g	average_remain_spikes Average amplitudes of remaining detected/corrected spikes	-	2	db	2*8 byte(s)
h	num_band_points Number of points in band (NA)	-	1	ul	4 byte(s)
i	wavenumber_first Wavenumber of first point in band	cm-1	1	db	8 byte(s)
j	wavenumber_last Wavenumber of last point in band	cm-1	1	db	8 byte(s)
k	complex_points Complex data points (N*2)	-		fl	4 byte(s)

19	band_info_ab band AB information	-	1	band_info_abStruct	262.0 byte(s)

a	deci_fac Decimation factor for current band	-	1	us	2 byte(s)
b	num_spikes Number of detected/corrected spikes	-	1	ul	4 byte(s)
c	igm_id Sweep ID of igms containing spikes (room for 10 values, unused entries set to zero)	-	10	us	10*2 byte(s)
d	spike_pos Spike positions in the interferogram (room for 10 values, unused entries set to zero)	-	10	ul	10*4 byte(s)
e	spike_amp Spike amplitudes (room for 10 complex values, each i followed by q. Unused entries set to	-	10*2	db	10*2*8 byte(s)

#	Description			Units	Count	Type	Size
		zero). Spikes occured at positions described by the corresponding entry in previous fields.					
	f	remain_spikes Number of remaining detected/corrected spikes	-		1	ul	4 byte(s)
	g	average_remain_spikes Average amplitudes of remaining detected/corrected spikes	-		2	db	2*8 byte(s)
	h	num_band_points Number of points in band (NA)	-		1	ul	4 byte(s)
	i	wavenumber_first Wavenumber of first point in band	cm-1		1	db	8 byte(s)
	j	wavenumber_last Wavenumber of last point in band	cm-1		1	db	8 byte(s)
	k	complex_points Complex data points (N*2)	-			fl	4 byte(s)
20	band_info_b band B information			-	1	band_info_bStruct	262.0 byte(s)
	a	deci_fac Decimation factor for current band	-		1	us	2 byte(s)
	b	num_spikes Number of detected/corrected spikes	-		1	ul	4 byte(s)
	c	igm_id Sweep ID of igms containing spikes (room for 10 values, unused entries set to zero)	-		10	us	10*2 byte(s)
	d	spike_pos Spike positions in the interferogram (room for 10 values, unused entries set to zero)	-		10	ul	10*4 byte(s)
	e	spike_amp Spike amplitudes (room for 10 complex values, each i followed by q. Unused entries set to zero). Spikes occured at positions described by the corresponding entry in previous fields.	-		10*2	db	10*2*8 byte(s)
	f	remain_spikes Number of remaining detected/corrected spikes	-		1	ul	4 byte(s)
	g	average_remain_spikes Average amplitudes of remaining detected/corrected spikes	-		2	db	2*8 byte(s)
	h	num_band_points Number of points in band (NA)	-		1	ul	4 byte(s)
	i	wavenumber_first Wavenumber of first point in band	cm-1		1	db	8 byte(s)
	j	wavenumber_last Wavenumber of last point in band	cm-1		1	db	8 byte(s)
	k	complex_points Complex data points (N*2)	-			fl	4 byte(s)
21	band_info_c band C information			-	1	band_info_cStruct	262.0 byte(s)
	a	deci_fac Decimation factor for current band	-		1	us	2 byte(s)

#	Description			Units	Count	Type	Size
	b	num_spikes Number of detected/corrected spikes	-	1		ul	4 byte(s)
	c	igm_id Sweep ID of igms containing spikes (room for 10 values, unused entries set to zero)	-	10		us	10*2 byte(s)
	d	spike_pos Spike positions in the interferogram (room for 10 values, unused entries set to zero)	-	10		ul	10*4 byte(s)
	e	spike_amp Spike amplitudes (room for 10 complex values, each i followed by q. Unused entries set to zero). Spikes occured at positions described by the corresponding entry in previous fields.	-	10*2		db	10*2*8 byte(s)
	f	remain_spikes Number of remaining detected/corrected spikes	-	1		ul	4 byte(s)
	g	average_remain_spikes Average amplitudes of remaining detected/corrected spikes	-	2		db	2*8 byte(s)
	h	num_band_points Number of points in band (NA)	-	1		ul	4 byte(s)
	i	wavenumber_first Wavenumber of first point in band	cm-1	1		db	8 byte(s)
	j	wavenumber_last Wavenumber of last point in band	cm-1	1		db	8 byte(s)
	k	complex_points Complex data points (N*2)	-			fl	4 byte(s)
22	band_info_d band D information		-		1	band_info_dStruct	262.0 byte(s)
	a	deci_fac Decimation factor for current band	-	1		us	2 byte(s)
	b	num_spikes Number of detected/corrected spikes	-	1		ul	4 byte(s)
	c	igm_id Sweep ID of igms containing spikes (room for 10 values, unused entries set to zero)	-	10		us	10*2 byte(s)
	d	spike_pos Spike positions in the interferogram (room for 10 values, unused entries set to zero)	-	10		ul	10*4 byte(s)
	e	spike_amp Spike amplitudes (room for 10 complex values, each i followed by q. Unused entries set to zero). Spikes occured at positions described by the corresponding entry in previous fields.	-	10*2		db	10*2*8 byte(s)
	f	remain_spikes Number of remaining detected/corrected spikes	-	1		ul	4 byte(s)
	g	average_remain_spikes Average amplitudes of remaining detected/corrected spikes	-	2		db	2*8 byte(s)
	h	num_band_points Number of points in band (NA)	-	1		ul	4 byte(s)
	i	wavenumber_first	cm-1	1		db	8 byte(s)

#	Description	Units	Count	Type	Size
	Wavenumber of first point in band				
j	wavenumber_last Wavenumber of last point in band	cm-1	1	db	8 byte(s)
k	complex_points Complex data points (N*2)	-		fl	4 byte(s)

Record Length : 1475

DS_NAME : Gain Calibration ADS #1

Format Version 114.0

6.5.31 Gain Calibration ADS #2

Table 6.54 Gain Calibration ADS #2

Gain Calibration ADS #2

#	Description	Units	Count	Type	Size
Data Record					
0	dsr_time Start time (MJD)(this time corresponds to the ZPD crossing time of the first sweep of the scan for which the data is valid or used)	MJD	1	mjd	12 byte(s)
1	attach_flag Attachment flag (always set to zero for this ADSR)	flag	1	BooleanFlag	1 byte(s)
2	create_time Time of creation	MJD	1	mjd	12 byte(s)
3	quality_flag Quality indicator (PCD)"""""0""""" non-corrupted, """""1""""" corrupted due to the instrument, """""2""""" corrupted due to the transmission and """""4""""" corrupted due to the observational validation, -1 = empty	flag	1	BooleanFlag	1 byte(s)
4	num_statistics Number of data sets cumulated in statistics, one value per band (A, AB, B, C, D)	-	5	ul	5*4 byte(s)
5	sweep_dir Sweep direction, """""F""""" forward and """""R""""" reverse	-	1	uc	1 byte(s)
6	spare_1 Spare	-	1	SpareField	34 byte(s)
7	band_info_a Radiometric accuracy statistics for band A	-	1	band_info_aStruct	12.0 byte(s)
	a — num_points Number of points in band (MA)	-	1	ul	4 byte(s)
	b — wavenumber_first	cm-1	1	db	8 byte(s)

#	Description		Units	Count	Type	Size
		Wavenumber of first point in band				
	c	wavenumber_last Wavenumber of last point in band	cm-1	1	db	8 byte(s)
	d	mean Mean data points (M points)	W/(cm2.sr.cm-1)		fl	4 byte(s)
	e	std_dev Standard deviation data points (M points)	W/(cm2.sr.cm-1)		fl	4 byte(s)
8	band_info_ab Radiometric accuracy statistics for band AB		-	1	band_info_abStruct	12.0 byte(s)
	a	num_points Number of points in band (MA)	-	1	ul	4 byte(s)
	b	wavenumber_first Wavenumber of first point in band	cm-1	1	db	8 byte(s)
	c	wavenumber_last Wavenumber of last point in band	cm-1	1	db	8 byte(s)
	d	mean Mean data points (M points)	W/(cm2.sr.cm-1)		fl	4 byte(s)
	e	std_dev Standard deviation data points (M points)	W/(cm2.sr.cm-1)		fl	4 byte(s)
9	band_info_b Radiometric accuracy statistics for band B		-	1	band_info_bStruct	12.0 byte(s)
	a	num_points Number of points in band (MA)	-	1	ul	4 byte(s)
	b	wavenumber_first Wavenumber of first point in band	cm-1	1	db	8 byte(s)
	c	wavenumber_last Wavenumber of last point in band	cm-1	1	db	8 byte(s)
	d	mean Mean data points (M points)	W/(cm2.sr.cm-1)		fl	4 byte(s)
	e	std_dev Standard deviation data points (M points)	W/(cm2.sr.cm-1)		fl	4 byte(s)
10	band_info_c Radiometric accuracy statistics for band C		-	1	band_info_cStruct	12.0 byte(s)
	a	num_points Number of points in band (MA)	-	1	ul	4 byte(s)
	b	wavenumber_first Wavenumber of first point in band	cm-1	1	db	8 byte(s)
	c	wavenumber_last Wavenumber of last point in band	cm-1	1	db	8 byte(s)
	d	mean Mean data points (M points)	W/(cm2.sr.cm-1)		fl	4 byte(s)
	e	std_dev Standard deviation data points (M points)	W/(cm2.sr.cm-1)		fl	4 byte(s)
11	band_info_d Radiometric accuracy statistics for band D		-	1	band_info_dStruct	12.0 byte(s)
	a	num_points	-	1	ul	4 byte(s)

#	Description		Units	Count	Type	Size
		Number of points in band (MA)				
	b	wavenumber_first Wavenumber of first point in band	cm-1	1	db	8 byte(s)
	c	wavenumber_last Wavenumber of last point in band	cm-1	1	db	8 byte(s)
	d	mean Mean data points (M points)	W/(cm2.sr.cm-1)		fl	4 byte(s)
	e	std_dev Standard deviation data points (M points)	W/(cm2.sr.cm-1)		fl	4 byte(s)

Record Length : 141

DS_NAME : Gain Calibration ADS #2

Format Version 114.0

6.5.32 Geolocation ADS (LADS)

Table 6.55 Geolocation ADS (LADS)

Geolocation ADS (LADS)

#	Description		Units	Count	Type	Size
Data Record						
0	dsr_time ZPD time of the first sweep in the scan		MJD	1	mjd	12 byte(s)
1	attach_flag Attachment Flag(set to 1 if all MDSRs associated with this ADSR are blank or missing. Set to zero otherwise.)		flag	1	BooleanFlag	1 byte(s)
2	time_mid ZPD time of the sweep closest in time to the center of the scan		MJD	1	mjd	12 byte(s)
3	time_last ZPD time of the last sweep in the scan		MJD	1	mjd	12 byte(s)
4	loc_first WGS84 latitude and longitude of first sweep in the scan		-	1	loc_firstStruct	8.0 byte(s)
	a	lat Latitude	(1e-6) degrees	1	GeoCoordinate	4 byte(s)
	b	lon Longitude	(1e-6) degrees	1	GeoCoordinate	4 byte(s)

#	Description	Units	Count	Type	Size
5	loc_mid WGS84 latitude and longitude of the sweep closest in time to the center of the scan	-	1	loc_midStruct	8.0 byte(s)
	a: lat, Latitude; (1e-6) degrees; 1; GeoCoordinate; 4 byte(s) b: lon, Longitude; (1e-6) degrees; 1; GeoCoordinate; 4 byte(s)				
6	loc_last WGS84 latitude and longitude of last sweep in the scan	-	1	loc_lastStruct	8.0 byte(s)
	a: lat, Latitude; (1e-6) degrees; 1; GeoCoordinate; 4 byte(s) b: lon, Longitude; (1e-6) degrees; 1; GeoCoordinate; 4 byte(s)				
7	spare_1 Spare	-	1	SpareField	8 byte(s)

Record Length : 69

DS_NAME : Geolocation ADS (LADS)

Format Version 114.0

6.5.33 Scan Information ADS

Table 6.56 Scan Information ADS

Scan Information ADS

#	Description	Units	Count	Type	Size
	Data Record				
0	dsr_time Time of last start elevation scan sequence (MJD)(this time corresponds to the ZPD crossing time of the first sweep of the scan for which the data is valid or used)	MJD	1	mjd	12 byte(s)
1	dsr_length Length of this DSR in bytes	bytes	1	ul	4 byte(s)
2	attach_flag Attachment flag (always set to zero for this ADSR)	flag	1	BooleanFlag	1 byte(s)
3	app_id Application process ID From Instrument Source Packet	-	1	us	2 byte(s)
4	filter_id Filter set ID	-	1	us	2 byte(s)

#	Description	Units	Count	Type	Size
	From Instrument Source Packet				
5	dec_factor Decimation factors.Order: detectors A1, A2,..,D2	-	8	uc	8*1 byte(s)
6	band_map Band mapping configuration From Instrument Source Packet	-	6	uc	6*1 byte(s)
7	num_sweeps Number of sweeps in current scan (M) From Instrument Source Packet	sweeps	1	us	2 byte(s)
8	num_fringe Number of fringe counts (samples at ADC) From Instrument Source Packet	-	1	ul	4 byte(s)
9	sait_id Commanded elevation and azimuth SAIT ID of current scan From Instrument Source Packet	-	2	uc	2*1 byte(s)
10	azi_ang Commanded start elevation and azimuth angles of current scan From Instrument Source Packet	-	2	ul	2*4 byte(s)
11	scan_count Elevation scan counter (reset to zero after a new valid offset calibration)	-	1	ul	4 byte(s)
12	num_fce Accumulated FCE corrected in gain calibration data, at end of current scan. (reset to zero at the start of each processing window)	-	1	ul	4 byte(s)
13	true_local_solar_time True local solar time at target	(1e-6) hours	1	sl	4 byte(s)
14	sat_target_azim Satellite to target azimuth	(1e-6) degrees	1	sl	4 byte(s)
15	target_sun_azim Target to sun azimuth	(1e-6) degrees	1	sl	4 byte(s)
16	target_sun_elev Target to sun elevation	(1e-6) degrees	1	sl	4 byte(s)
17	spare_1 spare	-	1	SpareField	70 byte(s)
18	time_start_elev_scan MJD start time of the first elevation scan (ZPD) from which scene data were extracted for actual spectral calibration.	MJD	1	mjd	12 byte(s)
19	qua_ind_pcd_flag Quality indicator (PCD) """"0"""" non_corrupted, """"-1"""" = default values filled in	flag	1	BooleanFlag	1 byte(s)
20	lin_spec_corr_fac Linear spectral correction factor (Ksc). Linear correction factor (same for all the bands). Doppler effect is treated separately and removed from the scene spectra before spectral calibration.	-	1	db	8 byte(s)
21	std_dev_corr_fac Standard deviation of correction factor	-	1	db	8 byte(s)
22	spare_2 spare	-	1	SpareField	24 byte(s)
23	num_pk_fit Number of peak fitted(S)	-	1	us	2 byte(s)
24	paw_gain_scal PAW gain scaling constants	-	8	fl	8*4 byte(s)
25	spare_3 Spare	-	1	SpareField	14 byte(s)
26	peak Peak #1 to #S	-		peakStruct	-32.0 byte(s)

a	mc_win_id Microwindow ID	-	8	uc	8*1 byte(s)
b	wvnum_spec_ln Exact wavenumber of spectral line	cm-1	1	db	8 byte(s)
c	dect_freq_shift Detected frequency shift	cm-1	1	db	8 byte(s)
d	correla_coeff Correlation coefficient	-	1	db	8 byte(s)
e	num_coadd_scene Number of coadded scene measurements(K)	-	1	us	2 byte(s)
f	seq_id_scene_coadd Sequential ID of scene measurements coadded	-		us	2 byte(s)

#	Description	Units	Count	Type	Size
27	nesr_data NESR data for M sweeps (N data)	r.u.		fl	4 byte(s)

Record Length : 210

DS_NAME : Scan Information ADS

Format Version 114.0

6.5.34 Offset Calibration ADS

Table 6.57 Offset Calibration ADS

Offset Calibration ADS

#	Description	Units	Count	Type	Size
Data Record					
0	dsr_time Start time (MJD) of the elevation scan to which this data pertains.(ZPD crossing time of first sweep in scan for which offset cal. data are valid)	MJD	1	mjd	12 byte(s)
1	attach_flag Attachment flag (always set to zero for this ADSR)	flag	1	BooleanFlag	1 byte(s)
2	band_valid_pcd Band Validity PCD for latest offset measurement (5 values for bands A, AB, B, C, and D). 0 = non-corrupted 1= corrupted due to instrument errors. 2= corrupted due to transmission errors. 4= corrupted due to observational validation.	-	5	uc	5*1 byte(s)
3	acc_fce_corr Accumulated FCE correction in gain calibration data, at end of offset measurement sequence (5 values for bands A, AB,B ,C , and D)	-	5	ss	5*2 byte(s)
4	sweep_dir Sweep direction, """"F"""" forward and """"R"""" reverse	ascii	1	AsciiString	1 byte(s)
5	det_non_linear_flux Detector non-linearity flux validity. (4 values, for detectors A1, A2, AB and B), """"0"""" = flux value is valid, """"1"""" = flux > upper threshold or < lower threshold for at least 1 offset	-	4	uc	4*1 byte(s)
6	spare_1 Spare	-	1	SpareField	46 byte(s)
7	band_a Band A offset	-	1	band_aStruct	256.0 byte(s)

	a	zpd_cross_time ZPD crossing time of first sweep in currently valid offset sequence for this band	MJD	1	mjd	12 byte(s)
	b	dec_factor Decimation factor	-	1	us	2 byte(s)

#	Description			Units	Count	Type	Size
	c	num_corr_spikes Number of corrected spikes	-	1		ul	4 byte(s)
	d	spike_sweep_id Sweep IDs of IGM containing spike	-	10		us	10*2 byte(s)
	e	spike_sample Sample position of spikes in IGM	-	10		ul	10*4 byte(s)
	f	spike_amp Amplitude of spikes	-	10*2		db	10*2*8 byte(s)
	g	spike_rem Number of remaining detected spikes	-	1		us	2 byte(s)
	h	avg_amp_spike_rem Average amplitude of remaining detected spikes	-	2		db	2*8 byte(s)
	i	num_points Number of data points (NA)Before decimation, low resolution sweep produces approximately 30769 data points while high resolution sweep produces approximately 307 692 data points. The decimation factor depends on the band and varies from 11 to 38	-	1		ul	4 byte(s)
	j	off_data Complex data pointsIGM data points are complex data output from FIR filter at the SPE. (N*2 fl)	-			fl	4 byte(s)
8	band_ab Band AB offset		-		1	band_abStruct	256.0 byte(s)
	a	zpd_cross_time ZPD crossing time of first sweep in currently valid offset sequence for this band	MJD	1		mjd	12 byte(s)
	b	dec_factor Decimation factor	-	1		us	2 byte(s)
	c	num_corr_spikes Number of corrected spikes	-	1		ul	4 byte(s)
	d	spike_sweep_id Sweep IDs of IGM containing spike	-	10		us	10*2 byte(s)
	e	spike_sample Sample position of spikes in IGM	-	10		ul	10*4 byte(s)
	f	spike_amp Amplitude of spikes	-	10*2		db	10*2*8 byte(s)
	g	spike_rem Number of remaining detected spikes	-	1		us	2 byte(s)
	h	avg_amp_spike_rem Average amplitude of remaining detected spikes	-	2		db	2*8 byte(s)
	i	num_points Number of data points (NA)Before decimation, low resolution sweep produces approximately 30769 data points while high resolution sweep produces approximately 307 692 data points. The decimation factor depends on the band and varies from 11 to 38	-	1		ul	4 byte(s)
	j	off_data Complex data pointsIGM data points are complex data output from FIR filter at the SPE. (N*2 fl)	-			fl	4 byte(s)

#	Description	Units	Count	Type	Size
9	band_b Band B Offset	-	1	band_bStruct	256.0 byte(s)

a	zpd_cross_time ZPD crossing time of first sweep in currently valid offset sequence for this band	MJD	1	mjd	12 byte(s)
b	dec_factor Decimation factor	-	1	us	2 byte(s)
c	num_corr_spikes Number of corrected spikes	-	1	ul	4 byte(s)
d	spike_sweep_id Sweep IDs of IGM containing spike	-	10	us	10*2 byte(s)
e	spike_sample Sample position of spikes in IGM	-	10	ul	10*4 byte(s)
f	spike_amp Amplitude of spikes	-	10*2	db	10*2*8 byte(s)
g	spike_rem Number of remaining detected spikes	-	1	us	2 byte(s)
h	avg_amp_spike_rem Average amplitude of remaining detected spikes	-	2	db	2*8 byte(s)
i	num_points Number of data points (NA)Before decimation, low resolution sweep produces approximately 30769 data points while high resolution sweep produces approximately 307 692 data points. The decimation factor depends on the band and varies from 11 to 38	-	1	ul	4 byte(s)
j	off_data Complex data pointsIGM data points are complex data output from FIR filter at the SPE. (N*2 fl)	-		fl	4 byte(s)

10	band_c Band C offset	-	1	band_cStruct	256.0 byte(s)

a	zpd_cross_time ZPD crossing time of first sweep in currently valid offset sequence for this band	MJD	1	mjd	12 byte(s)
b	dec_factor Decimation factor	-	1	us	2 byte(s)
c	num_corr_spikes Number of corrected spikes	-	1	ul	4 byte(s)
d	spike_sweep_id Sweep IDs of IGM containing spike	-	10	us	10*2 byte(s)
e	spike_sample Sample position of spikes in IGM	-	10	ul	10*4 byte(s)
f	spike_amp Amplitude of spikes	-	10*2	db	10*2*8 byte(s)
g	spike_rem Number of remaining detected spikes	-	1	us	2 byte(s)
h	avg_amp_spike_rem Average amplitude of remaining detected spikes	-	2	db	2*8 byte(s)
i	num_points Number of data points (NA)Before decimation, low resolution sweep produces approximately 30769 data points while high resolution sweep	-	1	ul	4 byte(s)

#	Description		Units	Count	Type	Size
		produces approximately 307 692 data points. The decimation factor depends on the band and varies from 11 to 38				
	j	off_data Complex data pointsIGM data points are complex data output from FIR filter at the SPE. (N*2 fl)	-		fl	4 byte(s)
11	band_d Band D ofset		-	1	band_dStruct	256.0 byte(s)
	a	zpd_cross_time ZPD crossing time of first sweep in currently valid offset sequence for this band	MJD	1	mjd	12 byte(s)
	b	dec_factor Decimation factor	-	1	us	2 byte(s)
	c	num_corr_spikes Number of corrected spikes	-	1	ul	4 byte(s)
	d	spike_sweep_id Sweep IDs of IGM containing spike	-	10	us	10*2 byte(s)
	e	spike_sample Sample position of spikes in IGM	-	10	ul	10*4 byte(s)
	f	spike_amp Amplitude of spikes	-	10*2	db	10*2*8 byte(s)
	g	spike_rem Number of remaining detected spikes	-	1	us	2 byte(s)
	h	avg_amp_spike_rem Average amplitude of remaining detected spikes	-	2	db	2*8 byte(s)
	i	num_points Number of data points (NA)Before decimation, low resolution sweep produces approximately 30769 data points while high resolution sweep produces approximately 307 692 data points. The decimation factor depends on the band and varies from 11 to 38	-	1	ul	4 byte(s)
	j	off_data Complex data pointsIGM data points are complex data output from FIR filter at the SPE. (N*2 fl)	-		fl	4 byte(s)

Record Length : 1359

DS_NAME : Offset Calibration ADS

Format Version 114.0

6.5.35 Summary Quality ADS

Table 6.58 Summary Quality ADS

Summary Quality ADS

#	Description	Units	Count	Type	Size
Data Record					
0	dsr_time ZPD time of the first sweep in the scan	MJD	1	mjd	12 byte(s)
1	attach_flag Attachment Flag (set to 1 if all MDSRs corresponding to this ADSR are blank, set to zero otherwise)	flag	1	BooleanFlag	1 byte(s)
2	num_corr_sweeps Number of corrupted sweeps	-	1	us	2 byte(s)
3	num_corr_ins Number of corrupted sweeps with instrument errors	-	1	us	2 byte(s)
4	spare_1 Spare	-	1	SpareField	2 byte(s)
5	num_corr_obs Number of corrupted sweeps with observational errors	-	1	us	2 byte(s)
6	num_excess_phase Number of sweeps for which the phase parameter exceeds 0.1. Sequence is : forward band AB, forward band B, reverse band AB, reverse band B	-	4	us	4*2 byte(s)
7	num_opd_shift Number of sweeps for which the OPD shift in band B differs from band AB. Sequence is : forward direction, reverse direction	-	2	us	2*2 byte(s)
8	num_sweeps_flux_oor Number of sweeps for which the flux is out of range for one or all detectors	-	1	us	2 byte(s)
9	spare_2 Spare	-	1	SpareField	22 byte(s)

Record Length : 57

DS_NAME : Summary Quality ADS

Format Version 114.0

6.5.36 Structure ADS

Table 6.59 Structure ADS

Structure ADS

#	Description	Units	Count	Type	Size
Data Record					
0	dsr_time Time of first scan info ADSR this record refers to	MJD	1	mjd	12 byte(s)
1	attach_flag Attachment flag (always set to 0)	flag	1	BooleanFlag	1 byte(s)
2	appl_proc_id Application process ID (c.f.field 4 in scan information ADSR)	-	1	us	2 byte(s)
3	dsr_len_scan_info DSR Length of scan information ADSR(s) to which this record refers	-	1	ul	4 byte(s)
4	num_sweeps_curr_scan Number of sweeps in current scan (M) (c.f.field 8 in scan information ADSR)	-	1	us	2 byte(s)
5	num_points_nesr Number of points in NESR (N) (c.f.field 22 in SPH)	-	1	ul	4 byte(s)
6	num_peaks_fitted Number of peaks fitted (S) (c.f.field 12.6 in scan information ADSR)	-	1	us	2 byte(s)
7	size_blocks_peaks_fitted Size of blocks reporting of peaks fitted. Size of field 27 of Scan info ADS. (= 34 x S + 2 x sigma-K(i), i = 1...S)	-	1	us	2 byte(s)
8	index_first_scan_info Index of first Scan Info ADSR to which Structure ADSR pertains	-	1	ul	4 byte(s)
9	num_scan_info_adsr Number of Scan Info ADSR to which Structure ADSR applies	-	1	ul	4 byte(s)
10	index_first_mdsr Index of first MDSR to which Structure ADSR pertains	-	1	ul	4 byte(s)
11	spare_1 Spare	-	1	SpareField	9 byte(s)

Record Length : 50

DS_NAME : Structure ADS

Format Version 114.0

6.5.37 Calibrated Spectra MDS

Table 6.60 Calibrated Spectra MDS

Calibrated Spectra MDS

#	Description	Units	Count	Type	Size
Data Record					
0	dsr_time ZPD crossing time (MJD)MJD time format is described in Annex A.	MJD	1	mjd	12 byte(s)
1	quality_flag Quality indicator (PCD). """"0""""=non-corrupted, """"1""""=one or more bands corrupted, """"-1""""=blank MDSR	flag	1	BooleanFlag	1 byte(s)
2	seq_id Sequential ID counter The sweep ID counter is a sequential counter that starts at 0 for each output file. It identifies each sweep contained within an output file (level 1B product).	-	1	us	2 byte(s)
3	sc_pos S/C position vector in earth-fixed reference	km	3	db	3*8 byte(s)
4	los_ang LOS pointing angles (azimuth and elevation)	degrees	2	db	2*8 byte(s)
5	loc_1 Geodetic tangent point geolocation (limb and error)	km	2	db	2*8 byte(s)
6	loc_2 Geodetic latitude and geographic longtitude of the tangent point geolocation (lat. then long.)	-	1	loc_2Struct	8.0 byte(s)
	a: lat, Latitude — (1e-6) degrees — 1 — GeoCoordinate — 4 byte(s) b: lon, Longitude — (1e-6) degrees — 1 — GeoCoordinate — 4 byte(s)				
7	rad_earth Radius of earth surface curvature in looking direction at nadir of LOS tangent point	km	1	db	8 byte(s)
8	range_rate Earth fixed target to satellite range rate	km/s	1	db	8 byte(s)
9	alt_rate Geodetic altitude rate of the target	km/s	1	db	8 byte(s)
10	igm_limit Interferogram min/max at ADC for each detector. Order: min for detectors A1, A2,...,D2 followed by max for A1, A2, ...,D2	-	16	ss	16*2 byte(s)
11	sweep_id Sweep ID counter (as in source packet)	-	1	us	2 byte(s)
12	ins_mode Instrument mode/activity	-	1	us	2 byte(s)
13	com_sweep Last commanded number of sweeps	-	1	us	2 byte(s)
14	rel_pos Relative position of current sweep in scan	-	1	us	2 byte(s)
15	dop_strch Doppler stretching factor calculated	-	1	db	8 byte(s)
16	num_spikes Number of detected/corrected spikes. Result of spike detection/correction for the current sweep and for each of the 6 channels/bands (A1, A2, B1, B2, C, and D). Are stored the number of spikes detected/corrected, the location of the bad pixel and the amplitude of the spikes (for the 10 highest) and the number and average of the remaining spikes. It is assumed that all detected spikes are corrected.	-	6	us	6*2 byte(s)
17	spike_pos Spike positions in the interferogramPosition of spike given in sampling number for each band. Ordered as follow: Channel A1, A2, B1, B2, C1, C2, D1, D2	-	60	ul	60*4 byte(s)
18	spike_amp Spike amplitudes. Amplitude (complex) of spike is given in arbitrary or normalized units as given at the output of the instrument. Ordered as follow: Channel A1, A2, B1, B2, C1, C2, D1, D2	-	120	db	120*8 byte(s)
19	remain_spike Number of remaining detected/corrected spikes Ordered as follow: Channel A1, A2, B1, B2, C1, C2, D1, D2	-	6	us	6*2 byte(s)
20	avg_amp	-	12	db	12*8 byte(s)

#	Description	Units	Count	Type	Size
	Average amplitudes of remaining detected (absolute values) Ordered as follow: Channel A1, A2, B1, B2, C1, C2, D1, D2				
21	fringe_count Commanded left and right fringe count Extracted from Instrument Source Packet	-	2	ul	2*4 byte(s)
22	asp_pos APS position at last scan gate start and stop (the variable name 'asp_pos' is not changed into 'aps_pos' to avoid useless compiling errors) Extracted from Instrument Source Packet	-	2	ul	2*4 byte(s)
23	num_errs Number of detected/corrected fringe counter errors (relative fringe count error wrt the gain; i.e., the number of fringe counts (to left (-) or right(+)) the IGM is shifted to match the gain)	-	1	ss	2 byte(s)
24	sweep_dir Sweep Direction F = forward, R = reverse	ascii	1	AsciiString	1 byte(s)
25	band_val Band Validity PCD (one value per band) 0=not corrupted, 2=corrupted due to transmission error, 4=corrupted due to observational validation	-	5	uc	5*1 byte(s)
26	detect_non_lin_flux Detector non-linearity flux validity. (4 values, for detectors A1,A2,AB and B),"""0""" = flux value is valid, """1""" = flux > upper threshold or < lower threshold	-	4	uc	4*1 byte(s)
27	warn_flag_isp Warning flag in isp	-	1	us	2 byte(s)
28	error_flag_isp Error flag in isp	-	1	us	2 byte(s)
29	spare_1 Spare	-	1	SpareField	18 byte(s)
30	band_a Spectral data points band A Single precision floating point data is assumed for the calculated spectra. Amplitude of points is given in radiance units [W/(cm2 sr cm-1)]. The given data points are real. (NA points)	r.u.		fl	4 byte(s)
31	band_ab Spectral data points band AB Single precision floating point data is assumed for the calculated spectra. Amplitude of points is given in radiance units [W/(cm2 sr cm-1)]. The given data points are real. (NAB points)	r.u.		fl	4 byte(s)
32	band_b Spectral data points band B Single precision floating point data is assumed for the calculated spectra. Amplitude of points is given in radiance units [W/(cm2 sr cm-1)]. (NB points)	r.u.		fl	4 byte(s)
33	band_c Spectral data points band C Single precision floating point data is assumed for the calculated spectra. Amplitude of points is given in radiance units [W/(cm2 sr cm-1)]. The given data points are real. (NC points)	r.u.		fl	4 byte(s)
34	band_d Spectral data points band D Single precision floating point data is assumed for the calculated spectra. Amplitude of points is given in radiance units [W/(cm2 sr cm-1)]. The given data points are real. (ND points)	r.u.		fl	4 byte(s)

Record Length : 1501

DS_NAME : Calibrated Spectra MDS

Format Version 114.0

6.5.38 Mipas Level 1B SPH

Table 6.61 Mipas Level 1B SPH

Mipas Level 1B SPH

#	Description	Units	Count	Type	Size
Data Record					
0	sph_descriptor_title SPH_DESCRIPTOR=	keyword	1	AsciiString	15 byte(s)
1	quote_1 quotation mark (""")	ascii	1	AsciiString	1 byte(s)
2	sph_descriptor SPH descriptorASCII string describing the product.	ascii	1	AsciiString	28 byte(s)
3	quote_2 quotation mark (""")	ascii	1	AsciiString	1 byte(s)
4	newline_char_1 newline character	terminator	1	AsciiString	1 byte(s)
5	strip_cont_ind_title STRIPLINE_CONTINUITY_INDICATOR=	keyword	1	AsciiString	31 byte(s)
6	stripline_continuity_indicator Value: +000= No stripline continuity, the product is a complete segment Other: Stripline Counter	-	1	Ac	4 byte(s)
7	newline_char_2 newline character	terminator	1	AsciiString	1 byte(s)
8	slice_pos_title SLICE_POSITION=	keyword	1	AsciiString	15 byte(s)
9	slice_position Value: +001 to NUM_SLICESDefault value if no stripline continuity = +001	-	1	Ac	4 byte(s)
10	newline_char_3 newline character	terminator	1	AsciiString	1 byte(s)
11	num_slice_title NUM_SLICES=	keyword	1	AsciiString	11 byte(s)
12	num_slices Number of slices in this striplineDefault value if no continuity = +001	-	1	Ac	4 byte(s)
13	newline_char_4 newline character	terminator	1	AsciiString	1 byte(s)
14	start_time_title START_TIME=	keyword	1	AsciiString	11 byte(s)
15	quote_3 quotation mark (""")	ascii	1	AsciiString	1 byte(s)
16	start_time ZPD time of first MDSR of the first scan in the product. UTC time format	UTC	1	UtcExternal	27 byte(s)
17	quote_4 quotation mark (""")	ascii	1	AsciiString	1 byte(s)
18	newline_char_5 newline character	terminator	1	AsciiString	1 byte(s)
19	stop_time_title STOP_TIME=	keyword	1	AsciiString	10 byte(s)
20	quote_5 quotation mark (""")	ascii	1	AsciiString	1 byte(s)
21	stop_time ZPD time of last MDSR of the last scan in the product. UTC time format	UTC	1	UtcExternal	27 byte(s)
22	quote_6 quotation mark (""")	ascii	1	AsciiString	1 byte(s)
23	newline_char_6 newline character	terminator	1	AsciiString	1 byte(s)
24	first_lat_title FIRST_TANGENT_LAT=	keyword	1	AsciiString	18 byte(s)
25	first_tangent_lat Latitude of LOS tangent point at center of scan (refraction corrected) of the first scan in the product. Positive north.	(1e-6) degrees	1	AsciiGeoCoordinate	11 byte(s)
26	first_lat_units <10-6degN>	units	1	AsciiString	10 byte(s)
27	newline_char_7 newline character	terminator	1	AsciiString	1 byte(s)
28	first_long_title	keyword	1	AsciiString	19 byte(s)

#	Description	Units	Count	Type	Size
	FIRST_TANGENT_LONG=				
29	first_tangent_long Longitude of LOS tangent point at center of scan (refraction corrected) of the first scan in the product. Positive north.	(1e-6) degrees	1	AsciiGeoCoordinate	11 byte(s)
30	first_long_units <10-6degE>	units	1	AsciiString	10 byte(s)
31	newline_char_8 newline character	terminator	1	AsciiString	1 byte(s)
32	last_lat_title LAST_TANGENT_LAT=	keyword	1	AsciiString	17 byte(s)
33	last_tangent_lat Latitude of LOS tangent point at center of scan (refraction corrected) of the last scan in the product. Positive East.	(1e-6) degrees	1	AsciiGeoCoordinate	11 byte(s)
34	last_lat_units <10-6degN>	units	1	AsciiString	10 byte(s)
35	newline_char_9 newline character	terminator	1	AsciiString	1 byte(s)
36	last_long_title LAST_TANGENT_LONG=	keyword	1	AsciiString	18 byte(s)
37	last_tangent_long Longitude of LOS tangent point at center of scan (refraction corrected) of the last scan in the product. Positive East.	(1e-6) degrees	1	AsciiGeoCoordinate	11 byte(s)
38	last_long_units <10-6degE>	units	1	AsciiString	10 byte(s)
39	newline_char_10 newline character	terminator	1	AsciiString	1 byte(s)
40	spare_1 Spare	-	1	SpareField	51 byte(s)
41	tot_sweeps_title TOT_SWEEPS=	keyword	1	AsciiString	11 byte(s)
42	tot_sweeps Total number of sweeps in product	-	1	As	6 byte(s)
43	newline_char_2 newline character	terminator	1	AsciiString	1 byte(s)
44	tot_scans_title TOT_SCANS=	keyword	1	AsciiString	10 byte(s)
45	tot_scans Total number of scans in product (N)The average number of scans in one orbit is N = 80.	-	1	As	6 byte(s)
46	newline_char_3 newline character	terminator	1	AsciiString	1 byte(s)
47	tot_nom_scans_title TOT_NOM_SCANS=	keyword	1	AsciiString	14 byte(s)
48	tot_nom_scans Number of nominal elevation scans in product	-	1	As	6 byte(s)
49	newline_char_4 newline character	terminator	1	AsciiString	1 byte(s)
50	num_sweeps_title NUM_SWEEPS_PER_SCAN=	keyword	1	AsciiString	20 byte(s)
51	num_sweeps_per_scan Number of sweeps per nominal elevation scan	-	1	As	6 byte(s)
52	newline_char_5 newline character	terminator	1	AsciiString	1 byte(s)
53	scan_off_cal_title SCANS_PER_OFF_CAL=	keyword	1	AsciiString	18 byte(s)
54	scans_per_off_cal Number of nominal elevation scans per offset calibration	-	1	As	6 byte(s)
55	newline_char_6 newline character	terminator	1	AsciiString	1 byte(s)
56	tot_sp_scans_title TOT_SP_SCANS=	keyword	1	AsciiString	13 byte(s)
57	tot_sp_scans Number of special event scans in product	-	1	As	6 byte(s)
58	newline_char_7 newline character	terminator	1	AsciiString	1 byte(s)
59	fringe_scene_title FRINGES_PER_SCENE=	keyword	1	AsciiString	18 byte(s)
60	fringes_per_scene Number of fringe counts (samples at ADC) in scene (nominal mode)	-	1	Al	11 byte(s)
61	newline_char_8 newline character	terminator	1	AsciiString	1 byte(s)

#	Description	Units	Count	Type	Size
62	num_points_title NUM_POINTS_PER_BAND=	keyword	1	AsciiString	20 byte(s)
63	num_points_per_band Number of points in bandsField for common spectral axis definition.(listed in order of band A, AB, B, C, D)	-	5	Al	5*11 byte(s)
64	newline_char_9 newline character	terminator	1	AsciiString	1 byte(s)
65	first_wavenum_title FIRST_WAVENUM=	keyword	1	AsciiString	14 byte(s)
66	first_wavenum Wavenumber of first point in bandsField for common spectral axis definition.(listed in order of band A, AB, B, C, D)	cm-1	5	Ado	5*25 byte(s)
67	first_wavenum_units <cm-1>	units	1	AsciiString	6 byte(s)
68	newline_char_10 newline character	terminator	1	AsciiString	1 byte(s)
69	last_wavenum_title LAST_WAVENUM=	keyword	1	AsciiString	13 byte(s)
70	last_wavenum Wavenumber of last point in bandsField for common spectral axis definition.(listed in order of band A, AB, B, C, D)	cm-1	5	Ado	5*25 byte(s)
71	last_wavenum_units <cm-1>	units	1	AsciiString	6 byte(s)
72	newline_char_11 newline character	terminator	1	AsciiString	1 byte(s)
73	num_nesr_title NUM_NESR_PNTS=	keyword	1	AsciiString	14 byte(s)
74	num_nesr_pnts Number of spectral points in NESR reported	-	1	Al	11 byte(s)
75	newline_char_12 newline character	terminator	1	AsciiString	1 byte(s)
76	nesr_first_wavenum_title NESR_FIRST_WAVENUM=	keyword	1	AsciiString	19 byte(s)
77	nesr_first_wavenum Wavenumber of first point in NESR reported	cm-1	1	Ado	25 byte(s)
78	nesr_first_wavenum_units <cm-1>	units	1	AsciiString	6 byte(s)
79	newline_char_13 newline character	terminator	1	AsciiString	1 byte(s)
80	nesr_last_wavenum_title NESR_LAST_WAVENUM=	keyword	1	AsciiString	18 byte(s)
81	nesr_last_wavenum Wavenumber of last point in NESR reported	cm-1	1	Ado	25 byte(s)
82	nesr_last_wavenum_units <cm-1>	units	1	AsciiString	6 byte(s)
83	newline_char_14 newline character	terminator	1	AsciiString	1 byte(s)
84	sweep_id_title SWEEP_ID=	keyword	1	AsciiString	9 byte(s)
85	sweep_id Sweep ID counter of first sweep in current product (as in source packet)	-	1	As	6 byte(s)
86	newline_char_15 newline character	terminator	1	AsciiString	1 byte(s)
87	max_path_diff_title MAX_PATH_DIFF=	keyword	1	AsciiString	14 byte(s)
88	max_path_diff Maximum path difference in nominal scene measurements.	cm-1	1	Afl	15 byte(s)
89	max_path_diff_units <cm>	units	1	AsciiString	4 byte(s)
90	newline_char_16 newline character	terminator	1	AsciiString	1 byte(s)
91	spare_2 Spare	-	1	SpareField	48 byte(s)

Record Length : 1160

DS_NAME : Mipas Level 1B SPH

Format Version 114.0

6.5.39 Scan Geolocation ADS

Table 6.62 Scan Geolocation ADS

Scan Geolocation ADS

#	Description	Units	Count	Type	Size
Data Record					
0	dsr_time Time of DSR (ZPD time of sweep closest to scans mean time)	MJD	1	mjd	12 byte(s)
1	attach_flag Attachment Flag (set to 1 if all MDSRs corresponding to this ADSR are blank, set to zero otherwise)	flag	1	BooleanFlag	1 byte(s)
2	loc_first Geolocation (lat. / long.) of first scene LOS tangent pointWGS84 reference, refraction corrected	-	1	loc_firstStruct	8.0 byte(s)
	a: lat, Latitude; (1e-6) degrees; 1; GeoCoordinate; 4 byte(s)				
	b: lon, Longitude; (1e-6) degrees; 1; GeoCoordinate; 4 byte(s)				
3	first_alt Tangent altitude of first scene LOS tangent point	km	1	db	8 byte(s)
4	loc_last Geolocation (lat. / long.) of last scene LOS tangent pointWGS84 reference, refraction corrected	-	1	loc_lastStruct	8.0 byte(s)
	a: lat, Latitude; (1e-6) degrees; 1; GeoCoordinate; 4 byte(s)				
	b: lon, Longitude; (1e-6) degrees; 1; GeoCoordinate; 4 byte(s)				
5	last_alt Tangent altitude of last scene LOS tangent point	km	1	db	8 byte(s)
6	loc_mid Geolocation (lat. / long.) of LOS tangent point closest to scans mean time (WGS84reference, refraction corrected)	-	1	loc_midStruct	8.0 byte(s)
	a: lat, Latitude; (1e-6) degrees; 1; GeoCoordinate; 4 byte(s)				
	b: lon, Longitude; (1e-6) degrees; 1; GeoCoordinate; 4 byte(s)				
7	spare_1 Spare	-	1	SpareField	47 byte(s)

Record Length : 100

DS_NAME : Scan Geolocation ADS

Format Version 114.0

6.5.40 Scan Information MDS

Table 6.63 Scan Information MDS

Scan Information MDS

#	Description	Units	Count	Type	Size
Data Record					
0	dsr_time Time of DSR. ZPD time of sweep closest to scans mean time, s.	MJD	1	mjd	12 byte(s)
1	dsr_length DSR length	-	1	ul	4 byte(s)
2	quality_flag Quality indicator (PCD).	flag	1	BooleanFlag	1 byte(s)
3	zpd_crossing_time ZPD crossing time of ith scene spectrun in elevation scan (i = 1, ..., Nsw)	MJD		mjd	12 byte(s)
4	geolocation_los_tangent Geolocation (lat./long.) of ith scene LOS tangent point (i = 1, ..., Nsw)	-		geolocation_los_tangentStruct	-8.0 byte(s)
	a: lat, Latitude — (1e-6) degrees — 1 — GeoCoordinate — 4 byte(s)				
	b: lon, Longitude — (1e-6) degrees — 1 — GeoCoordinate — 4 byte(s)				
5	tangent_altitude_los Tangent altitude of ith scene LOS tangent point (i = 1, ..., Nsw)	km		db	8 byte(s)
6	appl_process_id Application process ID	-	1	us	2 byte(s)
7	retrieval_p_t_flag Flag indicating successful p,T retrieval	flag	1	BooleanFlag	1 byte(s)
8	retrieval_vmr_flag Flag indicating successful VMR retrievals	flag	6	BooleanFlag	6*1 byte(s)
9	spare_1 Spare	-	1	SpareField	54 byte(s)
10	retrieval_p_t p, T retrievals.	-	1	retrieval_p_tStruct	-25.0 byte(s)
	a: lrv_p_t_flag, Logical retrieval vector for p,T retrieval (Nsw). Set to zero if N/A. — flag — — BooleanFlag — 1 byte(s)				
	b: pressure — hPa — — fl — 4 byte(s)				

#	Description	Units	Count	Type	Size
	Retrieved pressure for each sweep. Set to NaN if N/A				
c	pressure_variance Pressure variance for each sweep. Set to NaN if N/A	hPa ^ 2		fl	4 byte(s)
d	tangent_altitude Corrected tangent altitudes of sweeps. Set to NaN if N/A	km		fl	4 byte(s)
e	height_cor_variance Height correction variance for each sweep. Set to NaN if N/A	m ^ 2		fl	4 byte(s)
f	temp Retrieved temperatures for each sweep. Set to NaN if N/A	K		fl	4 byte(s)
g	temp_variance Temperature variance for each sweep. Set to NaN if N/A	K ^ 2		fl	4 byte(s)
11	retrieval_vmr VMR retrievals for species 1 to 6.	-	6	retrieval_vmrStruc	6*-33.0 byte(s)
a	lrv_vmr_flag Logical retrieval vector for VMR retrieval (Nsw). Set to zero if N/A.	flag		BooleanFlag	1 byte(s)
b	vmr Retrieved VMR for each sweep. Set to NaN if N/A	ppm		fl	4 byte(s)
c	vmr_variance VMR variance for each sweep. Set to NaN if N/A	ppm ^ 2		fl	4 byte(s)
d	concentration Concentration for each sweep. Set to NaN if N/A	cm ^ -3		fl	4 byte(s)
e	concentration_variance Concentration variance for each sweep. Set to NaN if N/A	(cm ^ -3) ^ 2		db	8 byte(s)
f	vertical_col_density Vertical column density for each sweep. Set to NaN if N/A	cm ^ -2		fl	4 byte(s)
g	vcd_variance Vertical column density variance for each sweep. Set to NaN if N/A	(cm ^ -2) ^ 2		db	8 byte(s)

Record Length : N/A

DS_NAME : Scan Information MDS

Format Version 114.0

6.5.41 Microwindows Occupation Matrices ADS

Table 6.64 Microwindows Occupation Matrices ADS

Microwindows Occupation Matrices ADS

#	Description	Units	Count	Type	Size
Data Record					
0	dsr_time Start time of validity of DSRZPD time of sweep closest to mean time of the corresponding scan	MJD	1	mjd	12 byte(s)
1	dsr_length Length of this DSR in bytes	bytes	1	ul	4 byte(s)
2	attach_flag Attachment flag (Always set to zero for this ADS)	flag	1	BooleanFlag	1 byte(s)
3	mw_lab_pt Labels of p,T retrieval microwindows selected for sweep #i, i = 1,..., Nsw. Not used fields are blanked out.	-		mw_lab_ptStruct	-8.0 byte(s)
	a: label, Microwindow Label; ascii; 1; AsciiString; 8 byte(s)				
4	mw_lrv_pt Logical retrieval vector for p,T retrieval	-		uc	1 byte(s)
5	mw_lab_vmr1 Labels of species #1 VMR retrieval microwindows selected for sweep #i,i = 1,..., Nsw.	-		mw_lab_vmr1Struct	-8.0 byte(s)
	a: label, Microwindow Label; ascii; 1; AsciiString; 8 byte(s)				
6	mw_lrv_vmr1 Logical retrieval vector for species #1 VMR retrieval	-		uc	1 byte(s)
7	mw_lab_vmr2 Labels of species #2 VMR retrieval microwindows selected for sweep #i,i = 1,..., Nsw.	-		mw_lab_vmr2Struct	-8.0 byte(s)
	a: label, Microwindow Label; ascii; 1; AsciiString; 8 byte(s)				
8	mw_lrv_vmr2 Logical retrieval vector for species #2 VMR retrieval	-		uc	1 byte(s)
9	mw_lab_vmr3 Labels of species #3 VMR retrieval microwindows selected for sweep #i,i = 1,..., Nsw.	-		mw_lab_vmr3Struct	-8.0 byte(s)
	a: label, Microwindow Label; ascii; 1; AsciiString; 8 byte(s)				
10	mw_lrv_vmr3 Logical retrieval vector for species #3 VMR retrieval	-		uc	1 byte(s)
11	mw_lab_vmr4 Labels of species #4 VMR retrieval microwindows selected for sweep #i,i = 1,..., Nsw.	-		mw_lab_vmr4Struct	-8.0 byte(s)
	a: label, Microwindow Label; ascii; 1; AsciiString; 8 byte(s)				

#	Description	Units	Count	Type	Size
12	mw_lrv_vmr4 Logical retrieval vector for species #4 VMR retrieval	-		uc	1 byte(s)
13	mw_lab_vmr5 Labels of species #5 VMR retrieval microwindows selected for sweep #i,i = 1,..., Nsw.	-		mw_lab_vmr5Struct	-8.0 byte(s)
	a: label Microwindow Label; ascii; 1; AsciiString; 8 byte(s)				
14	mw_lrv_vmr5 Logical retrieval vector for species #5 VMR retrieval	-		uc	1 byte(s)
15	mw_lab_vmr6 Labels of species #6 VMR retrieval microwindows selected for sweep #i,i = 1,..., Nsw.	-		mw_lab_vmr6Struct	-8.0 byte(s)
	a: label Microwindow Label; ascii; 1; AsciiString; 8 byte(s)				
16	mw_lrv_vmr6 Logical retrieval vector for species #6 VMR retrieval	-		uc	1 byte(s)
17	spare_1 Spare	-	1	SpareField	47 byte(s)

Record Length : 1

DS_NAME : Microwindows Occupation Matrices ADS

Format Version 114.0

6.5.42 Instrument and Processing Parameters ADS

Table 6.65 Instrument and Processing Parameters ADS

Instrument and Processing Parameters ADS

#	Description	Units	Count	Type	Size
Data Record					
0	dsr_time Time of granule. ZPD time of sweep closest to mean time of corresponding scan	MJD	1	mjd	12 byte(s)
1	dsr_length Length of this DSR in bytes	bytes	1	ul	4 byte(s)
2	attach_flag Attachment flag (Always set to zero for this ADS)	flag	1	BooleanFlag	1 byte(s)
3	elev_scans Vector of actual elevation scan angles	deg		fl	4 byte(s)
4	sg	-	1	uc	1 byte(s)

#	Description	Units	Count	Type	Size
	Retrieved profile switch. Switch indicating whether standard pressure grids (PT, PVMR(j), Pcont(pT), ,Pcont(V(j)) see below) are used to represent retrieved profile data [Sg]?S?: standard output grid?T?:tangent pressure grid. The switch will be set to T i				
5	pt Vector defining pressure levels at which temperature profile data are represented. PT (i), i = 1, ..., NT0if Sg set to ?T?,PT(i) = ptan (i)	hPa		fl	4 byte(s)
6	pv Vector defining pressure levels at which target species # j (j = 1, ..., 6) profile data are represented. PV(j) (i), i = 1, ..., NV(j)if Sg set to ?T?,PV(j)(i) = ptan (i)	hPa		fl	4 byte(s)
7	pcont_pt Vector defining pressure levels at which continuum data for p,T retrieval are represented. Pcont(pT) (i), i = 1, ..., Ncgrid(pT)if Sg set to ?T?,Pcont(pT)(i) = ptan(indexmin(pT) +i-1)	hPa		fl	4 byte(s)
8	pcont_vmr Vectors defining pressure levels at which continuum data for species #j (J + 1, ..., 6) VMR retrievals are represented. Pcont(V(j)) (i), i = 1, ..., Ncgrid(V(j))Ordering of species according to SPHif Sg set to ?T?,Pcont(V(j))(i) = ptan(indexmin(V(j)) +i-1	hPa		fl	4 byte(s)
9	max_macro_iter_pt Max. number of macro iterations of Newton / Marquardt algorithm for p,T retrieval	-	1	us	2 byte(s)
10	max_macro_iter_vmr Max. number of macro iterations of Newton / Marquardt algorithm for VMR retrievals Ordering of species according to SPH	-	6	us	6*2 byte(s)
11	max_micro_iter_pt Max. number of micro iterations of Newton / Marquardt algorithm for p,T retrieval	-	1	us	2 byte(s)
12	max_micro_iter_vmr Max. number of micro iterations of Newton / Marquardt algorithm for VMR retrievals	-	6	us	6*2 byte(s)
13	spare_1 Spare	-	1	SpareField	80 byte(s)
14	spare_2 Spare	-	1	SpareField	82 byte(s)

Record Length : 188

DS_NAME : Instrument and Processing Parameters ADS

Format Version 114.0

6.5.43 PCD Information of Individual Scans ADS

Table 6.66 PCD Information of Individual Scans ADS

PCD Information of Individual Scans ADS

#	Description	Units	Count	Type	Size
Data Record					

#	Description	Units	Count	Type	Size
0	dsr_time Time of granule ZPD time of sweep closest mean time of corresponding scan	MJD	1	mjd	12 byte(s)
1	dsr_length Length of this DSR in bytes	bytes	1	ul	4 byte(s)
2	attach_flag Attachment flag (Always set to zero for this ADS)	flag	1	BooleanFlag	1 byte(s)
3	num_macro_pt Number of macro iterations	-	1	ss	2 byte(s)
4	num_micro_pt Number of micro iterations	-	1	us	2 byte(s)
5	part_chi2_pt Partial chi2 for microwindows. #j at altitude #i,i = 1, ..., Nsw,j = 1, ..., NMWPT. Not used fields are set to -1	-		fl	4 byte(s)
6	evol_chi2_pt Evolution of chi2 during iteration procedure	-		fl	4 byte(s)
7	evol_lambda_pt Evolution of lambda (Marquardt damping factor) during iteration procedure	-		fl	4 byte(s)
8	ret_val_pt Values of retrieved parameters for each macro iteration	-		fl	4 byte(s)
9	pcd_vmr1 PCD info for species #1	-	1	pcd_vmr1Struct	-12.0 byte(s)

a	num_macro_vmr Number of macro iterations	-	1	us	2 byte(s)
b	num_micro_vmr Number of micro iterations	-	1	us	2 byte(s)
c	part_chi2_vmr Partial chi2 for microwindows. #j at altitude #i,i = 1, ..., Nsw,j = 1, ..., NMWPT. Not used fields are set to -1	-		fl	4 byte(s)
d	evol_chi2_vmr Evolution of chi2 during iteration procedure	-		fl	4 byte(s)
e	evol_lambda_vmr Evolution of lambda during iteration procedure	-		fl	4 byte(s)
f	ret_val_vmr Values of retrieved parameters for each macro iteration	-		fl	4 byte(s)

10	pcd_vmr2 PCD info for species #2	-	1	pcd_vmr2Struct	-12.0 byte(s)

a	num_macro_vmr Number of macro iterations	-	1	us	2 byte(s)
b	num_micro_vmr Number of micro iterations	-	1	us	2 byte(s)
c	part_chi2_vmr Partial chi2 for microwindows. #j at altitude #i,i = 1, ..., Nsw,j = 1, ..., NMWPT. Not used fields are set to -1	-		fl	4 byte(s)
d	evol_chi2_vmr Evolution of chi2 during iteration procedure	-		fl	4 byte(s)
e	evol_lambda_vmr Evolution of lambda during iteration procedure	-		fl	4 byte(s)
f	ret_val_vmr Values of retrieved parameters for each macro iteration	-		fl	4 byte(s)

11	pcd_vmr3 PCD info for species #3	-	1	pcd_vmr3Struct	-12.0 byte(s)

a	num_macro_vmr	-	1	us	2 byte(s)

#	Description	Units	Count	Type	Size
	Number of macro iterations				
b	num_micro_vmr Number of micro iterations	-	1	us	2 byte(s)
c	part_chi2_vmr Partial chi2 for microwindows. #j at altitude #i,i = 1, ..., Nsw,j = 1, ..., NMWPT. Not used fields are set to -1	-		fl	4 byte(s)
d	evol_chi2_vmr Evolution of chi2 during iteration procedure	-		fl	4 byte(s)
e	evol_lambda_vmr Evolution of lambda during iteration procedure	-		fl	4 byte(s)
f	ret_val_vmr Values of retrieved parameters for each macro iteration	-		fl	4 byte(s)
12	pcd_vmr4 PCD info for species #4	-	1	pcd_vmr4Struct	-12.0 byte(s)
a	num_macro_vmr Number of macro iterations	-	1	us	2 byte(s)
b	num_micro_vmr Number of micro iterations	-	1	us	2 byte(s)
c	part_chi2_vmr Partial chi2 for microwindows. #j at altitude #i,i = 1, ..., Nsw,j = 1, ..., NMWPT. Not used fields are set to -1	-		fl	4 byte(s)
d	evol_chi2_vmr Evolution of chi2 during iteration procedure	-		fl	4 byte(s)
e	evol_lambda_vmr Evolution of lambda during iteration procedure	-		fl	4 byte(s)
f	ret_val_vmr Values of retrieved parameters for each macro iteration	-		fl	4 byte(s)
13	pcd_vmr5 PCD info for species #5	-	1	pcd_vmr5Struct	-12.0 byte(s)
a	num_macro_vmr Number of macro iterations	-	1	us	2 byte(s)
b	num_micro_vmr Number of micro iterations	-	1	us	2 byte(s)
c	part_chi2_vmr Partial chi2 for microwindows. #j at altitude #i,i = 1, ..., Nsw,j = 1, ..., NMWPT. Not used fields are set to -1	-		fl	4 byte(s)
d	evol_chi2_vmr Evolution of chi2 during iteration procedure	-		fl	4 byte(s)
e	evol_lambda_vmr Evolution of lambda during iteration procedure	-		fl	4 byte(s)
f	ret_val_vmr Values of retrieved parameters for each macro iteration	-		fl	4 byte(s)
14	pcd_vmr6 PCD info for species #6	-	1	pcd_vmr6Struct	-12.0 byte(s)

#	Description	Units	Count	Type	Size
	a: num_macro_vmr — Number of macro iterations	-	1	us	2 byte(s)
	b: num_micro_vmr — Number of micro iterations	-	1	us	2 byte(s)
	c: part_chi2_vmr — Partial chi2 for microwindows. #j at altitude #i,i = 1, ..., Nsw,j = 1, ..., NMWPT. Not used fields are set to -1	-		fl	4 byte(s)
	d: evol_chi2_vmr — Evolution of chi2 during iteration procedure	-		fl	4 byte(s)
	e: evol_lambda_vmr — Evolution of lambda during iteration procedure	-		fl	4 byte(s)
	f: ret_val_vmr — Values of retrieved parameters for each macro iteration	-		fl	4 byte(s)
15	num_valid_info_strings — Number of valid PCD information strings [Npcd]	-	1	us	2 byte(s)
16	info_strings — PCD information strings	-		info_stringsStruct	-80.0 byte(s)
	a: pcd_info — PCD information string	ascii	1	AsciiString	80 byte(s)
17	spare_1 — Spare	-	1	SpareField	47 byte(s)

Record Length : N/A

DS_NAME : PCD Information of Individual Scans ADS

Format Version 114.0

6.5.44 Residual Spectra mean values and standard deviation data ADS

Table 6.67 Residual Spectra mean values and standard deviation data ADS

Residual Spectra , mean values and standard deviation data ADS

#	Description	Units	Count	Type	Size
Data Record					
0	dsr_time Star time of DSRZPD time of sweep closest to the mean time of the corresponding scan	MJD	1	mjd	12 byte(s)
1	dsr_length Length of this DSR in bytes	bytes	1	ul	4 byte(s)
2	attach_flag Attachment flag (Always set to zero for this ADS)	flag	1	BooleanFlag	1 byte(s)
3	num_points Vector defining number of spectral grid points for each microwindow used in p, T retrievals [nspec_pT (i),i = 1, ..., Ntot(pT)]	-		us	2 byte(s)
4	spectral_mask Spectral mask	-		uc	1 byte(s)
5	num_ret Number of p,T retrievals for which mean values and standard deviations are computed	-	1	us	2 byte(s)
6	mean Mean value of residual spectra for spectral grid points in p,T retrieval microwindows [Ntot_grid(pT) = Si nspec_pT (i)]	r.u.		fl	4 byte(s)
7	std_dev Standard deviation of residual spectra for spectral grid points in p,T retrieval microwindows [Ntot_grid(pT) = Si nspec_pT (i)]	r.u.		fl	4 byte(s)
8	vmr1 info for VMR 1	-	1	vmr1Struct	-9.0 byte(s)

a	num_points Vector defining number of spectral grid points for each microwindow used in species #1 VMR retrievals [nspec_v(1,i),i = 1, ..., Ntot(V(1))]	-		us	2 byte(s)
b	spectral_masks Spectral masks	-		uc	1 byte(s)
c	num_ret Number of species VMR retrievals for which mean values and standard deviations are computed	-	1	us	2 byte(s)
d	mean Mean value of residual spectra for spectral grid points in species VMR retrieval microwindows. [Ntot_grid(V(1)) = Si nspec_v(1,i)]	r.u.		fl	4 byte(s)
e	std_dev Standard deviation of residual spectra for spectral grid points in species VMR retrieval microwindows. [Ntot_grid(V(1)) = Si nspec_v(1,i)]	r.u.		fl	4 byte(s)

9	vmr2 info for VMR 2	-	1	vmr2Struct	-9.0 byte(s)

a	num_points Vector defining number of spectral grid points for each microwindow used in species #1 VMR retrievals [nspec_v(1,i),i = 1, ..., Ntot(V(1))]	-		us	2 byte(s)
b	spectral_masks Spectral masks	-		uc	1 byte(s)
c	num_ret Number of species VMR retrievals for which mean values and standard deviations are computed	-	1	us	2 byte(s)
d	mean Mean value of residual spectra for spectral grid	r.u.		fl	4 byte(s)

#	Description			Units	Count	Type	Size
		points in species VMR retrieval microwindows. [Ntot_grid(V(1)) = Si nspec_v(1,i)]					
	e	std_dev Standard deviation of residual spectra for spectral grid points in species VMR retrieval microwindows. [Ntot_grid(V(1)) = Si nspec_v(1,i)]	r.u.			fl	4 byte(s)
10	vmr3 info for VMR 3			-	1	vmr3Struct	-9.0 byte(s)
	a	num_points Vector defining number of spectral grid points for each microwindow used in species #1 VMR retrievals [nspec_v(1,i),i = 1, ..., Ntot(V(1))]	-			us	2 byte(s)
	b	spectral_masks Spectral masks	-			uc	1 byte(s)
	c	num_ret Number of species VMR retrievals for which mean values and standard deviations are computed	-	1		us	2 byte(s)
	d	mean Mean value of residual spectra for spectral grid points in species VMR retrieval microwindows. [Ntot_grid(V(1)) = Si nspec_v(1,i)]	r.u.			fl	4 byte(s)
	e	std_dev Standard deviation of residual spectra for spectral grid points in species VMR retrieval microwindows. [Ntot_grid(V(1)) = Si nspec_v(1,i)]	r.u.			fl	4 byte(s)
11	vmr4 info for VMR 4			-	1	vmr4Struct	-9.0 byte(s)
	a	num_points Vector defining number of spectral grid points for each microwindow used in species #1 VMR retrievals [nspec_v(1,i),i = 1, ..., Ntot(V(1))]	-			us	2 byte(s)
	b	spectral_masks Spectral masks	-			uc	1 byte(s)
	c	num_ret Number of species VMR retrievals for which mean values and standard deviations are computed	-	1		us	2 byte(s)
	d	mean Mean value of residual spectra for spectral grid points in species VMR retrieval microwindows. [Ntot_grid(V(1)) = Si nspec_v(1,i)]	r.u.			fl	4 byte(s)
	e	std_dev Standard deviation of residual spectra for spectral grid points in species VMR retrieval microwindows. [Ntot_grid(V(1)) = Si nspec_v(1,i)]	r.u.			fl	4 byte(s)
12	vmr5 info for VMR 5			-	1	vmr5Struct	-9.0 byte(s)

#	Description	Units	Count	Type	Size
	a — num_points: Vector defining number of spectral grid points for each microwindow used in species #1 VMR retrievals [nspec_v(1,i),i = 1, ..., Ntot(V(1))]	-		us	2 byte(s)
	b — spectral_masks: Spectral masks	-		uc	1 byte(s)
	c — num_ret: Number of species VMR retrievals for which mean values and standard deviations are computed	-	1	us	2 byte(s)
	d — mean: Mean value of residual spectra for spectral grid points in species VMR retrieval microwindows. [Ntot_grid(V(1)) = Si nspec_v(1,i)]	r.u.		fl	4 byte(s)
	e — std_dev: Standard deviation of residual spectra for spectral grid points in species VMR retrieval microwindows. [Ntot_grid(V(1)) = Si nspec_v(1,i)]	r.u.		fl	4 byte(s)
13	vmr6 Residual spectra in target species for VMR 6	-	1	vmr6Struct	-9.0 byte(s)
	a — num_points: Vector defining number of spectral grid points for each microwindow used in species #1 VMR retrievals [nspec_v(1,i),i = 1, ..., Ntot(V(1))]	-		us	2 byte(s)
	b — spectral_masks: Spectral masks	-		uc	1 byte(s)
	c — num_ret: Number of species VMR retrievals for which mean values and standard deviations are computed	-	1	us	2 byte(s)
	d — mean: Mean value of residual spectra for spectral grid points in species VMR retrieval microwindows. [Ntot_grid(V(1)) = Si nspec_v(1,i)]	r.u.		fl	4 byte(s)
	e — std_dev: Standard deviation of residual spectra for spectral grid points in species VMR retrieval microwindows. [Ntot_grid(V(1)) = Si nspec_v(1,i)]	r.u.		fl	4 byte(s)
14	spare_1 Spare	-	1	SpareField	49 byte(s)

Record Length : 3

DS_NAME : Residual Spectra , mean values and standard deviation data ADS

Format Version 114.0

6.5.45 Summary Quality ADS

Table 6.68 Summary Quality ADS

Summary Quality ADS

#	Description	Units	Count	Type	Size
Data Record					
0	dsr_time Time of DSR (ZPD time of sweep closest to first scans mean time)	MJD	1	mjd	12 byte(s)
1	attach_flag Attachment Flag (set to 1 if all MDSRs corresponding to this ADSR are blank, set to zero otherwise)	flag	1	BooleanFlag	1 byte(s)
2	p_T_term_macro_micro Total no. of p, T retrievals terminated due to excess number of macro / micro iterations	-	2	us	2*2 byte(s)
3	vmr_term_macro_micro Total no. of VMR retrievals terminated due to due to excess number of macro / micro iterations	-	6*2	us	6*2*2 byte(s)
4	p_T_term_run_time Total no. of p,T retrievals terminated due to run time limitation	-	1	us	2 byte(s)
5	vmr_term_run_time Total no. of VMR retrievals terminated due to run time limitation1 value for each species	-	6	us	6*2 byte(s)
6	spare_1 Spare	-	1	SpareField	65 byte(s)

Record Length : 120

DS_NAME : Summary Quality ADS

Format Version 114.0

6.5.46 Structure ADS

Table 6.69 Structure ADS

Structure ADS

#	Description	Units	Count	Type	Size
Data Record					
0	dsr_time Time of DSR (ZPD time of sweep closest to mean time of first scan this ADSR refers to)	MJD	1	mjd	12 byte(s)
1	attach_flag Attachment flag	flag	1	BooleanFlag	1 byte(s)
2	num_sweeps Number of sweeps per scan	-	1	us	2 byte(s)
3	num_press_temp_pts Number of retrieved pressure/temperature profile points	-	1	us	2 byte(s)
4	num_vmr_pts Number of retrieved VMR profile points	-	6	us	6*2 byte(s)
5	flags_p_t_error_flag Flags indicating existence of p,T error propagation data	flag	6	us	6*2 byte(s)
6	num_con_params_p_t Number of fitted continuum parameters in p,T retrievals	-	1	us	2 byte(s)
7	num_con_params_vmr Number of fitted continuum parameters in VMR retrievals	-	6	us	6*2 byte(s)
8	num_instr_offset_p_t Number of fitted instrument offset values in p,T retrievals	-	1	us	2 byte(s)
9	num_instr_offset_vmr Number of fitted instrument offset values in VMR retrievals	-	6	us	6*2 byte(s)
10	max_num_micro_p_t Max number of microwindows per acquisition tangent height used for p, T retrieval	-	1	us	2 byte(s)
11	max_num_micro_vmr Max number of microwindows per acquisition tangent height used for VMR retrieval	-	6	us	6*2 byte(s)
12	tot_num_p_t_micro_all_alt Total number of p, T microwindows (all altitudes) processed in current scan	-	1	us	2 byte(s)
13	tot_num_vmr_micro_all_alt Total number of VMR retrieval microwindows (all altitudes) processed in current scan	-	6	us	6*2 byte(s)
14	tot_num_spect_grid_p_t Total number of spectral grid points contained in selected p,T microwindows	-	1	us	2 byte(s)
15	tot_num_spect_vmr Total number of spectral grid points contained in selected microwindows for VMR removals	-	6	us	6*2 byte(s)
16	num_grid_con_p_t Number of profile grid points to represent continuum profile data for p,T retrieval	-	1	us	2 byte(s)
17	num_grid_con_vmr Number of profile grid points to represent continuum profile data for VMR retrievals	-	6	us	6*2 byte(s)
18	num_evo_steps_p_t Maximum number of evolution steps reported for p,T retrievals. Refers to corresponding PCD info ADSR.	-	1	ss	2 byte(s)
19	num_evo_steps_vmr Maximum number of evolution steps reported for VMR retrievals. Refers to corresponding PCD info ADSR.	-	6	ss	6*2 byte(s)
20	num_pcd_info Maximum number of PCD information strings in corresponding PCD info ADSR.	-	1	us	2 byte(s)
21	mds_scan_info_pointer Offset and size of first corresponding record in Scan Info MDS	-	1	mds_scan_info_pointerStruct	8.0 byte(s)
	a: dsr_offset Offset of first DSR. Set to -1 if DSR is missing.	-	1	sl	4 byte(s)
	b: dsr_length Size of DSR's	-	1	ul	4 byte(s)
22	mds_p_t_pointer Offset and size of first corresponding record in p, T profile MDS	-	1	mds_p_t_pointerStruct	8.0 byte(s)

#	Description	Units	Count	Type	Size
	a: dsr_offset — Offset of first DSR. Set to -1 if DSR is missing.	-	1	sl	4 byte(s)
	b: dsr_length — Size of DSR's	-	1	ul	4 byte(s)
23	mds_vmr1_pointer — Offset and size of first corresponding record in VMR #1 profile MDS	-	1	mds_vmr1_pointerStruct	8.0 byte(s)
	a: dsr_offset — Offset of first DSR. Set to -1 if DSR is missing.	-	1	sl	4 byte(s)
	b: dsr_length — Size of DSR's	-	1	ul	4 byte(s)
24	mds_vmr2_pointer — Offset and size of first corresponding record in VMR #2 profile MDS	-	1	mds_vmr2_pointerStruct	8.0 byte(s)
	a: dsr_offset — Offset of first DSR. Set to -1 if DSR is missing.	-	1	sl	4 byte(s)
	b: dsr_length — Size of DSR's	-	1	ul	4 byte(s)
25	mds_vmr3_pointer — Offset and size of first corresponding record in VMR #3 profile MDS	-	1	mds_vmr3_pointerStruct	8.0 byte(s)
	a: dsr_offset — Offset of first DSR. Set to -1 if DSR is missing.	-	1	sl	4 byte(s)
	b: dsr_length — Size of DSR's	-	1	ul	4 byte(s)
26	mds_vmr4_pointer — Offset and size of first corresponding record in VMR #4 profile MDS	-	1	mds_vmr4_pointerStruct	8.0 byte(s)
	a: dsr_offset — Offset of first DSR. Set to -1 if DSR is missing.	-	1	sl	4 byte(s)
	b: dsr_length — Size of DSR's	-	1	ul	4 byte(s)
27	mds_vmr5_pointer — Offset and size of first corresponding record in VMR #5 profile MDS	-	1	mds_vmr5_pointerStruct	8.0 byte(s)
	a: dsr_offset — Offset of first DSR. Set to -1 if DSR is missing.	-	1	sl	4 byte(s)
	b: dsr_length — Size of DSR's	-	1	ul	4 byte(s)
28	mds_vmr6_pointer — Offset and size of first corresponding record in VMR #6 profile MDS	-	1	mds_vmr6_pointerStruct	8.0 byte(s)
	a: dsr_offset — Offset of first DSR. Set to -1 if DSR is missing.	-	1	sl	4 byte(s)
	b: dsr_length — Size of DSR's	-	1	ul	4 byte(s)
29	mds_cont_pointer — Offset and size of first corresponding record in Offset and Continuum MDS	-	1	mds_cont_pointerStruct	8.0 byte(s)
	a: dsr_offset — Offset of first DSR. Set to -1 if DSR is missing.	-	1	sl	4 byte(s)
	b: dsr_length — Size of DSR's	-	1	ul	4 byte(s)

#	Description	Units	Count	Type	Size
30	pcd_ads_pointer Offset and size of first corresponding record in PCD ADS	-	1	pcd_ads_pointerStruct	8.0 byte(s)
	a: dsr_offset Offset of first DSR. Set to -1 if DSR is missing.	-	1	sl	4 byte(s)
	b: dsr_length Size of DSR's	-	1	ul	4 byte(s)
31	mw_ads_pointer Offset and size of first corresponding record in Microwindows Ocupation Matrix ADS	-	1	mw_ads_pointerStruct	8.0 byte(s)
	a: dsr_offset Offset of first DSR. Set to -1 if DSR is missing.	-	1	sl	4 byte(s)
	b: dsr_length Size of DSR's	-	1	ul	4 byte(s)
32	res_spect_ads_pointer Offset and size of first corresponding record in Residual Spectra ADS	-	1	res_spect_ads_pointerStruct	8.0 byte(s)
	a: dsr_offset Offset of first DSR. Set to -1 if DSR is missing.	-	1	sl	4 byte(s)
	b: dsr_length Size of DSR's	-	1	ul	4 byte(s)
33	param_ads_pointer Offset and size of first corresponding record in Parameters ADS	-	1	param_ads_pointerStruct	8.0 byte(s)
	a: dsr_offset Offset of first DSR. Set to -1 if DSR is missing.	-	1	sl	4 byte(s)
	b: dsr_length Size of DSR's	-	1	ul	4 byte(s)
34	spare_1 Spare	-	1	SpareField	55 byte(s)

Record Length : 300

DS_NAME : Structure ADS

Format Version 114.0

6.5.47 Continuum Contribution and Radiance Offset MDS

Table 6.70 Continuum Contribution and Radiance Offset MDS

Continuum Contribution and Radiance Offset MDS

#	Description	Units	Count	Type	Size
Data Record					
0	dsr_time Time of DSR, ZPD time of sweep closest to scans mean time	MJD	1	mjd	12 byte(s)
1	dsr_length Length of this DSR in bytes	bytes	1	ul	4 byte(s)
2	quality_flag Quality indicator(set to -1 if all retrieval failed. Set to 0 otherwise.)	flag	1	BooleanFlag	1 byte(s)
3	fitted_off_pt Fitted instrument offset in p , T retrieval microwindowsoffset (i), i = 1, ..., Noffset(pT)	r.u.		fl	4 byte(s)
4	off_var Instrument offset variance data Elements of diagonal of variance/covariance matrix	(r.u.)2		fl	4 byte(s)
5	def_pt_mw_off Definition of p, T retrieval microwindows in which offset values are fitted:Each entry is an 8 character stringi = 1, ..., Noffset(pT)	-		def_pt_mw_offStruct	-8.0 byte(s)
	a: label Microwindow Label — ascii — 1 — AsciiString — 8 byte(s)				
6	ind_first_last Indices of tangent heights for which continuum absorption coefficients are fitted. If no continuum is fitted, values are set to -1.	-		us	2 byte(s)
7	cont p, T retrievals: Radiometric offset values fitted in different spectral intervals	-		contStruct	10.0 byte(s)
	a: def_mw Definition of p, T retrieval microwindows used at altitude #indexCon(pT). — ascii — 1 — AsciiString — 8 byte(s)				
	b: type_mw Types of grouping for above MWs used at altitude #indexCon(pT) 0: not used1: isolated2: edge of a loose group3: leftmost edge of a tight group4: leftmost edge of a tight group and edge of a loose group5: member of a tight group but not at the corner of th — - — ss — 2 byte(s)				
	c: fitted_cont Fitted continuum values used at altitude #indexCon(pT) — (1e-30) cm2/molec — fl — 4 byte(s)				
	d: fitted_cont_var Variance data of continuums fitted used at altitude #indexCon(pT) — (1e-60) cm4/molec2 — fl — 4 byte(s)				
	e: cont_press_cov Covariance data of fitted continuums and retrieved pressure used at altitude #indexCon(pT) — (1e-30) hPa*cm2/molec — fl — 4 byte(s)				
	f: cont_temp_cov Covariance data of fitted continuums and retrieved temperature used at altitude #indexCon(pT) — (1e-30) K*cm2/molec — fl — 4 byte(s)				
8	fitted_off_vmr1 Fitted instrument offset in VMR #1 retrieval microwindows	r.u.		fl	4 byte(s)
9	off_var_vmr1 Instrument offset variance data. Elements of diagonal of variance/covariance matrix	(r.u.)2		fl	4 byte(s)
10	def_mw_vmr1 Definition of VMR #1 retrieval microwindows in which offset values are fitted	ascii	1	AsciiString	1 byte(s)

#	Description	Units	Count	Type	Size
11	indecies_vmr1 Indices of tangent height for which continuum absorption coefficients are fitted. [indexmin(V(i)), indexmax(V(i))]If no continuum is fitted, set to -1	-		us	2 byte(s)
12	cont_alt_vmr1 VMR #1 continuum values fitted in different spectral intervals for each altitude index	-		cont_alt_vmr1Struct	13.0 byte(s)

a	def_mw Definition of VMR retrieval microwindows. Used at altitude #indexCon(V(1)). row relating to this altitude of matrix for VMR retrieval in corresponding Scan Info ADS	ascii	1	AsciiString	1 byte(s)
b	type_mw Types of grouping for above MWs used at altitude #indexCon(V(i))	-		ss	2 byte(s)
c	fitted_cont Fitted continuum values at altitude #indexCon(V(i))	(1e-30) cm2/molec		fl	4 byte(s)
d	fitted_cont_var Variance data of continuums fitted at altitude #indexCon(V(i))	(1e-60) cm4/molec2		fl	4 byte(s)
e	fitted_cont_cov Covariance data of fitted continuums and retrieved VMR profile point at altitude #indexCon(V(i))	(1e-30) ppm*cm2/molec		fl	4 byte(s)

#	Description	Units	Count	Type	Size
13	fitted_off_vmr2 Fitted instrument offset in VMR #2 retrieval microwindows	r.u.		fl	4 byte(s)
14	off_var_vmr2 Instrument offset variance data. Elements of diagonal of variance/covariance matrix	(r.u.)2		fl	4 byte(s)
15	def_mw_vmr2 Definition of VMR #2 retrieval microwindows in which offset values are fitted	ascii	1	AsciiString	1 byte(s)
16	indecies_vmr2 Indices of tangent height for which continuum absorption coefficients are fitted. [indexmin(V(i)), indexmax(V(i))]If no continuum is fitted, set to -1	-		us	2 byte(s)
17	cont_alt_vmr2 VMR #2 continuum values fitted in different spectral intervals for each altitude index	-		cont_alt_vmr2Struct	13.0 byte(s)

a	def_mw Definition of VMR retrieval microwindows. Used at altitude #indexCon(V(1)). row relating to this altitude of matrix for VMR retrieval in corresponding Scan Info ADS	ascii	1	AsciiString	1 byte(s)
b	type_mw Types of grouping for above MWs used at altitude #indexCon(V(i))	-		ss	2 byte(s)
c	fitted_cont Fitted continuum values at altitude #indexCon(V(i))	(1e-30) cm2/molec		fl	4 byte(s)
d	fitted_cont_var Variance data of continuums fitted at altitude #indexCon(V(i))	(1e-60) cm4/molec2		fl	4 byte(s)
e	fitted_cont_cov Covariance data of fitted continuums and retrieved VMR profile point at altitude #indexCon(V(i))	(1e-30) ppm*cm2/molec		fl	4 byte(s)

#	Description	Units	Count	Type	Size
18	fitted_off_vmr3 Fitted instrument offset in VMR #3 retrieval microwindows	r.u.		fl	4 byte(s)
19	off_var_vmr3 Instrument offset variance data. Elements of diagonal of variance/covariance matrix	(r.u.)2		fl	4 byte(s)

#	Description	Units	Count	Type	Size
20	def_mw_vmr3 Definition of VMR #3 retrieval microwindows in which offset values are fitted	ascii	1	AsciiString	1 byte(s)
21	indecies_vmr3 Indices of tangent height for which continuum absorption coefficients are fitted. [indexmin(V(i)), indexmax(V(i))]If no continuum is fitted, set to -1	-		us	2 byte(s)
22	cont_alt_vmr3 VMR #3 continuum values fitted in different spectral intervals for each altitude index	-		cont_alt_vmr3Struct	13.0 byte(s)

a	def_mw Definition of VMR retrieval microwindows. Used at altitude #indexCon(V(1)). row relating to this altitude of matrix for VMR retrieval in corresponding Scan Info ADS	ascii	1	AsciiString	1 byte(s)
b	type_mw Types of grouping for above MWs used at altitude #indexCon(V(i))	-		ss	2 byte(s)
c	fitted_cont Fitted continuum values at altitude #indexCon(V(i))	(1e-30) cm2/molec		fl	4 byte(s)
d	fitted_cont_var Variance data of continuums fitted at altitude #indexCon(V(i))	(1e-60) cm4/molec2		fl	4 byte(s)
e	fitted_cont_cov Covariance data of fitted continuums and retrieved VMR profile point at altitude #indexCon(V(i))	(1e-30) ppm*cm2/molec		fl	4 byte(s)

23	fitted_off_vmr4 Fitted instrument offset in VMR #4 retrieval microwindows	r.u.		fl	4 byte(s)
24	off_var_vmr4 Instrument offset variance data. Elements of diagonal of variance/covariance matrix	(r.u.)2		fl	4 byte(s)
25	def_mw_vmr4 Definition of VMR #4 retrieval microwindows in which offset values are fitted	ascii	1	AsciiString	1 byte(s)
26	indecies_vmr4 Indices of tangent height for which continuum absorption coefficients are fitted. [indexmin(V(i)), indexmax(V(i))]If no continuum is fitted, set to -1	-		us	2 byte(s)
27	cont_alt_vmr4 VMR #4 continuum values fitted in different spectral intervals for each altitude index	-		cont_alt_vmr4Struct	13.0 byte(s)

a	def_mw Definition of VMR retrieval microwindows. Used at altitude #indexCon(V(1)). row relating to this altitude of matrix for VMR retrieval in corresponding Scan Info ADS	ascii	1	AsciiString	1 byte(s)
b	type_mw Types of grouping for above MWs used at altitude #indexCon(V(i))	-		ss	2 byte(s)
c	fitted_cont Fitted continuum values at altitude #indexCon(V(i))	(1e-30) cm2/molec		fl	4 byte(s)
d	fitted_cont_var Variance data of continuums fitted at altitude #indexCon(V(i))	(1e-60) cm4/molec2		fl	4 byte(s)
e	fitted_cont_cov Covariance data of fitted continuums and retrieved VMR profile point at altitude #indexCon(V(i))	(1e-30) ppm*cm2/molec		fl	4 byte(s)

28	fitted_off_vmr5 Fitted instrument offset in VMR #5 retrieval microwindows	r.u.		fl	4 byte(s)

#	Description	Units	Count	Type	Size
29	off_var_vmr5 Instrument offset variance data. Elements of diagonal of variance/covariance matrix	(r.u.)2		fl	4 byte(s)
30	def_mw_vmr5 Definition of VMR #5 retrieval microwindows in which offset values are fitted	ascii	1	AsciiString	1 byte(s)
31	indecies_vmr5 Indices of tangent height for which continuum absorption coefficients are fitted. [indexmin(V(i)), indexmax(V(i))]If no continuum is fitted, set to -1	-		us	2 byte(s)
32	cont_alt_vmr5 VMR #5 continuum values fitted in different spectral intervals for each altitude index	-		cont_alt_vmr5Struct	13.0 byte(s)

a	def_mw Definition of VMR retrieval microwindows. Used at altitude #indexCon(V(1)). row relating to this altitude of matrix for VMR retrieval in corresponding Scan Info ADS	ascii	1	AsciiString	1 byte(s)
b	type_mw Types of grouping for above MWs used at altitude #indexCon(V(i))	-		ss	2 byte(s)
c	fitted_cont Fitted continuum values at altitude #indexCon(V(i))	(1e-30) cm2/molec		fl	4 byte(s)
d	fitted_cont_var Variance data of continuums fitted at altitude #indexCon(V(i))	(1e-60) cm4/molec2		fl	4 byte(s)
e	fitted_cont_cov Covariance data of fitted continuums and retrieved VMR profile point at altitude #indexCon(V(i))	(1e-30) ppm*cm2/molec		fl	4 byte(s)

33	fitted_off_vmr6 Fitted instrument offset in VMR #6 retrieval microwindows	r.u.		fl	4 byte(s)
34	off_var_vmr6 Instrument offset variance data. Elements of diagonal of variance/covariance matrix	(r.u.)2		fl	4 byte(s)
35	def_mw_vmr6 Definition of VMR #6 retrieval microwindows in which offset values are fitted	ascii	1	AsciiString	1 byte(s)
36	indecies_vmr6 Indices of tangent height for which continuum absorption coefficients are fitted. [indexmin(V(i)), indexmax(V(i))]If no continuum is fitted, set to -1	-		us	2 byte(s)
37	cont_alt_vmr6 VMR #6 continuum values fitted in different spectral intervals for each altitude index	-		cont_alt_vmr6Struct	13.0 byte(s)

a	def_mw Definition of VMR retrieval microwindows. Used at altitude #indexCon(V(1)). row relating to this altitude of matrix for VMR retrieval in corresponding Scan Info ADS	ascii	1	AsciiString	1 byte(s)
b	type_mw Types of grouping for above MWs used at altitude #indexCon(V(i))	-		ss	2 byte(s)
c	fitted_cont Fitted continuum values at altitude #indexCon(V(i))	(1e-30) cm2/molec		fl	4 byte(s)
d	fitted_cont_var Variance data of continuums fitted at altitude #indexCon(V(i))	(1e-60) cm4/molec2		fl	4 byte(s)
e	fitted_cont_cov Covariance data of fitted continuums and retrieved VMR profile point at altitude #indexCon(V(i))	(1e-30) ppm*cm2/molec		fl	4 byte(s)

#	Description	Units	Count	Type	Size
38	spare_1 Spare	-	1	SpareField	47 byte(s)

Record Length : 80

DS_NAME : Continuum Contribution and Radiance Offset MDS

Format Version 114.0

6.5.48 P T and Height Correction Profiles MDS

Table 6.71 P T and Height Correction Profiles MDS

P, T, and Height Correction Profiles MDS

#	Description	Units	Count	Type	Size
Data Record					
0	dsr_time Time of DSR ZPD time of sweep closest to scans mean time	MJD	1	mjd	12 byte(s)
1	dsr_length Length of this DSR in bytes	bytes	1	ul	4 byte(s)
2	quality_flag Quality indicator (set to -1 if retrieval failed. Set to 0 otherwise.)	flag	1	BooleanFlag	1 byte(s)
3	conv_id ID of convergence condition terminating the iteration : 0=maximum number of micro-iterations exceeded ; 1=maximum number of macro-iterations exceeded ; 2=convergence reached ; 3=maximum run-time exceeded ; 4=retrieval failed	-	1	us	2 byte(s)
4	last_chi2 Last chi2 test value	-	1	fl	4 byte(s)
5	ig_flag Flag indicating source of used initial guess data : I = Initial guess from pre-stored profiles in MIP_IG2_AX ; M = Intial guess derived from meteorological preprocessor using AUX_ECF_AX or AUX_ECA_AX ; P = Initial guess derived using pre-stored forward calculation results (only p,T retrieval) in MIP_FM2_AX ; S = Initial guess taken from results of the processing of the previous scan ; Blank spece = retrieval failed	flag	1	BooleanFlag	1 byte(s)
6	tan_press Tangent pressure of ith LOS tangent altitude. (i = 1, ..., Npt)Ordered from highest to lowest altitude	hPa		fl	4 byte(s)
7	tan_press_var_cov Tangent pressure variance / covariance dataElements of diagonal and off-diagonal elements of var./cov. matrix	hPa2		fl	4 byte(s)
8	h_corr Height increment correction (dz) for ith LOS tangent altitude. (i = 1, ..., (Npt - 1). If Npt<=0, the byte length of the array is zero.	m		fl	4 byte(s)
9	h_corr_var_cov Height correction variance / covariance data. Elements of diagonal and off-diagonal elements of var./cov. matrix. The matrix contains Npt*(Npt-1)/2 items. If Npt<=0, the byte length of the array is zero.	m2		fl	4 byte(s)
10	temp	K		fl	4 byte(s)

#	Description	Units	Count	Type	Size
	Temperature of ith grid point. (i = 1, ..., Npt)				
11	temp_var_cov Temperature profile variance / covariance data. Elements of diagonal and off-diagonal elements of var./cov. matrix	K2		fl	4 byte(s)
12	pres_temp_var_cov Tangent pressure / temperature profile covariance data. Elements ptan-T profile covariance matrix. The value will be set to -10e30 for sweeps where pressure is not fitted	hPa*K		fl	4 byte(s)
13	spare_1 Spare	-	1	SpareField	56 byte(s)

Record Length : 52

DS_NAME : P, T, and Height Correction Profiles MDS

Format Version 114.0

6.5.49 H2O Target Species MDS

Table 6.72 H2O Target Species MDS

H2O Target Species MDS

#	Description	Units	Count	Type	Size
Data Record					
0	dsr_time Time of DSRZPD time of sweep closest to scans mean time.	MJD	1	mjd	12 byte(s)
1	dsr_length Length of this DSR in bytes	bytes	1	ul	4 byte(s)
2	quality_flag Quality indicator(set to -1 if all retrieval failed. Set to 0 otherwise.)	flag	1	BooleanFlag	1 byte(s)
3	conv_id ID of convergence condition terminating the iteration : 0=maximum number of micro-iterations exceeded ; 1=maximum number of macro-iterations exceeded ; 2=convergence reached ; 3=maximum run-time exceeded ; 4=retrieval failed	-	1	us	2 byte(s)
4	last_chi2 Last chi2 test value	-	1	fl	4 byte(s)
5	ig_flag Flag indicating source of used initial guess data : I = Initial guess from pre-stored profiles in MIP_IG2_AX ; M = Intial guess derived from meteorological preprocessor using AUX_ECF_AX or AUX_ECA_AX ; P = Initial guess derived using pre-stored forward calculation results (only p,T retrieval) in MIP_FM2_AX ; S = Initial guess taken from results of the processing of the previous scan ; Blank spece = retrieval failed	flag	1	BooleanFlag	1 byte(s)
6	vmr VMR of ith LOS tangent altitude. VMR1(i)(i = 1, ..., NV(1))	ppm		fl	4 byte(s)
7	vmr_var_cov VMR profile variance / covariance data. Elements of diagonal and off-diagonal elements of var./cov. matrix	ppm2		fl	4 byte(s)
8	conc_alt	cm-3		fl	4 byte(s)

#	Description	Units	Count	Type	Size
	Concentration of ith LOS tangent altitude, [r1 (i)] (i = 1, ..., NV(1))				
9	conc_var_cov Concentration profile variance / covariance data. Elements of diagonal and off-diagonal elements of var./cov. matrix	(cm-3)2		db	8 byte(s)
10	vert_col Vertical column density of ith LOS tangent altitude, h1 (i) (i = 1, ..., NV(1))	cm-2		fl	4 byte(s)
11	vert_col_var_cov Vertical column density profile variance / covariance dataElements of diagonal and off-diagonal elements of var./cov. matrix	(cm-2)2		db	8 byte(s)
12	error_p_t_prop_flag Flag indicating used approach for p,T error propagation	flag	1	BooleanFlag	1 byte(s)
13	error_p_t_vcm p,T error VCM	-		fl	4 byte(s)
14	spare_1 Spare	-	1	SpareField	39 byte(s)

Record Length : 28

DS_NAME : H2O Target Species MDS

Format Version 114.0

6.5.50 Level 2 product SPH

Table 6.73 Level 2 product SPH

Level 2 product SPH

#	Description	Units	Count	Type	Size
Data Record					
0	sph_descriptor_title SPH_DESCRIPTOR=	keyword	1	AsciiString	15 byte(s)
1	quote_1 quotation mark (""")	ascii	1	AsciiString	1 byte(s)
2	sph_descriptor SPH descriptorASCII string describing the product.	ascii	1	AsciiString	28 byte(s)
3	quote_2 quotation mark (""")	ascii	1	AsciiString	1 byte(s)
4	newline_char_1 newline character	terminator	1	AsciiString	1 byte(s)
5	strip_cont_ind_title STRIPLINE_CONTINUITY_INDICATOR=	keyword	1	AsciiString	31 byte(s)
6	stripline_continuity_indicator Value: +000= No stripline continuity, the product is a complete segment Other: Stripline Counter	-	1	Ac	4 byte(s)
7	newline_char_2 newline character	terminator	1	AsciiString	1 byte(s)

#	Description	Units	Count	Type	Size
8	slice_pos_title SLICE_POSITION=	keyword	1	AsciiString	15 byte(s)
9	slice_position Value: +001 to NUM_SLICESDefault value if no stripline continuity = +001	-	1	Ac	4 byte(s)
10	newline_char_3 newline character	terminator	1	AsciiString	1 byte(s)
11	num_slice_title NUM_SLICES=	keyword	1	AsciiString	11 byte(s)
12	num_slices Number of slices in this striplineDefault value if no continuity = +001	-	1	Ac	4 byte(s)
13	newline_char_4 newline character	terminator	1	AsciiString	1 byte(s)
14	start_time_title START_TIME=	keyword	1	AsciiString	11 byte(s)
15	quote_3 quotation mark (""")	ascii	1	AsciiString	1 byte(s)
16	start_time ZPD time of first MDSR of the first scan in the product. UTC time format	UTC	1	UtcExternal	27 byte(s)
17	quote_4 quotation mark (""")	ascii	1	AsciiString	1 byte(s)
18	newline_char_5 newline character	terminator	1	AsciiString	1 byte(s)
19	stop_time_title STOP_TIME=	keyword	1	AsciiString	10 byte(s)
20	quote_5 quotation mark (""")	ascii	1	AsciiString	1 byte(s)
21	stop_time ZPD time of last MDSR of the last scan in the product.UTC time format	UTC	1	UtcExternal	27 byte(s)
22	quote_6 quotation mark (""")	ascii	1	AsciiString	1 byte(s)
23	newline_char_6 newline character	terminator	1	AsciiString	1 byte(s)
24	first_lat_title FIRST_TANGENT_LAT=	keyword	1	AsciiString	18 byte(s)
25	first_tangent_lat Latitude of LOS tangent point at center of scan (refraction corrected) of the first scan in the product. Positive north.	(1e-6) degrees	1	AsciiGeoCoordinate	11 byte(s)
26	first_lat_units <10-6degN>	units	1	AsciiString	10 byte(s)
27	newline_char_7 newline character	terminator	1	AsciiString	1 byte(s)
28	first_long_title FIRST_TANGENT_LONG=	keyword	1	AsciiString	19 byte(s)
29	first_tangent_long Longitude of LOS tangent point at center of scan (refraction corrected) of the first scan in the product. Positive north.	(1e-6) degrees	1	AsciiGeoCoordinate	11 byte(s)
30	first_long_units <10-6degE>	units	1	AsciiString	10 byte(s)
31	newline_char_8 newline character	terminator	1	AsciiString	1 byte(s)
32	last_lat_title LAST_TANGENT_LAT=	keyword	1	AsciiString	17 byte(s)
33	last_tangent_lat Latitude of LOS tangent point at center of scan (refraction corrected) of the last scan in the product. Positive East.	(1e-6) degrees	1	AsciiGeoCoordinate	11 byte(s)
34	last_lat_units <10-6degN>	units	1	AsciiString	10 byte(s)
35	newline_char_9 newline character	terminator	1	AsciiString	1 byte(s)
36	last_long_title LAST_TANGENT_LONG=	keyword	1	AsciiString	18 byte(s)
37	last_tangent_long Longitude of LOS tangent point at center of scan (refraction corrected) of the last scan in the product. Positive East.	(1e-6) degrees	1	AsciiGeoCoordinate	11 byte(s)
38	last_long_units <10-6degE>	units	1	AsciiString	10 byte(s)
39	newline_char_10 newline character	terminator	1	AsciiString	1 byte(s)
40	spare_1 Spare	-	1	SpareField	49 byte(s)
41	num_scans_title	keyword	1	AsciiString	10 byte(s)

#	Description	Units	Count	Type	Size
	NUM_SCANS=				
42	num_scans No. of acquired elevation scans in Level 1 B input file	-	1	As	6 byte(s)
43	newline_char_2 newline character	terminator	1	AsciiString	1 byte(s)
44	num_los_title NUM_LOS_GEOMS=	keyword	1	AsciiString	14 byte(s)
45	num_los_geoms Number of LOS geometries per elev. scan in nominal mode [Nacq]	-	1	As	6 byte(s)
46	newline_char_3 newline character	terminator	1	AsciiString	1 byte(s)
47	num_scans_ds_title NUM_SCANS_PER_DS=	keyword	1	AsciiString	17 byte(s)
48	num_scans_per_ds Number of elevation scans per D.S. calibration cycle in nominal mode	-	1	As	6 byte(s)
49	newline_char_4 newline character	terminator	1	AsciiString	1 byte(s)
50	num_scans_proc_title NUM_SCANS_PROC=	keyword	1	AsciiString	15 byte(s)
51	num_scans_proc No. of elevation scans in nominal mode processed	-	1	As	6 byte(s)
52	newline_char_5 newline character	terminator	1	AsciiString	1 byte(s)
53	num_sp_not_title NUM_SP_NOT_PROC=	keyword	1	AsciiString	16 byte(s)
54	num_sp_not_proc No. of elevation scans in special events mode not processed	-	1	As	6 byte(s)
55	newline_char_6 newline character	terminator	1	AsciiString	1 byte(s)
56	num_spec_title NUM_SPECTRA=	keyword	1	AsciiString	12 byte(s)
57	num_spectra No. of scene spectra in measurement interval	-	1	As	6 byte(s)
58	newline_char_7 newline character	terminator	1	AsciiString	1 byte(s)
59	num_spec_proc_title NUM_SPECTR_PROC=	keyword	1	AsciiString	16 byte(s)
60	num_spectr_proc No. of scene spectra processed	-	1	As	6 byte(s)
61	newline_char_8 newline character	terminator	1	AsciiString	1 byte(s)
62	num_gain_title NUM_GAIN_CAL=	keyword	1	AsciiString	13 byte(s)
63	num_gain_cal No. of gain calibration cycles in measurement time interval. This value will be 0 if no Gain Calibration ADSRs appeared in the input Level-1B product and 1 otherwise	-	1	As	6 byte(s)
64	newline_char_9 newline character	terminator	1	AsciiString	1 byte(s)
65	tot_gran_title TOT_GRANULES=	keyword	1	AsciiString	13 byte(s)
66	tot_granules Total number of elevation scans (?granules?) processed [Nscan]	-	1	As	6 byte(s)
67	newline_char_10 newline character	terminator	1	AsciiString	1 byte(s)
68	max_path_diff_title MAX_PATH_DIFF=	keyword	1	AsciiString	14 byte(s)
69	max_path_diff Maximum path difference in nominal scene measurements	cm	1	Afl	15 byte(s)
70	max_path_diff_units <cm>	units	1	AsciiString	4 byte(s)
71	newline_char_11 newline character	terminator	1	AsciiString	1 byte(s)
72	order_title ORDER_OF_SPECIES=	keyword	1	AsciiString	17 byte(s)
73	order_quote_1 quotation mark(""")	ascii	1	AsciiString	1 byte(s)
74	order_of_species String describing the sequence of species within this product. Example: H2O,N2O,HNO3,CH4,O3 unused characters set to blank. String is left justified.	ascii	1	AsciiString	30 byte(s)
75	order_quote_2	ascii	1	AsciiString	1 byte(s)

#	Description	Units	Count	Type	Size
	quotation mark(""")				
76	order_newline_char newline character	terminator	1	AsciiString	1 byte(s)
77	num_sweeps_per_scan_title NUM_SWEEPS_PER_SCAN=	keyword	1	AsciiString	20 byte(s)
78	num_sweeps_per_scan Number of sweeps per nominal elevation scan	-	1	As	6 byte(s)
79	newline_char_11a newline character	terminator	1	AsciiString	1 byte(s)
80	spare_2 Spare	-	1	SpareField	21 byte(s)
81	dsd_spare DSD Spare (279 blank space character followed by 1 newline character)	-	1	dsd_sp	0 byte(s)

Record Length : 729

DS_NAME : Level 2 product SPH

Format Version 114.0

6.5.51 Scan information MDS

Table 6.74 Scan information MDS

Scan information MDS

#	Description	Units	Count	Type	Size
	Data Record				
0	dsr_time Time of DSR. ZPD time of sweep closest to scans mean time, s.	MJD	1	mjd	12 byte(s)
1	dsr_length DSR length	-	1	ul	4 byte(s)
2	quality_flag Quality indicator (PCD).	flag	1	BooleanFlag	1 byte(s)
3	zpd_crossing_time ZPD crossing time of ith scene spectrun in elevation scan (i = 1, ..., Nsw)	MJD		mjd	12 byte(s)
4	geolocation_los_tangent Geolocation (lat./long.) of ith scene LOS tangent point (i = 1, ..., Nsw)	-		geolocation_los_tangentStruct	-8.0 byte(s)
	a: lat Latitude	(1e-6) degrees	1	GeoCoordinate	4 byte(s)
	b: lon Longitude	(1e-6) degrees	1	GeoCoordinate	4 byte(s)
5	tangent_altitude_los Tangent altitude of ith scene LOS tangent point (i = 1, ..., Nsw)	km		db	8 byte(s)

#	Description	Units	Count	Type	Size
6	appl_process_id Application process ID	-	1	us	2 byte(s)
7	retrieval_p_t_flag Flag indicating successful p,T retrieval	flag	1	BooleanFlag	1 byte(s)
8	retrieval_vmr_flag Flag indicating successful VMR retrievals	flag	2	BooleanFlag	2*1 byte(s)
9	spare_1 Spare	-	1	SpareField	58 byte(s)
10	retrieval_p_t p, T retrievals.	-	1	retrieval_p_tStruct	-25.0 byte(s)

a	lrv_p_t_flag Logical retrieval vector for p,T retrieval (Nsw). Set to zero if N/A.	flag		BooleanFlag	1 byte(s)
b	pressure Retrieved pressure for each sweep. Set to NaN if N/A	hPa		fl	4 byte(s)
c	pressure_variance Pressure variance for each sweep. Set to NaN if N/A	hPa ^ 2		fl	4 byte(s)
d	tangent_altitude Corrected tangent altitudes of sweeps. Set to NaN if N/A	km		fl	4 byte(s)
e	height_cor_variance Height correction variance for each sweep. Set to NaN if N/A	m ^ 2		fl	4 byte(s)
f	temp Retrieved temperatures for each sweep. Set to NaN if N/A	K		fl	4 byte(s)
g	temp_variance Temperature variance for each sweep. Set to NaN if N/A	K ^ 2		fl	4 byte(s)

11	retrieval_vmr VMR retrievals for O3 and H20	-	2	retrieval_vmrStruc	2*-33.0 byte(s)

a	lrv_vmr_flag Logical retrieval vector for VMR retrieval (Nsw). Set to zero if N/A.	flag		BooleanFlag	1 byte(s)
b	vmr Retrieved VMR for each sweep. Set to NaN if N/A	ppm		fl	4 byte(s)
c	vmr_variance VMR variance for each sweep. Set to NaN if N/A	ppm ^ 2		fl	4 byte(s)
d	concentration Concentration for each sweep. Set to NaN if N/A	cm ^ -3		fl	4 byte(s)
e	concentration_variance Concentration variance for each sweep. Set to NaN if N/A	(cm ^ -3) ^ 2		db	8 byte(s)
f	vertical_col_density Vertical column density for each sweep. Set to NaN if N/A	cm ^ -2		fl	4 byte(s)
g	vcd_variance Vertical column density variance for each sweep. Set to NaN if N/A	(cm ^ -2) ^ 2		db	8 byte(s)

Record Length : N/A

DS_NAME : Scan information MDS

Format Version 114.0

6.5.52 Microwindows occupation matrices for p T and trace gas retrievals

Table 6.75 Microwindows occupation matrices for p T and trace gas retrievals

Microwindows occupation matrices for p, T and trace gas retrievals

#	Description	Units	Count	Type	Size
Data Record					
0	dsr_time Start time of validity of DSR. ZPD time of sweep closest to mean time of the corresponding scan	MJD	1	mjd	12 byte(s)
1	dsr_length Length of this DSR in bytes	bytes	1	ul	4 byte(s)
2	attach_flag Attachment flag. (Always set to zero for this ADS)	flag	1	BooleanFlag	1 byte(s)
3	mw_lab_pt Labels of p,T retrieval microwindows selected for sweep #i, i = 1,..., Nsw. Not used fields are blanked out.	-		mw_lab_ptStruct	-8.0 byte(s)
	a: label, Microwindow Label; ascii; 1; AsciiString; 8 byte(s)				
4	mw_lrv_pt Logical retrieval vector for p,T retrieval	-		uc	1 byte(s)
5	mw_lab_vmr1 Labels of species #1 VMR retrieval microwindows selected for sweep #i,i = 1,..., Nsw.	-		mw_lab_vmr1Struct	-8.0 byte(s)
	a: label, Microwindow Label; ascii; 1; AsciiString; 8 byte(s)				
6	mw_lrv_vmr1 Logical retrieval vector for species #1 VMR retrieval	-		uc	1 byte(s)
7	mw_lab_vmr2 Labels of species #2 VMR retrieval microwindows selected for sweep #i,i = 1,..., Nsw.	-		mw_lab_vmr2Struct	-8.0 byte(s)
	a: label, Microwindow Label; ascii; 1; AsciiString; 8 byte(s)				
8	mw_lrv_vmr2 Logical retrieval vector for species #2 VMR retrieval	-		uc	1 byte(s)
9	spare_1	-	1	SpareField	113 byte(s)

#	Description	Units	Count	Type	Size
	Spare				

Record Length : 103

DS_NAME : Microwindows occupation matrices for p, T and trace gas retrievals

Format Version 114.0

6.5.53 Instrument and Processing Parameters ADS

Table 6.76 Instrument and Processing Parameters ADS

Instrument and Processing Parameters ADS

#	Description	Units	Count	Type	Size
Data Record					
0	dsr_time Time of granule. ZPD time of sweep closest to mean time of corresponding scan	MJD	1	mjd	12 byte(s)
1	dsr_length Length of this DSR in bytes	bytes	1	ul	4 byte(s)
2	attach_flag Attachment flag. (Always set to zero for this ADS)	flag	1	BooleanFlag	1 byte(s)
3	elev_scans Vector of actual elevation scan angles	deg		fl	4 byte(s)
4	sg Retrieved profile switch. Switch indicating whether standard pressure grids (PT, PVMR(j), Pcont(pT), ,Pcont(V(j)) see below) are used to represent retrieved profile data [Sg]?S?: standard output grid?T?:tangent pressure grid. The switch will be set to T i	-	1	uc	1 byte(s)
5	pt Vector defining pressure levels at which temperature profile data are represented. PT (i), i = 1, ..., NT0if Sg set to ?T?,PT(i) = ptan (i)	hPa		fl	4 byte(s)
6	pv Vector defining pressure levels at which target species # j (j = 1, ..., 6) profile data are represented. PV(j) (i), i = 1, ..., NV(j)if Sg set to ?T?,PV(j)(i) = ptan (i)	hPa		fl	4 byte(s)
7	pcont_pt Vector defining pressure levels at which continuum data for p,T retrieval are represented. Pcont(pT) (i), i = 1, ..., Ncgrid(pT)if Sg set to ?T?,Pcont(pT)(i) = ptan(indexmin(pT) +i-1)	hPa		fl	4 byte(s)
8	pcont_vmr Vectors defining pressure levels at which continuum data for species #j (J + 1, ..., 6) VMR retrievals are represented. Pcont(V(j)) (i), i = 1, ..., Ncgrid(V(j))Ordering of species according to SPHif Sg set to ?T?,Pcont(V(j))(i) = ptan(indexmin(V(j)) +i-1	hPa		fl	4 byte(s)
9	max_macro_iter_pt Max. number of macro iterations of Newton / Marquardt algorithm for p,T retrieval	-	1	us	2 byte(s)
10	max_macro_iter_vmr Max. number of macro iterations of Newton / Marquardt algorithm for VMR retrievals Ordering of species according to SPH	-	2	us	2*2 byte(s)

#	Description	Units	Count	Type	Size
11	max_micro_iter_pt Max. number of micro iterations of Newton / Marquardt algorithm for p,T retrieval	-	1	us	2 byte(s)
12	max_micro_iter_vmr Max. number of micro iterations of Newton / Marquardt algorithm for VMR retrievals	-	2	us	2*2 byte(s)
13	spare_1 Spare	-	1	SpareField	80 byte(s)
14	spare_2 Spare	-	1	SpareField	82 byte(s)

Record Length : 172

DS_NAME : Instrument and Processing Parameters ADS

Format Version 114.0

6.5.54 Summary Quality ADS

Table 6.77 Summary Quality ADS

Summary Quality ADS

#	Description	Units	Count	Type	Size
Data Record					
0	dsr_time Time of DSR. ZPD time of sweep closest to first scans mean time.	MJD	1	mjd	12 byte(s)
1	attach_flag Attachment Flag. Set to 1 if all MDSRs corresponding to this ADSR are blank, set to zero otherwise.	flag	1	BooleanFlag	1 byte(s)
2	p_T_term_macro_micro Total no. of p, T retrievals terminated due to excess number of macro / micro iterations	-	2	us	2*2 byte(s)
3	vmr_term_macro_micro Total no. of VMR retrievals terminated due to due to excess number of macro / micro iterations	-	2*2	us	2*2*2 byte(s)
4	p_T_term_run_time Total no. of p,T retrievals terminated due to run time limitation	-	1	us	2 byte(s)
5	vmr_term_run_time Total no. of VMR retrievals terminated due to run time limitation. 1 value for each species	-	2	us	2*2 byte(s)
6	spare_1 Spare	-	1	SpareField	65 byte(s)

Record Length : 96

DS_NAME : Summary Quality ADS

Format Version 114.0

6.5.55 MIP_NLE_2P SPH

Table 6.78 MIP_NLE_2P SPH

MIP_NLE_2P SPH

#	Description	Units	Count	Type	Size
Data Record					
0	sph_descriptor_title SPH_DESCRIPTOR=	keyword	1	AsciiString	15 byte(s)
1	quote_1 quotation mark (""")	ascii	1	AsciiString	1 byte(s)
2	sph_descriptor SPH descriptorASCII string describing the product.	ascii	1	AsciiString	28 byte(s)
3	quote_2 quotation mark (""")	ascii	1	AsciiString	1 byte(s)
4	newline_char_1 newline character	terminator	1	AsciiString	1 byte(s)
5	strip_cont_ind_title STRIPLINE_CONTINUITY_INDICATOR=	keyword	1	AsciiString	31 byte(s)
6	stripline_continuity_indicator Value: +000= No stripline continuity, the product is a complete segment Other: Stripline Counter	-	1	Ac	4 byte(s)
7	newline_char_2 newline character	terminator	1	AsciiString	1 byte(s)
8	slice_pos_title SLICE_POSITION=	keyword	1	AsciiString	15 byte(s)
9	slice_position Value: +001 to NUM_SLICESDefault value if no stripline continuity = +001	-	1	Ac	4 byte(s)
10	newline_char_3 newline character	terminator	1	AsciiString	1 byte(s)
11	num_slice_title NUM_SLICES=	keyword	1	AsciiString	11 byte(s)
12	num_slices Number of slices in this striplineDefault value if no continuity = +001	-	1	Ac	4 byte(s)
13	newline_char_4 newline character	terminator	1	AsciiString	1 byte(s)
14	start_time_title START_TIME=	keyword	1	AsciiString	11 byte(s)
15	quote_3 quotation mark (""")	ascii	1	AsciiString	1 byte(s)
16	start_time ZPD time of first MDSR of the first scan in the product. UTC time format	UTC	1	UtcExternal	27 byte(s)
17	quote_4 quotation mark (""")	ascii	1	AsciiString	1 byte(s)

#	Description	Units	Count	Type	Size
18	newline_char_5 newline character	terminator	1	AsciiString	1 byte(s)
19	stop_time_title STOP_TIME=	keyword	1	AsciiString	10 byte(s)
20	quote_5 quotation mark (""")	ascii	1	AsciiString	1 byte(s)
21	stop_time ZPD time of last MDSR of the last scan in the product.UTC time format	UTC	1	UtcExternal	27 byte(s)
22	quote_6 quotation mark (""")	ascii	1	AsciiString	1 byte(s)
23	newline_char_6 newline character	terminator	1	AsciiString	1 byte(s)
24	first_lat_title FIRST_TANGENT_LAT=	keyword	1	AsciiString	18 byte(s)
25	first_tangent_lat Latitude of LOS tangent point at center of scan (refraction corrected) of the first scan in the product. Positive north.	(1e-6) degrees	1	AsciiGeoCoordinate	11 byte(s)
26	first_lat_units <10-6degN>	units	1	AsciiString	10 byte(s)
27	newline_char_7 newline character	terminator	1	AsciiString	1 byte(s)
28	first_long_title FIRST_TANGENT_LONG=	keyword	1	AsciiString	19 byte(s)
29	first_tangent_long Longitude of LOS tangent point at center of scan (refraction corrected) of the first scan in the product. Positive north.	(1e-6) degrees	1	AsciiGeoCoordinate	11 byte(s)
30	first_long_units <10-6degE>	units	1	AsciiString	10 byte(s)
31	newline_char_8 newline character	terminator	1	AsciiString	1 byte(s)
32	last_lat_title LAST_TANGENT_LAT=	keyword	1	AsciiString	17 byte(s)
33	last_tangent_lat Latitude of LOS tangent point at center of scan (refraction corrected) of the last scan in the product. Positive East.	(1e-6) degrees	1	AsciiGeoCoordinate	11 byte(s)
34	last_lat_units <10-6degN>	units	1	AsciiString	10 byte(s)
35	newline_char_9 newline character	terminator	1	AsciiString	1 byte(s)
36	last_long_title LAST_TANGENT_LONG=	keyword	1	AsciiString	18 byte(s)
37	last_tangent_long Longitude of LOS tangent point at center of scan (refraction corrected) of the last scan in the product. Positive East.	(1e-6) degrees	1	AsciiGeoCoordinate	11 byte(s)
38	last_long_units <10-6degE>	units	1	AsciiString	10 byte(s)
39	newline_char_10 newline character	terminator	1	AsciiString	1 byte(s)
40	spare_1 Spare	-	1	SpareField	49 byte(s)
41	num_scans_title NUM_SCANS=	keyword	1	AsciiString	10 byte(s)
42	num_scans No. of acquired elevation scans in Level 1 B input file	-	1	As	6 byte(s)
43	newline_char_2 newline character	terminator	1	AsciiString	1 byte(s)
44	num_los_title NUM_LOS_GEOMS=	keyword	1	AsciiString	14 byte(s)
45	num_los_geoms Number of LOS geometries per elev. scan in nominal mode [Nacq]	-	1	As	6 byte(s)
46	newline_char_3 newline character	terminator	1	AsciiString	1 byte(s)
47	num_scans_ds_title NUM_SCANS_PER_DS=	keyword	1	AsciiString	17 byte(s)
48	num_scans_per_ds Number of elevation scans per D.S. calibration cycle in nominal mode	-	1	As	6 byte(s)
49	newline_char_4 newline character	terminator	1	AsciiString	1 byte(s)
50	num_scans_proc_title NUM_SCANS_PROC=	keyword	1	AsciiString	15 byte(s)
51	num_scans_proc	-	1	As	6 byte(s)

#	Description	Units	Count	Type	Size
	No. of elevation scans in nominal mode processed				
52	newline_char_5 newline character	terminator	1	AsciiString	1 byte(s)
53	num_sp_not_title NUM_SP_NOT_PROC=	keyword	1	AsciiString	16 byte(s)
54	num_sp_not_proc No. of elevation scans in special events mode not processed	-	1	As	6 byte(s)
55	newline_char_6 newline character	terminator	1	AsciiString	1 byte(s)
56	num_spec_title NUM_SPECTRA=	keyword	1	AsciiString	12 byte(s)
57	num_spectra No. of scene spectra in measurement interval	-	1	As	6 byte(s)
58	newline_char_7 newline character	terminator	1	AsciiString	1 byte(s)
59	num_spec_proc_title NUM_SPECTR_PROC=	keyword	1	AsciiString	16 byte(s)
60	num_spectr_proc No. of scene spectra processed	-	1	As	6 byte(s)
61	newline_char_8 newline character	terminator	1	AsciiString	1 byte(s)
62	num_gain_title NUM_GAIN_CAL=	keyword	1	AsciiString	13 byte(s)
63	num_gain_cal No. of gain calibration cycles in measurement time interval. This value will be 0 if no Gain Calibration ADSRs appeared in the input Level-1B product and 1 otherwise	-	1	As	6 byte(s)
64	newline_char_9 newline character	terminator	1	AsciiString	1 byte(s)
65	tot_gran_title TOT_GRANULES=	keyword	1	AsciiString	13 byte(s)
66	tot_granules Total number of elevation scans (?granules?) processed [Nscan]	-	1	As	6 byte(s)
67	newline_char_10 newline character	terminator	1	AsciiString	1 byte(s)
68	max_path_diff_title MAX_PATH_DIFF=	keyword	1	AsciiString	14 byte(s)
69	max_path_diff Maximum path difference in nominal scene measurements	cm	1	Afl	15 byte(s)
70	max_path_diff_units <cm>	units	1	AsciiString	4 byte(s)
71	newline_char_11 newline character	terminator	1	AsciiString	1 byte(s)
72	order_title ORDER_OF_SPECIES=	keyword	1	AsciiString	17 byte(s)
73	order_quote_1 quotation mark(""")	ascii	1	AsciiString	1 byte(s)
74	order_of_species String describing the sequence of species within this product. Example: H2O,N2O,HNO3,CH4,O3 unused characters set to blank. String is left justified.	ascii	1	AsciiString	30 byte(s)
75	order_quote_2 quotation mark(""")	ascii	1	AsciiString	1 byte(s)
76	order_newline_char newline character	terminator	1	AsciiString	1 byte(s)
77	num_sweeps_per_scan_title NUM_SWEEPS_PER_SCAN=	keyword	1	AsciiString	20 byte(s)
78	num_sweeps_per_scan Number of sweeps per nominal elevation scan	-	1	As	6 byte(s)
79	newline_char_11a newline character	terminator	1	AsciiString	1 byte(s)
80	spare_2 Spare	-	1	SpareField	21 byte(s)
81	dsd_spare DSD Spare (279 blank space character followed by 1 newline character)	-	1	dsd_sp	0 byte(s)

Record Length : 729

DS_NAME : MIP_NLE_2P SPH

Format Version 114.0

6.5.56 P T occupation matrices ADS

Table 6.79 P T occupation matrices ADS

VMR #6 occupation matrices ADS

#	Description	Units	Count	Type	Size
Data Record					
0	dsr_time Time of creation	MJD	1	mjd	12 byte(s)
1	dsr_length DSR length	-	1	ul	4 byte(s)
2	attach_flag Attachment flag (Always set to zero for this ADS)	flag	1	BooleanFlag	1 byte(s)
3	lab_occ_matrix Label for occupation matrix	-	1	lab_occ_matrixStruct	10.0 byte(s)
	a: label, Matrix Label; ascii; 1; AsciiString; 10 byte(s)				
4	num_rows_current_occ_matrix Number of rows of current occupation matrix	-	1	us	2 byte(s)
5	band_occ Band occupation matrix for current occupation matrix	-		us	2 byte(s)
6	vect_bands Vector containing valid ranges for each row of occupation matrix	km		fl	4 byte(s)
7	log_retr_vector Logical retrieval vector indicating sweeps where parameters shall be fitted	-		us	2 byte(s)
8	dsr_offset_mds1 Offset of DSR within data set containing occupation matrix data	-	1	ul	4 byte(s)

Record Length : 25

DS_NAME : VMR #6 occupation matrices ADS

Format Version 114.0

6.5.57 Priority of p T retrieval occupation matices

Table 6.80 Priority of p T retrieval occupation matices

Priority of VMR#6 retrieval occupation matices

#	Description	Units	Count	Type	Size
Data Record					
0	dsr_time Time of creation	MJD	1	mjd	12 byte(s)
1	dsr_length DSR length	-	1	ul	4 byte(s)
2	attach_flag Attachment flag	flag	1	BooleanFlag	1 byte(s)
3	num_occ_matrices Number of occupation matrices with Nsw(1) rows valid for latitude#1	-	1	us	2 byte(s)
4	labs_occ_matrices Labels of occupation matrices with Nsw(1) rows valid for latitude#1	-		labs_occ_matricesStruct	-10.0 byte(s)
	a: label Matrix Label; ascii; 1; AsciiString; 10 byte(s)				
5	dsr_offsets_ads8 Offsets of DRSs within occumpation matrix ADS containing annotation data for above occupation matrices	-		ul	4 byte(s)

Record Length : 5

DS_NAME : Priority of VMR#6 retrieval occupation matices

Format Version 114.0

6.5.58 General GADS

Table 6.81 General GADS

General GADS

#	Description	Units	Count	Type	Size
Data Record					
0	dsr_time Time of creation	MJD	1	mjd	12 byte(s)
1	num_lat_bands Number of latitude bands for which data is contained [Nlat]	-	1	us	2 byte(s)
2	lat_bands Vector of latitude bands	deg		fl	4 byte(s)
3	num_spectral_bands Number of spectral bands	-	1	us	2 byte(s)
4	spect_bands_used_mw Spectral bands in which used microwindows are located	cm-1		fl	4 byte(s)
5	ref_tropo_height Reference tropopause height for contained altitude data	km	1	fl	4 byte(s)
6	num_diff_nums_sweeps Number of different numbers of sweeps for which occupation matrices are contained	-	1	us	2 byte(s)
7	num_sweeps_occ_matrices Numbers of sweeps for which occupation matrices are contained	-		us	2 byte(s)
8	dsr_offsets_p_t_retr Offsets of DSRs within p, T piority ADS defining priority of p,T retrieval occupation matrices with Nsw(1) rows valid for latitude band #i, i = 1, ..., Nlat	-		ul	4 byte(s)
9	dsr_offsets_vmr1_retr Offsets of DSRs within VMR#1 priority ADS defining priority of species#1 VMR retrieval occupation matrices with Nsw(1) rows valid for latitude band #i, i = 1, ..., Nlat	-		ul	4 byte(s)
10	dsr_offsets_vmr2_retr Offsets of DSRs within VMR#2 priority ADS defining priority of species#2 VMR retrieval occupation matrices with Nsw(1) rows valid for latitude band #i, i = 1, ..., Nlat	-		ul	4 byte(s)
11	dsr_offsets_vmr3_retr Offsets of DSRs within VMR#3 priority ADS defining priority of species#3 VMR retrieval occupation matrices with Nsw(1) rows valid for latitude band #i, i = 1, ..., Nlat	-		ul	4 byte(s)
12	dsr_offsets_vmr4_retr Offsets of DSRs within VMR#4 priority ADS defining priority of species#4 VMR retrieval occupation matrices with Nsw(1) rows valid for latitude band #i, i = 1, ..., Nlat	-		ul	4 byte(s)
13	dsr_offsets_vmr5_retr Offsets of DSRs within VMR#5 priority ADS defining priority of species#5 VMR retrieval occupation matrices with Nsw(1) rows valid for latitude band #i, i = 1, ..., Nlat	-		ul	4 byte(s)
14	dsr_offsets_vmr6_retr Offsets of DSRs within VMR#6 priority ADS defining priority of species#6 VMR retrieval occupation matrices with Nsw(1) rows valid for latitude band #i, i = 1, ..., Nlat	-		ul	4 byte(s)

Record Length : N/A

DS_NAME : General GADS

Format Version 114.0

6.5.59 Occupation matrices for p T retrieval MDS

Table 6.82 Occupation matrices for p T retrieval MDS

Occupation matrices for p,T retrieval MDS

#	Description	Units	Count	Type	Size
Data Record					
0	dsr_time Time of creation	MJD	1	mjd	12 byte(s)
1	dsr_length DSR length	-	1	ul	4 byte(s)
2	quality_flag Quality indicator (PCD)	flag	1	BooleanFlag	1 byte(s)
3	occ_label Label for occupation matrix	-	1	occ_labelStruct	10.0 byte(s)
	a: label, Matrix Label; ascii; 1; AsciiString; 10 byte(s)				
4	num_sweeps Number of sweeps. (rows of occupation matrix)	-	1	us	2 byte(s)
5	num_mw Number of microwindows. (columns of occupation matrix)	-	1	us	2 byte(s)
6	labs_mw Labels of microwindows	-		labs_mwStruct	-8.0 byte(s)
	a: label, Microwindow Label; ascii; 1; AsciiString; 8 byte(s)				
7	occ occupation matrix	-		us	2 byte(s)

Record Length : 21

DS_NAME : Occupation matrices for p,T retrieval MDS

Format Version 114.0

6.5.60 Occupation matrices for vmr#1 retrieval MDS

Table 6.83 Occupation matrices for vmr#1 retrieval MDS

Occupation matrices for vmr#6 retrieval MDS

#	Description	Units	Count	Type	Size
Data Record					
0	dsr_time Time of creation	MJD	1	mjd	12 byte(s)
1	dsr_length DSR length	-	1	ul	4 byte(s)
2	quality_flag Quality indicator	flag	1	BooleanFlag	1 byte(s)
3	occ_label Label for occupation matrix	-	1	occ_labelStruct	10.0 byte(s)
	a: label, Matrix Label; ascii; 1; AsciiString; 10 byte(s)				
4	num_sweeps Number of sweeps. (rows of occupation matrix)	-	1	us	2 byte(s)
5	num_mw Number of microwindows. (columns of occupation matrix)	-	1	us	2 byte(s)
6	labs_mw Labels of microwindows	-		labs_mwStruct	-8.0 byte(s)
	a: label, Microwindow Label; ascii; 1; AsciiString; 8 byte(s)				
7	occ Occupation matrix	-		us	2 byte(s)
8	num_fitted_params Number of fitted parameters	-	1	us	2 byte(s)
9	ref_vmr_profile Reference VMR profile	ppm		fl	4 byte(s)
10	eo Matrix E0	-		fl	4 byte(s)
11	matrix_s_flag Flag for use of matrix S	flag	1	us	2 byte(s)
12	ref_press_profile Reference pressure profile	hPa		fl	4 byte(s)
13	ref_temp_profile Reference temperature profile	K		fl	4 byte(s)
14	s Matrix S	-		fl	4 byte(s)

Record Length : 5

DS_NAME : Occupation matrices for vmr#6 retrieval MDS

Format Version 114.0

6.5.61 General GADS

Table 6.84 General GADS

General GADS

#	Description	Units	Count	Type	Size
Data Record					
0	dsr_time Time of creation	MJD	1	mjd	12 byte(s)
1	num_mpd_ranges Number of MPD ranges for which data is contained	-	1	us	2 byte(s)
2	mpd_ranges MPD ranges for which matrices are contained	-		db	8 byte(s)
3	offsets Offset of DSR in MDS containing VCM for MPD range #i, i = 1, ..., Nmpd	-		sl	4 byte(s)

Record Length : 2

DS_NAME : General GADS

Format Version 114.0

6.5.62 Inverse LOS VCM matrices MDS

Table 6.85 Inverse LOS VCM matrices MDS

Inverse LOS VCM matrices MDS

#	Description	Units	Count	Type	Size
Data Record					
0	dsr_time Time of creation	MJD	1	mjd	12 byte(s)
1	dsr_length DSR length	-	1	ul	4 byte(s)
2	quality_flag	flag	1	BooleanFlag	1 byte(s)

#	Description	Units	Count	Type	Size
	Quality indicator (PCD)				
3	matrix_dimension Dimension of current matrix	-	1	us	2 byte(s)
4	vcm_matrix VCM matrix	-		db	8 byte(s)

Record Length : 11

DS_NAME : Inverse LOS VCM matrices MDS

Format Version 114.0

6.5.63 Processing Parameters GADS

Table 6.86 Processing Parameters GADS

1 MDSR per MDS

#	Description	Units	Count	Type	Size
Data Record					
0	dsr_time Start time (MJD)	MJD	1	mjd	12 byte(s)
1	quality_flag Quality indicator (PCD)"""""0""""" non-corrupted,"""""-1""""" = corrupted, default values filled in	flag	1	BooleanFlag	1 byte(s)
2	samp_time Sampling time (UTC)Last modification time of file section using UTC time format	UTC	1	UtcExternal	27 byte(s)
3	nom_laser_freq Nominal metrology laser wavenumber	cm-1	1	db	8 byte(s)
4	spare_1 Spare	-	1	SpareField	50 byte(s)
5	axis_time Axis time (UTC)Last modification time of file section using UTC time format	UTC	1	UtcExternal	27 byte(s)
6	num_points_per_band Number of points per band	-	5	ul	5*4 byte(s)
7	first_wavenum Wavenumber of first point in band	cm-1	5	db	5*8 byte(s)
8	last_wavenum Wavenumber of last point in band	cm-1	5	db	5*8 byte(s)
9	spare_2 Spare	-	1	SpareField	50 byte(s)
10	fce_time FCE time (UTC)Last modification time of file section using UTC time format	UTC	1	UtcExternal	27 byte(s)
11	spare_3 spare	-	1	SpareField	4 byte(s)
12	num_points	-	2	ul	2*4 byte(s)

#	Description	Units	Count	Type	Size
	Number of points around ZPD band AB and B				
13	spare_4 Spare	-	1	SpareField	50 byte(s)
14	nesr_time NESR time (UTC) Last modification time of NESR file section using UTC time format	UTC	1	UtcExternal	27 byte(s)
15	nesr_std_dev_thresh Standard deviation threshold	-	1	db	8 byte(s)
16	nesr_thresh_rej Threshold of rejection	%	1	db	8 byte(s)
17	nesr_reduc_factor Template reduction factor	-	1	us	2 byte(s)
18	spare_5 Spare	-	1	SpareField	50 byte(s)
19	rad_time Radiometric time (UTC)Last modification time of file section using UTC time format	UTC	1	UtcExternal	27 byte(s)
20	rad_std_dev_thresh Standard deviation threshold	-	1	db	8 byte(s)
21	rad_rej_thresh Threshold of rejection	%	1	db	8 byte(s)
22	rad_reduc_factor Template reduction factor	-	1	us	2 byte(s)
23	spare_6 Spare	-	1	SpareField	50 byte(s)
24	quality_time Quality time (UTC)Last modification time of file section using UTC time format	UTC	1	UtcExternal	27 byte(s)
25	qual_std_dev_thresh Standard deviation threshold	-	1	db	8 byte(s)
26	qual_rej_thresh Threshold of rejection	%	1	db	8 byte(s)
27	qual_reduc_factor Template reduction factor	-	1	us	2 byte(s)
28	spare_7 Spare	-	1	SpareField	50 byte(s)
29	spike_time Spike time (UTC)Last modification time of file section using UTC time format	UTC	1	UtcExternal	27 byte(s)
30	num_per_block Number of points per block	-	1	ul	4 byte(s)
31	spike_std_dev_thresh Standard deviation threshold	-	1	db	8 byte(s)
32	spare_8 Spare	-	1	SpareField	50 byte(s)
33	sinc_time Sinc time (UTC)Last modification time of file section using UTC time format	UTC	1	UtcExternal	27 byte(s)
34	sinc_num_rows Number of rows (N)	-	1	ul	4 byte(s)
35	sinc_num_cols Number of columns (J)	-	1	ul	4 byte(s)
36	sinc_coef Interpolation coefficients (N*J doubles)	-		db	8 byte(s)
37	spare_9 Spare	-	1	SpareField	50 byte(s)
38	spec_time Spectral time (UTC) Last modification time of spectrqal calibration section using UTC time format	UTC	1	UtcExternal	27 byte(s)
39	spec_asc_node_time Time since ascending node crossing from which the search for the first valid scene data shall start, in seconds	s	1	db	8 byte(s)
40	spec_update_period Update period	#of nominal scans	1	us	2 byte(s)
41	spec_tan_ht_intv Tangent height interval within which scene data shall be extracted	km	2	fl	2*4 byte(s)
42	spec_scene_coadd Number of scenes to be co-added	-	1	us	2 byte(s)
43	spec_simplex_conv_tol Simplex convergence tolerance	-	1	db	8 byte(s)
44	spec_max_iter Maximum number of iterations	-	1	ul	4 byte(s)
45	spec_valid_thresh Validity threshold	-	1	db	8 byte(s)

#	Description	Units	Count	Type	Size
46	cal_method calibration Method (0=peak find, 1=cross correlation method)	-	1	uc	1 byte(s)
47	spare_10 Spare	-	1	SpareField	29 byte(s)
48	ils_time ILS time (UTC).Last modification time of file section using UTC time format	UTC	1	UtcExternal	27 byte(s)
49	ils_asc_node_time Time since ascending node crossing from which the search for the valid scene data shall start	s	1	db	8 byte(s)
50	ils_tan_ht_intv Tangent height interval within which scene data shall be extracted	km	2	fl	2*4 byte(s)
51	ils_max_scene_coadd Maximum number of scenes to be co-added	-	1	us	2 byte(s)
52	ils_max_subseq_scan Maximum number of subsequent scans from which scenes are to be extracted.	-	1	us	2 byte(s)
53	ils_simplex_conv_tol Simplex convergence tolerance	-	1	db	8 byte(s)
54	ils_max_iter Maximum number of iterations	-	1	ul	4 byte(s)
55	init_guess_para Initial guess parameters: height and offset	km	2	fl	2*4 byte(s)
56	max_opd Maximum optical path difference	cm	1	fl	4 byte(s)
57	shear_y Shear at ZPD along Y	cm	1	fl	4 byte(s)
58	shear_z Shear at ZPD along Z	cm	1	fl	4 byte(s)
59	mis_y Systematic IR misalignment along Y	rad	1	fl	4 byte(s)
60	mis_z Systematic IR misalignment along Z	rad	1	fl	4 byte(s)
61	interfer_div_y Interferometer divergence (total angle) along Y	rad	1	fl	4 byte(s)
62	interfer_div_z Interferometer divergence (total angle) along Z	rad	1	fl	4 byte(s)
63	laser_mis_y Systematic laser misalignment along Y	rad	1	fl	4 byte(s)
64	laser_mis_z Systematic laser misalignment along Z	rad	1	fl	4 byte(s)
65	num_subdiv_y Number of field of view subdivisions along Y	-	1	ul	4 byte(s)
66	num_subdiv_z Number of field of view subdivisions along Z	-	1	ul	4 byte(s)
67	spare_11 Spare	-	1	SpareField	4 byte(s)
68	blur_width_y Blur angular width along Y	rad	1	fl	4 byte(s)
69	blur_width_z Blur angular width along Z	rad	1	fl	4 byte(s)
70	nomi_opt_speed Nominal optical speed	cm/sec	1	fl	4 byte(s)
71	init_pert Sampling perturbation first sample	cm	1	fl	4 byte(s)
72	init_pert_time_const Time constant for attenuation of sampling perturbation	sec	1	fl	4 byte(s)
73	init_rel_speed_fluc Relative speed fluctuation on the first sample	-	1	fl	4 byte(s)
74	init_rel_speed_fluc_time_const Time constant for attenuation of speed fluctuation	sec	1	fl	4 byte(s)
75	gain_slope Slope of relative gain vs relative frequency	-	1	fl	4 byte(s)
76	mismatch_delay Delay mismatch between IR electrical response and ADC trigger signal	sec	1	fl	4 byte(s)
77	relative_drift Relative drift rate of laser wavenumber per second	sec-1	1	fl	4 byte(s)
78	noise_bw Laser bandwidth due to white frequency noise	Hz	1	fl	4 byte(s)
79	lin_shear_y Linear shear variation along Y	-	1	fl	4 byte(s)
80	lin_shear_z	-	1	fl	4 byte(s)

#	Description	Units	Count	Type	Size
	Linear shear variation along Z				
81	spare_12 Spare	-	1	SpareField	42 byte(s)
82	los_time LOS time (UTC) Last modification time of file section using UTC time format	UTC	1	UtcExternal	27 byte(s)
83	min_azi_angle_side Minimum azimuth angle in side observation geometry	-	1	db	8 byte(s)
84	max_azi_angle_side Maximum azimuth angle in side observation geometry	-	1	db	8 byte(s)
85	spare_13 Spare	-	1	SpareField	56 byte(s)
86	min_azi_angle_rear Minimum azimuth angle in rearward observation geometry	-	1	db	8 byte(s)
87	max_azi_angle_rear Maximum azimuth angle in rearward observation geometry	-	1	db	8 byte(s)
88	spare_14 Spare	-	1	SpareField	50 byte(s)
89	alt_orb_def Altitude and orbit control system defaults - pitch, roll, and yaw	deg	3	db	3*8 byte(s)
90	alt_orb_mis_angle Altitude and orbit control system mispointing angle - pitch, roll, and yaw	deg	3	db	3*8 byte(s)
91	alt_orb_mis_rate Altitude and orbit control system mispointing rate - pitch, roll, and yaw	deg/s	3	db	3*8 byte(s)
92	targ_mode TARGET mode	-	1	ss	2 byte(s)
93	targ_ray TARGET ray tracing mode switch	-	1	us	2 byte(s)
94	trag_ext TARGET extended results vector switch	-	1	us	2 byte(s)
95	spare_15 spare	-	1	SpareField	50 byte(s)

Record Length : 1414

DS_NAME : 1 MDSR per MDS

Format Version 114.0

6.5.64 Framework Parameters GADS

Table 6.87 Framework Parameters GADS

Framework Parameters GADS

#	Description	Units	Count	Type	Size
	Data Record				

#	Description	Units	Count	Type	Size
0	dsr_time Time of creation	MJD	1	mjd	12 byte(s)
1	spec_ev_switch Switch for processing of special events	-	1	uc	1 byte(s)
2	spare_1 Spare	-	1	SpareField	2 byte(s)
3	max_path_diff Maximum optical path difference	cm	1	db	8 byte(s)
4	ref_char Reference character to be compared with PCD	-	1	sc	1 byte(s)
5	spike_thresh Threshold of spike location wrt ZPD	-	1	ul	4 byte(s)
6	spike_thresh_rms Threshold for maximum rms amplitude of spikes	-	1	db	8 byte(s)
7	laser_wvn Wavenumber of laser	cm-1	1	db	8 byte(s)
8	spare_2 Spare	-	1	SpareField	4 byte(s)
9	num_fr_counts Number of fringe counts valid for nominal measurement at MPD	-	1	ul	4 byte(s)
10	num_nesr_thresh Number of NESR thresholds [NNESRth]	-	1	us	2 byte(s)
11	wvn_nesr_thresh1 Wavenumber related to the first NESR threshold	cm-1	1	db	8 byte(s)
12	wvn_nesr_thresh2 Wavenumber related to the last NESR threshold	cm-1	1	db	8 byte(s)
13	nesr_thresh Vector containing NESR thresholds	r.u.		db	8 byte(s)
14	max_mw Maximum number of MW?s used in retrieval	-	1	us	2 byte(s)
15	tropopause_height Height of tropopause at poles	km	1	db	8 byte(s)
16	tropopause_height_incr Increment of tropopause height	km	1	db	8 byte(s)
17	spare_3 Spare	-	1	SpareField	70 byte(s)
18	spec_res_coarse Spectral resolution of the general coarse wavenumber grid	cm-1	1	db	8 byte(s)
19	max_dev Maximum allowed deviation between input grid and general coarse wavenumber grid	cm-1	1	db	8 byte(s)
20	num_sinc Number of sinc interpolation coefficients	-	1	us	2 byte(s)
21	num_off Number of offsets used for interpolation	-	1	ss	2 byte(s)
22	num_coef Number of coefficients defining analytical Norton-Beer apodisation function [NCn]	-	1	us	2 byte(s)
23	coef Coefficients of analytical Norton-Beer apodisation function	-		db	8 byte(s)
24	num_wvn Number of wavenumbers at which the ILS has been characterised [NcILS]	-	1	us	2 byte(s)
25	wnm Vector containing wavenumbers at which the ILS has been characterised	cm-1		db	8 byte(s)
26	lin_shear Vector containing for each wavenumber the retroreflector linear shear along Z vs. OPD	cm		db	8 byte(s)
27	ir_misalign Vector containing for each wavenumber the systematic IR misalignment along Y	rad		db	8 byte(s)
28	spec_res_fine Spectral resolution of the general fine wavenumber grid	cm-1	1	db	8 byte(s)
29	req_spec_width Requested spectral width of the AILS in each spectral band	cm-1	1	db	8 byte(s)
30	min_res_ails Required minimum resolution of computed AILS	cm-1	1	db	8 byte(s)
31	min_res_opd Minimum resolution of sampling grid in OPD domain	cm	1	us	2 byte(s)
32	max_fft Maximum number of FFT samples to be used	-	1	us	2 byte(s)
33	min_div_mir Minimum divergence for which the modulation MIR is computed	deg	1	db	8 byte(s)

#	Description	Units	Count	Type	Size
34	spare_4 Spare	-	1	SpareField	8 byte(s)
35	z_ir_misalign Systematic IR misalignment along Z	rad	1	db	8 byte(s)
36	y_lin_shear Retroreflector linear shear along Y vs. OPD	cm	1	db	8 byte(s)
37	y_interfer_div Interferometer divergence along Y	rad	1	db	8 byte(s)
38	z_interfer_div Interferometer divergence along Z	rad	1	db	8 byte(s)
39	laser_misalign_opd_y Systematic OPD measuring laser misalignment along Y	rad	1	db	8 byte(s)
40	laser_misalign_opd_z Systematic OPD measuring laser misalignment along Z	rad	1	db	8 byte(s)
41	lin_shear_var_y Linear shear variation along Y	-	1	db	8 byte(s)
42	lin_shear_var_z Linear shear variation along Z	-	1	db	8 byte(s)
43	blur_ang_width_y Blur angular width along Y	rad	1	db	8 byte(s)
44	blur_ang_width_z Blur angular width along Z	rad	1	db	8 byte(s)
45	opt_speed_interfer Optical speed of interferometer	cm/s	1	db	8 byte(s)
46	init_perturb Initial perturbation on sampling of first sample	cm	1	db	8 byte(s)
47	time_const_init_perturb Time constant of exponential attenuation of initial sampling perturbation	double	1	db	8 byte(s)
48	rel_speed_fluc Initial relative speed fluctuation at the beginning of scan	-	1	db	8 byte(s)
49	time_const_speed_fluc Time constant of exponential attenuation of the initial speed fluctuation	s	1	db	8 byte(s)
50	gain_slope Gain slope of electrical response of IR detector and preamplifer	-	1	db	8 byte(s)
51	mismatch_delay Mismatch delay between IR electronics response and ADC trigger	s	1	db	8 byte(s)
52	rel_drift_rate Relative drift rate of laser wavenumber	cm-1	1	db	8 byte(s)
53	white_noise_bw Bandwidth of laser white noise	Hz	1	db	8 byte(s)
54	laser_noise_bw Bandwidth of laser 1/f noise	Hz	1	db	8 byte(s)
55	num_samples_y Number of discrete samples of integral approximation along Y	-	1	us	2 byte(s)
56	num_samples_z Number of discrete samples of integral approximation along Z	-	1	us	2 byte(s)
57	coeff_c Coefficient C used for ILS/AILS interpolation	-	1	db	8 byte(s)
58	coeff_b Coefficient B used for ILS/AILS interpolation	cm	1	db	8 byte(s)
59	coeff_a Coefficient A used for ILS/AILS interpolation	cm2	1	db	8 byte(s)
60	const_spec_corr Constant spectral correction coefficient of AILS	cm-1	1	db	8 byte(s)
61	lin_spec_corr Linear spectral correction coefficient of AILS	-	1	db	8 byte(s)
62	quad_spec_corr Quadratic spectral correction coefficient of AILS	cm	1	db	8 byte(s)
63	spare_5 Spare	-	1	SpareField	4 byte(s)
64	num_samples_apo Number of samples of apodisation vector in spectral domain	-	1	us	2 byte(s)
65	num_element_apo Number of elements of apodisation vector in OPD domain	-	1	us	2 byte(s)
66	spare_6 Spare	-	1	SpareField	10 byte(s)
67	thresh_ils Threshold for spectral grid error on which the ILS is computed	cm-1	1	db	8 byte(s)
68	lowest_apo Lowest value of apodisation vector	-	1	db	8 byte(s)

#	Description	Units	Count	Type	Size
69	thresh_ratio Threshold of ratio for which inversed squared apodisation function is computed	-	1	db	8 byte(s)
70	spare_7 Spare	-	1	SpareField	2 byte(s)
71	thresh_min_eigen Threshold defining minimum value of eigenvalue	-	1	db	8 byte(s)
72	max_spec_lines Maximum number of spectral lines per MW	-	1	us	2 byte(s)
73	seq_vmr_ret Sequence of processing of VMR retrievals each is a 4 character string	ascii	1	AsciiString	24 byte(s)
74	switch_p_t_retrieval Switch for skipping p,T retrieval	-	1	us	2 byte(s)
75	max_hitran_code Maximum HITRAN code to be considered	-	1	us	2 byte(s)
76	spare_8 Spare	-	1	SpareField	8 byte(s)
77	up_alt_thresh Upper altitude threshold for use of spectral lines	km	1	db	8 byte(s)
78	low_alt_thresh Lower altitude threshold for use of spectral lines	km	1	db	8 byte(s)
79	max_alt_step Maximum altitude step for hydrostatic equilibrium	km	1	db	8 byte(s)
80	spare_9 Spare	-	1	SpareField	40 byte(s)

Record Length : 552

DS_NAME : Framework Parameters GADS

Format Version 114.0

6.5.65 P t Retrieval GADS

Table 6.88 P t Retrieval GADS

P, t, Retrieval GADS

#	Description	Units	Count	Type	Size
Data Record					
0	dsr_time Time of creation	MJD	1	mjd	12 byte(s)
1	min_val_non_sing Minimum value used to check non-singularity of matrix	-	1	db	8 byte(s)
2	a_priori_switch Switch for usage of a priori pointing information	-	1	us	2 byte(s)
3	spare_1 Spare	-	1	SpareField	12 byte(s)

#	Description	Units	Count	Type	Size
4	max_elements Maximum number of elements in profiles	-	1	us	2 byte(s)
5	num_unsuccess Number of allowed unsuccessful previous retrievals	-	1	us	2 byte(s)
6	enh_spec_range Enhanced spectral range of MW?s used to decide whether a line inside the MW shall be considered as line or as nearby continuum	cm-1	1	db	8 byte(s)
7	max_samples_fine Maximum number of spectral samples on fine grid	-	1	us	2 byte(s)
8	chi2_thresh Threshold to check convergence of chi-square	-	1	db	8 byte(s)
9	thresh_fitted_press Threshold to check convergence of fitted pressure	-	1	db	8 byte(s)
10	thresh_fitted_temp Threshold to check convergence of fitted temperature	-	1	db	8 byte(s)
11	spare_2 Spare	-	1	SpareField	2 byte(s)
12	max_macro_iter_gauss Maximum number of Gauss-Newton macro-iterations	-	1	us	2 byte(s)
13	spare_3 Spare	-	1	SpareField	2 byte(s)
14	max_num_marq Maximum number of Marquardt micro-iterations	-	1	us	2 byte(s)
15	low_thresh_press Lower threshold of estimated pressure	hPa	1	db	8 byte(s)
16	up_thresh_press Upper threshold of estimated pressure	hPa	1	db	8 byte(s)
17	low_thresh_temp Lower threshold of estimated temperature	K	1	db	8 byte(s)
18	up_thresh_temp Upper threshold of estimated temperature	K	1	db	8 byte(s)
19	low_thresh_cont Lower threshold of estimated continuum parameter	cm2	1	db	8 byte(s)
20	up_thresh_cont Upper threshold of estimated continuum parameter	cm2	1	db	8 byte(s)
21	spare_4 Spare	-	1	SpareField	24 byte(s)
22	diff_spec_res Difference between spectral resolution of general fine wavenumber grid and spectral grid of cross section look-up tables	cm-1	1	db	8 byte(s)
23	pre_stored_switch Switch for using pre-stored spectra and jacobian matrix	-	1	us	2 byte(s)
24	cont_param Control parameter for fitting of continuum and instrumental offset	-	1	us	2 byte(s)
25	up_alt_cont Upper altitude limit where continuum shall be fitted	km	1	db	8 byte(s)
26	zero_alt_cont Altitude above which the continuum shall be set to zero	km	1	db	8 byte(s)
27	spare_5 Spare	-	1	SpareField	8 byte(s)
28	max_fitted Maximum number of fitted parameters	-	1	us	2 byte(s)
29	spec_overlap Overlap of spectral range between two adjacent MW?s	%	1	db	8 byte(s)
30	temp_inc Temperature increment used to compute perturbed temperature profile	K	1	db	8 byte(s)
31	cent_wvn Central wavenumber of the line used as reference	cm-1	1	db	8 byte(s)
32	temp_coef_lorentz Coefficient of temperature dependence of Lorentz half-width of the line used as reference	-	1	db	8 byte(s)
33	guess_alt Guess of altitude increment above highest level	km	1	db	8 byte(s)
34	red_fact Reduction factor applied to guess of altitude increment	-	1	db	8 byte(s)
35	up_lim_atm Upper limit of atmosphere	km	1	db	8 byte(s)
36	half_width_ref Half-width of the line used as reference	cm-1	1	db	8 byte(s)
37	max_temp_var_low Maximum allowed temperature variation between atmospheric levels for lower	K	1	db	8 byte(s)

#	Description	Units	Count	Type	Size
	altitudes				
38	max_temp_var_high Maximum allowed temperature variation between atmospheric levels for higher altitudes	K	1	db	8 byte(s)
39	alt_thresh_change Altitude threshold where temperature thresholds are changed	km	1	db	8 byte(s)
40	max_var_half_width Maximum allowed variation of half-width of the line between adjacent atmospheric levels	cm-1	1	db	8 byte(s)
41	num_max_atm Number of maximum levels for modelling of the atmosphere	-	1	us	2 byte(s)
42	max_diff_gas Maximum number of different gases	-	1	us	2 byte(s)
43	max_geom Maximum number of simulated geometries	-	1	us	2 byte(s)
44	max_param_pt Maximum number of parameters to be retrieved for p, T and continuum	-	1	us	2 byte(s)
45	coef_corr_grav Coefficients for latitude dependent correction of gravity acceleration	-	2	db	2*8 byte(s)
46	eq_ref_temp Equivalent reference temperature	K	1	db	8 byte(s)
47	eq_ref_press Reference equivalent pressure at equivalent reference temperature used for line computation	hPa	1	db	8 byte(s)
48	approx_err_int Approximation error of integrals (Curtis-Godson)	-	1	db	8 byte(s)
49	init_temp_pert Initial temperature of perturbed equivalent temperature	K	1	db	8 byte(s)
50	max_layers Maximum number of layers	-	1	us	2 byte(s)
51	max_samp_integrand Minimum number of samples at which the integrand of each integral shall be computed	-	1	us	2 byte(s)
52	max_base_profile_elems Maximum number of elements in base profiles	-	1	us	2 byte(s)
53	min_integrate_var Minimum value of integration variable	-	1	db	8 byte(s)
54	num_add_iapt_num Number of additional IAPT numbers for each geometry above the lowest geometry	-	1	us	2 byte(s)
55	half_width_mult_lorentz Multiplier for Lorentz and Doppler half width used for Lorentz lineshape computations on the local coarse wavenumber grid	-	1	db	8 byte(s)
56	half_width_mult_voigt Multiplier for Doppler half width used for Voigt lineshape computations on the local fine wavenumber grid	-	1	db	8 byte(s)
57	interp_switch Switch for interpolation of absorption cross sections for geometries above the lowest geometry	-	1	ss	2 byte(s)
58	cross_switch Switch for usage of cross section lookup tables	-	1	us	2 byte(s)
59	spare_6 Spare	-	1	SpareField	8 byte(s)
60	co2_chi_switch Switch for computation of CO2 chi factor	-	1	us	2 byte(s)
61	mult_fact_voigt Multiplication factor applied to approximate Voigt half width to determine the local fine grid	-	1	db	8 byte(s)
62	mult_fact_coarse Multiplier for definition of local coarse wavenumber grid	-	1	us	2 byte(s)
63	spare_7 Spare	-	1	SpareField	8 byte(s)
64	num_samp_x Number of samples along x coordinate	-	1	us	2 byte(s)
65	num_samp_y Number of samples along y coordinate	-	1	us	2 byte(s)
66	great_base Greater base of trapezium defining the vertical FOV	km	1	db	8 byte(s)
67	small_base Smaller base of trapezium defining the vertical FOV	km	1	db	8 byte(s)
68	spare_8 Spare	-	1	SpareField	8 byte(s)
69	lambda_damp_fact	-	1	db	8 byte(s)

#	Description	Units	Count	Type	Size
	Lambda damping factor				
70	scale_lambda_damp_fact Scaling of lambda damping factor related to continuum parameters	-	1	db	8 byte(s)
71	scale_dec_lambda Scaling factor used to decrease lambda at each macro iteration	-	1	db	8 byte(s)
72	scale_inc_lambda Scaling factor used to increase lambda at each micro iteration	-	1	db	8 byte(s)
73	max_rel_press_error Threshold for maximum relative error of retrieved pressure	-	1	db	8 byte(s)
74	temp_thresh_err Temperature threshold used to check the maximum error of retrieved temperature	K	1	db	8 byte(s)
75	prev_prof_switch Switch for usage of previous retrieved profiles	-	1	us	2 byte(s)
76	half_width_const Constants for computation of half-width	-	3	db	3*8 byte(s)
77	spare_9 Spare	-	1	SpareField	2 byte(s)
78	samp_inter_x_voigt Sampling interval of x coordinate of Voigt LUT	-	1	db	8 byte(s)
79	samp_inter_y_voigt Sampling interval of y coordinate of Voigt LUT	-	1	db	8 byte(s)
80	ref_half_width_exp Reference half width exponent of lineshape to be computed	-	1	db	8 byte(s)
81	ref_half_width Reference half-width of lineshape to be computed	cm-1	1	db	8 byte(s)
82	sd_ig2_profile Standard deviation of IG2 profile at reference pressure	-	1	db	8 byte(s)
83	ref_pressure_sd_ig2_profile Reference pressure for standard deviation of IG2 profile	hPa	1	db	8 byte(s)
84	grad_sd_ig2_profile Gradient of standard deviation of IG2 profile	-	1	db	8 byte(s)
85	corr_factor_first_diag_elem Correlation factor for first diagonal elements of interpolated VCM for IG2	-	1	db	8 byte(s)
86	sd_ecmwf_profile Standard deviation of ECMWF profile at reference pressure	-	1	db	8 byte(s)
87	ref_pressure_sd_ecmwf_profile Reference pressure for standard deviation of ECMWF profile	hPa	1	db	8 byte(s)
88	grad_sd_ecmwf_profile Gradient of standard deviation of ECMWF profile	-	1	db	8 byte(s)
89	Corr_factor_ecmwf Correlation factor for first diagonal elements of interpolated VCM for ECMWF	-	1	db	8 byte(s)
90	time_const_aging_VCM Time constant for aging VCM of retrieved profiles	s	1	db	8 byte(s)
91	height_tropopause Height of tropopause at poles	km	1	db	8 byte(s)
92	incr_tropopause_height Increment of tropopause height	km	1	db	8 byte(s)
93	sim_geom_below_trop Maximum distance of simulated geometries below tropopause	km	1	db	8 byte(s)
94	sim_distance_above_trop Maximum distance of simulated geometries above tropopause	km	1	db	8 byte(s)
95	enabling_profile_reg Switch for enabling profile regularisation	-	1	us	2 byte(s)
96	param_tuning_profile_reg Parameter for tuning profile regularisation	-	1	db	8 byte(s)
97	diag_reg_matrix Diagonal and first off-diagonal element of regularisation matrix referring to pressure	-	2	db	2*8 byte(s)
98	diag_reg_matrix_temp Diagonal and first off-diagonal element of regularisation matrix referring to temperature	-	2	db	2*8 byte(s)
99	diag_reg_matrix_cont Diagonal and first off-diagonal element of regularisation matrix referring to continuum	-	2	db	2*8 byte(s)
100	diag_reg_matrix_offset Diagonal and first off-diagonal element of regularisation matrix referring to offset	-	2	db	2*8 byte(s)
101	switch_fov_tab_func Switch for usage of FOV tabulated function	-	1	us	2 byte(s)
102	max_sim_geom_fov Maximum number of simulated geometries for FOV	-	1	us	2 byte(s)

#	Description	Units	Count	Type	Size
103	num_points_fov_tab_band_a Number of points for FOV tabulation for spectral band A	-	1	us	2 byte(s)
104	heights_fov_func_band_a Heights of FOV function for spectral band A	-		db	8 byte(s)
105	grid_fov_func_band_a Grid for FOV function for spectral band A	-		db	8 byte(s)
106	num_points_fov_tab_band_ab Number of points for FOV tabulation for spectral band AB	-	1	us	2 byte(s)
107	heights_fov_func_band_ab Heights of FOV function for spectral band AB	-		db	8 byte(s)
108	grid_fov_func_band_ab Grid for FOV function for spectral band AB	-		db	8 byte(s)
109	num_points_fov_tab_band_b Number of points for FOV tabulation for spectral band B	-	1	us	2 byte(s)
110	heights_fov_func_band_b Heights of FOV function for spectral band B	-		db	8 byte(s)
111	grid_fov_func_band_b Grid for FOV function for spectral band B	-		db	8 byte(s)
112	num_points_fov_tab_band_c Number of points for FOV tabulation for spectral band C	-	1	us	2 byte(s)
113	heights_fov_func_band_c Heights of FOV function for spectral band C	-		db	8 byte(s)
114	grid_fov_func_band_c Grid for FOV function for spectral band C	-		db	8 byte(s)
115	num_points_fov_tab_band_d Number of points for FOV tabulation for spectral band D	-	1	us	2 byte(s)
116	heights_fov_func_band_d Heights of FOV function for spectral band D	-		db	8 byte(s)
117	grid_fov_func_band_d Grid for FOV function for spectral band D	-		db	8 byte(s)

Record Length : 654

DS_NAME : P, t, Retrieval GADS

Format Version 114.0

6.5.66 VMR Retrieval Parameters GADS

Table 6.89 VMR Retrieval Parameters GADS

VMR Retrieval Parameters GADS

#	Description	Units	Count	Type	Size
Data Record					
0	dsr_time Time of creation	MJD	1	mjd	12 byte(s)

#	Description	Units	Count	Type	Size
1	dsr_length DSR length	-	1	ul	4 byte(s)
2	min_val_non_sing Minimum value used to check non-singularity of matrix	-	1	db	8 byte(s)
3	usage_matrix_s_p_t_error Switch for usage of matrix S in p,T error propagation	-	1	us	2 byte(s)
4	spare_1 Spare	-	1	SpareField	12 byte(s)
5	max_elements Maximum number of elements in profiles	-	1	us	2 byte(s)
6	num_unsuccess Number of allowed unsuccessful previous retrievals	-	1	us	2 byte(s)
7	enh_spec_range Enhanced spectral range of MW?s used to decide whether a line inside the MW shall be considered as line or as nearby continuum	cm-1	1	db	8 byte(s)
8	max_samples_fine Maximum number of spectral samples on fine grid	-	1	us	2 byte(s)
9	chi2_thresh Threshold to check convergence of chi-square	-	1	db	8 byte(s)
10	thresh_fitted_vmr Threshold to check convergence of fitted VMR	-	1	db	8 byte(s)
11	spare_2 Spare	-	1	SpareField	2 byte(s)
12	max_macro_iter_gauss Maximum number of Gauss-Newton macro-iterations	-	1	us	2 byte(s)
13	spare_3 Spare	-	1	SpareField	2 byte(s)
14	max_num_marq Maximum number of Marquardt micro-iterations	-	1	us	2 byte(s)
15	low_thresh_vmr Lower threshold of estimated VMR	ppm	1	db	8 byte(s)
16	up_thresh_vmr Upper threshold of estimated VMR	ppm	1	db	8 byte(s)
17	low_thresh_cont Lower threshold of estimated continuum parameter	cm2	1	db	8 byte(s)
18	up_thresh_cont Upper threshold of estimated continuum parameter	cm2	1	db	8 byte(s)
19	spare_4 Spare	-	1	SpareField	24 byte(s)
20	diff_spec_res Difference between spectral resolution of general fine wavenumber grid and spectral grid of cross section look-up tables	cm-1	1	db	8 byte(s)
21	cont_param Control parameter for fitting of continuum and instrumental offset0:exclude continuum and offset1:include continuum, exclude offset2:include continuum and offset	-	1	us	2 byte(s)
22	up_alt_cont Upper altitude limit where continuum shall be fitted	km	1	db	8 byte(s)
23	spare_5 Spare	-	1	SpareField	8 byte(s)
24	max_fitted Maximum number of fitted parameters	-	1	us	2 byte(s)
25	spec_overlap Overlap of spectral range between two adjacent MW?s	%	1	db	8 byte(s)
26	zero_alt_cont Altitude above which the continuum shall be set to zero	km	1	db	8 byte(s)
27	cent_wvn Central wavenumber of the line used as reference	cm-1	1	db	8 byte(s)
28	temp_coef_lorentz Coefficient of temperature dependence of Lorentz half-width of the line used as reference	-	1	db	8 byte(s)
29	guess_alt Guess of altitude increment above highest level	km	1	db	8 byte(s)
30	red_fact Reduction factor applied to guess of altitude increment	-	1	db	8 byte(s)
31	up_lim_atm Upper limit of atmosphere	km	1	db	8 byte(s)
32	half_width_ref Half-width of the line used as reference	cm-1	1	db	8 byte(s)
33	max_temp_var_low Maximum allowed temperature variation between atmospheric levels for lower altitudes	K	1	db	8 byte(s)

#	Description	Units	Count	Type	Size
34	max_temp_var_high Maximum allowed temperature variation between atmospheric levels for higher altitudes	K	1	db	8 byte(s)
35	alt_thresh_change Altitude threshold where temperature thresholds are changed	km	1	db	8 byte(s)
36	max_var_half_width Maximum allowed variation of half-width of the line between adjacent atmospheric levels	cm-1	1	db	8 byte(s)
37	num_max_atm Number of maximum levels for modelling of the atmosphere	-	1	us	2 byte(s)
38	max_diff_gas Maximum number of different gases	-	1	us	2 byte(s)
39	max_geom Maximum number of simulated geometries	-	1	us	2 byte(s)
40	max_param_vmr Maximum number of parameters to be retrieved for VMR and continuum	-	1	us	2 byte(s)
41	coef_corr_grav Coefficients for latitude dependent correction of gravity acceleration	-	2	db	2*8 byte(s)
42	approx_err_int Approximation error of integrals (Curtis-Godson)	-	1	db	8 byte(s)
43	init_temp_pert Initial temperature of perturbed equivalent temperature	K	1	db	8 byte(s)
44	max_layers Maximum number of layers	-	1	us	2 byte(s)
45	max_samp_integrand Minimum number of samples at which the integrand of each integral shall be computed	-	1	us	2 byte(s)
46	max_base_profile_elems Maximum number of elements in base profiles	-	1	us	2 byte(s)
47	min_integrate_var Minimum value of integration variable	-	1	db	8 byte(s)
48	num_add_iapt_num Number of additional IAPT numbers for each geometry above the lowest geometry	-	1	us	2 byte(s)
49	eq_ref_press Reference equivalent pressure at equivalent reference temperature used for line computation	hPa	1	db	8 byte(s)
50	eq_ref_temp Equivalent reference temperature	K	1	db	8 byte(s)
51	half_width_mult_lorentz Multiplier for Lorentz and Doppler half width used for Lorentz lineshape computations on the local coarse wavenumber grid	-	1	db	8 byte(s)
52	half_width_mult_voigt Multiplier for Doppler half width used for Voigt lineshape computations on the local fine wavenumber grid	-	1	db	8 byte(s)
53	interp_switch Switch for interpolation of absorption cross sections for geometries above the lowest geometry	-	1	ss	2 byte(s)
54	cross_switch Switch for usage of cross section lookup tables	-	1	us	2 byte(s)
55	spare_6 Spare	-	1	SpareField	6 byte(s)
56	hitran_code HITRAN code of the lineshape to be pre-computed	-	1	us	2 byte(s)
57	isotope_num_lineshape Isotope number of lineshape to be precomputed	-	1	us	2 byte(s)
58	co2_chi_switch Switch for computation of CO2 chi factor0: no factor1: N2/O2 broadening2: N2 broadening only	-	1	us	2 byte(s)
59	ref_half_width_exp Reference half width exponent of lineshape to be computed	-	1	db	8 byte(s)
60	ref_half_width Reference half-width of lineshape to be computed	cm-1	1	db	8 byte(s)
61	mult_fact_voigt Multiplication factor applied to approximate Voigt half width to determine the local fine grid	-	1	db	8 byte(s)
62	mult_fact_coarse Multiplier for definition of local coarse wavenumber grid	-	1	us	2 byte(s)
63	spare_7 Spare	-	1	SpareField	8 byte(s)
64	num_samp_x Number of samples along x coordinate	-	1	us	2 byte(s)
65	num_samp_y	-	1	us	2 byte(s)

#	Description	Units	Count	Type	Size
	Number of samples along y coordinate				
66	great_base Greater base of trapezium defining the vertical FOV	km	1	db	8 byte(s)
67	small_base Smaller base of trapezium defining the vertical FOV	km	1	db	8 byte(s)
68	spare_8 Spare	-	1	SpareField	16 byte(s)
69	scale_fact_vmr_base Scaling factor used to scale base VMR profile	-	1	db	8 byte(s)
70	thresh_temp_diff Threshold of temperature difference between two model layers	K	1	db	8 byte(s)
71	lambda_damp_fact Lambda damping factor	-	1	db	8 byte(s)
72	scale_lambda_damp_fact Scaling of lambda damping factor related to continuum parameters	-	1	db	8 byte(s)
73	scale_dec_lambda Scaling factor used to decrease lambda at each macro iteration	-	1	db	8 byte(s)
74	scale_inc_lambda Scaling factor used to increase lambda at each micro iteration	-	1	db	8 byte(s)
75	prev_prof_switch Switch for usage of previous retrieved profiles	-	1	us	2 byte(s)
76	spare_9 Spare	-	1	SpareField	2 byte(s)
77	vcm_thresh VCM threshold used to check the maximum error of retrieved VMR	ppm	1	db	8 byte(s)
78	half_width_const Constants for computation of half-width	-	3	db	3*8 byte(s)
79	spare_10 Spare	-	1	SpareField	8 byte(s)
80	samp_inter_x_voigt Sampling interval of x coordinate of Voigt LUT	-	1	db	8 byte(s)
81	samp_inter_y_voigt Sampling interval of y coordinate of Voigt LUT	-	1	db	8 byte(s)
82	sd_ig2_profile Standard deviation of IG2 profile at reference pressure	-	1	db	8 byte(s)
83	ref_pressure_sd_ig2_profile Reference pressure for standard deviation of IG2 profile	hPa	1	db	8 byte(s)
84	grad_sd_ig2_profile Gradient of standard deviation of IG2 profile	-	1	db	8 byte(s)
85	corr_factor_first_diag_elem Correlation factor for first diagonal elements of interpolated VCM for IG2	-	1	db	8 byte(s)
86	sd_ecmwf_profile Standard deviation of ECMWF profile at reference pressure	-	1	db	8 byte(s)
87	ref_pressure_sd_ecmwf_profile Reference pressure for standard deviation of ECMWF profile	hPa	1	db	8 byte(s)
88	grad_sd_ecmwf_profile Gradient of standard deviation of ECMWF profile	-	1	db	8 byte(s)
89	Corr_factor_ecmwf Correlation factor for first diagonal elements of interpolated VCM for ECMWF	-	1	db	8 byte(s)
90	time_const_aging_VCM Time constant for aging VCM of retrieved profiles	s	1	db	8 byte(s)
91	height_tropopause Height of tropopause at poles	km	1	db	8 byte(s)
92	incr_tropopause_height Increment of tropopause height	km	1	db	8 byte(s)
93	sim_geom_below_trop Maximum distance of simulated geometries below tropopause	km	1	db	8 byte(s)
94	sim_distance_above_trop Maximum distance of simulated geometries above tropopause	km	1	db	8 byte(s)
95	enabling_profile_reg Switch for enabling profile regularisation	-	1	us	2 byte(s)
96	param_tuning_profile_reg Parameter for tuning profile regularisation	-	1	db	8 byte(s)
97	diag_reg_matrix_temp Diagonal and first off-diagonal element of regularisation matrix referring to VMR	-	2	db	2*8 byte(s)
98	diag_reg_matrix_cont Diagonal and first off-diagonal element of regularisation matrix referring to continuum	-	2	db	2*8 byte(s)
99	diag_reg_matrix_offset Diagonal and first off-diagonal element of regularisation matrix referring to offset	-	2	db	2*8 byte(s)

#	Description	Units	Count	Type	Size
100	switch_fov_tab_func Switch for usage of FOV tabulated function	-	1	us	2 byte(s)
101	max_sim_geom_fov Maximum number of simulated geometries for FOV	-	1	us	2 byte(s)
102	num_points_fov_tab_band_a Number of points for FOV tabulation for spectral band A	-	1	us	2 byte(s)
103	heights_fov_func_band_a Heights of FOV function for spectral band A	-		db	8 byte(s)
104	grid_fov_func_band_a Grid for FOV function for spectral band A	-		db	8 byte(s)
105	num_points_fov_tab_band_ab Number of points for FOV tabulation for spectral band AB	-	1	us	2 byte(s)
106	heights_fov_func_band_ab Heights of FOV function for spectral band AB	-		db	8 byte(s)
107	grid_fov_func_band_ab Grid for FOV function for spectral band AB	-		db	8 byte(s)
108	num_points_fov_tab_band_b Number of points for FOV tabulation for spectral band B	-	1	us	2 byte(s)
109	heights_fov_func_band_b Heights of FOV function for spectral band B	-		db	8 byte(s)
110	grid_fov_func_band_b Grid for FOV function for spectral band B	-		db	8 byte(s)
111	num_points_fov_tab_band_c Number of points for FOV tabulation for spectral band C	-	1	us	2 byte(s)
112	heights_fov_func_band_c Heights of FOV function for spectral band C	-		db	8 byte(s)
113	grid_fov_func_band_c Grid for FOV function for spectral band C	-		db	8 byte(s)
114	num_points_fov_tab_band_d Number of points for FOV tabulation for spectral band D	-	1	us	2 byte(s)
115	heights_fov_func_band_d Heights of FOV function for spectral band D	-		db	8 byte(s)
116	grid_fov_func_band_d Grid for FOV function for spectral band D	-		db	8 byte(s)

Record Length : 634

DS_NAME : VMR Retrieval Parameters GADS

Format Version 114.0

6.5.67 P T Retrieval MW ADS

Table 6.90 P T Retrieval MW ADS

VMR Retrieval MW ADS for species #6

#	Description	Units	Count	Type	Size
Data Record					
0	dsr_time Time of creation	MJD	1	mjd	12 byte(s)
1	attach_flag Attachment flag (Always set to zero for this ADS)	flag	1	BooleanFlag	1 byte(s)
2	mw_id Microwindow identifier 8 character string	ascii	1	AsciiString	8 byte(s)
3	num_lines Number of spectral lines	-	1	ul	4 byte(s)
4	dsr_num DSR in Spectral Lines MDS containing data of first line	-	1	ul	4 byte(s)

Record Length : 29

DS_NAME : VMR Retrieval MW ADS for species #6

Format Version 114.0

6.5.68 Spectral Lines MDS

Table 6.91 Spectral Lines MDS

Spectral Lines MDS

#	Description	Units	Count	Type	Size
Data Record					
0	dsr_time Time of creation	MJD	1	mjd	12 byte(s)
1	quality_flag Quality indicator (always set to zero)	flag	1	BooleanFlag	1 byte(s)
2	wvn Wavenumber	cm-1	1	db	8 byte(s)
3	intensity Intensity	cm-1/molec*cm-2	1	fl	4 byte(s)
4	air_broad_296 Air broadened half-width at 296K	cm-1	1	fl	4 byte(s)
5	air_broad_hw_temp_dep Coefficient of temperature dependence of air broadened half-width	-	1	fl	4 byte(s)
6	low_energy Lower state energy	cm-1	1	fl	4 byte(s)
7	wing_flag Flag for line wing treatment0: interpolation possible1: full treatment (calculation at each grid point in the MW)	flag	1	us	2 byte(s)
8	isotope_num Isotope number	-	1	us	2 byte(s)
9	hitran_mol	-	1	us	2 byte(s)

#	Description	Units	Count	Type	Size
	HITRAN molecular code				
10	up_lim Upper limit where line has to be considered	km	1	fl	4 byte(s)
11	low_lim Lower limit where line has to be considered	km	1	fl	4 byte(s)

Record Length : 51

DS_NAME : Spectral Lines MDS

Format Version 114.0